Texas Water Resources Institute
Annual Technical Report
FY 2001

Introduction

Research Program

Texas Groundwater Management and Global Applications

Basic Information

Title:	Texas Groundwater Management and Global Applications
Project Number:	2001TX3101B
Start Date:	3/1/2001
End Date:	2/28/2002
Funding Source:	104B
Congressional District:	10
Research Category:	Not Applicable
Focus Category:	Groundwater, Law, Institutions, and Policy, Management and Planning
Descriptors:	groundwater, management
Principal Investigators:	Daniel Stein

Publication

1. Stein, Daniel R., 2002, Texas-Mexico Groundwater and Global Applications, M.S. thesis, Lyndon B. Johnson School of Public Affairs, The University of Texas, Austin, Texas

Texas-Mexico Groundwater and Global Policy Applications

Daniel Reuben Stein, B.A.
Thesis
The University of Texas at Austin
May, 2002
Project: TX3101

The debate over groundwater aquifers that underlie more than one sovereign nation is not peculiar to Texas and Mexico. When one nation withdraws groundwater from a transboundary aquifer, the other side may perceive that it loses a portion of its own supply. Groundwater users are typically unwilling to surrender their beneficial utilization of these waters, even while this use causes damage or depletion of the aquifer or exacerbates existing tensions with a neighboring state. Unlike surface water, groundwater flows through underground geologic formations, so it is less tangible, measurable, and quantifiable than surface water. The facts regarding aquifer capacity or quality can be difficult to estimate, particularly as the volume of recharge in a given year is hard to predict. National and state groundwater laws among different nations can conflict or be incompatible. In the absence of a common policy on groundwater, neither party is obligated to conserve the resource.

The establishment of jointly accepted rules of aquifer withdrawal, whether or not through a groundwater treaty, would be a tangible step toward conserving a natural resource and improving relations with a neighboring country. In the case of Texas and Mexico, there is a need for such rules due to patterns of groundwater mining both in Mexico and in the United States over the past five years. This thesis does not seek to argue for a common transboundary groundwater policy between the United States and Mexico. It does suggest options for the administration Texas-Mexico aquifers, should the parties decide to develop common groundwater policies. These options are based on a review of current studies of bilateral transboundary groundwater management between Texas and Mexico and between the Palestinian Authority and Israel.\

Texas-Mexico Groundwater

The second and third chapters of this thesis deal with the issues related to transboundary groundwater between Texas and Mexico. Chapter two contains an overview of the hydrologic situation, as well as the duties and purview of existing water management institutions. It summarizes of water laws on both sides of the border and applicable international water law. Chapter three reports on the views of experts as they seek to analyze the situation and develop potential solutions. The literature addressed in the third chapter provides examples of existing opinions on the issues raised in this thesis. Items mentioned in the literature review are not the only articles available on the subject, but illustrate professional viewpoints related to the issue of transboundary groundwater.

Texas shares five major aquifers with Mexico: the Hueco-Mesilla Bolson (two aquifers divided by a rock ridge); the Edwards-Trinity Plateau; the Carrizo-Wilcox; and the Gulf Coast Aquifer. A series of minor aquifers called West Texas Bolsons also cross Texas' border with Mexico.

In an area as dry as the border region, water management is important to secure adequate supplies for years to come. A continued increase in population developing along the border, particularly in cities such as Tijuana and Ciudad Juárez, strains an underground water supply that

Incorporation of Salinity in Evaluating Water Availability

Basic Information

Title:	Incorporation of Salinity in Evaluating Water Availability
Project Number:	2001TX3121B
Start Date:	3/1/2001
End Date:	2/28/2002
Funding Source:	104B
Congressional District:	8
Research Category:	Engineering
Focus Category:	Water Quality, Surface Water, Models
Descriptors:	river basin management, water supply,natural salt pollution
Principal Investigators:	Richard Hoffpauir

Publication

Incorporation of Salinity in Evaluating Water Availability

PI: Richard Hoffpauir
Professor: Ralph Wurbs
Department of Civil Engineering
Texas A&M University
Project T3121

This research will address associated with salinity in evaluating and modeling the availability of water rights. Most of the work focuses on modifying the Water Rights Analysis Package (WRAP) model Wurbs developed to better deal with issues associated with saline surface waters.

So far, work on the WRAP model has stressed modeling the extent to which waters may be available at specific points in a watershed, based on hydrologic and water use data.

Recently, Wurbs and a team of graduate students have worked to improve the model by incorporating new features, including assessing how salinity constrains usable water supplies, and, in a different project, examining conditional water availability.

In this project, Hoffpauir is developing new computer codes for WRAP, using FORTRAN, that address issues related to salinity. He is also reviewing research that TAMU conducted throughout the 1990s that examined how salinity may affect reservoir operations.

A TWRI-funded research project is helping a Texas A&M University graduate student examine how to incorporate salinity problems into water modeling efforts.

This project worked to expand the modeling capabilities of the WRAP computer model to include the ability to assess issues related to natural salt pollution. The study identified how salinity may limit the availability and reliability of water supplies.

Conditional Reliability Modeling to Support Short-Term River Basin Management Decisions

Basic Information

Title:	Conditional Reliability Modeling to Support Short-Term River Basin Management Decisions
Project Number:	2001TX3141B
Start Date:	3/1/2001
End Date:	2/28/2002
Funding Source:	104B
Congressional District:	8
Research Category:	Not Applicable
Focus Category:	Models, Surface Water, Management and Planning
Descriptors:	simulation modeling, reservoir system operations, drought management, water rights,water supply reliability
Principal Investigators:	Adalberto Salazar-Polania

Publication

1. Salazar, Adalberton. 2002. Conditional Reliability Modeling To Support Short Term River Basin Management Decisions, Texas Water Resources Institute, Texas A&M University, College Station, Texas, SR 2002-023.

Conditional Reliability Modeling to Support Short-Term River Basin Management Decisions

PI: Adalberto Andres Salazar
Professor: Ralph Wurbs
Department of Civil Engineering
Texas A&M University
Project: TX 3141

The objective of this research was to develop a conditional reliability model that would support short-term river basin management activities in which consideration of current reservoir storage levels is important. The results are the probability of meeting water demands and instream flow requirements given specific storage conditions and water management premises. The model is a part of the Water Rights Analysis Package (WRAP), which is the set of computer programs adopted by the State of Texas through the Texas Natural Resources Conservation Commission (TNRCC) for the development of water availability studies. Two new programs, WRAP-CON and TAB-CON, were developed for incorporation in the WRAP package.

The research studied a methodology for the prediction of inflows based on conditional frequency duration curves developed for specific storage intervals. The reservoir storage is considered as a link between past flows and future flows, performing a similar role to the autocorrelation coefficient. Usually, streamflows have some degree of autocorrelation, meaning that the flow tomorrow will depend partially on the flow recorded today. In the proposed model, the reservoir level takes the place of the autocorrelation coefficient and the flow tomorrow depends on reservoir storage today. Since the reservoir preserves some memory of the flows in the past, the storage behavior contains inherently the autocorrelational properties of inflows. This model is designed to override the assumption of all alternative flow sequences being equally likely to occur. Portions of historical inflows are routed in separate simulations, and the exceedence probability of flows is related to the diversion amountor storage achieved in each simulation. This produces the likelihood of meeting water requirements and storage levels. The reliability in the basin is expressed with parameters such as the probability of meeting or exceeding percentages of target diversions, volume and period reliability, distribution of storage in the next months, and other statistical parameters.

The model can be applied in the formulation and evaluation of drought contingency plans and operational activities. It was tested in two river basins in Texas: Guadalupe-San Antonio and Nueces. The research included the development of methodologies for the application of the model and investigation of pertinent modeling complexities.

Arsenic Concentrations in Water Resources of the Choke Canyon/Lake Corpus Christi Reservoir Systems: Surface and Ground Waters

Basic Information

Title:	Arsenic Concentrations in Water Resources of the Choke Canyon/Lake Corpus Christi Reservoir Systems: Surface and Ground Waters
Project Number:	2001TX3161B
Start Date:	3/1/2001
End Date:	2/28/2002
Funding Source:	104B
Congressional District:	27
Research Category:	Not Applicable
Focus Category:	Surface Water, Water Quality, Radioactive Substances
Descriptors:	Uranium Mining, Trace Metals, Nueces River Basin,Arsenic
Principal Investigators:	Jill Brandenberger

Publication

1. Brandenberger, J. and P. Louchouarn. 2001. Arsenic Concentrations in Water Resources of the Choke Canyon/Lake Corpus Christi Reservoir System: Surface and Ground Waters, Masters Thesis, Department of Environmental Science, Texas A&M University--Corpus Christi, Texas
2. Brandenberger, J.M., P. Louchouarn, B. Herbert, P. Tissot, P. Michaud, R. Parker, M. Williams, J. Bonner, M. Beaman. 2001. Behavior of Trace metal Concentrations in Water Profiles from Lake Corpus Christi Subsequent to Overturn Event. NOAA--Expanding Opportunities in Oceanic and Atmospheric Science. April 1-3, Jackson, MS.
3. Parker, R., B. Herbert, J.M. Brandenberger, P. Louchouarn. 2001 Ground Water Discharge from Mid-tertiary Rhyolitic Ash-Rich Sediments as the Source of Elevated Arsenic in South Texas Surface Waters. GSA Abstracts with Programs, v. 33, n. 6, p. A53
4. Brandenberger, Jill M., 2002, Geochemical characterization of trace metal cycling in the waters and sediments of the Lower Nueces River Basin, Texas, Texas A&M University--Corpus Christi, Texas

Arsenic Concentrations in Water Resources of the Choke Canyon/Lake Corpus Christi Reservoir System: Surface and Ground Waters

Project funded in part by the TWRI for the period of Feb. 2001 to January 2002

The above-mentioned project focused on understanding the cycling and fate of heavy metals in Nueces River Watershed including both its surface and ground waters. The objectives of the project were to perform temporal and spatial monitoring of trace element concentrations, focusing on arsenic, in 1) waters of Lake Corpus Christi, Choke Canyon, and points along the tributary rivers: Nueces, Atascosa and Frio, as well as 2) selected ground water wells in this region. Surface water samples have been collected throughout the year 2001during three seasons (winter, spring and summer), and flood events represented by high water discharges into the reservoir system. Ground waters were sampled throughout a wide "grid" covering an extended area around Lake Corpus Christi. For each of the water samples, the total and dissolved fractions have been analyzed by Inductively Coupled Plasma Mass Spectrometry (ICPMS) for arsenic and a suite of other trace metals of interest. The results were interpreted in terms of temporal and spatial changes for surface waters and in terms of spatial variability for ground waters. Our data yielded a substantial suite of findings that are presented in the Abstract and project report below. The abstract represents the completed thesis work of Jill Brandenberger, whereas the project report encompasses only the chapter in the thesis focusing on freshwater resources in the lower Nueces River basin. A copy of the thesis manuscript will be delivered to TWRI upon binding. The research detailed in this thesis manuscript is funded in part by the TWRI project funds and have led to several presentations (see below) and will lead to further planned submissions of manuscripts to peer-reviewed journals (see below)

Presentations.

Brandenberger, J. M., Patrick Louchouarn, Bruce Herbert, Philippe Tissot, Patrick Michaud, Ron Parker, Martha Williams, Jim Bonner, and Mark Beaman. 2001. Behavior of Trace Metal Concentrations in Water Profiles from Lake Corpus Christi Subsequent to an Overturn Event. NOAA – Expanding Opportunities in Oceanic and Atmospheric Sciences. April 1-3, 2001, Jackson, MS.

Parker, Ronald, Bruce Herbert, Jill Brandenberger, and Patrick Louchouarn. 2001. Ground Water Discharge From Mid-Tertiary Rhyolitic Ash-Rich Sediments as the Source of Elevated Arsenic in South Texas Surface Waters. GSA Abstracts with Programs, Volume 33, Number 6, p. A 53.

Publications in Preparation

Brandenberger J., Louchouarn P., Herbert B., Tissot P., Michaud P., Parker R., and Beaman M. (2002 – In preparation). Geochemical behavior of trace metals in a sub-tropical fresh-water lake subsequent to an overturn event. **Chemical Geology**.

Brandenberger J., Louchouarn P., Herbert B., Tissot P., Michaud P., Parker R. (2002 – In preparation). A historical reconstruction of heavy metal non-point source inputs to the Nueces River/Lake Corpus Christi System, Texas. **Applied Geochemistry.**

ABSTRACT

GEOCHEMICAL CHARACTERIZATION OF TRACE METAL CYCLING IN THE WATERS AND SEDIMENTS OF THE LOWER NUECES RIVER BASIN, TX

Jill M. Brandenberger

Thesis for a M.Sc. in Environmental Sciences, Texas A&M University Corpus Christi

Co-Chairpersons of Advisory Committee: Dr. Patrick Louchouarn and Dr. Bruce Herbert

During the last several decades, human-related activities and populations have increased markedly along the Texas Gulf Coast, intensifying pressures on the water resources and ecosystems of this area. The Lake Corpus Christi/Choke Canyon reservoir system mitigates issues of water quantity while perturbing the quality of available fresh water resources. A driving force in the degradation of water quality is the potential loading and deposition of colloidal particles with a high affinity for trace metals and their incorporation into bedded sediments of the system. This "sequestration" may not be permanent, as redox sensitive metals (Mn, Fe, U, As and Mo) are susceptible to diagenetic remobilization due to oscillations in the hydrodynamic regime. This process may in turn result in a positive flux of metals to the water column adding a substantial stress to the aquatic environment and decreasing the quality of our freshwater supply.

This research thus assessed the water quality of Lake Corpus Christi as a function of 1) tributaries and ground waters within the Nueces River basin, 2) present geochemical cycling of trace metals during temporal, spatial, and event driven oscillations of dissolved oxygen, and 3) sedimentary reservoirs in diverse sections of the lake (historic water quality as inferred from sediment cores).

Water column profiles for trace metals assessed seasonal variations (summer vs. winter), an inflow event (episodic floods) and spatial distributions (oxygenated vs. stratified water column). The hypolimnetic cycling of Mn, Fe, Pb, Cr, V, Co and Ni resulted in higher enrichment factors in summer vs. winter and at the deeper station (stratified water column). The strong correlation of Pb and Mn cycling suggests diagenetic remobilization of Pb. However, the mildly reducing conditions did not entrain the cycling of As, Mo and U. Moreover, whereas Mo and U concentrations remain constant at background levels within surface waters of the whole system of study, dissolved As values in the Lower Nueces River basin (8-12 μg/L), are enriched by two orders of magnitude with respect to background levels measured in the upper basin (0.5 μg/L). The conservative behavior of As results in seasonally cycling with dilution during periods of higher inflow (winter and spring) and evapoconcentration in the summer. This contributes to the degradation of water quality and results in seasonal concentrations above the recently adopted standard for arsenic in drinking water (10 μg/L).

Sediment cores encompassed the three reservoir zones: riverine, transition, and lacustrine, each with unique depositional environments. Average metal concentrations in surface sediments are below the threshold effect level (TEL) with the exception of Ni, but discrete depths indicate layers of enriched metal content. Normalized sediment profiles give further evidence of periods of enrichment and depletion of As, Co, Cu, Pb, Ni and Mn suggesting historic fluctuations in metal accumulation throughout the sediment profiles. Historical changes in material inputs to the sedimentary environments of the lake are further supported by significant changes in total organic matter and its isotopic signatures ($\delta^{13}C$ and $\delta^{15}N$). Temporal trends, provided by the pre-reservoir conditions show decreasing values of Hg and Pb due to changes in atmospheric cycling and basin-wide collection/redistribution processes. The uniform distribution of U and Mo around average sediment values suggests that the transport of these metals from upstream uranium mines has not impacted the sediments of Lake Corpus Christi. However, sedimentary peaks in As may support the selective transport and sequestration of this heavy metal due to uranium mining activities in Live Oak County.

The extreme heterogeneity of As, Mo and U in ground waters suggests a mechanism for sequestration, such as sulfidization upon contact with water discharging along faults in Live Oak County enriched in H_2S. The concentrations of these metals in selected ground waters are elevated well above the drinking water standards. An emphasis was placed on As because elevated levels are seen in the surface waters as well as ground waters (~10 and ~20 μg/L, respectively) . However, the ground water samples provide the first indication of enrichment in U (47 μg/L) in the Nueces River basin well above drinking water standard (30 μg/L). Sources for these selective enrichments can include both anthropogenic activities such as past mining processes and agricultural pesticide used in the drainage/aquifer basin, and natural geological inputs to ground water reservoirs.

GEOCHEMICAL CHARACTERIZATION OF TRACE METAL CYCLING IN THE LOWER NUECES RIVER BASIN, TX

Jill M. Brandenberger

Thesis chapter for a M.Sc. in Environmental Sciences, Texas A&M University Corpus Christi

In the semi-arid climate of the south Texas Gulf Coast region, the availability of freshwater resources is a critical issue stressing the stability of communities. An additional stress on the naturally limited freshwater resources is the marked growth in population over the last several decades (Kufus, 2000). In an attempt to mitigate growing water demands, the City of Corpus Christi constructed, in 1982 and 1958, the Choke Canyon / Lake Corpus Christi reservoir system in the lower Nueces River basin (Figure 1). The reservoirs provide water to over 300,000 people in Corpus Christi and surrounding communities. The irony of reservoirs is that they mitigate water quantity concerns, while generating issues on water quality (Thornton et al., 1990).

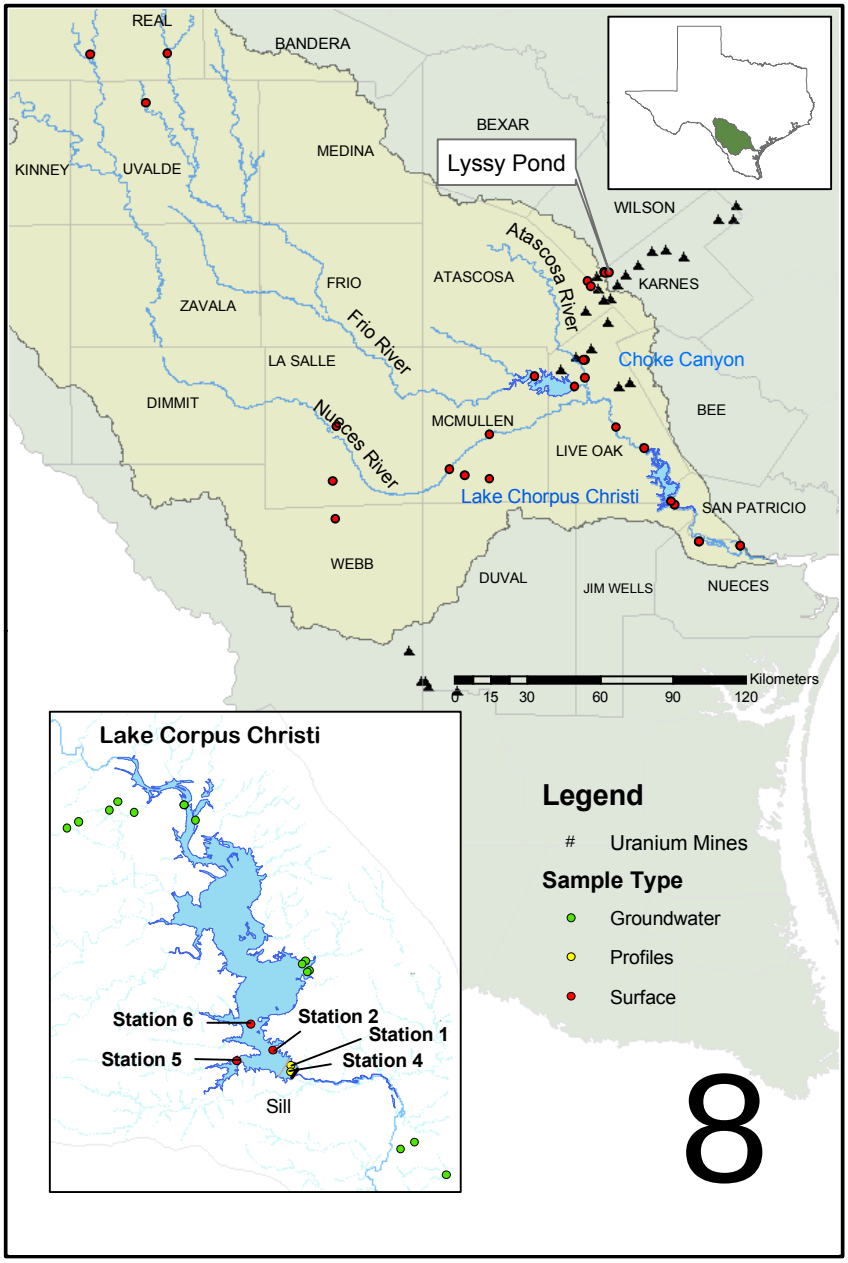

Figure 1. Sampling locations in the Nueces River basin, Lyssy Pond, and the inset of Lake Corpus Christi marking station and ground water sample locations.

The degradation of water quality is often associated to the high loading of particulate and colloidal materials (Thornton et al., 1990), such as clay and silt, which tend to sequester trace metals (Louchouarn and Lucotte, 1998; Santschi et al., 1999; Balogh et al., 1999; Sharma et al., 1999a; Forstner and Wittmann, 1979; Louchouarn et al., 1993; Martin et

al., 1995; Menounou and Presley, 1996; Wen et al., 1999; Baskaran and Santschi, 1993). The adsorption processes enhances the riparian transport of trace metals, as suspended particulates, through a watershed (Manahan, 2000), allowing the deposition of colloidal material in the relatively quiescent waters of reservoirs. Subsequently, incorporating sequester contaminants into the sedimentary record (Hemond and Fechner-Levy, 2000). However, the sedimentary record may not be permanent, as some metals, particularly redox sensitive metals (Mn, Fe, U, As and Mo) are susceptible to diagenetic remobilization due to oscillations in the hydrodynamic regime. Physiochemical alteration in the aquatic ecosystem may effectively reverse the role of sediments from a sink to a source for metals in the hypolimnion, degrading water quality by increasing metal bioavailability (Manahan, 2000; Salbu and Steinnes, 1995).

The dynamic hydrologic cycle typical in south Texas emphaizes the need to characterize contaminant sources, identify depositional environments and understand processes (i.e. temporal cycling) affecting remobilization and sequestration of trace metals. Managing water quality in reservoirs such as Lake Corpus Christi in the Nueces River basin (Roulet et al., 2000; Salbu and Steinnes, 1995; U. S. Environmental Protection Agency, 1999a) requires a holistic basin-wide scale. Initiatives such as the National Water-Quality Assessment (NAWQA) program identified potential contaminant sources and assessed the water quality in the Nueces River basin from 1996-1998 (Bush et al., 2000). The study focused specifically on the upper basin because it is the recharge zone for the Edwards aquifer, but failed to address water quality in the lower basin containing the reservoir system. Other initiatives assessed the susceptibility and loading of contaminants in the Nueces River basin to both freshwater resources -Safe Drinking Water Act Amendments of 1996 (Focazio et al., 2000), Clean Water Act (U. S. Environmental Protection Agency, 1999b) and Texas Clean Rivers (Fisher, 1996; Nueces River Authority, 2001) and the estuarine ecosystem (National Estuaries Program; Baird, et al., 1996). A common theme in all these programs is the lack of data on trace metal concentrations in Lake Corpus Christi reservoir. Compounding this lack of data is the failure to address the previously extensive uranium mining in South Texas as a potential source of trace metals. This could be a significant omission since the transport of mine tailings are widely recognized as substantial anthropogenic contributors of trace metals

and radionuclides to aquatic systems and their sediments (Langedal, 1997; Macdonald et al., 1991; Odhiambo et al., 1996; Ruttenber et al., 1984; U. S. Department of Energy, 1996; Van Metre et al., 1997c).

A zone of uranium mineralization extends across Texas from east central to the southern tip and into Mexico (Nugent et al., 1994). The zone contains clusters of uranium deposits enriched with a minimum of 500 tons of uranium oxide (U_3O_8) each (Finch, 1996). The uranium clusters resulted from the oxidation of volcanic ash by meteoric waters effectively mobilizing uranium along with other redox-sensitive metals (As, Mo V and Se), until remineralization in reducing environments (Eargle et al., 1971; Galloway, 1977; Galloway et al., 1982; Galloway and Kaiser, 1980; Henry et al., 1982; Henry and Kapadia, 1980; Ledger, 1981). By the 1970's, over 40 mines were located in Karnes, Atascosa, Gonzales, and Live Oak counties (Figure 1), ranking Texas third in uranium ore reserves with an estimated 6.6 million tons (Eargle et al., 1971). The pervasive uranium mining activities in Karnes County resulted in the transport of trace metals and radionuclides to both ground water (Blount et al., 1992; U. S. Department of Energy, 1995) and surface waters ecosystems (Batson et al., 1996; Blount et al., 1992; Bryson et al., 1988; Harrington et al., 1998; Parker et al., 1999; U. S. Department of Energy, 1991). Consequently, uranium mining is a major contributor to the degradation of water quality on a local level. The high geochemical mobility of trace metals associated with uranium mining highlights the need to assess their impacts on the Nueces River watershed since tributaries to Lake Corpus Christi drain areas of previous mining activities in Live Oak County.

The identification of Lake Corpus Christi reservoir as a potential recipient of trace metals associated to uranium mining activities emphasizes the need to better understand water quality as a function of the distribution and temporal cycling of trace metals in this aquatic system. Oscillations in dissolved oxygen due to seasonal stratification or episodic mixing events drives the cycling of trace metals (Salbu and Steinnes, 1995). Many studies characterized the cycling of trace metals in response to changes in redox state in seasonal or permanently anoxic hypolimnetic waters (Achterberg et al., 1997; Balistrieri et al., 1992a; Balistrieri et al., 1992b; Elbaz-Poulichet et al., 1997; Harrington et al., 1998; Kneebone and Hering, 2000; Morfett et al., 1988; Murray, 1987; Sigg et al.,

1987; Taillefert et al., 2000; Viollier et al., 1995; Viollier et al., 1997). These studies developed models for the biogeochemical cycling of trace elements across the oxic-anoxic interface in the water column (redox-cline) (Elbaz-Poulichet et al., 1997). Applying a stratified basin model to Lake Corpus Christi provides information on the potential cycling of redox sensitive trace elements as changes in heat balance, wind stress, and lake level affect the efficiency of mixing and depth of oxygen penetration in the water column. Therefore, it is paramount to consider these cycles when addressing water quality concerns, as redox-driven phase transformation of trace metals from particulate to dissolved phase deteriorates water quality by increasing metal bioavailability by orders of magnitude (Neff, 1984; Salbu and Steinnes, 1995). The substantial presence of trace metals in Lake Corpus Christi or its tributaries could substantiate a public health concern since the reservoir is a primary source of water for Corpus Christi and the only source for smaller surrounding communities.

This research evaluates impacts on water quality related to the distribution of trace elements in the lower Nueces River basin and Lake Corpus Christi reservoir. Seasonal and event driven depth profiles in Lake Corpus Christi provided information on the geochemical cycling of trace metals while surface and ground waters collected throughout the lower Nueces River basin provide information on the basin wide distribution of trace metals. The initial assessment of ground waters serves as the cornerstone for the modeling of trace metals in ground waters of Live Oak County.

STUDY AREA

The use of a reference site (Figure 1 - Lyssy Pond) in this study provided information on the geochemical cycling of trace metals in a system- 1) demonstrating elevated levels of trace metals and radionuclides directly attributed to uranium mining activities (Parker et al., 1999) and 2) undergoes strong seasonal stratification with installation of anoxia in the hypolimnion. Lyssy Pond is a stock pond located in Karnes County near the federally funded Uranium Mill Tailings Remedial Action (UMTRA) Project. For a detailed characterization of Lyssy Pond, see (Parker et al., 1999).

The Nueces River Basin covers approximately 44,000 km^2, encompassing all or part of 23 counties (Figure1). Presently, the major land use is farming and ranching with no major metropolitan areas in the immediate drainage basin, only larger communities

including Uvalde, Pleasanton, George West, and Three Rivers (Nueces River Authority, 2001). However, from 1967 until the early 1980's several uranium mines (Figure 1) operated in Live Oak County extracting ore from the Oakville Formation, which also hosts a major aquifer providing water for municipal, domestic and agricultural uses (Galloway et al., 1982).

The Choke Canyon/Lake Corpus Christi Reservoir system provides water to the City of Corpus Christi, as well as, South Texas Water Authority, Alice, Beeville, Port Aransas, Rockport, Mathis, Three Rivers, San Patricio Authority and Lamar Peninsula (Fisher, 1996). Lake Corpus Christi reservoir is the focus of this research and is located in Live Oak County (Figure 1). The major tributaries to the reservoir are the Frio (from Choke Canyon reservoir releases), Atascosa, and Nueces Rivers. The Nueces River flows into Lake Corpus Christi downstream of the confluence of the three rivers (Figure 1). The reservoir was impounded in 1958 with the completion of the Wesley Seale Dam located ~ 305 m downstream of the pre-existing reservoir's dam (La Fruta reservoir) (Cunningham, 1998). The remnants of the earthen La Fruta Dam remain and act as a sill (as denoted in Figure 1), restricting flow and altering the deposition regime near the new dam.

Summer conditions in Lake Corpus Christi have the potential to allow stratified conditions to develop in the water column as a result of minimal inflows and substantial evaporative losses potentially reaching 152 cm a year (Cunningham, 1998). Winter conditions are a marked contrast, as strong winds associated with cold fronts efficiently homogenize the water column. During this time, the winds are primarily out of the north, producing significant wave action, as the long axis of the lake is oriented to the north, enhancing the fetch along the lake. Consequently, geochemical cycles of trace metals may be dominated by wind-driven mixing in the winter (fully oxidized), periodic flood events (mixing), and large-scale evaporative losses in the summer.

SAMPLING AND ANALYTICAL TECHNIQUES

Water Column Profiles

Water column profiles for trace elements include three sampling events from Lake Corpus Christi (July, August and January) and one profile from Lyssy Pond (April 2001).

Profiles in Lake Corpus Christi are from two stations (1 & 4; Figure 1) in the lacustrine zone near the dam (Thornton et al., 1990). They are located less than a kilometer apart and selected to represent the deeper section with more restricted mixing (station 1) and a control station indicative of better-mixed shallower environments (station 4). The three sampling events encompass conditions in the water column subsequent to a mixing event and seasonal variations. The July 7, 2000 profiles provide information on the conditions in the lake following a large inflow and subsequent mixing event (Figure 2). Seasonal sampling events include summer (August 25, 2000) and winter (January 26, 2001).

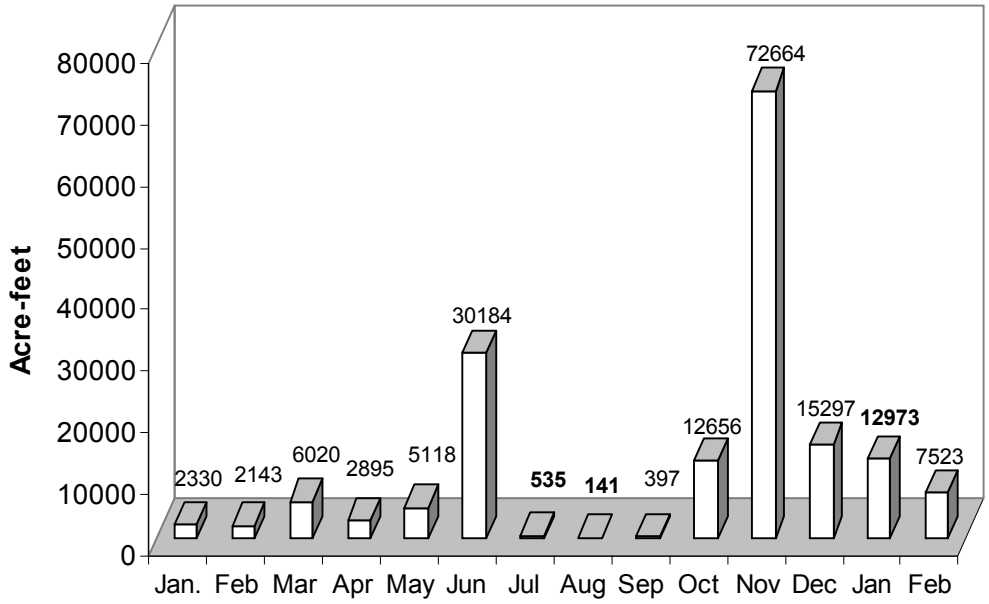

Figure 2. Inflow into Lake Corpus Christi from January 2000 to February 2001. Water column sampling occurred in July, August and January.

Figure 3. Multiple Underwater Syringe Sampling Tool (MUSST).

Physiochemical parameters (pH, DO, temperature, and depth) were collected using a Hydrolab®. Water column profiles were retrieved by *in-situ* sampling using a customized 4" polyvinyl chloride (PVC) sampling device (Multiple Underwater Syringe Sampling Tool – MUSST; Figure 3). The MUSST allows remote sample collection into two 50 ml acid-cleaned polypropylene syringes, minimizing perturbation of the water column while preserving *in-situ* water chemistry. The two-syringe design facilitated the simultaneous collection of samples for dissolved and particulate fractions eliminating the need to later split one sample for two fractions, potentially altering the *in-situ* chemistry.

All water samples were collected following EPA Method 1669: Sampling Ambient Water for Trace Metals at EPA Water Quality Criteria Levels (U. S. Environmental Protection Agency, 1996c). This method includes procedures specifically designed to reduce the possibility of contamination during collection and analysis of water samples. In accordance with this method, all equipment was acid cleaned and clean techniques were strictly followed throughout water sample collection and analysis.

Surface and Ground waters in the Nueces River Basin

The collection of surface water grabs encompassed three other stations (2, 5 and 6) in Lake Corpus Christi and 17 tributary samples of the three rivers in the Nueces River basin– three in the upper and 13 in the lower basin (Figure 1). Tributary samples taken along the Frio River progressed from points in the upper Nueces River basin to upstream and downstream of Choke Canyon Reservoir (Figure 1 –locations in red). The Atascosa River was sampled above the confluence of the three rivers. The Nueces River was progressively sampled in La Salle and McMullen counties.

Sixteen ground waters samples were collected from wells around Lake Corpus Christi (Figure 1- inset of Lake Corpus Christi) in acid clean low-density polyethylene (LDPE) bottles. Samples were retrieved from the well spigot, before any pre-treatment, by allowing water to flow for five minutes prior to collection.

Sample Processing

Upon collection, water samples were stored at 4°C to reduce reaction kinetics. A portion of each sample was filtered through acid-clean 0.45 μm nylon syringe filters, either in the field using a field-portable glove box as a clean environment or in a Class 100 clean bench. The filtered portion represents the "dissolved" metal fraction. Profile samples collected from waters with DO < 3.00 mg/L were filtered in an ultra-high purity nitrogen atmosphere in the field-portable glove box to prevent alteration of metal speciation due to oxidizing conditions or metal scavenging by Fe and Mn oxy-hydroxides. The dissolved and unfiltered (particulate by subtraction) fractions were acidified to 0.2% Optima® nitric acid or a pH <2.0.

Trace Elements Analysis

In accordance with EPA Method 1669, the dissolved fraction is operationally defined as passing through a 0.45 μm filter. However, many studies have shown that a significant percentage of trace metals are associated with the colloidal fractions between 1nm and 1 μm (Baskaran and Santschi, 1993; Benoit et al., 1994; Greenamoyer and Moran, 1997; Hoffman et al., 1981; Martin et al., 1995; Wen et al., 1999). Therefore, both the dissolved and total fractions were acid solubilized to destroy colloidal complexes, dissolving trace metals potentially adsorbed onto colloidal matter. EPA Method 1640

Section 12.2.7 - Total Recoverable Analytes (U. S. Environmental Protection Agency, 1996b) details the digestion method for water samples. Following pre-treatment, samples were analyzed on a Hewlett-Packard 4500 Inductively Coupled Plasma-Mass Spectrometer (ICP-MS) following EPA Method 1638 (U. S. Environmental Protection Agency, 1996a) utilizing in-line addition of the internal standards Sc, Y, Ho, Tb. The ICP-MS was calibrated prior to analysis using a five-point calibration curve prepared with certified standards. The calibration curve for each metal showed a correlation coefficient of $r^2 > 0.999$. Table 1 shows the accuracy and precision of the instrument for each metal as assessed by the analysis of the NIST 1643d: Trace Elements in Drinking Water Standard. Table 1 also lists the method detection limits for each element (MDL) determined by the analysis of seven replicates of a 0.1 part-per-billion (ppb) standard. Other quality control measures included the analysis of continuing calibration verification (CCV) standards showing greater than 90% accuracy throughout the analysis, three types of blanks (sampling, method and reagent) which revealed no contamination of the samples and duplicates/triplicates indicating greater than 90% precision.

Table 1. Accuracy and precision of NIST 1643d and MDLs for trace metals in water.

Trace Metal	NIST 1643d Measure Value (9 samples)		**NIST 1643d Certified Value**		Average Accuracy	Percent Difference	
	Median	Range	Median	Range			MDL
As	55.9	± 1.7	**56.0**	**± 0.73**	100%	2.6%	0.0217
Cd	6.44	± 0.58	**6.47**	**± 0.37**	100%	6.9%	0.0458
Co	24.9	± 0.57	**25.0**	**± 0.59**	100%	1.6%	0.00922
Cr	19.6	± 2.3	**18.5**	**± 0.20**	106%	10%	0.114
Cu	22.8	± 0.48	**20.5**	**± 3.8**	111%	11%	0.0920
Fe	na	na	**na**	**na**	na	na	na
Mn	38.2	± 0.55	**37.7**	**± 0.83**	101%	1.7%	0.0683
Mo	113	± 3.2	**113**	**± 1.7**	100%	2.5%	0.0713
Ni	57.3	± 1.4	**58.1**	**± 2.7**	99%	2.3%	0.0284
Pb	17.9	± 0.54	**18.2**	**± 0.64**	98%	2.6%	0.0254
U	na	na	**na**	**na**	96%[1]	1.6%[2]	0.00945
V	35.3	± 1.02	**35.1**	**± 1.4**	100%	2.5%	0.0233

Concentrations determined by ICP-MS and reported in μg/L (ppb)

[1] Value determined by high purity standards

[2] Value determined by sample replicates

RESULTS

Lyssy Pond

The physiochemical conditions of Lyssy Pond (Figure 4) in April 2001 show partially stratified conditions in the water column with a slight redox-cline and thermocline around 250 cm. Because traces of DO were still measured in the hypolimnion, anoxic conditions existed only in the sedimentary layer. Despite the lack of anoxia in the hypolimnion, variations in vertical distributions of Mn, U and Pb suggest that the declining DO concentrations are enough to generate reducing conditions and entrain geochemical cycling of these metals between particulate and dissolved phase. This substantiates the use of Mn as a geochemical indicator of reduction in the oxidation potential (Eh) of the water column (Balistrieri et al., 1992b; Viollier et al., 1995). The distinct profile for Mn in Lyssy Pond, results from remineralization of organic matter and reductive dissolution of Mn oxy-hydroxides increasing dissolved Mn by nine orders of magnitude in the sub-oxic hypolimnion. The peak in particulate Mn at 325 cm suggests diffusive fluxes of reduced Mn^{2+} from the sediment-water interface into the water column where it is oxidized to the less soluble Mn^{4+} (Balistrieri et al., 1992a; Davison and Tipping, 1984; Mayer et al., 1982; Morfett et al., 1988; Mortimer, 1941; Viollier et al., 1995).

As the oxidation potential of the hypolimnion changes, the profiles of redox sensitive metals such as U, As and Mo should also indicate alterations in speciation resulting in a shift between particulate and dissolved phases (Achterberg et al., 1997; Elbaz-Poulichet et al., 1997; Hamilton-Taylor and Davison, 1995; van der Weijden et al., 1990; Viollier et al., 1995; Viollier et al., 1997). However, in Lyssy Pond only the U profile shows near perfect mass balance with peaks in the particulate phase corresponding to declines in dissolved phase which results from the changing oxidation states between dissolved U^{6+} and reduced, more highly scavenged, U^{4+} (Figure 4). These observations suggest the oxidation potential in the water column may not be reducing enough to produce a phase transformation in As (Figure 4) and Mo species (not shown).

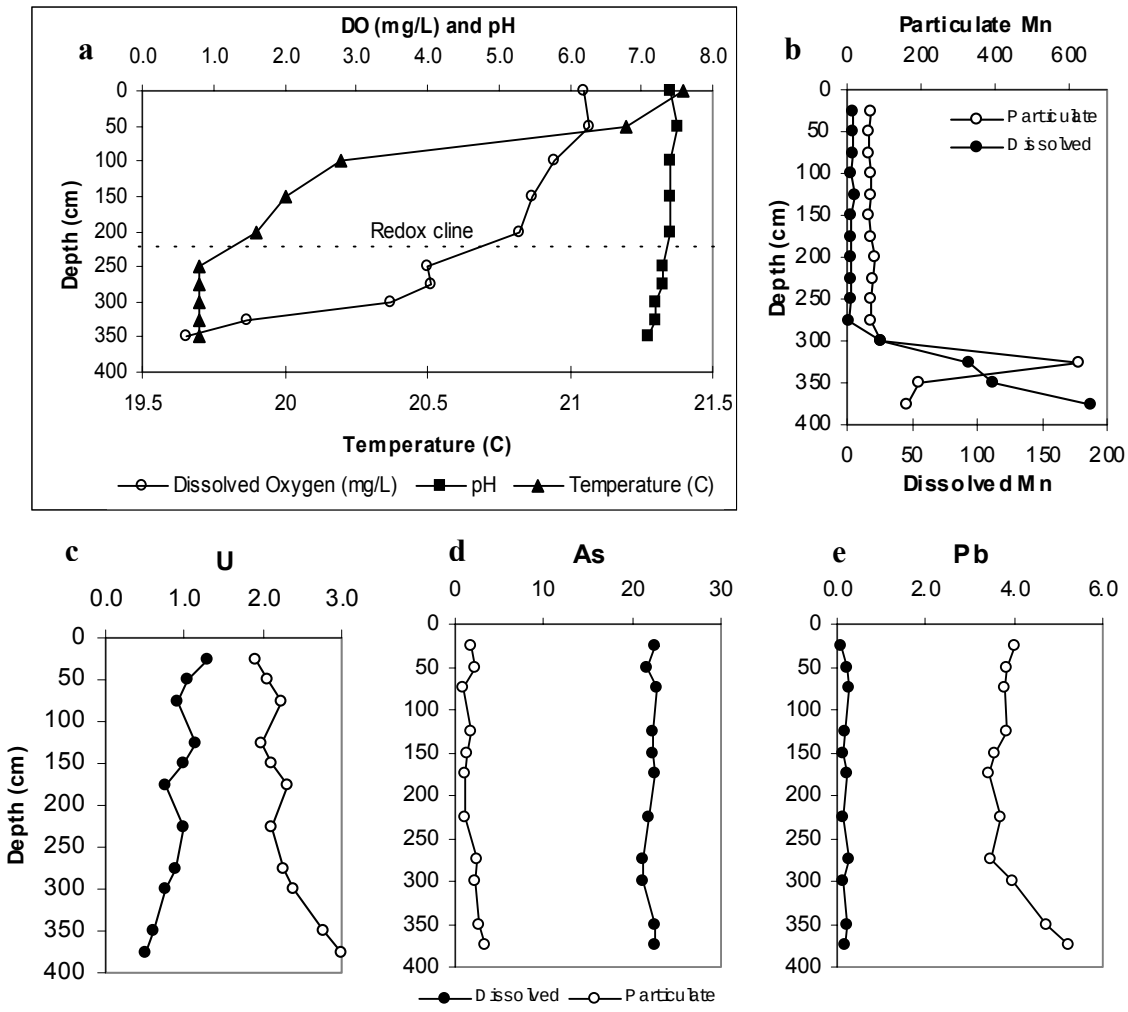

Figure 4. Lyssy Pond water profiles for (a) physical parameters, and the particulate and dissolved fractions of (b) Mn, (c) U, (d) As and (e) Pb. (Values reported in μg/L.)

Lake Corpus Christi Profiles

Physical Parameters

Figure 5 presents the water column profiles of DO, water temperature and pH in Lake Corpus Christi produced by seasonal variations (August vs. January), an inflow event (July 2000), and spatial distributions (stations 1 vs. 4). Dissolved oxygen is the only

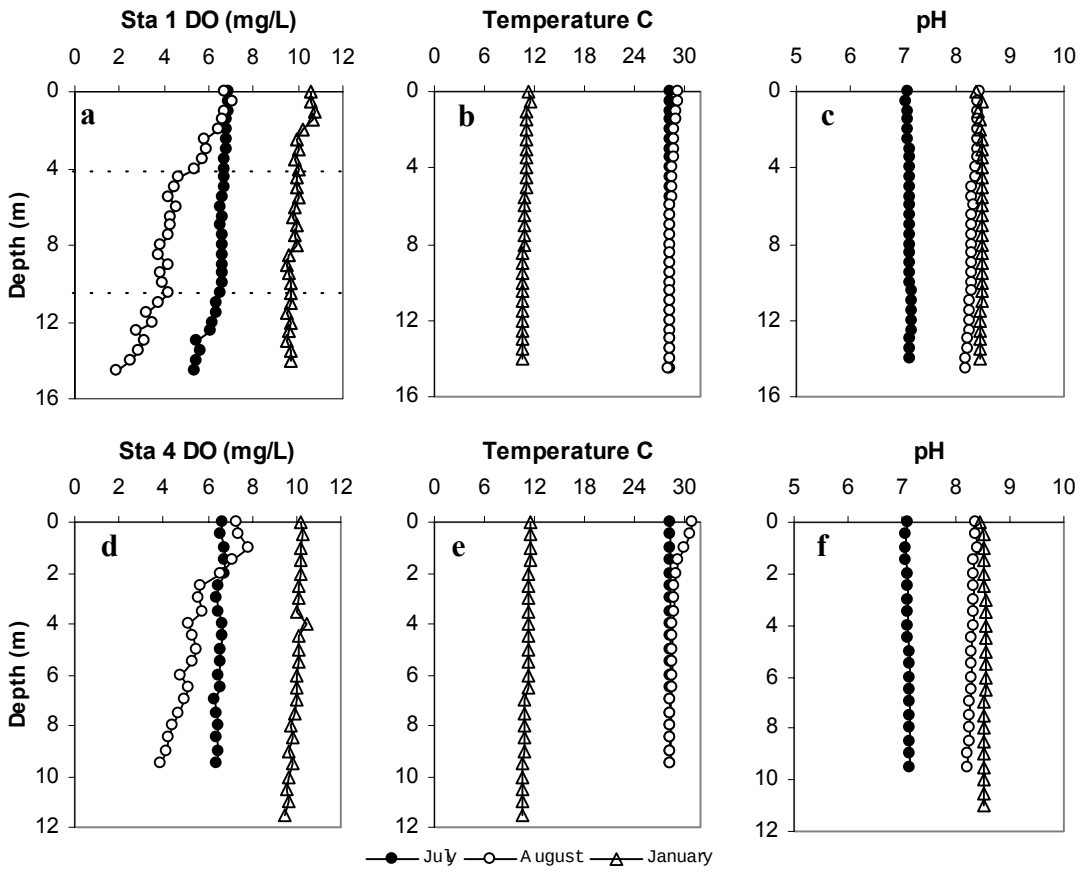

Figure 5. Physiochemical conditions in Lake Corpus Christi for July, August and January. Depth profiles for station 1 (a) DO, (b) temperature and (c) pH and for station 4 (d) DO, (e) temperature and (f) pH.

parameter with a marked seasonal variation in vertical distribution, as seen by a virtually homogenous water column in January versus a partially stratified water column in August. The seasonal differences in DO may be typical, however, the generally shallow depths of the lake allow changing hydrologic conditions to rapidly alter seasonal physiochemical conditions. For example, substantial inflows to Lake Corpus Christi in June 2000 (Figure 2) lead to virtually homogenous conditions within the water column in July compared to the stratified conditions seen in August.

The collection of two profiles during each sampling event in Lake Corpus Christi provides data to assess any spatial variations in physiochemical conditions, and ultimately metal cycling within the lake. Spatial variation in the lake occurs as a function of depth, with seasonal and follow event driven mixing.

Trace Metal Profiles

Figure 6 presents the water column profiles of V, Cr, Mn, Co, Fe, Ni, Cu, As, Mo, Pb, and U as a function of seasonal variations in water chemistry, spatial variations between the two stations, and episodic mixing. The profiles consist of dissolved and particulate fractions for each metal during the three sampling periods (horizontally - July, August and January) for two stations (vertically – 1, 4).

The seasonal profiles illustrate the response of trace metals to partial stratification in August and a mixed water column in January. Comparing the characteristic profile of Mn obtained in Lyssy Pond to August profiles for Lake Corpus Christi, provides information on the oxidation potential of the water column. In Lake Corpus Christi, Fe values were used in conjunction with Mn to evaluate the oxidation potential of the water column since they have similar geochemical profiles offset slightly by differences in oxidation kinetics (Hites and Eisenreich, 1987; Salbu and Steinnes, 1995; Viollier et al., 1995). Station 1 profiles for both seasons show pronounced peaks in the hypolimnion of particulate Mn and Fe, while only August profiles for station 4 have peaks, although of smaller magnitude. The enrichment of particulate Mn and Fe at station 1 is, respectively, by factors of 7.3 and 10 in August and 6.6 and 2.8 in January. In comparison, enrichment factors for station 4 in August are notably lower enrichment factors (3.4 and 2.7, respectively). The profiles of both metals in August are mirror images of the DO profile with epilimnetic peaks in the metals corresponding to the decline in DO at 5.5 m. The peaks in particulate Mn and Fe suggest the oxidation potential is sufficiently reducing to alter the speciation of these metals. However, the oxidation potential favors only the reductive dissolution of Mn in station 1.

The particulate values of V, Cr, Co, Ni and Pb also increase in the hypolimnion, analogous to peaks in Mn and Fe. The August profiles at station 1 show greater hypolimnetic enrichments of the particulate metals by factors of 26, 11, 6.6, 16 and 6.4, respectively; relative to January; which had enrichments values of 3.9, 2.7, 4.0, 5.1 and 3.7, respectively. At station 1, only particulate Co and Pb increase by factors 2.2 and 2.9. Among the dissolved phase metals, only Pb shows significantly higher values in the hypolimnion at station 1 in January.

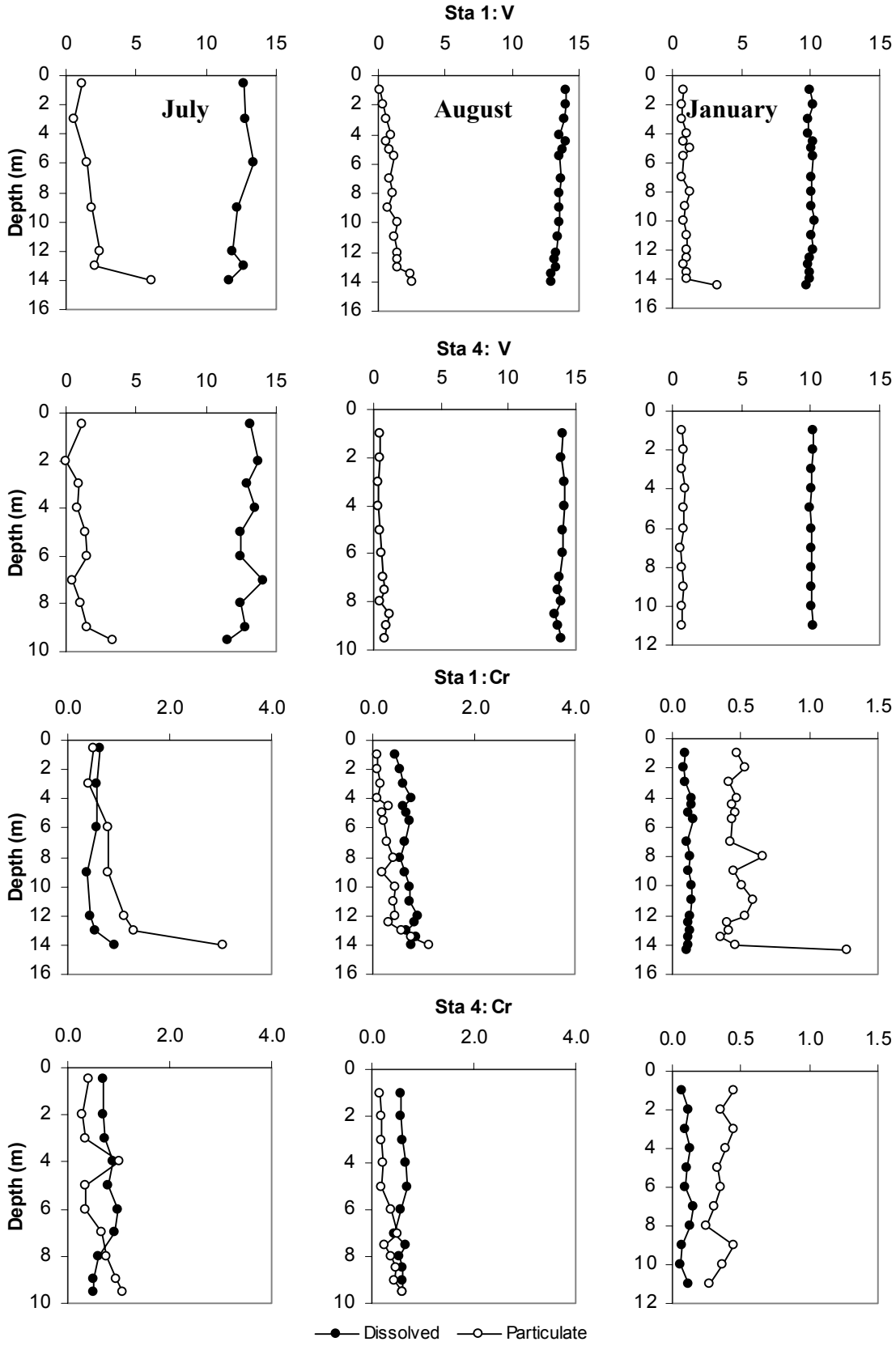

Figure 6. Trace metal profiles for July, August and January at stations 1 and 4.

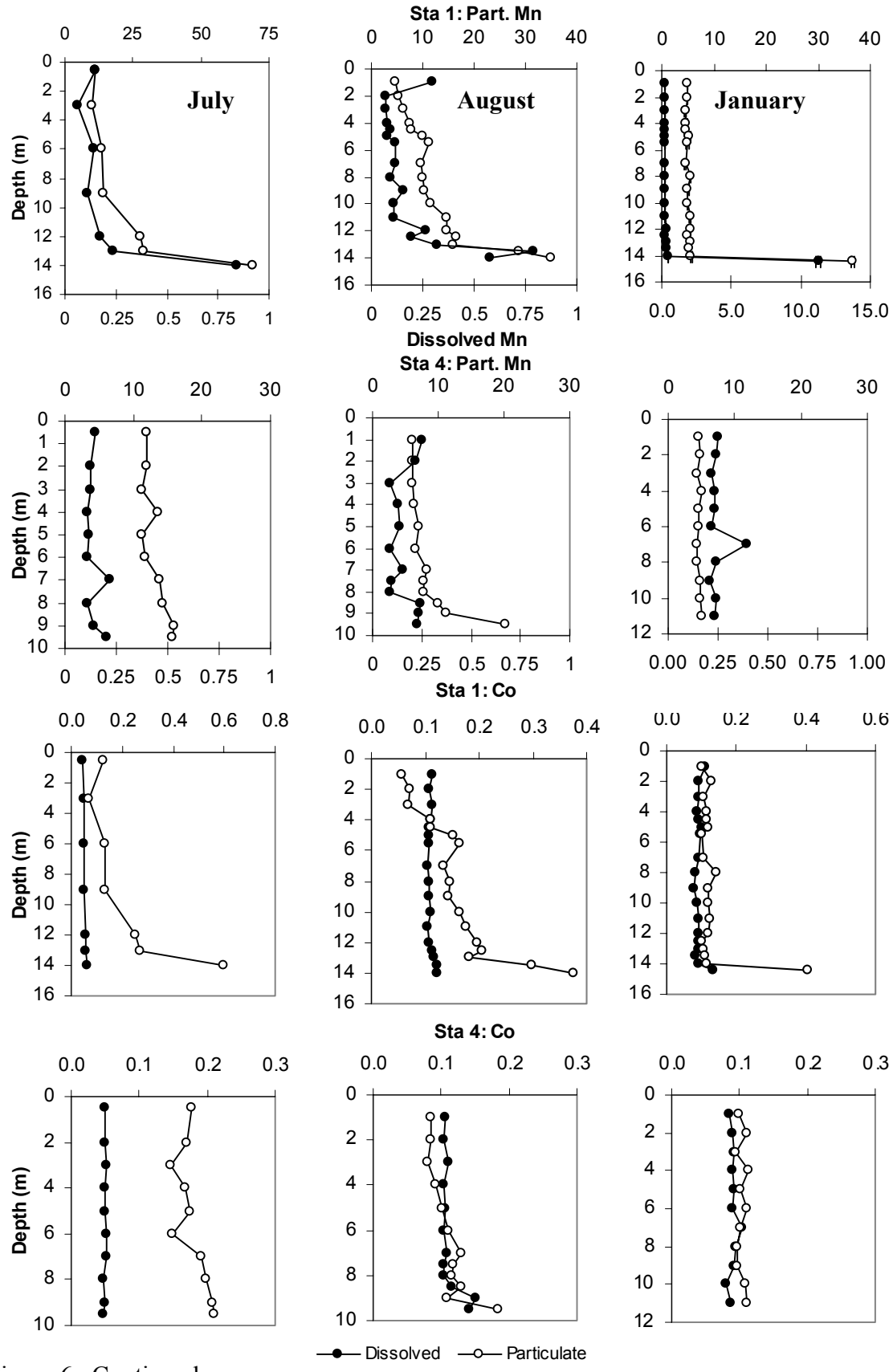

Figure 6. Continued.

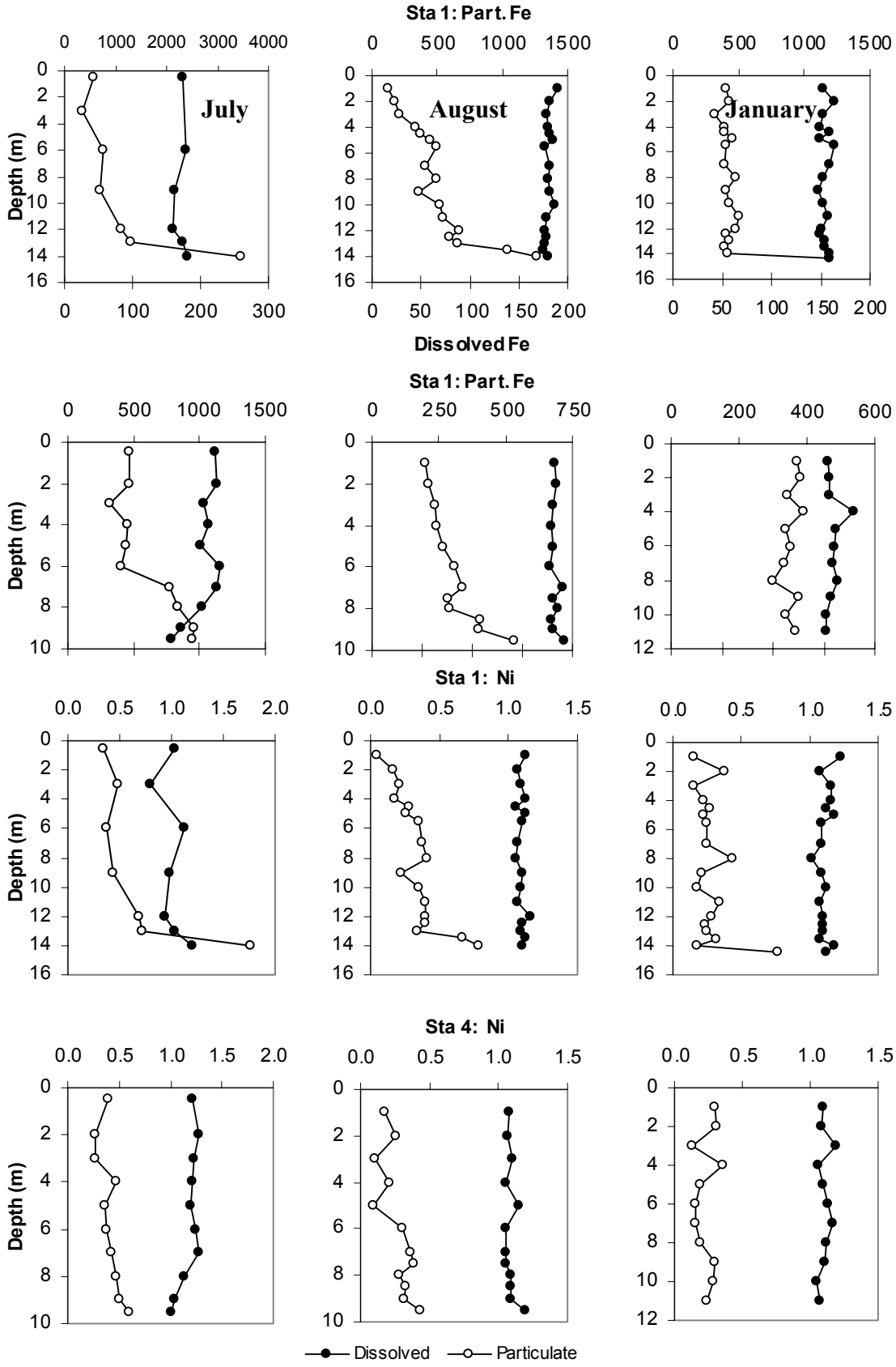

Figure 6. Continued.

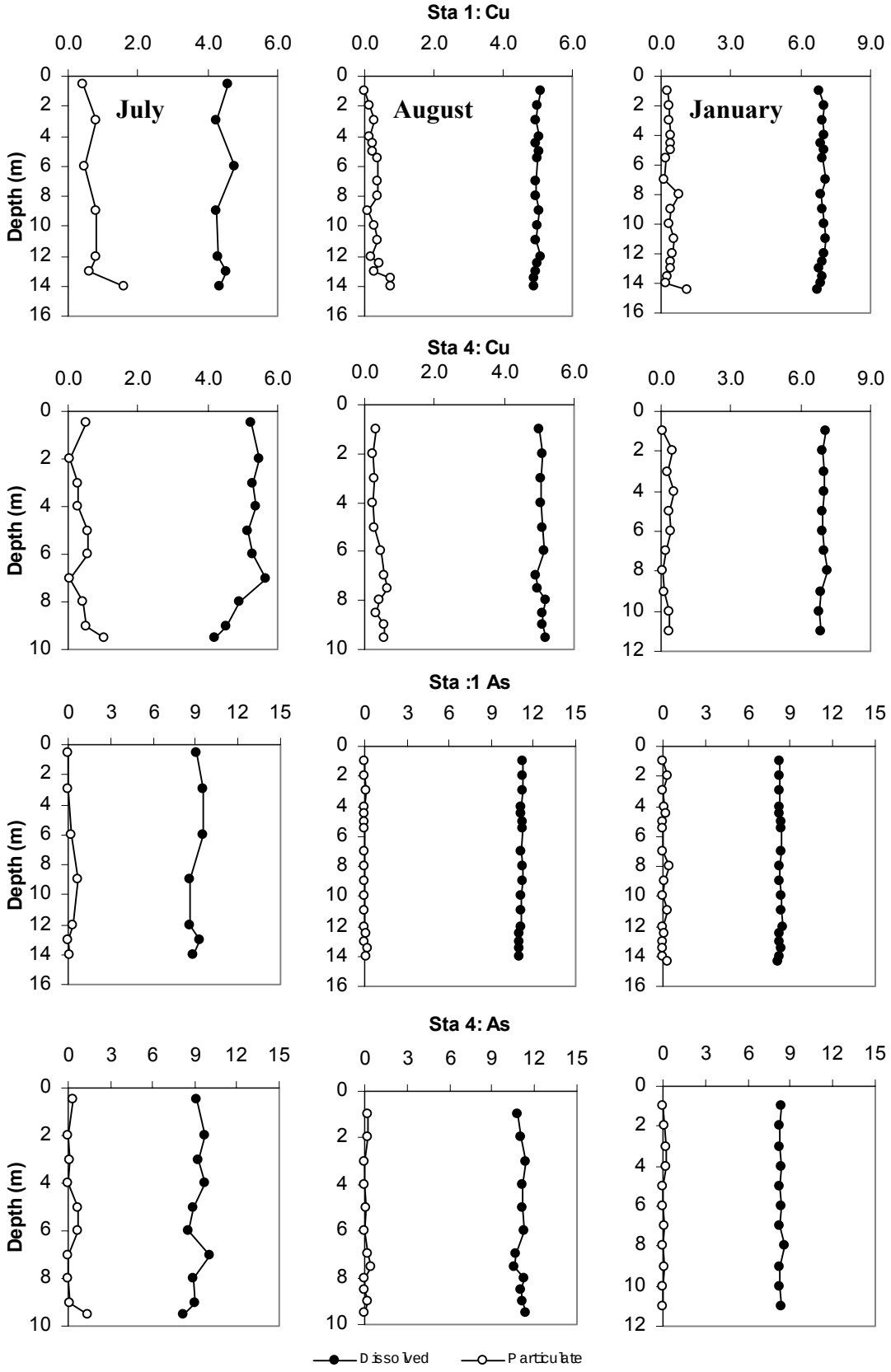

Figure 6. Continued.

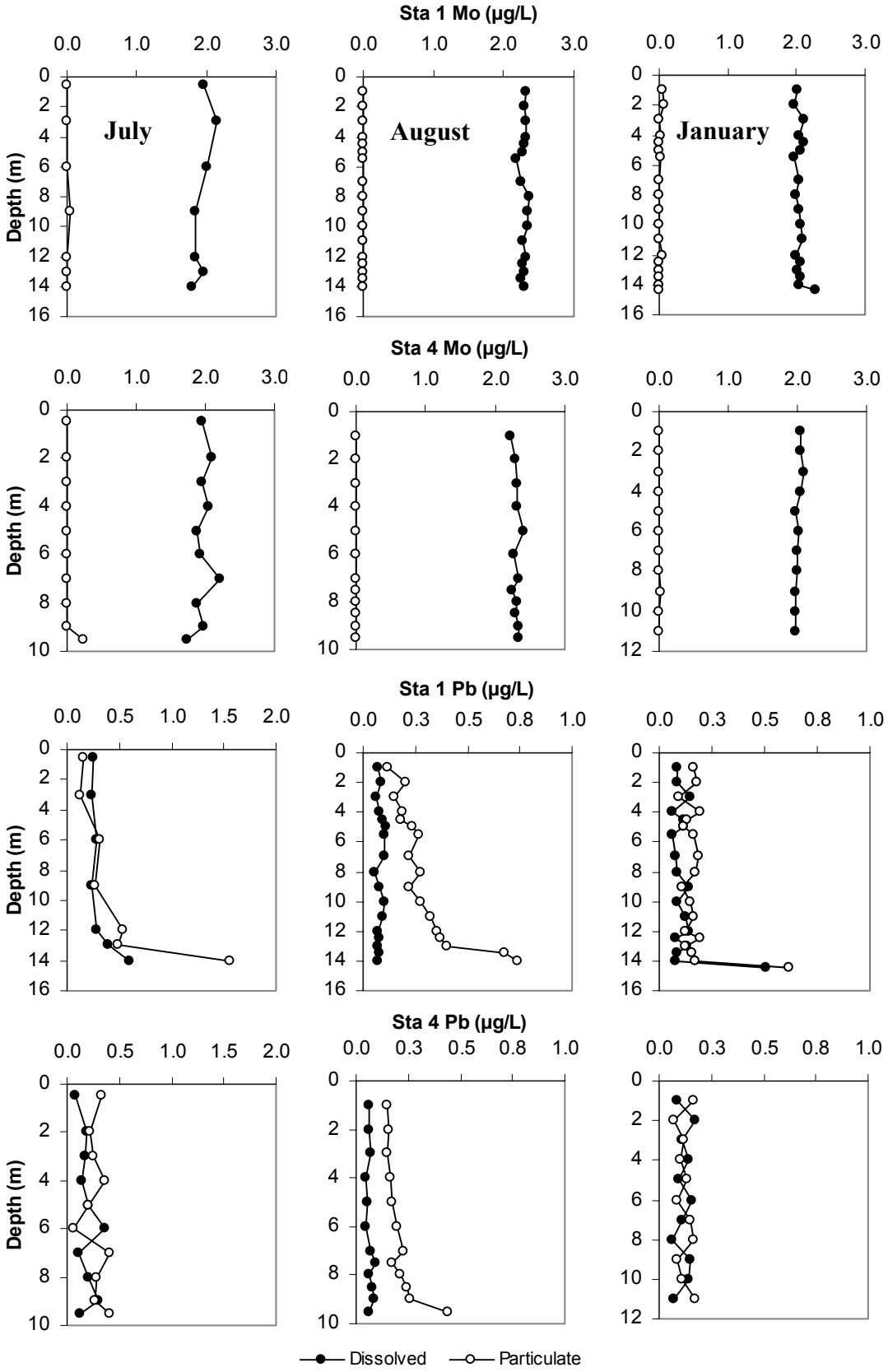

Figure 6. Continued.

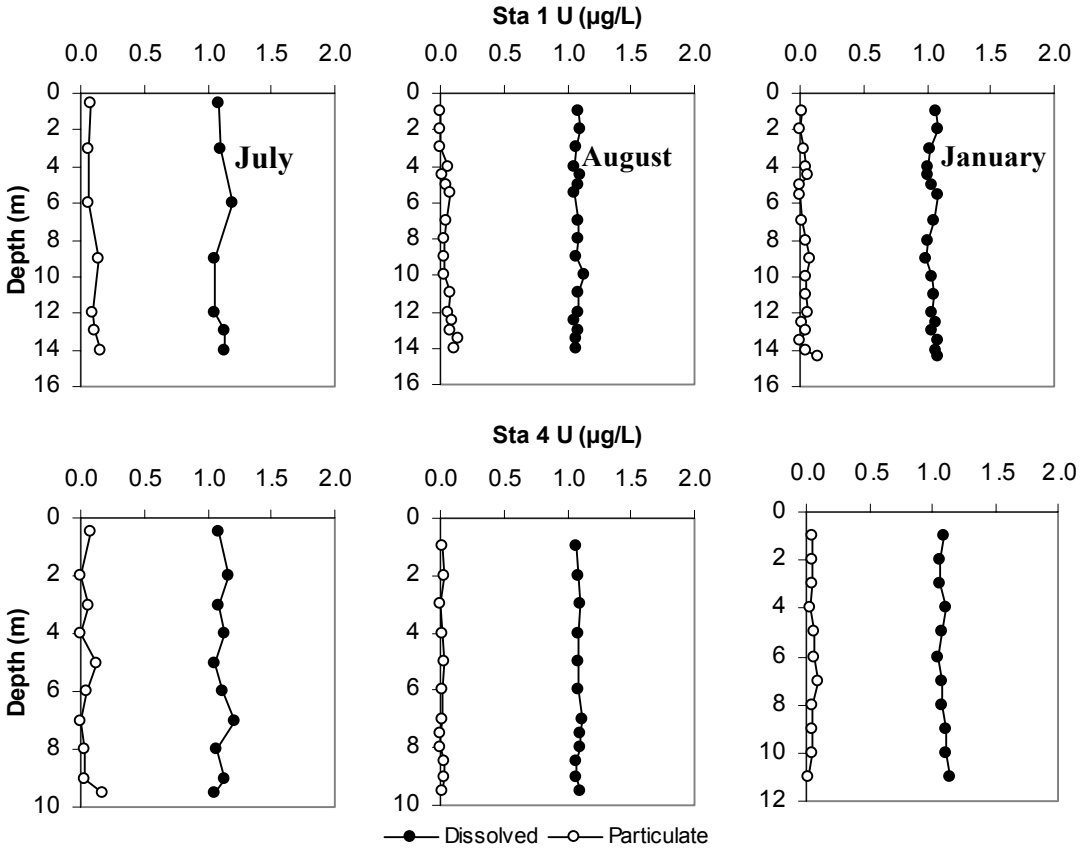

Figure 6. Continued.

In Lake Corpus Christi, the oxidation potential of the water column during both seasons, as inferred from Mn and Fe profiles, does not appear to be sufficiently reducing to catalyze the phase transformation of redox sensitive metals such as U, Mo and As, since they all occur exclusively in the dissolved phase during all sampling periods.

The average epilimnetic metal values show little seasonal variations in concentrations with the exception of higher V and As in the summer and higher Cu in the winter. The summer values for V and As averaged 14 and 11 µg/L, respectively, vs. 10 and 8 µg/L, respectively, during the winter. Value for Cu increased from 5 to 7 µg/L from summer to winter. The noted seasonal cycling of As in Lake Corpus Christi is of particular importance since the levels in the lake are an order of magnitude above reported background levels in uncontaminated lakes ranging from 0.2 µg/L (Salbu and Steinnes, 1995) to 3.75 µg/L (Anderson and Bruland, 1991).

The two stations sampled in the lacustrine zone of Lake Corpus Christi provided

information on the spatial variations in trace metals as a function of depth. On average, the epilimnetic waters show very little spatial variation in metals. The heterogeneity in hypolimnetic DO consistently produced spatial variations of Mn, Fe, V, Cr, Co, Ni and Pb at station 1. In contrast, station 4 profiles show the vertical distribution of trace metals is relatively homogenous, except in August.

Trace metal profiles were also evaluated for responses to an episodic mixing event driven by a substantial inflow of meteoric waters from the Nueces River in June. The DO profiles indicate the near complete oxygenation of the water column. This resulted in the oxidation of Fe and Mn oxy-hydroxides, marked by higher particulate values for these metals in the July sampling. In July, particulate Mn at station 1 ranged between 11.0 - 69.4 μg/L, showing an overall enrichment factor of 1.9 relative to August (4.77 – 34.9 μg/L). Particulate Fe shows a slightly greater enrichment in July (583 – 3476 μg/L) by a factor of 2.3 relative to August (123 – 1260 μg/L). However, the cycling of As is marked by dilution following the inflow event with dissolved values of 9.1 ± 0.94 μg/L compared to August (11.1 ± 0.34 μg/L).

Surface and Ground waters in the Nueces River Basin

The tributaries and ground water samples enhanced the understanding of the distribution of As in the Nueces River basin, since Lake Corpus Christi values are elevated above background. Figure 7 illustrates the distribution of As from the ambient levels in the upper Nueces River basin to the tap water in Corpus Christi. The low concentrations of As in the Frio and Nueces Rivers (upper Nueces River basin), averaging 0.56 μg/L, are characteristic of background surface values. This is in marked contrast to the average 6.0 μg/L measured in the Frio River near Choke Canyon and 6.4 μg/L in the Atascosa River. The distribution of As in the Nueces River also shows a gradient of increasing values toward Lake Corpus Christi ranging from 2.5 μg/L at Holland Dam in La Salle County to 6.17 μg/L at the entrance to the lake.

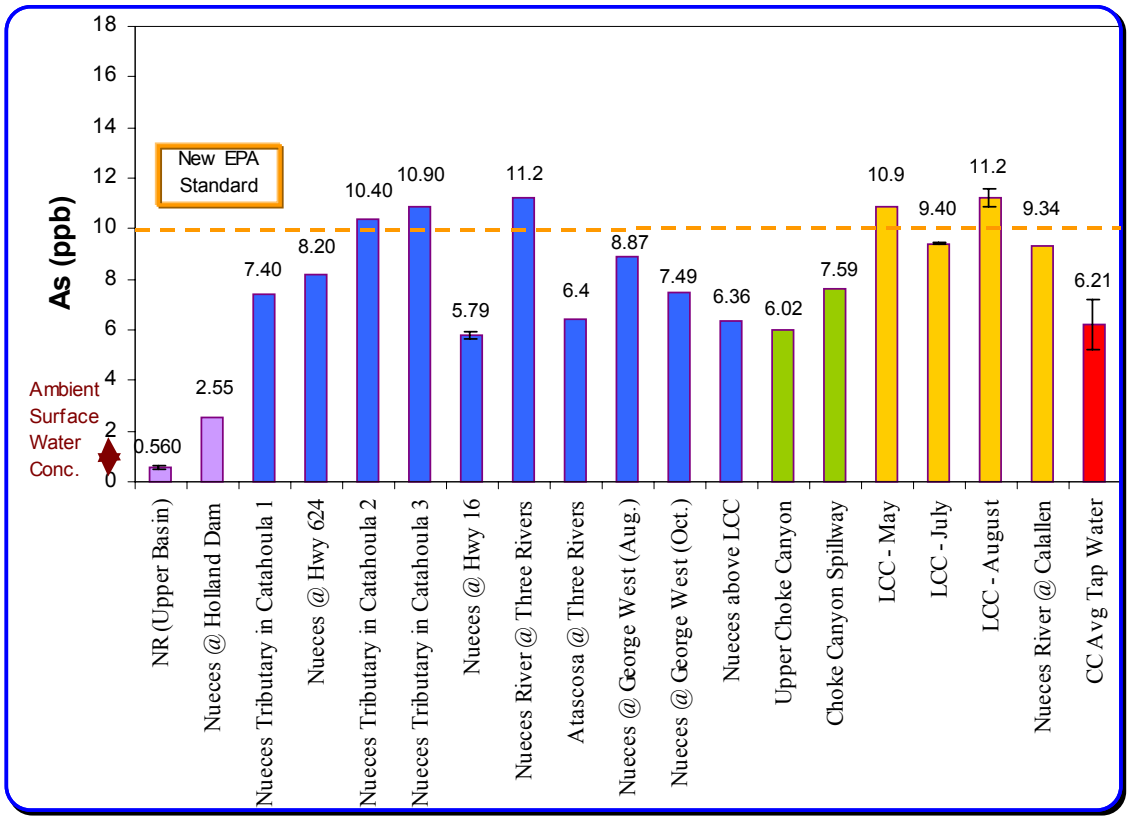

Figure 7. The distribution of arsenic in the Nueces River (NR) basin, including Lake Corpus Christi (LCC). Samples grade from the upper basin (left) to the tap water of the City of Corpus Christi. The dashed line represents the new EPA standard for arsenic in drinking water.

Figure 8 illustrates the distribution of As, U and Mo in the 16 ground waters sampled. The values illustrate the typical heterogeneity of complex ground water systems. Concentrations range from 0.34 – 47 µg/L for U and 0 – 16 µg/L for Mo. The values for As range from ambient levels of around 0.6 µg/L to 24 µg/L, which is more than twice the new EPA arsenic drinking water standard of 10 µg/L (Todd Whitman, 2001).

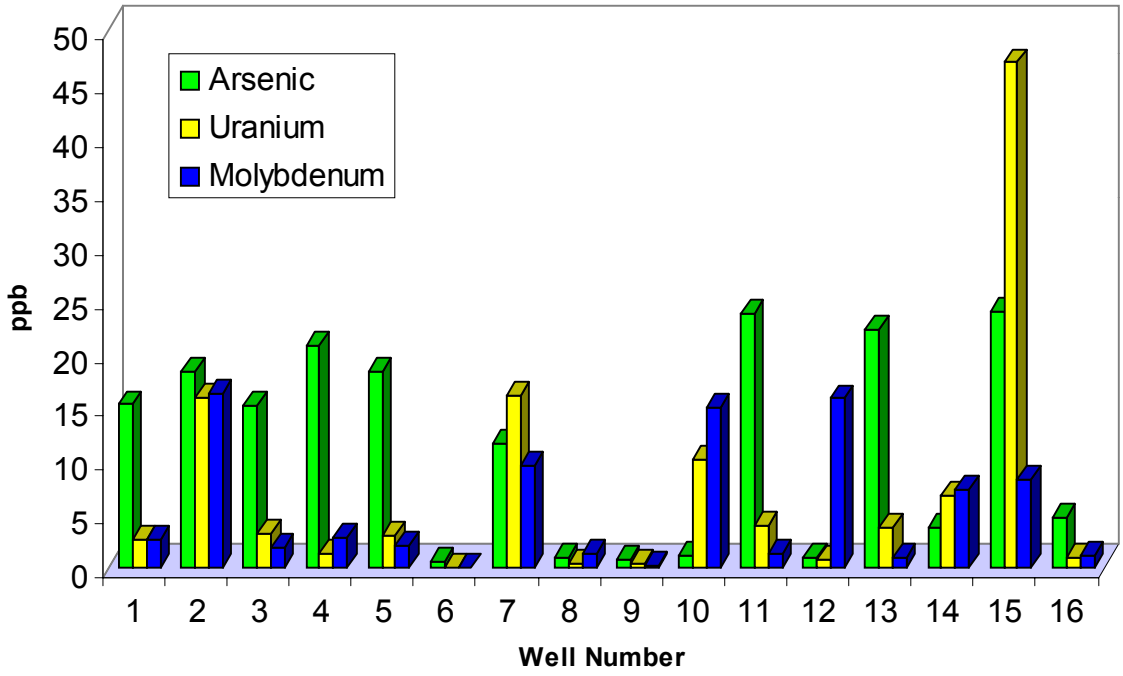

Figure 8. Concentrations of arsenic, uranium and molybdenum in ground water samples.

DISCUSSION

The enrichment and cycling of trace metals in the water column of Lake Corpus Christi due to alterations in redox conditions may have a tremendous influence on water quality. In Lake Corpus Christi, redox driven cycles of trace metals seems to be controlled by variations in dissolved oxygen both temporally and spatially. These oscillations in dissolved oxygen entrain changes in the speciation of Mn and Fe characterized by increasing particulates just above the redox cline and increasing dissolved Mn in the more reducing hypolimnion. These characteristic depth profiles indicate the redox boundary migrates within the water column in the summer creating

partially stratified conditions in the summer and well-mixed conditions in winter and following hydrological mixing events, January and July. As in Kneebone and Hering (2000), the hypolimnetic increases in dissolved Mn at station 1, regardless of hydrologic conditions, suggesting that even during well-mixed conditions the sediments remained reduced. This implies the sediments remain a constant source of reduced Mn (dissolved) diffusing across the sediment-water interface into the hypolimnion. The seasonal and event driven mixing of the water column at station 4, however, suggests the sediments may reverse from a sink to a source for metals in the hypolimnion, degrading water quality as the cycling of Mn and Fe oxy-hydroxides results in the scavenging of trace metals in oxic regimes and the release of associated trace metals in reducing regimes (Balistrieri et al., 1992b; Viollier et al., 1995; Viollier et al., 1997).

Metals enriched in the hypolimnion with Mn and Fe are particulate Cr, V, Co, Ni and Pb. Two processes appear to control the cycling of hypolimnetic metals. The distribution of metals such as Cr may be attributed to changes in speciation driven by redox reactions (Achterberg et al., 1997). While, the enrichment of metals such as V, Co, Ni and Pb may be attributed to scavenging by Mn and Fe oxy-hydroxides (Achterberg et al., 1997; Balistrieri and Murray, 1986; Balistrieri et al., 1992b; Hamilton-Taylor and Davison, 1995; Pohl and Hennings, 1999; Taillefert et al., 2000; Viollier et al., 1995; Viollier et al., 1997). Previous studies have proposed the adsorption of V and Pb are intrinsically linked to the cycling of Fe (Hamilton-Taylor and Davison, 1995; Viollier et al., 1995), whereas Co is linked to Mn (Balistrieri and Murray, 1986; Balistrieri et al., 1992b; Taillefert et al., 2000; Viollier et al., 1995). However, in both Lake Corpus Christi and Lyssy Pond linear regression analysis indicates a much stronger correlation between Pb and Mn (Figure 9) than between Pb and Fe ($r^2 = 0.33$ in Lyssy Pond and 0.865 in Lake Corpus Christi). This is in agreement with (Pohl and Hennings, 1999) who suggest the phase distribution of Pb in the water column is specifically controlled by the cycling of Mn. Many studies document the diagenetic remobilization of Mn (Balistrieri et al., 1992a; Davison and Tipping, 1984; Mayer et al., 1982; Mortimer, 1941; Viollier et al., 1995; Viollier et al., 1997), which inferring from the correlation above, may led to the remobilization of Pb. This directly contradicts the assumption that the high affinity of Pb to particulate matter limits the aquatic residence time of Pb by favoring sedimentation

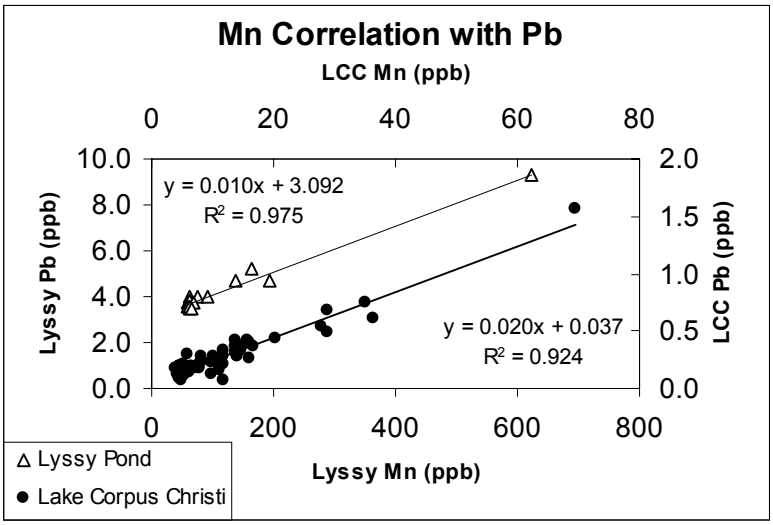

Figure 9. Correlation between Mn and Pb in Lyssy Pond and Lake Corpus Christi.

with minimal diagenetic remobilization (Hites and Eisenreich, 1987).

The profiles show the enrichment of Mn, Fe and Cr and their associated metals (Pb, V, Co and Ni) are inversely proportional to the oxidation potential of the water column. This relationship produces seasonal variations as metals have higher enrichment factors in summer when oxidation potentials are lower. In fact, the enrichment factors measured in August may be underestimates of summer conditions as the water column was completely oxygenated just prior to sampling. The relatively high values for particulate Mn and Fe in July substantiate enrichment of the hypolimnion with respect to these metals prior to the inflow event. This relationship also provides an explanation for the spatial variations between the hypolimnion of the two stations, as the sediments at station 1 remain reducing resulting in greater hypolimnetic enrichment of metals.

Although both stations were in the lacustrine zone near the dam, dissolved oxygen measurements indicate only slightly reducing conditions corroborated by the phase distribution of Mn and Fe. The relatively shallow depths and large fetch of the lake may drive episodic and seasonal hypolimnetic mixing (Thornton et al., 1990). Although true equilibrium in trace metal cycling is rarely achieved in reservoirs, the dynamic nature of Lake Corpus Christi may even prevent the achievement of steady state (Manahan, 2000). This might explain why U, Mo and As occur entirely in the dissolved phase and only U values in Lyssy Pond, under suboxic conditions, indicate phase transformation.

Arsenic

The occurrence of As in the waters of Lake Corpus Christi is elevated above ambient levels (0.5- 1 μg/L (National Academy of Sciences, 1997) by almost an order of magnitude and occurs entirely in the dissolved phase both seasonally and even under mildly reducing conditions. This stability may be attributed to the lack of strongly reducing conditions since profiles of Lyssy Pond similarly reported no As cycling. Additionally, the high pH values, of ~ 8.5, in the lake further contributes to the redox stability of the more soluble As (V) even under moderately reducing conditions, while decreasing adsorption affinity to mineral surfaces (Levy et al., 1999). Furthermore, the relative depletion of Fe in this system (Brandenberger et al., in preparation) suggests a strong lack of preferential adsorption of As onto Fe oxy-hydroxides (Aurillo et al., 1994; Belzile and Tessier, 1990; Crecelius, 1975).

This conservative behavior of As allows for dilution during periods of higher inflow resulting from events (July) or seasonal variations marked by higher inflows into Lake Corpus Christi. Additionally, the substantial evaporative losses and minimal inflows to the lake lead to evapoconcentration of As in the summer (La Force et al., 2000; Levy et al., 1999; McLaren and Kim, 1995; Michel et al., 1999; Riedel et al., 2000; Welch and Lico, 1998). The conservative behavior resulting in temporal enrichment of As up to 12 μg/L contributes to the degradation of water quality in Lake Corpus Christi reservoir and ultimately the drinking water it provides, as only a small percentage of As is removed during standard water treatment. This data is particularly timely, as the USEPA finally adopted the new arsenic in drinking water standard of 10 μg/L (Todd Whitman, 2001). The new standard is in agreement with World Health Organization standards and was guided by studies (National Academy of Sciences, 1999) indicating the old standard of 50 μg/L was not sufficiently low enough to protect human health. According to USEPA, arsenic is the only known substance for which there is adequate evidence of carcinogenic risk by both inhalation and ingestion routes of exposure (U. S. Environmental Protection Agency, 1998) and for which exposure through drinking water has been clearly demonstrated to cause skin, bladder, lung and prostate cancer in humans (Christen, 1999; Morales et al., 2000; National Academy of Sciences, 1999). Tap water for the City of Corpus Christi in August averaged 6.2 μg/L, which is below the standard. The dilution

relative to the lake values in August, averaging 12 μg/L, may be attributed to the blending of Lake Corpus Christi waters with Lake Texana waters from the Mary Rhodes Pipeline prior to incorporation into the public water supply system. However, this is not an option for several small communities using Lake Corpus Christi as the sole source for freshwater and may result in arsenic concentrations above the new drinking water standard.

Arsenic – Basin Review

The distribution of As in the Nueces River basin provides information on potential sources. Values for As in the basin range from the ambient levels reported in the upper basin (0.5 μg/L) to values in Nueces Bay of > 10 μg/L (Fisher, 1996). Even the urbanized areas around San Antonio, subject to anthropogenic contamination, only reported values around 2 μg/L As (Bush et al., 2000). In addition, values along the Nueces River increase considerably downstream of Holland Dam. This suggests the sources for As occurs within the basin itself. Compiling arsenic concentrations from National Uranium Resource Evaluation (NURE), Texas Water Development Board (TWDB) and National Water Information System (NWIS) into a GIS database provides an unambiguous assumption that the dominant sources for As in the Nueces River basin are the formations enriched in uranium ore, such as the Catahoula and the Oakville Formations (Parker et al., 2001). Therefore, the significant increase in As in the Nueces River downstream of Holland Dam results from the meander of the river across these formations. The values in the Nueces River basin are in direct contrast with the neighboring San Antonio basin, similarly impacted by uranium mining and potentially to a greater extent, as Karnes County is the origin of uranium mining and now hosts the UMTRA project. Arsenic levels in the San Antonio and San Marcos Rivers average 2.98 ± 0.9 μg/L.

Evaluating the basin data using ratios of As to Mo and U, all enriched in uranium ore deposits, identifies areas of selective enrichment of As by creating unique signatures for identifying potential sources of waters. Figure 10 illustrates the signatures of different water sources such as the three sampling events in Lake Corpus Christi, the upper basin, uranium mine drainages, and ground waters. The ratio signatures identify the selective

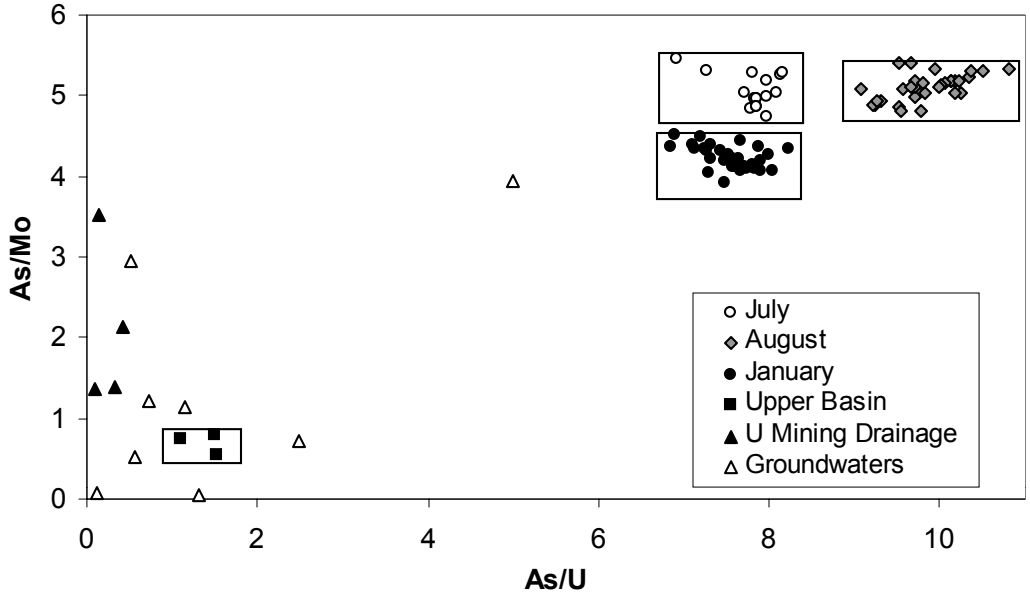

Figure 10. Ratios of As to U and Mo showing signatures of the three sampling events in Lake Corpus Christi, the upper Nueces River basin, uranium mining and ground waters.

enrichment of As during periods of evaporative concentration in August relative to January and the selective dilution of As in July. In comparison, the ratio signatures in the upper basin confirm its relative isolation from uranium mining, and provide the signatures expected in systems un-impacted by uranium deposits. However, surface water drainages near uranium mines indicate selective enrichment of U relative to As and As relative to Mo, subsequently altering the ratio signatures. In comparison, ratios for the Lyssy Pond profile are not shown as they overlap Lake Corpus Christi water profiles, but the signatures within the depth profile are distributed between July and January signatures as a function of the distribution of Mo in the water column.

Ground Waters

The extreme heterogeneity of As, Mo and U in ground waters suggests a mechanism for sequestration, such as sulfidization upon contact with water discharging along faults in Live Oak County enriched in H_2S (Henry et al., 1982). The concentrations of selected ground waters are elevated above the new drinking water standard. An emphasis was placed on As because elevated levels are seen in the surface waters as well as ground

waters. However, the ground water samples provide the first indication of enrichment in U and Mo in the Nueces River basin. The occurrence of U (48 μg/L) above the drinking water standard of 30 μg/L is significant, not only as a health concern for U, but also suggest the potential for elevated levels of the U daughter products, radium and radon. The ratios of As, U and Mo in ground waters reveal a scattering of signatures suggesting As is not selectively enriched. This results from the non-conservative behavior of these redox sensitive trace metals in ground waters produced by the removal of evapoconcentration and dilution as factors potentially influencing the selective enrichment of arsenic. Therefore, significant investigations are required to further understand the distribution of As, U and Mo in the ground waters of the lower Nueces River basin.

LITERATURE CITED

Achterberg, E.P., Van den Berg, C.M.G., Boussemart, M. and Davison, W., 1997. Speciation and cycling of trace metals in Esthwaite Water: A productive English lake with seasonal deep-water anoxia. Geochimica et Cosmochimica Acta, 61(24): 5233-5253.

Anderson, L.C.D. and Bruland, K.W., 1991. Biogeochemistry of arsenic in natural waters: The importance of methylated species. Environ. Sci. Technol., 25: 420-427.

Aurillo, A.C., Mason, R.P. and Hemond, H.F., 1994. Speciation and fate of arsenic in three lakes of the Aberjona watershed. Environ. Sci. Technol., 28: 577-585.

Baird, C.M., Jennings, M., Ockerman, D. and Dybala, T., 1996. Characterization of Nonpoint Sources and Loadings to the Corpus Christi Bay National Estuary Program Study Area., Corpus Christi Bay National Estuary Program.

Balistrieri, L.S. and Murray, J.W., 1986. The surface chemistry of sediments from the Panama Basin: the influence of Mn oxides on metal adsorption. Geochim. Cosmochim. Acta, 50: 2235-2243.

Balistrieri, L.S., Murray, J.W. and Paul, B., 1992a. The cycling of iron and manganese in the water column of Lake Sammamish, Washington. Limnol. Oceanogr., 37(3): 510-528.

Balistrieri, L.S., Murray, J.W. and Paul, B., 1992b. The Biogeochemical Cycling of Trace Metals in the Water Column of Lake Sammamish, Washington: Response to Seasonally Anoxic Conditions. Limnology Oceanography, 37(3): 529-548.

Balogh, S.J., Engstrom, D.R., Almendinger, J.E., Meyer, M.L. and Johnson, K.D., 1999. History of mercury loading in the upper Mississippi River reconstructed from the sediments of Lake Pepin. Environ. Sci. Technol., 33: 3297-3302.

Baskaran, M. and Santschi, P., 1993. The role of particles and colloids in the transport of radionuclides in coastal environments of Texas. Mar. Chem., 43: 95-114.

Batson, V.L., Bertsch, P.M. and Herbert, B.E., 1996. Transport of Anthropogenic Uranium from Sediments to Surface Waters During Episodic Storm Events. J. Environ. Qual., 25: 1129-1137.

Belzile, N. and Tessier, A., 1990. Interactions between arsenic and iron oxyhydroxides in lacustrine sediments. Geochimica et Cosmochimica Acta, 54: 103-109.

Benoit, G. et al., 1994. Partitioning of Cu, Pb, Ag, Zn, Fe, Al, and Mn between filter-retained particles, colloids and solution in six Texas estuaries. Mar. Chem., 45: 307-336.

Blount, J.G., Kreitler, C.W. and Dickerson, P.W., 1992. Geological and Geochemical Controls on Contamination from Uranium Mill Tailings at the Falls City UMTRA Site in South Texas. v. 24, Geological Society of America.

Brandenberger, J.M., Louchouarn, P., Herbert, B.E. and Parker, R., in preparation. Geochemical Cycling of Trace Metals in Lake Corpus Christi Reservoir, TX - Implications to Historic Water Quality using Age Dated Sediment Cores.

Bryson, H.C., Bostick, K. and Longmire, P., 1988. Hydrogeologic and Geochemical Aspects of Contaminant Transport at the Falls City Texas UMTRA Site, FOCUS Conference of Southwestern Ground Water Issues, pp. 559-577.

Bush, P.W. et al., 2000. Water Quality in South-Central Texas, Texas, 1996-1998. Circular 1212, United States Geological Survey, Denver.

Christen, K., 1999. Arsenic standard for drinking water too high, NRC says. Environmental Science and Technology, 33: 188.

Crecelius, E.A., 1975. The geochemical cyle of arsenic in Lake Washington and its relation to other elements. Limnol. Oceanography, 20: 441-451.

Cunningham, A.M., 1998. Corpus Christi Water Supply Documented History 1852-1997. Quality Bindery, Inc., San Antonio, 588 pp.

Davison, W. and Tipping, E., 1984. Treading in Mortimer's footsteps: The geochemical cycling of iron and manganese in Esthwaite Water. 52, Freshwater Biol. Assoc.

Eargle, D.H., Hinds, G.W. and Weeks, A.M.D., 1971. Uranium Geology and Mines, South Texas., Bureau of Economic Geology, University of Texas at Austin, Austin, TX.

Elbaz-Poulichet, F., Nagy, A. and Cserny, T., 1997. The Distribution of Redox Sensitive Elements (U, As, Sb, V, and Mo) along a River-WetlandLake System (Balaton Region, Hungary). Aquatic Geochemistry, 3: 267-282.

Erickson, B.E. and Helz, G.R., 2000. Molybenum (VI) speciation in sulfidic waters: Stability and lability of thiomolybdates. Geochimica et Cosmochimica Acta, 64: 1149-1158.

Finch, W.I., 1996. Uranium Provinces of North America--Their Definition, Distribution and Models, U.S. Geological Survey.

Fisher, N.M., 1996. 1996 Regional Assessment of Water Quality in the Nueces Coastal Basins, Texas Natural Resources Conservation Commission, Corpus Christi, TX.

Focazio, M.J., Welch, A.H., Watkins, S.A., Helsel, D.R. and Horn, M.A., 2000. A Retrospective Analysis on the Occurence of Arsenic in Ground-Water Resources of the United States and Limitations in Drinking-Water-Supply Characterizations. 99-4279, United States Geological Survey, Reston.

Forstner, U. and Wittmann, G.T.W., 1979. Metal Pollution in the Aquatic Environment. Springer-Verlag, New York, 289 pp.

Galloway, W.E., 1977. Catahoula Formation of the Texas Coastal Plain: Depositional Systems, Composition, Structural Development, Ground-water Flow History, and Uranium Distribution. 87, Buraeu of Economic Geology, Austin.

Galloway, W.E., Henry, C.D. and Smith, G.E., 1982. Depositional Framework, Hydrostratigraphy, and Uranium Mineralization of the Oakville Sandstone (Miocene), Texas Coastal Plain. 113, Bureau of Economic Geology, Austin.

Galloway, W.E. and Kaiser, W.R., 1980. Catahoula Formation of the Texas Coastal Plain: Origin, Geochemical Evolution, and Characteristics of Uranium Deposits. 100, Bureau of Economic Geology, Austin.

Greenamoyer, J.M. and Moran, S.B., 1997. Invesigation of Cd, Cu, Ni and Th-234 in the colloidal size range in the Gulf of Maine. Mar. Chem., 57: 217-226.

Hamilton-Taylor, J. and Davison, W., 1995. Redox-driven cycling of trace elements in lakes. In: A. Lerman and e. al. (Editors), Physics and Chemistry of Lakes. Springer Verlag., pp. 217-236.

Harrington, J.M., Laforce, M.J., Rember, W.C., Fendorf, S.E. and Rosenweig, R.F., 1998. Phase associations and mobilization of iron and trace elements in Coeur d'Alene Lake, Idaho. Environ. Sci. Technol., 32: 650-656.

Hemond, H.F. and Fechner-Levy, E.J., 2000. Chemical Fate and Transport in the Environment. Academic Press, San Diego, 433 pp.

Henry, C.D. et al., 1982. Geochemistry of ground water in the Miocene Oakville Sandstone - A major aquifer and uranium host of the Texas Coastal Plain. 118, Bureau of Economic Geology, Austin.

Henry, C.D. and Kapadia, R.R., 1980. Trace Elements in Soils of the South Texas Uranium District: Concentrations, Origin, and Environmental Significance. 101, Bureau of Econcomic Geology, Austin, TX.

Hites, R.A. and Eisenreich, S.J. (Editors), 1987. Sources and Fates of Aquatic Pollutants. Advannces in Chemistry, 216. American Chemical Society, Washington, 391 pp.
Hoffman, M.R., Yost, E.C., Eisenreich, S.J. and Maler, W.J., 1981. Characterization of soluble and colloidal-phase metal complexes in river water by ultrafiltration. A mass-balance approach. Environ. Sci. Technol., 15: 655-661.
Kneebone, P.E. and Hering, J.G., 2000. Behavior of arsenic and other redox-sensitive elements in Crowley Lake, CA: A reservoir in the Los Angeles Aqueduct System. Environ. Sci. Technol., 34: 4307-4312.
Kufus, M., 2000. Water Futures. Texas Parks and Wildlife, 58(8): 11-12.
La Force, M.J., Hansel, C.M. and Fendorf, S., 2000. Arsenic speciation, seasonal transformations, and co-distribution with iron in a mine waste-influenced palustrine emergent wetland. Environmental Science and Technology, 34(18): 3937-3943.
Langedal, M., 1997. Dispersion of tailings in the Knabeana-Kvina drainage basin, Norwr, 2: Mobility of Cu and Mo in tailings-derived fluvial sediments. Journal of Geochemical Exploration, 58: 173-183.
Langmuir, D., 1997. Aqueous Environmental Geochemistry. Prentice-Hall, Inc., Upper Saddle River, NJ, 600 pp.
Ledger, E.B., 1981. Evaluation of the Catahoula Formation as a Source Rock for Uranium Mineralization, with Emphasis on East Texas. Ph. D. Dissertation Thesis, Texas A&M University, College Station, TX, 249 pp.
Levy, D.B., Schramke, J.A., Esposito, K.J., Erickson, T.A. and Moore, J.C., 1999. The shallow ground water chemistry of arsenic, fluorine, and major elements: Eastern Owens Lake, California. Applied Geochemistry, 14: 53-65.
Louchouarn, P. and Lucotte, M., 1998. A historical reconstruction of organic and inorganic contamination events in the Saguenay/St-Lawrence system from preindustrial times to the present. The Science of the Total Environment, 213: 139-150.
Louchouarn, P., Lucotte, M., Mucci, A. and Pichet, P., 1993. Geochemistry of mercury in two hydroelectric reservoirs of Quebec, Canada. Canadian Journal of Fisheries and Aquatic Sciences, 50: 269-281.
Macdonald, R.W., Macdonald, D.M., O'Brien, M.C. and Gobeil, C., 1991. Accumulation of heavy metals (PB, Zn, Cu, Cd), carbon and nitrogen in sediments from Strait of Georgia, B. C., Canada. Marine Chemistry, 34: 109-135.
Manahan, S.E., 2000. Environmental Chemistry. Lewis Publishers, Boca Raton, 898 pp.
Martin, J., Dai, M.-H. and Cauwet, G., 1995. Significance of colloids in the biogeochemical cycling of organic carbon and trace metals in the Venice Lagoon (Italy). Limnol. Oceanogr., 40: 119-131.
Mayer, L.M., Liotta, F.P. and Norton, S.A., 1982. Hypolimnetic redox and phophorus cycling in hypereutrophic Lake Sebasticook, Maine. Water Resources, 16: 1189-1196.
McLaren, S. and Kim, N.D., 1995. Evidence for a seasonal fluctuation of arsenic in New Zealand's longest river and the effect of treatment on concentrations in drinking water. Environmental Pollution, 90: 67-73.
Menounou, N. and Presley, B.J., 1996. Mercury in sediment cores from central Texas Lakes, 28th Annual Meeting. Geological Society of America, p. 32.
Michel, P., Chiffoleau, J.F., Averty, B., Auger, D. and Chartier, E., 1999. High resolution profiles for arsenic in the Seine Estuary. Seasonal variations and net fluxes to the English Channel. Continental Shelf Research, 19: 2041-2061.
Morales, K.H., Ryan, L., Kuo, T.L., Wu, M.M. and Chen, C.J., 2000. Risk of internal cancers from arsenic in drinking water. Environ. Health Perspectives, 108(7): 655-661.
Morfett, K., Davison, W. and Hamilton-Taylor, J., 1988. Trace metal dynamics in a seasonally anoxic lake. Environ. Geol. Water Sci., 11: 107-114.
Mortimer, C.H., 1941. The exchange of dissolved substances between mud and water in lakes. J. Ecol., 29: 280-329.
Murray, J.W., 1987. Mechanisms controlling the distribution of trace elements in oceans and lakes. In: R.A. Hites and S.J. Eisenreich (Editors), Sources and Fates of Aquatic Pollutants. American Chemical Society, pp. 153-184.
National Academy of Sciences (Editor), 1997. Arsenic: Medical and Biological Effects of Environmental Pollutants. National Academy of Sciences, Washington, 332 pp.
National Academy of Sciences, 1999. Arsenic in Drinking Water, National Academy of Sciences Press.

Neff, J.M., 1984. Bioaccumulation of organic micropollutants from sediments and suspended particulates by aquatic animals, *Fresenius Z.* Analytical Chemistry, 319: 132-136.
Nueces River Authority, 2001. Basin Highlights Report for the Nueces River Basin and the San Antonio-Nueces and Nueces-Rio Grande Coastal Basins, Nueces River Authority, Corpus Christi, TX.
Nugent, J.E., Nabers, M.S. and Williamson, B., 1994. South Texas Uranium District Abandoned Mine Land Inventory., Railroad Commission of Texas, Austin.
Odhiambo, B.K., Macdonald, R.W., O'Brien, M.C., Harper, J.R. and Yunker, M.B., 1996. Transport and fate of mine tailings in a coastal fjord of British Columbia as inferred from sediment record. The Science of the Total Environment, 191: 77-94.
Parker, R., Herbert, B.E., Brandenberger, J.M. and Louchouarn, P., 2001. Ground water discharge from mid-tertiary rhyolitic ash-rich sediments as the source of elevated arsenic in south Texas surface waters., Geological Society of America, Boston, MA, pp. 2.
Parker, R.L., Herbert, B.E., Tissot, P.E. and Ussery, G., 1999. Gamma Spectroscopy of Livestock Pond Sediments from the Fall City, Texas, UMTRA Site: Scrutiny of DOE Contamination Classification, 1999 Annual Meeting of the Geological Society of America, Denver, Colorado.
Pohl, C. and Hennings, U., 1999. The effect of redox processes on the partitioning of Cd, Pb, Cu, and Mn between dissolved and particulate phases in the Baltic Sea. Marine Chemistry, 65: 41-53.
Riedel, G.F., Williams, S.A., Riedel, G.S., Gilmour, C.C. and Sanders, J.G., 2000. Temporal and spatial patterns of trace elements in the Patuxent River: A whole watershed approach. Estuaries, 23: 521-535.
Roulet, M. et al., 2000. Increases in mercury contamination recorded in lacustrine sediments following deforestation in Central Amazon. Chemical Geology, 165: 243-266.
Ruttenber, A.J., Kreiss, K., Douglas, R.L., Buhl, T.E. and Millard, J., 1984. The assessment of human exposure to radionuclides from uranium mill tailings release and mine dewatering effluent. Health Physics, 47: 21-35.
Salbu, B. and Steinnes, E. (Editors), 1995. Trace Elements in Natural Waters. CRC Press, Boca Raton, 302 pp.
Santschi, P. et al., 1999. Sediment transport and Hg recovery in Lavaca Bay, as evaluated from radionuclide and Hg distribution. Environ. Sci. Technol., 33: 378-391.
Sharma, V. et al., 1999a. Metals in sediments of Texas estuaries, USA. J. Environ. Sci. and Health, A34: 2061-2073.
Sigg, L., Sturm, M. and Kistler, D., 1987. Vertical transport of heavy metals by settling particles in Lake Zurich. Limnology & Oceanography, 32(1): 112.
Taillefert, M., Lienemann, C.-P., Gaillard, F.-F. and Perret, D., 2000. Speciation, reactivity, and cycling of Fe and Pb in a meromictic lake. Geochimica et Cosmochimica Acta, 64: 169-183.
Thornton, K., Kimmel, B.L. and Payne, F.E. (Editors), 1990. Reservoir Limnology: Ecological Perspectives. John Wiley & Sons, New York, 246 pp.
Todd Whitman, C., 2001. Letter from EPA Administrator Christie Whitman to Veterans Affairs, Housing and Urban Development and Independent Agencies Conferees on the New Rule for Arsenic in Drinking Water, U.S. Environmental Protection Agency, Washington.
U. S. Department of Energy, 1991. Environmental Analysis and Data Report Prepared for the Environmental Assessment of Remedial Action at the Inactive Uranium Mill Tailings Site Near Falls City, Texas. DOE/UMTRA-150320-EADR, U. S. Department of Energy, Washington, DC.
U. S. Department of Energy, 1995. Baseline Risk Assessment of Ground Water Contamination at the Uranium Mill Tailings Site near Falls City, Texas. DOE/EIA/62350-64, U. S. Department of Energy, Albuquerque, New Mexico.
U. S. Department of Energy, 1996. Final programmatic environmental impact statement for the uranium mill tailings remedial action ground water project: Volume I. DOE/EIA-0198, U. S. Department of Energy, Albuquerque, New Mexico.
U. S. Environmental Protection Agency, 1996a. Method 1638: Determination of Trace Elements in Ambient Waters by Inductively Coupled Plasma - Mass Spectrometry, Office of Water Engineering and Analysis Division, Washington, D.C.
U. S. Environmental Protection Agency, 1996b. Method 1640: Determination of Trace Elements in Ambient Waters by On-Line Chelation Preconcentration and Inductively Coupled Plasma-Mass Spectrometry, Office of Water Engineering and Analysis Division, Washington, D.C.

U. S. Environmental Protection Agency, 1996c. Method 1669: Sampling Ambient Water for Determination of Metals at EPA Water Quality Criteria Levels, Office of Water Engineering and Analysis Division, Washington, D.C.

U. S. Environmental Protection Agency, 1998. Research plan for arsenic in drinking water., U. S. Environmental Protection Agency, National Center for Environmental Assessment, Cincinnati, OH.

U. S. Environmental Protection Agency, 1999a. Ecological conditions of estuaries in the Gulf of Mexico., U.S. Environmental Protection Agency, Office of Research and Development, National Health and Environmental Effects Research Laboratory, Gulf Ecology Division, Gulf Breeze, Florida.

U. S. Environmental Protection Agency, 1999b. Index of Watershed Indicators. Department of Water.

van der Weijden, C.H. et al., 1990. Profiles of the redox sensitive trace elements As, Sb, V, Mo and U in the Tyro and Bannock basins, East Mediterranean. Mar. Chem., 31: 171-186.

Van Metre, P.C., Wirt, L., Lopes, T.J. and Ferguson, S.A., 1997c. Effects of Uranium-Mining Releases on Ground-Water Quality in the Puerco River Basin, Arizona and New Mexico. Water Supply Paper 2476, United States Geological Survey.

Viollier, E. et al., 1995. Geochemical study of a crater lake (Pavin Lake, France): Trace-element behaviour in the monimolimnion. Chem. Geol., 125: 61-72.

Viollier, E., Michard, G., Jezequel, D., Pepe, M. and Sarazin, G., 1997. Geochemical study of a crater lake: Lake Pavin, Puy de Dome, France. Contrants afforded by the particulate matter distribution in the element cycling within the lake. Chem. Geol., 142: 225-241.

Welch, A.H. and Lico, M.S., 1998. Factors controlling As and U in shallow ground water, southern Carson Desert, Nevada. Applied Geochemistry, 13: 521-539.

Wen, L.-S., Santschi, P., Gill, G. and Paternostro, C., 1999. Estuarine trace metal distributions in Galveston Bay: Importance of colloidal forms in the speciation of the dissolved phase. Mar. Chem., 63: 185-212.

Plankton succession: Investigations regarding new approaches to management

Basic Information

Title:	Plankton succession: Investigations regarding new approaches to management
Project Number:	2001TX3181B
Start Date:	3/1/2001
End Date:	2/28/2002
Funding Source:	104B
Congressional District:	8
Research Category:	Biological Sciences
Focus Category:	Wetlands, Waste Water, Ecology
Descriptors:	management schemes, pulsed nutrient flow,plankton succession
Principal Investigators:	Yesim Buyukates

Publication

1. Roelke, Daniel and Yesim Buyukates, 2002, Dynamics of phytoplankton succession coupled to species diversity as a system-level tool for study of Microcystis population dynamics in eutrophic lakes, in Limnology and Oceanography, v. 47(4), July 2002
2. Buyukates, Yesim, 2002, The effect of inntial community composition on phytoplankton succession under continuous pulsed-flow conditions, Texas Water Resources Institute, SR 2002-043, Texas A&M University, College Station, Texas
3. Buyukates, Yesim and Daniel Roelke, 2002, The Effect of Initial Commuity Composition on Phytoplankton Succession under Continuous and Pulsed-Flow Conditions, in 105th Texas Academy of Science conference, 2002, Laredo, Texas

Authors:

Buyukates, Y., D. L. Roelke
The effect of initial community composition on phytoplankton succession under continuous and pulsed-flow conditions

Three pulsed vs. continuous nutrient loading experiments were conducted to investigate phytoplankton competition in mixed assemblages from the Rincon Delta, Texas, in March, June and September 2001. Flow-through incubators received the same amount of nutrient loading and hydraulic flushing over the course of each experiment, as well as identical photoperiod and irradiance. Initial conditions in the incubators were assumed identical because water samples were drawn from the same well-mixed carboy that contained the field sample. Our findings showed that in one experiment pulsed flows supported greater secondary productivity with less accumulated phytoplankton biomass, and greater phytoplankton diversity, than continuous flow, while another experiment showed the opposite trend, and a third experiment, as yet, shows no trend. In one of the experiments the variability within a treatment was also high. We anticipated our observed results between treatments, but we did not anticipate the differences sometimes observed within treatments comprising an experiment, or the differences between experiments. This raised the question of what might be causing these differences in phytoplankton succession patterns. Differences between the experiments may be due to the initial presence or absence of phytoplankton species characteristic of minimum cell quotas that are below grazer food-quality thresholds, i.e., when in a starved state are unsuitable food sources. In turn, this would allow phytoplankton blooms of low diversity. However this does not explain the differences observed within treatments of the same experiment. It may be that phytoplankton succession in these assemblages behaves chaotically. In which case, minute variations in the initial phytoplankton community composition would have a profound impact on secondary productivity, phytoplankton standing biomass, and species diversity.

Sublethal Effects of Cadmum and Linear Alkylbenzene Sulfonate Mixtures on Pimephales promelas Exposure and Effect Endpoints: Laboratory and Field Assessments

Basic Information

Title:	Sublethal Effects of Cadmum and Linear Alkylbenzene Sulfonate Mixtures on Pimephales promelas Exposure and Effect Endpoints: Laboratory and Field Assessments
Project Number:	2001TX3201B
Start Date:	3/1/2001
End Date:	2/28/2002
Funding Source:	104B
Congressional District:	26
Research Category:	Biological Sciences
Focus Category:	Ecology, Toxic Substances, Waste Water
Descriptors:	Primephales promelas, LAS, cadmium, chemical mixtures,municipal effluents
Principal Investigators:	Bryan Brooks, THOMAS W LA POINT

Publication

1. Brooks, B.W., P.K. Turner, J. Weston, E.Glidewell, C.M. Foran, M. Slattery, D.B. Huggett, Waterborne and sediment toxicity of fluoxetine (Prozac) to selected organisms, Poster, 2002 Annual meeting of Society of Environmental Toxicology and Chemistry, Salt Lake City, UT
2. Brooks, B.W., P.K. Turner, J. Weston, E.Glidewell, C.M. Foran, M. Slattery, D.B. Huggett, Fathead minnow resopnses to Cadmium in effluent-dominated streams, 2002, Poster presented at 2002 Annual Meeting of the Society of Environmental Toxicology and Chemistry, Salt Lake City, Utah
3. Brooks, B.W., P.K. Turner, J. Weston, E.Glidewell, C.M. Foran, M. Slattery, D.B. Huggett, TIE and TMDL Approaches for Legacy Sediment Contaminants: Aresenic and Petrochemical Case Studies, presented at 2002 Annual meeting of the Society of Environmental Toxicoloyg and Chemistry, Salt Lake City, Utah.

Sublethal Effects of Cadmum and Linear Alkylbenzene Sulfonate Mixtures on Pimephales promelas Exposure and Effect Endpoints: Laboratory and Field Assessments

PI: Bryan Brooks
Professor: Thomas LaPoint
University of North Texas
Denton, Texas
Department of Biological Sciences
UNT Institute of Applied Sciences

Biologists at the University of North Texas (UNT) and the city of Denton have recently developed a research facility that will facilitate the study of how pollutants may affecting water quality in lakes, rivers, aquatic habitats, and wetlands in the region. The UNT Experimental Stream Facility opened in May. The center is located at the City of Denton Pecan Creek Wastewater Management Plant. Tom LaPoint, the Director of the UNT Institute for Applied Sciences, heads a team of scientists who conduct studies at the site.

The research center consists of 12 man-made "streams" that imitate natural rivers found throughout the region. Each experimental stream is 16 feet long and two feet wide. To mimic real world conditions, the streams were built with a gravel substrate, and pools were placed at the end of each stream segment. Water is supplied by the wastewater plant. A variety of aquatic organisms (including insects, larvae, snails, invertebrates, and fish) was obtained from Pecan Creek for use in this system. Wastewaters that flow through the facility will be rout routed back to the treatment plant to prevent possible contamination.

Throughout the summer of 2000, LaPoint and colleagues have been using this site to study how pollutants affect aquatic life in the surface waters. Minnows, bluegill sunfish, and other fish have been added to the downstream pools, where they have been exposed to contaminants throughout a 30- to 60-day period. Changes in the growth, behavior, and mortality of fish at the research site are being compared to laboratorystudies in which fish are exposed to individual contaminants.

Determination of Regional Scale Evapotranspiration of Texas from NOAA-AVHRR satellite

Basic Information

Title:	Determination of Regional Scale Evapotranspiration of Texas from NOAA-AVHRR satellite
Project Number:	2001TX3221B
Start Date:	3/1/2001
End Date:	2/28/2002
Funding Source:	104B
Congressional District:	8
Research Category:	Not Applicable
Focus Category:	Water Use, Climatological Processes, Models
Descriptors:	modeling, evapotranspiration, remote sensing,GIS
Principal Investigators:	Balaji Narasimhan, Raghavan Srinivasan

Publication

1. Narasimhan, Balaji. R. Srinivasan., 2002. Determination of Regional Scale Evapotranspiration of Texas from NOAA AVHRR satellite, Texas Water Resources Institute, Texas A&M University, College Station, Texas, SF2002-009
2. Narasimhan, Balaji, R. Srinivasan, 2002, Hydrological Applications of Land Surface Temperatures (LST) Derived from AVHRR, Texas Water Resources Institute, Texas A&M University, College Station, Texas, SR 2002-005

Determination of Regional Scale Evapotranspiration of Texas from NOAA – AVHRR satellite

Principle Investigators: -

Balaji Narasimhan
Graduate Student
Department of Agricultural Engineering
201 Scoates Hall,
Texas A&M University,
College Station, TX – 77843 – 2117.
Phone: (979) 845 – 3600
Fax : (979) 845 – 3932
E-mail: balaji@tamu.edu

Dr. Raghavan Srinivasan
Director and Associate Professor
Spatial Sciences Laboratory
Department of Forest Science
Spatial Sciences Laboratory
700 University Drive, Suit # 104
College Station, TX – 77840 – 2120.
Phone: (979) 845 - 5069
Fax : (979) 845 - 2273
E-mail: srin@brc.tamus.edu

Final Report
Submitted to Texas Water Resources Institute

Date of submission: March 5, 2002

Determination of Regional Scale Evapotranspiration of Texas from NOAA – AVHRR satellite

INTRODUCTION

Evapotranspiration (ET) is defined as the combined loss of water by evaporation from soil and transpiration from plants. Depending on the geographic location, 60-80% of total annual precipitation is lost in the form of evapotranspiration. Since ET accounts for a major portion of water lost to the atmosphere, accurate estimation is essential for the success of hydrologic modeling studies. ET is estimated using climatic data like net radiation, air temperature, wind velocity, vapor pressure deficit and relative humidity obtained from the nearest weather stations. However, interpolating ET using data obtained from a point data source to derive regional ET could introduce errors of large magnitude. During the last two decades, GIS and Remote Sensing have evolved as an indispensable tool for monitoring natural resources. Due to the availability of spatially distributed data from satellites, and adopting GIS principles, accurate determination of ET is possible. The present study aims at deriving spatially distributed ET using NOAA-AVHRR satellite data.

Advanced Very High Resolution Radiometer (AVHRR) is a sensor aboard NOAA series of polar orbiting earth satellites that are in operation for more than three decades. The main purpose of these satellites is to forecast weather and monitor regional climatic conditions. However, its potential for monitoring crop growth, assessing crop yield and monitoring forest cover has been realized only during the past decade. AVHRR is a broadband scanner, sensing in the visible (Channel 1), near-infrared (Channel 2) and thermal infrared portions (Channel 3, Channel 4 and Channel 5) of the electromagnetic spectrum. Currently NOAA-14 and NOAA-15 satellites are in orbit. The spectral ranges of different channels are given in Table 1.

Table.1 Spectral range of AVHRR

Channel	Wavelength (μm)
1	0.58 – 0.68
2	0.73 – 1.10
3	3.55 – 3.93
4	10.3 – 11.3
5	11.5 – 12.5

Data from Channel 1 and Channel 2 are used extensively for Land Use/Land Cover monitoring. However data obtained from thermal channels have been put to very little use. In this research project, data obtained from thermal channels 4 and 5 have been used in addition to the use of channel 1 and 2 in the estimation of ET.

PREVIOUS STUDIES

Few studies have been done in the past for the estimation of regional scale evapotranspiration from satellites. Seguin et al. (1994) conducted field experiments in France, the Sahel and North Africa and demonstrated the existence of a linear relationship between $(ET - R_n)$ and $(T_s - T_a)$ and the potential to derive ET from AVHRR satellite where, ET – Evapotranspiration, R_n – net radiation, T_s – Surface temperature and T_a – Air temperature. The disadvantage of this method is that the coefficients in this equation are site specific and separate equations have to be derived for different sites. Granger (1995) developed a feedback algorithm for the estimation of ET from AVHRR thermal channels. This study established a relationship between saturated vapor pressure at surface temperature T_s and vapor pressure deficit. The vapor pressure deficit estimated from surface temperature measurements is used to estimate evapotranspiration. Granger (1995) suggested that the equation developed could be applied for wide range of surface cover types. However, comparison of the model estimates with the field observations of vapor pressure deficit for Panhandle, Texas showed poor correlation. Tan and Shih (1997) adopted a similar approach suggested by Seguin et al (1994) for South Florida. Jiang and Islam (1999) adopted an approach similar to that of Priestly-Taylor method (ASCE, 1990) for estimation of ET. However, the values of _ are derived from inverse

relationship between NDVI (Normalized difference Vegetation Index and T_s). This equation doesn't take into account the advective flux and hence can be useful only for regions with low advective flux.

The objectives of this study are:

1. to develop a relationship between satellite surface temperature T_s and maximum air temperature T_a
2. to use minimal ground based inputs for deriving potential ET

METHODOLOGY

There are several methods available for estimating ET. The level of accuracy needed, quality and availability of weather parameters determine the adoption of a particular method for estimating ET. Penman-Monteith method is widely adopted because of its applicability to wide range of climatic conditions. Accurate estimates of ET could also be obtained using the energy budget method. This method is not widely adopted because of the non-availability of surface temperature (T_s) estimates from weather stations. With the help of AVHRR channel 4 and channel 5, surface temperature could be accurately estimated by using a split window algorithm developed by Price (1984). In the present study, ET is estimated using Energy Budget Method. Air temperature is one of the important input in the estimation of ET. In the following section a procedure to estimate air temperature from surface temperature and to ultimately estimate ET has been described

Estimation of Maximum Air temperature from Surface Temperature:

Surface Temperature:

Land Surface Temperature (LST) is the temperature measured just few inches above the surface of the land or the vegetation sensed by the thermal bands of AVHRR satellite. Infrared radiation sensed by AVHRR satellites is influenced due to atmospheric absorption by water vapor and other gases (principally CO_2). These make it difficult to accurately predict the surface temperature. This is further complicated because the land

surface does not behave as a perfect emitter of infrared radiation and presents a high variability.

Split window algorithms take advantage of the differential absorption in two close infrared bands to account for the effects of absorption by atmospheric gases. Several split window algorithm are currently available to derive LST from brightness temperature [Becker and Li (1990); Keer et al. (1992); and Price (1984); Ulivieri et al. (1992)]. A study conducted by Vázquez et al. (1997) showed that the split widow algorithm developed by Price (1984) performed better over other split window algorithms. Hence the algorithm developed by Price (1984) has been used to derive the Land Surface Temperature, which is given by:

$$LST = T_4 + 3.3 \times (T_4 - T_5) \times \frac{5.5 - \varepsilon_4}{4.5} + 0.75 \times T_5 \times \Delta\varepsilon \quad (1)$$

Where:

LST = Land Surface Temperature [° C],

T_4 = Brightness temperature obtained from Channel 4 [° C],

T_5 = Brightness temperature obtained from Channel 4 [° C],

$\Delta\varepsilon$ = $\varepsilon_4 - \varepsilon_5$,

ε_4 = Surface emissivity in AVHRR channel 4,

ε_5 = Surface emissivity in AVHRR channel 5.

Cihlar et al. (1997) developed an algorithm to calculate the surface emissivities ε_4 and ε_5 from NDVI (Normalized Difference Vegetation Index):

$$\varepsilon_4 = 0.9897 + 0.029 \times \ln(NDVI) \quad (2)$$

$$\Delta\varepsilon = \varepsilon_4 - \varepsilon_5 = 0.01019 + 0.01344 \times \ln(NDVI) \quad (3)$$

Relationship between T_s and T_a:

Comparison of surface temperature obtained from the satellite and the maximum air temperature measured at weather stations across Texas show that there is a strong linear relationship between T_s and T_a. This is because the overpass time of the satellite coincides with the occurrence of the maximum air temperature during noon. Hence a simple regression approach has been adopted for deriving T_a from T_s. However this

linear relationship varied spatially among weather stations across Texas even within the same climatic division [Texas is divided into ten climatic divisions (Fig. 1) by NWS based on the climatological parameters like temperature, precipitation, etc.,]. Hence

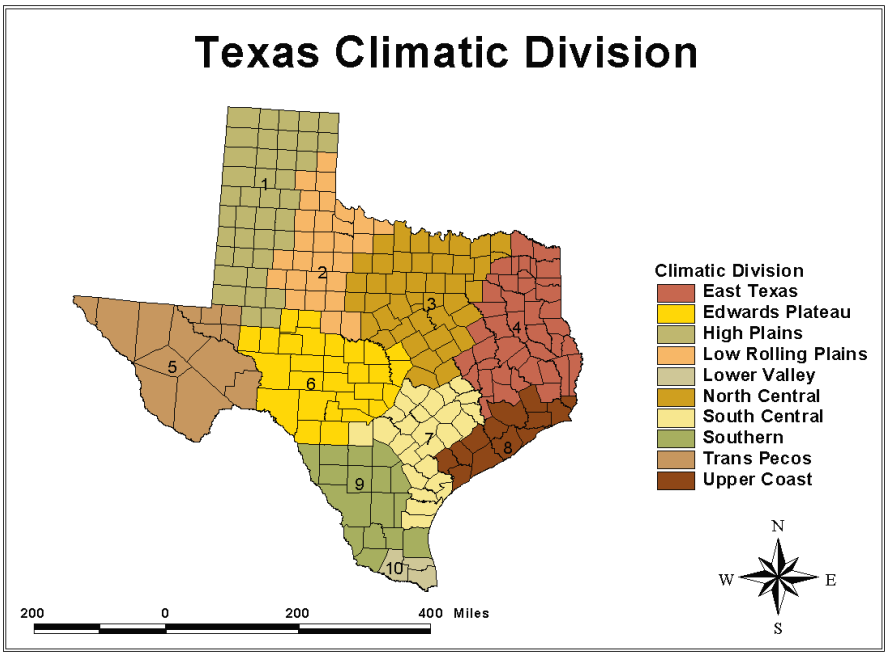

Figure 1. Climatic Divisions of Texas.

long-term maximum air temperature (T_{lm}) obtained from 30 years of historical weather data was incorporated into the regression model to account for spatial variation in the relationship among weather stations. Incorporation of T_{lm} in the regression model reduced the spatial variation in the relationship among weather stations within a given climatic division. Since there are ten climatic divisions in Texas, one such regression model has been developed for each climatic division. The regression model adopted in the study is of the form:

$$\hat{T}_a(i) = m(i)\sqrt{T_s \leftrightarrow T_{lm}} + C(i) \qquad (4)$$

Where:

$\hat{T}_a(i)$ - estimated daily maximum air temperature for climatic zone i

T_s - land surface temperature (˚F)

T_{lm} - long-term monthly maximum air temperature (˚F)

m(i) and C(i) are regression constants for climatic zone I (where i = 1,…..10). In this study daily weather data (September, 1999 to August, 2000) from 57 weather stations distributed across Texas were available for model development and validation (Fig.2).

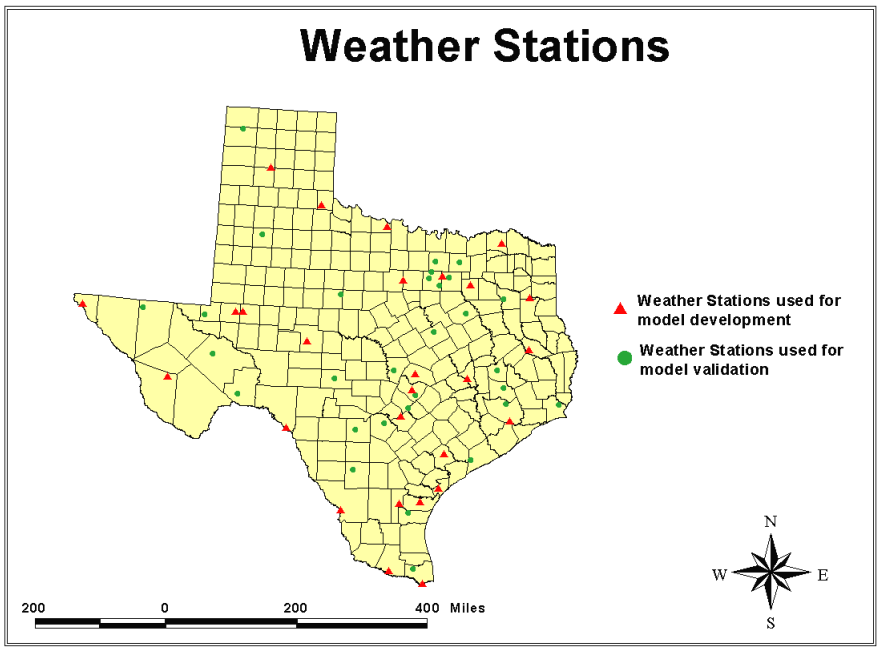

Figure 2. NWS weather stations used for model development and validation.

Daily weather data from 27 weather stations were used for model development and data from 30 weather stations were used for model validation. Comparison of model estimated $\hat{T}_a$ with that of the measured T_a (Fig. 3) show that the model estimated air temperatures are in good agreement with the measured air temperature ($r^2 = 0.79$ and slope ≈ 1).

Table 2. Regression coefficients used for deriving T_a from T_s

Climatic Division	m(i)	c(i)	R^2
1	0.78	15.60	0.74
2	0.89	9.29	0.8
3	0.87	12.10	0.82
4	0.91	11.21	0.84
5	0.83	9.98	0.76
6	0.87	11.05	0.78
7	0.78	18.45	0.74
8	0.86	13.46	0.79
9	0.82	16.24	0.72
10	0.81	17.35	0.75

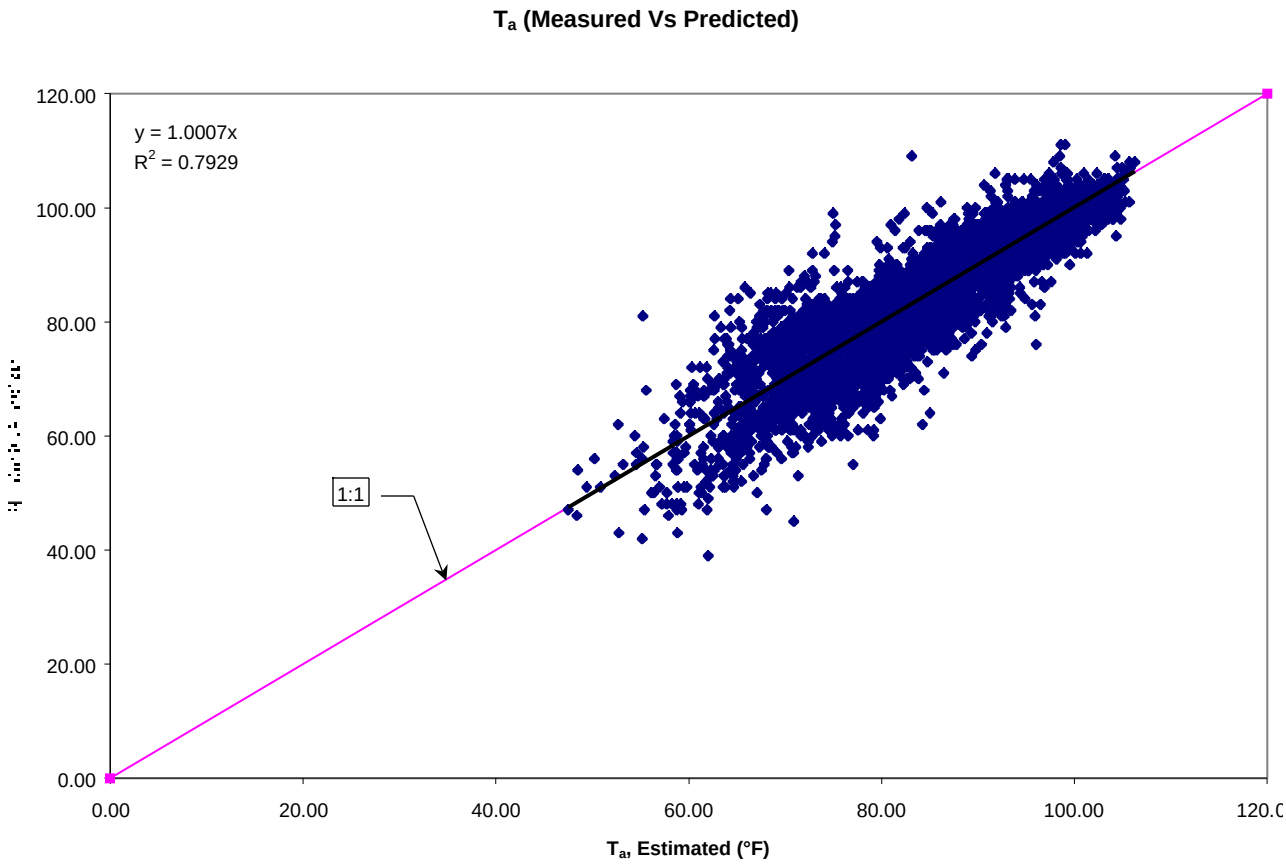

Figure 3. Comparison of model estimated air temperature with air temperature measured at NWS weather stations.

Estimation of potential ET:

The procedure for estimating ET on the vertical energy budget of a vegetated surface has been described in this section. The Energy Balance Equation is given by (ASCE 1990):

$$R_n = \lambda E + H + G \tag{5}$$

Where:

R_n - net radiation flux at the surface [MJ m^{-2} day^{-1}],

_E - latent heat flux [MJ m^{-2} day^{-1}],

H - sensible heat flux to the air [MJ m^{-2} day^{-1}],

G - sensible heat flux to the soil [MJ m^{-2} day^{-1}].

The sensible heat flux to the air is given by (ASCE 1990):

$$H = \frac{\rho_a C_p}{r_a} U_2 (T_s - T_a) \quad (6)$$

Where:

ρ_a - density of the air [kg m^{-3}],

C_p - specific heat of the air at constant pressure [MJ kg^{-1} °C^{-1}],

r_a - aerodynamic resistance [s m^{-1}],

U_2 - wind speed at a height 2m [m s^{-1}],

T_s - surface temperature [°C],

T_a - air Temperature [°C].

The roughness coefficient is given by (FAO 1998):

$$r_a = \frac{\ln \frac{z-d}{z_{om}} \quad \ln \frac{z-d}{z_{ov}}}{k^2 U_2} \quad (7)$$

Where:

k - Von Karman constant [0.41],

d - zero-plan displacement parameter [m],

Z_{om} - roughness parameter for momentum [m],

Z_{ov} - roughness parameter for head and vapor transfer [m].

Adopting coefficients for a grass reference crop suggested by FAO (FAO 1998) and substituting in eq. 3, eq.2 becomes:

$$H = \gamma \frac{900}{T_a + 273} \lambda U_2 (T_s - T_a) \quad (8)$$

Where:

γ - Psychrometric constant [kPa °C^{-1}].

Assuming sensible heat flux to the soil (G) as negligible, ET can be found by:

$$E = \frac{R_n - H}{\lambda} \quad (9)$$

where:

E - Evapotranspiration in [mm day^{-1}],

λ - Latent heat of vaporization at 20 °C [2.45 MJ kg^{-1}].

Net radiation (R_n):

Net radiation is the amount of radiation absorbed by the land surface from the incoming solar radiation:

$$R_n = (1-\alpha)R_s + \varepsilon R_l \text{ ø} - \varepsilon\sigma (T_s + 273.16)^4 \quad (10)$$

where:

R_n - net radiation [MJ m^{-2} d^{-1}],

R_s - incoming short wave radiation [MJ m^{-2} d^{-1}],

R_l - incoming long-wave radiation [MJ m^{-2} d^{-1}],

α - surface albedo,

T_s - Surface temperature [°C],

ε - emissivity,

_ - Stefan-Boltzman constant (4.90 X 10-9 MJ m^{-2} d^{-1} K^{-4}).

Incoming short wave radiation is estimated using empirical relationship suggested by FAO (FAO 1998). Surface albedo was calculated from the channel 1 and channel 2 of AVHRR, by adopting the method proposed by Gutman (1988). The algorithm developed by SwinBank (1963) was used to calculate the incoming long-wave radiation.

Psychrometric Constant (γ):

The psychrometric constant is given by (FAO 1998):

$$\gamma = \frac{C_p P}{\varepsilon\lambda} = 0.665 \leftrightarrow 10^{-3} P \quad (11)$$

where:

γ - psychrometric constant [kPa °C^{-1}],

P - atmospheric pressure [kPa],

λ - Latent heat of vaporization, 2.45 [MJ kg^{-1}],

C_p - Specific heat at constant pressure, 1.013 × 10^{-3} [MJ kg^{-1} °C^{-1}],

ε - ratio of molecular weight of water vapor/dry air = 0.622.

The atmospheric pressure varies with elevation. A 1km resolution DEM (Digital Elevation Model) is used in the calculation of atmospheric pressure (FAO 1998):

$$P = 101.3 \left(\frac{293 - 0.0065z}{293}\right)^{5.26} \quad (12)$$

where:

P - atmospheric pressure [kPa],

z - elevation above sea level [m].

Wind Velocity:

A constant wind velocity of 2m/s was assumed for estimation of grass reference ET since it cannot be derived from the satellite.

RESULTS AND DISCUSSION

By adopting the methodology outlined in this report, potential ET was calculated for cloud free days between May 1999 to April 2000 satellite images. Arc/Info 8.1 was used for processing the satellite images. During the same days potential ET was calculated for 16 FAA weather stations (Fig.4) from its ground based weather observations.

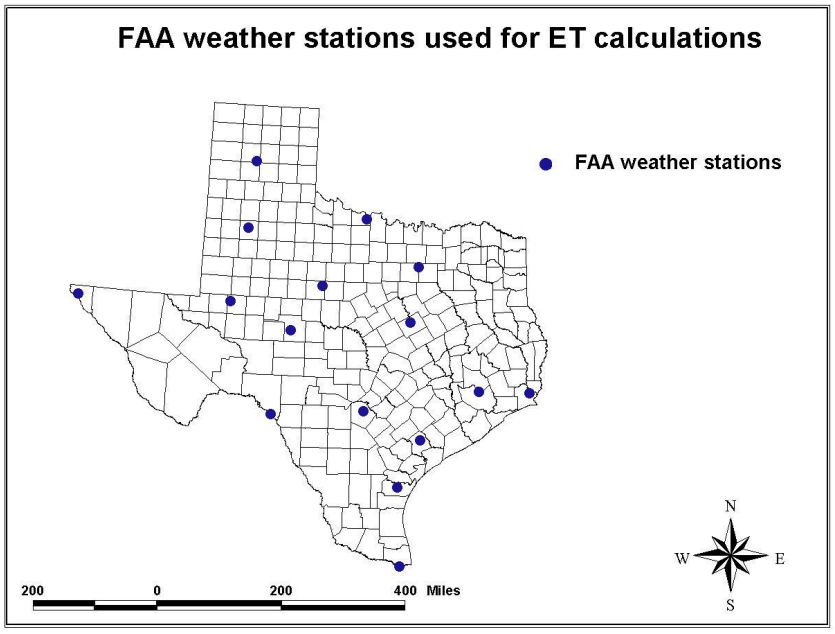

Figure 4. FAA weather stations used for calculated potential ET.

Ta, Rn, and ET0 (Potential ET) calculated for cloud free days from satellite were compared with the FAA weather station estimates (Figs. 5, 6, and 7).

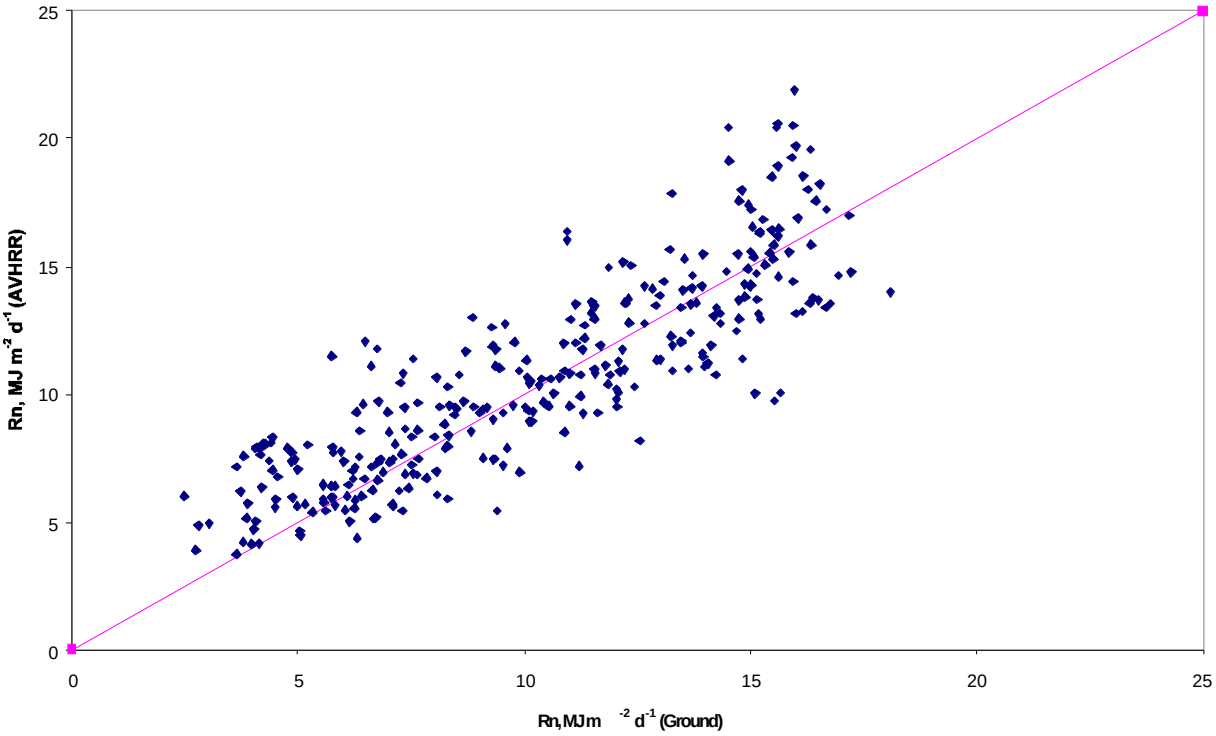

Figure 5. Comparison of net radiation derived from FAA stations and AVHRR

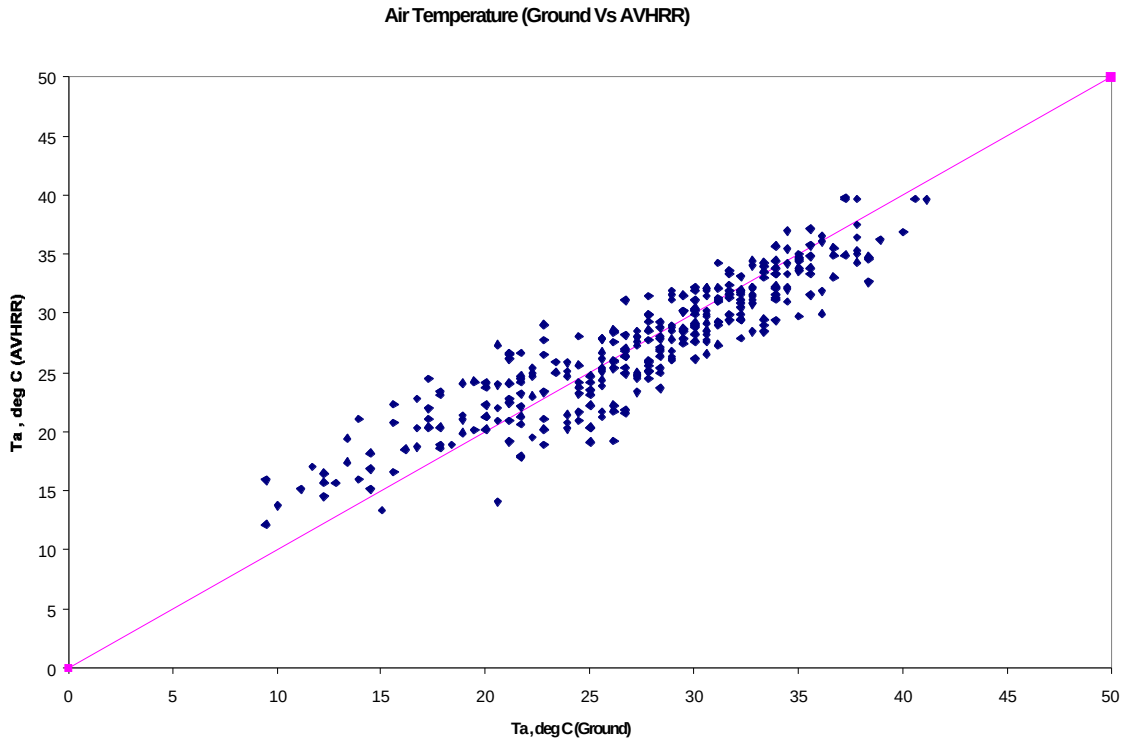

Figure 6. Comparison of maximum air temperature derived from FAA stations and AVHRR

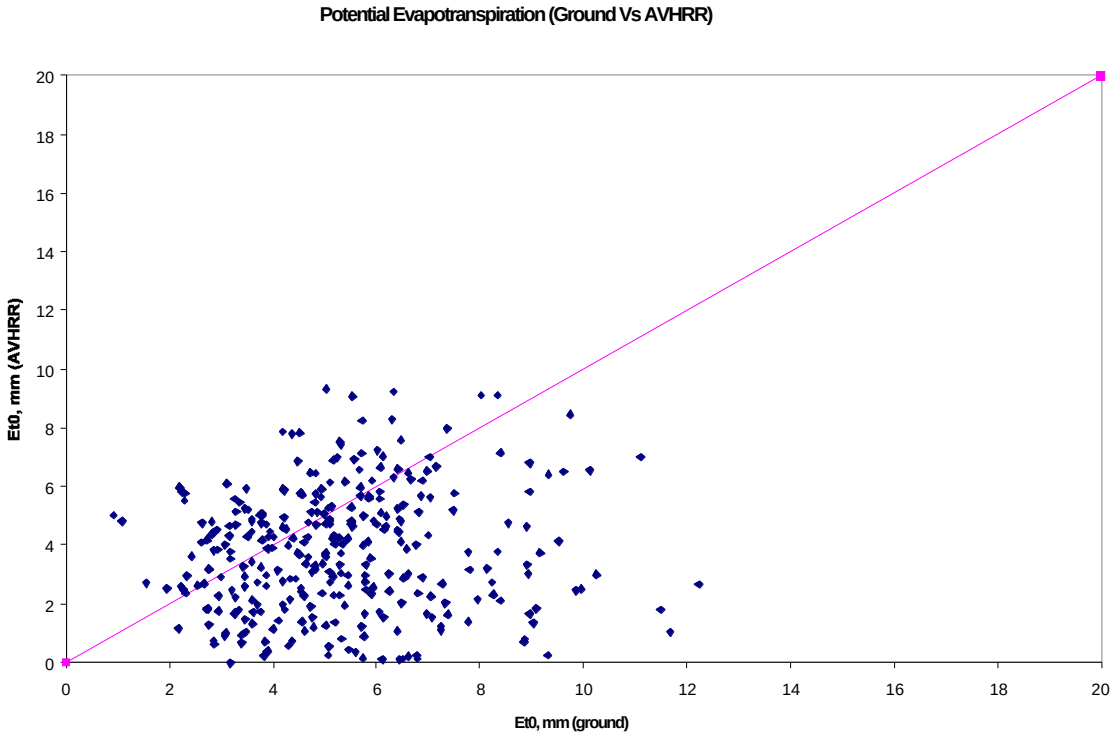

Figure 7. Comparison of potential ET derived from FAA stations and AVHRR

Comparison of Figs. 5, 6, 7 show that the air temperature and net radiation derived from AVHRR satellite compare well with the ground based estimates. However, the potential ET derived from ground based observations didn't match well with the ET derived from AVHRR. There are several reasons for this:

1. Penman-Monteith combination equation has been used to derive ET from ground based estimates. But an energy balance approach has been used to derive ET from AVHRR satellites. Because all the parameters needed for the estimation of ET using Penman-Monteith method cannot be derived from AVHRR satellite.
2. A constant wind velocity of 2m/s was used for the calculation of ET from AVHRR satellite; however, measured wind velocity was used for calculating ET from FAA weather stations.
3. The ET derived from FAA stations is derived from point observations. However, ET derived from AVHRR satellite is obtained by using parameters measure over an area of 1 km X 1km.

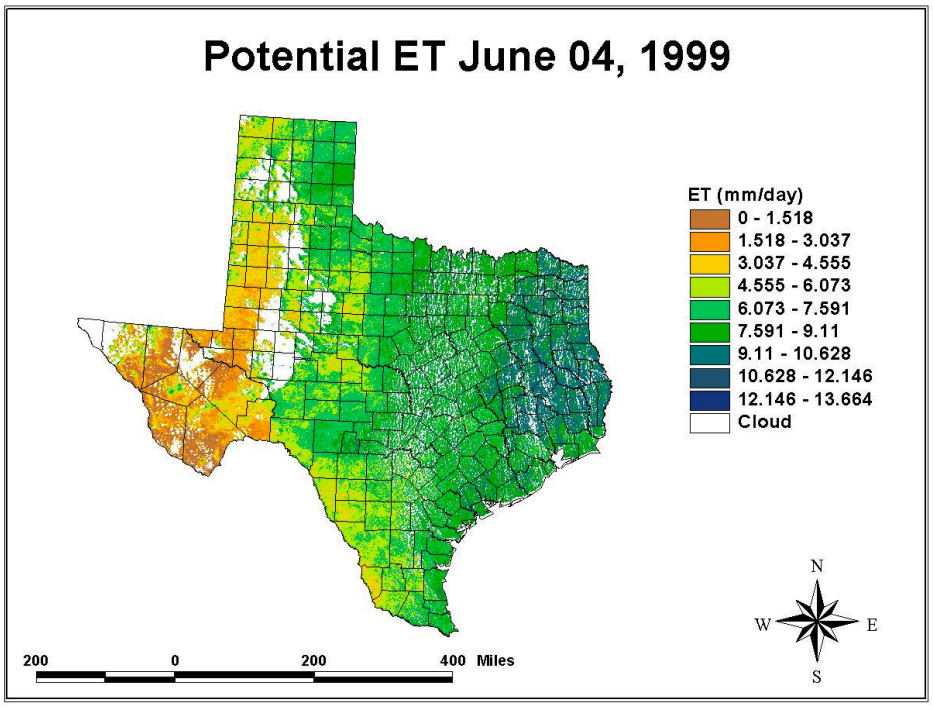

Figure 8. Potential ET derived from AVHRR satellite on June 4, 1999.

CONCLUSION

This research study developed a good understanding of the basic processes involved in the derivation of potential ET from AVHRR satellite. Preliminary results show that AVHRR satellite could be used for deriving potential ET. However some more research needs to be done to improve the accuracy of the ET estimates from AVHRR satellite. Research is in progress at the Spatial Sciences Laboratory to improve the methodology involved in the calculation of potential ET from AVHRR satellite.

REFERENCES

1. ASCE. 1990. Evapotranspiration and Irrigation Water Requirements. ASCE manuals and Reports on Engineering Practice No. 70. ASCE, New York, USA.
2. Becker, F., and Z. L. Li. 1990. Towards a local split window method over land surface. International journal of Remote Sensing. 3:369-393.
3. Cihlar, J., H. Ly, Z. Li, J. Chen, H. Pokrant, and F. Hung. 1997. Multi-temporal, Multi-channel AVHRR data sets for land biosphere studies – Artifacts and corrections. Remote Sensing and Environment. 60: 35 – 57.

4. FAO. 1998. Crop Evapotranspiration: Guidelines for computing crop water requirements. FAO Irrigation and Drainage Paper No.56. FAO, Rome, Italy.
5. Granger, R.J. 1995. A feedback Approach for the estimate of evapotranspiration using remotely-sensed data. Application of Remote Sensing in Hydrology. 211-222.
6. Gutman, G. 1988. A simple method for estimating monthly mean albedo of land surfaces from AVHRR data. Journal of Applied Meteorology. 27: 973-988.
7. Jiang. L, and S. Islam. 1999. A methodology for estimation of surface evapotranspiration over large areas using remote sensing observations. Geophysical Research Letter, 26(17): 2773 – 2776.
8. Kerr, Y. H., J. P. Lagouarde, and J. Imbernon. 1992. Accurate land surface temperature retrieval from AVHRR data with use of an improved split window. Remote Sensing and Environment. 41: 197-209.
9. Price, J. C. 1984. Land Surface Temperature measurements from the split window channels of the NOAA 7 Advanced Very High Resolution Radiometer. Journal of Geophysical Research, 89: 7231 – 7237.
10. Seguin.B, D. Courault, and M.Guérif. 1994. Surface Temperature and Evapotranspiration: Application of Local Scale Methods to Regional Scales Using Satellite Date. 49(3):287-295.
11. Swinbank, W. C. 1963. Long-wave radiation from clear skies. Quarterly Journal of Royal Meteorological Society. 89:339-348.
12. Tan, C. H. and S. F. Shih. 1997. Using NOAA Satellite Thermal Infrared Data for Evapotranspiration Estimation in South Florida. Soil Crop Science Society, Florida Proceedings, 56: 109 – 113.
13. Ulivieri, C., M. M. Castronouvo, R. Francioni, and A. Cardillo. 1992. A Split-window algorithm for estimating land surface temperature from Satellites. Advances in Space Research. 14(3): 59-65.
14. Vázquez, D. P., F. J. Olmo Reyes and L. A. Arboledas. 1997. A comparative study of algorithms for estimating land surface temperature from AVHRR data. Remote sensing and Environment. 62: 215-222.

Regional Economic Impacts of Aquifer Decline in the Southern High Plains of Texas

Basic Information

Title:	Regional Economic Impacts of Aquifer Decline in the Southern High Plains of Texas
Project Number:	2001TX3241B
Start Date:	3/1/2001
End Date:	2/28/2002
Funding Source:	104B
Congressional District:	19
Research Category:	Not Applicable
Focus Category:	Groundwater, Economics, Agriculture
Descriptors:	and irrigation, regional economics,Ogallala Aquifer
Principal Investigators:	Jeffrey W. Johnson

Publication

State:	Texas
Project Number:	TX3241
Title:	Regional Economic Impacts of Aquifer Decline in the Southern High Plains of Texas
Project Type:	Research Project
Focus Category:	Groundwater, Economics, Agriculture
Keywords:	and irrigation, regional economics,Ogallala Aquifer
Start Date:	03/01/2001
End Date:	02/28/2002
Congressional District:	19
PI:	Jeffrey W. Johnson Student, Texas Tech University email:jeff.johnson@ttu.edu phone:(806) 742-2808

Abstract

The goal of this study is to determine the long-term economic impacts of restrictive groundwater conservation measures on the economy of the Texas High Plains region. The study will include a 23-county area that utilizes the Ogallala Aquifer as a groundwater source. The project will develop dynamic optimization models to analyze crop production under different water conservation scenarios, and will assess how these conservation strategies may affect when the Aquifer would be economically exhausted.

1. **Title**: Regional Economic Impacts of Aquifer Decline in the Southern High Plains of Texas

2. **Focus Categories (to be completed by Institution personnel):**

3. **Keywords**: Ogallala Aquifer, regional economics, and irrigation

4. **Duration**: March 1, 2001 through February 28, 2002

5. **Federal Funds Requested**: $5,000

6. **Non-Federal (matching) Funds Pledged**: $10,000

7. **Principal Investigator (graduate student**): Jeffrey W. Johnson

   Co-Principal Investigator (faculty advisor): Dr. Phillip Johnson

8. **Congressional District**: 19th Congressional District

9. **Statement of Critical Regional Water Problems**:

The southern portion of the Ogallala Aquifer underlies and provides water for the Southern High Plains of Texas. The primary water consumer is agriculture, which uses about 96% of the water pumped from the aquifer for irrigation. Irrigated agriculture constitutes a significant portion of the regional economy with 55% of the 4.98 million acres of harvested cropland being irrigated. The 21 counties of the Llano Estacado Region are dependent on agriculture income for economic activity; with a 31% agricultural sales to retail sales ratio for the non-metropolitan counties in the region.

The Ogallala Aquifer is considered a closed aquifer and as a result is a nonrenewable resource. Although recent studies show that some recharge does occur, the amount of recharge is insignificant in relation to the rate of extraction. Because the extraction rate is much greater than the negligible recharge rate, the amount of water in the aquifer is decreasing toward the point of depletion. As the aquifer is depleted, irrigators will transition from irrigated to dryland cropping systems. Yield, crop revenues, and crop expenses will decline for the irrigator as he makes this transition.

The regional economy will be affected as farms transition to dryland cropping systems. This transition may result in a negative impact on the regional economy. Crop input suppliers, such as fertilizer and chemical dealers, and other supporting businesses, such as banks, department stores, and car dealerships may experience a decline in the volume of business as more farmers transition to dryland agriculture.

With open access to a nonrenewable resource, economic theory suggests that an individual irrigator should use available water as long as marginal benefits are greater than marginal costs. The decision of farmers as to the optimal rate of water use for irrigation over time is related to their individual discount rate (time preference). When evaluated at investment level discount rates individuals have less incentive to conserve water for the future because of its reduced future value. However, from a societal standpoint the decision as to the optimal rate of water use to sustain the

regional economy may be quite different given a lower social discount rate and the multiplier effect of agricultural income within the regional economy.
The implementation of policies that would result in a longer time horizon before economic depletion of the aquifer could result in a benefit to the regional economy. Restrictive water conservation measures could include a restriction on the amount of water pumped for each irrigator, a tax on the water pumped, or a tax on irrigated crop inputs or outputs. This study will investigate the regional economic impacts of the transition from irrigated to non-irrigated crop production and determine if the regional economy will benefit from extending the life to the aquifer. This study will investigate the benefits of conserving the water from the standpoint of the regional economy including farm-related and supporting businesses of the region

10. **Nature, Scope, and Objectives of the Research**:

The general objective of this study is to determine the long run economic impacts on the regional economy as a result of using restrictive water conservation measures to extend the life of the Ogallala Aquifer. The region for this study is the 21 county Llano Estacado Region. The specific objectives of this study are to:

1) Develop dynamic optimization models to analyze crop production under alternative restrictive water conservation scenarios.
2) Determine the time of economic exhaustion for the Ogallala Aquifer in the region under different levels of water restriction.
3) Analyze the economic impact on the regional economy as a result of the different levels of water restriction.

The study will develop dynamic optimization models of crop production that consider changes in the saturated thickness of the aquifer, pumping costs, crop prices, crop rotations, and other factors to allow analysis of the restrictive water conservation scenarios. The restrictive water conservation scenarios to be considered are no restriction, restriction to delay depletion, and restriction to allow sustained irrigation at a reduced level. County level optimization models will be formulated to take into account the variation across the region in aquifer characteristics and cropping patterns.

An input-output model using IMPLAN will be used to analyze the regional economic impacts of the restrictive water conservation scenarios on agricultural production. Input-output models are used to estimate the direct and indirect effects of dollar value changes in the output of economic sectors of the economy. The results of the input-output model will be used to estimate the impacts on the regional economy of changes in agricultural production brought about by the depletion of the Ogallala aquifer. A comparison of the changes in regional economic activity under each alternative restrictive water conservation measure will be used to evaluate the benefits of such measures.

11. **Results Expected from this Project**:

The evaluation of different restrictive water conservation measures using an input-output model of the regional economy will allow the analysis of the effectiveness of the policy tools available to regional and state decision makers.

Fluctuating environmental parameters in red drum nursery habitats: the influence of habitat quality on larval growth and endocrine function

Basic Information

Title:	Fluctuating environmental parameters in red drum nursery habitats: the influence of habitat quality on larval growth and endocrine function
Project Number:	2001TX3261B
Start Date:	3/1/2001
End Date:	2/28/2002
Funding Source:	104B
Congressional District:	27
Research Category:	Biological Sciences
Focus Category:	Ecology, Surface Water, Climatological Processes
Descriptors:	cortisol, thyroid hormones, diel cycles, growth, settlement, habitat quality, larval development,red drum
Principal Investigators:	Rafael Perez

Publication

1. Perez-Dominguez, Rafael, Joan Holt,. 2002 Effects of nursery environmental cycles on larval red drum (Sciaenops ocellatus) growth and survival, TWRI Special Report 02-02. Texas Water Resources Institute, Texas A&M University, College Station, Texas

TWRI Special Report 02-02, January 2002

Texas Water Resources Institute
make every drop count

Effects of nursery environmental cycles on larval red drum (*Sciaenops ocellatus*) growth and survival

RAFAEL PÉREZ-DOMÍNGUEZ, AND JOAN G. HOLT
Fisheries and Mariculture Laboratory, Marine Science Institute, The University of Texas at Austin, 750 Channel View Dr., Port Aransas, TX 78373, USA (rperez@utmsi.utexas.edu)

SUMMARY: Red drum early larval stages migrate through coastal inlets and settle into shallow seagrass meadows within estuaries. This study describes environmental rhythms (ER) in red drum nursery habitats and evaluates their role in larval growth. Well-defined diel ER were observed in temperature (amplitude: 2 to 4.5ºC) and dissolved oxygen (DO) (range: 2.9-7.5 mg O_2 L^{-1}), and sporadic cooling caused by cold fronts. We exposed groups of settlement sized larvae (4.9 mm standard length) to two oscillating temperature treatments (amplitudes: 3 and 6ºC; daily mean 27ºC), an oscillating DO treatment (range: 2.4-6.1 mg O_2 L^{-1}; daily mean 4.2 mg O_2 L^{-1}) and a control (no cycles; daily mean 27ºC, 6.4 mg O_2 L^{-1}). Relative to controls, growth was significantly reduced in the DO treatment but not in the temperature treatments. Survival was similar in all treatments. Fish previously exposed to temperature cycles maintained faster growth rates and higher food intake than control fish when exposed to a simulated cold front. These results suggest that (1) ER may impart a physiological advantage to fish, (2) acclimation to oscillating DO environments is unlikely, and (3) field estimates of environmental characteristics based upon averaged daily point samples are inadequate for predicting fish growth.

KEY WORDS: **red drum, settlement, recruitment, temperature, dissolved oxygen, diel rhythms**

INTRODUCTION

Fish recruitment is a central issue for understanding fish population dynamics. Fish nursery areas are thought to play a critical role in determining adult population size by influencing year class recruitment.[1,2] Red drum is a valuable resource along the Gulf and East coast of North America. From late August through October, red drum produce numerous planktonic larvae in offshore waters near estuarine inlets. After two to three weeks in the plankton, the larvae settle in seagrass beds within estuaries.[3,4] Seagrass beds serve as settlement and primary nursery habitat for young red drum. Rapid larval growth during this extremely vulnerable period greatly increases the probability of survival of larvae,[5] and therefore recruitment.[6]

Seagrass beds are structurally complex and highly productive habitats which provide shelter for larval red drum as well as abundant food to fuel their rapid growth. However, these shallow estuarine habitats experience substantial fluctuations in environmental characteristics to which settled larvae will be exposed.[7] Environmental parameters may fluctuate widely in estuaries as a result of diel and tidal cycles, and stochastic events (storms and cold fronts). Diel temperature cycles of 3 to 5ºC have been reported in shallow estuarine environments.[8] Similarly, water cooling associated with frontal systems is common during the settlement season. Dissolved oxygen (DO) oscillations may be large in shallow subtropical seagrasses due to photosynthesis-respiration rhythms of benthic communities.[8] Temperature and DO fluctuations in seagrass beds

are perhaps the most important abiotic factors controlling growth during the larval period and hence recruitment to adult stocks.

Although the effects of temperature and DO on growth and survival have been studied intensively in numerous species, very few studies have addressed the effect of fluctuating environmental conditions (diel and tidal rhythms) and short-term atmospheric events (storms, cold fronts) on fish growth. The aim of the present study was two fold: 1) describe naturally occurring environmental rhythms (range and patterns of variation) within prospective red drum nursery habitats during the settlement period, and 2) determine the effects of temperature and DO cycles on larval growth and survival in laboratory studies.

MATERIALS AND METHODS

Identification of cyclical environmental patterns in red drum nursery habitats (seagrass beds):

Environmental data surveys were compiled from three locations in the Aransas-Corpus Christi estuary system during the fall of 2000. Two stations were located in shallow seagrass beds (SG1 and SG2) within the estuary where red drum larvae have been found previously.[3)] A third station (INLET) was located in the Aransas Pass Ship Channel linking the estuary to the Gulf of Mexico.

Temperature, dissolved oxygen (DO), pH, conductivity, turbidity and water height in the seagrass stations were recorded at 30 min intervals for six weeks by YSI multiparameter water quality data sondes placed within the seagrass canopy. The sondes were checked and data downloaded weekly to ensure proper working conditions and to prevent data loss. Environmental data from the INLET was obtained from the automated monitoring program established at the University of Texas Marine Science Institute Pier Laboratory. The study was coincident with the peak period of larval red drum settlement to the seagrass beds.

Effects of diel temperature and DO fluctuation on the growth and survival of settlement sized red drum:

Red drum larvae were initially raised in 300 L circular tanks. Larvae of approximately 5-6 mm SL (19-22 d) were randomly assigned to experimental tanks at a density of 5-10 larvae L^{-1}. Two groups of three replicate tanks (150 L) were used in all experiments. Tanks from each treatment were connected to a 150 L reservoir for water conditioning. Water was recirculated through each system 1.2 times $hour^{-1}$ to ensure a homogeneous environment between the three replicate tanks within treatments. Temperature, DO, pH and salinity were recorded in at least one tank from each treatment at 15 min intervals by YSI multiparameter water quality data sondes. Preliminary tests have shown that due to the high recirculation rate used, there are no differences in water quality among replicate tanks. To estimate treatment effects on fish growth a total of 20-25 fish from each tank were sampled at regular intervals throughout the experiment and the standard length (SL) measured to the closest 0.1 mm.

Diel temperature cycles. Settlement sized red drum larvae (4.9 mm standard length; SL) were exposed to two oscillating temperature treatments (OSC T_{Lo} and OSC T_{Hi}) (amplitudes: 3 and 6ºC; daily mean 27ºC) and their growth and survival compared to larvae held at constant temperature (CONTROL) (no cycles; daily mean 27ºC). Temperature cycles were simulated using timer-controlled heaters (total 1500 watts) and a water chiller unit connected to the reservoir. The experiment was repeated twice; once to test the high fluctuation and the other the low fluctuation regimen. The experiments lasted for 20-22 days.

Diel DO cycles . Settlement sized red drum larvae (5.2 mm standard length; SL) were exposed to an oscillating dissolved oxygen treatment (OSC DO) (range 2.4 to 6.1 mg O_2 L^{-1}) and growth and survival compared to larvae held in constantly well-oxygenated water (CONTROL) (6.4 mg O_2 L^{-1}). The experiments lasted for 22 days. An oxygen depletion column was placed between the reservoir and the experimental tanks to generate the desired fluctuating DO conditions. DO levels were controlled by the flow of nitrogen injected into the column. All tanks were kept at constant 27ºC.

Effects of storm related cooling on the growth and survival of red drum grown in stable and oscillating temperature:

Fish previously exposed to temperature cycles (OSC T) and fish grown at constant temperature (CONTROL) were subjected to a simulated cold front. Water temperature was dropped in all tanks from 27ºC to 17ºC over a 36 hour period. The temperature was kept at 17ºC for 48 hours (day 2 and 3) and then raised back to 27ºC on day 4. The experiment lasted for six days. Water parameters

were monitored at 15 min intervals as described previously. Samples were obtained five days before the beginning of the experiment (from the conditioning tanks) and on days 0, 3 and 6. Groups of 25-30 fish from each tank were measured on each sampling date. Food level was adjusted daily ensuring that fish ate to satiation. Every morning the tanks were carefully siphoned and the unconsumed food collected and dried at 60ºC for 36 h. Food consumption was then estimated by subtracting the food recovered (corrected for leaching) from the total food provided during the day.

RESULTS

Identification of cyclical environmental patterns in red drum nursery habitats (seagrass beds):

Well-defined diel environmental rhythms were observed in temperature (amplitude: 2 to 4.5ºC) and dissolved oxygen (DO) (range: 2.9-7.5 mg O_2 L^{-1}) in seagrass beds (Fig. 1). DO levels were high during daytime and decreased during the night to low levels (2-4 mg/L). Sporadic cooling episodes with temperature drops greater than 10ºC in two to three days were recorded

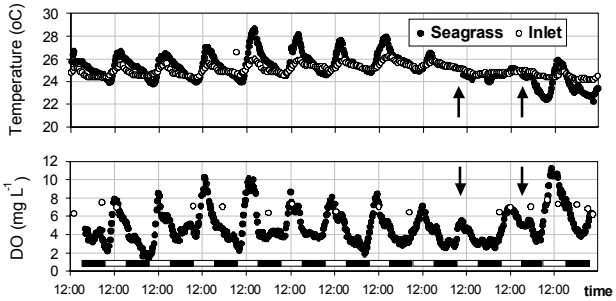

Fig. 1 Temperature and DO levels in the INLET and SG1. The arrows indicate the passage of cold fronts. Clear rectangles indicate daytime.

during the passage of cold fronts. Much less variability was observed in the others parameters in the survey (data not shown). Relative to seagrass beds, diel patterns and overall variability were greatly reduced in the INLET. Diel temperature fluctuation was only 1 to 1.5ºC. Diel DO cycles were absent in the inlet with DO levels remaining near to saturation levels at all times (Fig. 1). All other parameters remained nearly constant during the study (data not shown).

Effects of diel temperature and DO fluctuation on the growth and survival of settlement sized red drum:

Since the fish were exposed to different thermal treatments a cumulative degree index (15 min interval) was used. Relative to controls, growth was significantly reduced ($p<0.01$) in the DO treatment (Fig. 2) but no differences in growth relative to control fish were observed in either of the two temperature cycles used (Fig. 3). Survival was similar in all treatments.

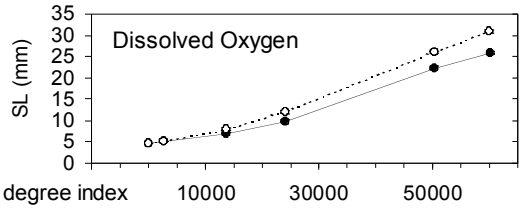

Fig.2 Growth of red drum under cyclic DO conditions (OSC DO; close circles) and stable conditions (CONTROL; open circles). Means ± SE (n=3).

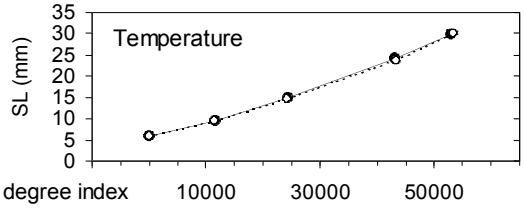

Fig.3 Growth of red drum under cyclic temperature conditions (OSC T_{Hi}; close circles) and stable constant (CONTROL; open circles). Means ± SE (n=3).

Effects of storm related cooling on the growth and survival of red drum grown in stable and oscillating temperature:

Fish previously exposed to temperature cycles maintained faster growth rates during the cooling phase (days 0-3) of the cold front ($p<0.05$). The difference in growth was no longer apparent by day six (Fig. 4). Food consumption was on average higher for fish previously grown under cycling conditions than control fish during the simulated cold front ($p<0.01$) (Fig. 5). No fish died during the 6-day experiment.

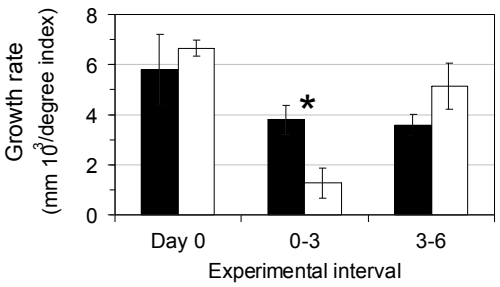

Fig.4 Growth rate of juvenile red drum during the simulated cold front experiment. Black columns represent fish previously exposed to temperature cycles. White columns represent CONTROL fish. Means ± SE (n=3). The asterisk indicates significant difference between groups ($p<0.05$).

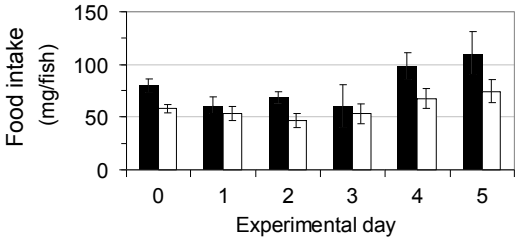

Fig.5 Food consumption during the simulated cold front experiment. Black columns represent fish previously exposed to temperature cycles. White columns represent CONTROL fish. Means ± SE (n=3).

DISCUSSION

Naturally occurring environmental cycles are linked to different patterns of energetic input within the relatively small nursery habitat. Circadian rhythms arise from day-night and tidal cycles while stochastic fluctuation are linked to meteorological disturbances. Diel temperature and DO cycles weaken or completely disappear on cloudy days. Both cycles were clearly related to irradiation. In shallow, productive seagrass beds there is an extensive primary productivity (photosynthesis) [9] and respiration confined to a small volume of water, resulting in large diel DO changes.

Red drum larvae are very tolerant of temperature fluctuations. Diel temperature fluctuation in excess of that found in our environmental surveys did not impair growth in the laboratory. Nevertheless the simulated cold front experiment seems to suggest that exposure to diel temperature rhythms may impart a physiological memory to the fish that allows for faster growth compared to CONTROLS during rapid cooling events. Food consumption during that experiment was on average higher in fish previously exposed to diel temperature fluctuation. However, no significant differences were detected at any particular day. Herzka [10] found that the isotopic composition of settlement sized red drum changed significantly faster in larvae stocked in the field than siblings held in laboratory and concluded that metabolic turnover (changes in isotopic composition not explained by growth) was accelerated in the caged fish. It can be inferred that the cost of growth (i.e. energy used per unit weight gain) was higher in the natural environment. Since no predation and unrestricted food access was assumed in both caged and laboratory fish, it seems possible to hypothesize that environmental fluctuations may drive these physiological differences in growth.

Fish in the OSC DO grew significantly less than CONTROL fish, while survival was not affected. Taylor and Miller[11] reported growth reduction in southern flounder (*Paralichthys lethostigma*) cyclically exposed to nocturnal hypoxia (2.8 mg O_2 L^{-1}). Although the lowest DO concentration used in the experiment (2.4 mg O_2 L^{-1}) was similar to the lowest observed values in the seagrass, these levels were reached only occasionally in the seagrass beds. The levels administered in the laboratory were well into the range where oxygen acts as a limiting factor resulting in retarded growth. A reduced growth potential is predicted in estuarine areas where strong diel DO cycles are present even when daytime DO levels are high. These experiments also indicate that the use of field estimates of environmental characteristics based solely upon averaged daily samples is inadequate for predicting fish growth in the pristine seagrass beds studied.

The benefit of evolving an estuarine dependent lifestyle strongly argues for an overall increased growth potential in these fluctuating environments and the possibility for specific adaptations to meet environmental challenges of the nursery habitat. Larval growth and survival in fluctuating environments of estuaries is a crucial aspect for understanding recruitment variability/mechanism and ultimately fish population dynamics in estuarine dependent species like red drum.

ACKNOWLEDGMENTS

This work has being supported in part by contributions from Perry R. and Nancy Lee Bass, and by the Texas Water Resource Institute (TAMU). The authors thank M.C. Alvarez, S. Applebaum, S. Holt, I. McCarthy, C. Pratt, and M. Tanaka for their comments and continuous support during this study.

REFERENCES

1. Underwood A.J. and Fairweather P.G. Supply-side ecology and benthic assemblages. Trends in Ecology and Evolution. 1989; **4**(1): 16-20
2. Sale P.F. Recruitment of marine species: Is the bandwagon rolling in the right direction? Trends in Ecology and Evolution. 1990; **5**(1): 25-27
3. Rooker J.R. and Holt S.A. Utilization of subtropical sea-grass meadows by newly settled red drum (*Sciaenops ocellatus*), patterns of distribution and growth. Marine Ecology Progress Series. 1997; **158**: 139-149
4. Rooker J.R., Holt S.A., Holt G.J. and Fuiman L.A. Spatial and temporal variability in growth, mortality, and recruitment potential of post-settlement red drum (*Sciaenops ocellatus*) in a subtropical estuary. Fisheries Bulletin. 1999; **97**: 581-590
5. Fuiman L.A. and Magurran A.E., 1994. Development of predator defenses in fishes. Rev. Fish Biol Fish **4**: 145-183
6. Houde E.D. Comparative growth, mortality, and energetics of marine fish larvae: temperature and implied latitudinal effects. Fisheries Bulletin. 1989; **87**(3): 471-495
7. Robbins B.D. and Bell S.S. Dynamics of a subtidal seagrass landscape: Seasonal and annual change in relation to water depth. Ecology 2000; **81**(15): 1193-1205
8. Beck N.G. and Bruland K.W. Diel biogeochemical cycling in a hyperventilating shallow estuarine environment. Estuaries 2000; **23**(2): 177-187
9. Moncreiff C.A., Sullivan M.J. and Daehnick A.E. Primary production dynamics in seagrass beds of Mississippi Sound: the contributions of seagrass, epiphytic algae, sand microflora, and phytoplankton. Marine Ecology Progress Series. 1992; **87**: 161-172
10. Herzka S.Z. and G.J. Holt. Changes in isotopic composition of red drum (*Sciaenops ocellatus*) larvae in response to dietary shifts: potential applications to settlement studies. Can. J. Fish Aquat. Sci. 2000; **57**: 137-147
11. Taylor J.C. and Miller J.M. Physiological performance of juvenile southern flounder, *Paralichthys lethostigma* (Jordan and Gilbert, 1884), in chronic and episodic hypoxia. Journal of Experimental Marine Biology and Ecology. 2001; **258**: 195-214

Resolution of Fluvial Sediment Sources, Residence Times and Resuspension Using Lithogenic, Atmospheric and Cosmogenic Radionuclides, Bayou Loco, Texas

Basic Information

Title:	Resolution of Fluvial Sediment Sources, Residence Times and Resuspension Using Lithogenic, Atmospheric and Cosmogenic Radionuclides, Bayou Loco, Texas
Project Number:	2001TX3281B
Start Date:	3/1/2001
End Date:	2/28/2002
Funding Source:	104B
Congressional District:	10
Research Category:	Not Applicable
Focus Category:	Sediments, Surface Water, Radioactive Substances
Descriptors:	sediment, fingerprinting, resuspension, residence time, radionuclides
Principal Investigators:	Kevin Yeager

Publication

1. Yeager, K.M., Santschi, P.H., Phillips, J.D. and B.E. Herbert, 2002, Sources of alluvium in a coastal plain stream based on radionuclide signatures from the 238U and 232Th decay series, Water Resources Research, vol. 38, no. 11, p. 24-1 - 24-11.
2. Yeager, Kevin M., Peter H. Santschi, Jonathan D. Phillips, Bruce E. Herbert. 2002. Sources of alluvium in a coastal plain stream based on radionuclide signatures from the 238U and 232 TH decay series. Water Resources Journal, v. 38, n. 11.

Sources of alluvium in a coastal plain stream based on radionuclide signatures from the ^{238}U and ^{232}Th decay series

Kevin M. Yeager,[1,2] Peter H. Santschi,[3] Jonathan D. Phillips,[4] and Bruce E. Herbert[1]

Received 18 September 2001; revised 19 April 2002; accepted 19 April 2002; published 16 November 2002.

[1] Discerning alluvial sources and their change over time or distance is a fundamental question in hydrology and geology, often critical in identifying impacts of human and natural perturbations on fluvial systems. Surfaces of upland interfluves and subsoils, sources of alluvium in the lower Loco Bayou basin, Texas, were distinguished using the isotope ratios ^{226}Ra/^{232}Th, ^{226}Ra/^{230}Th, and ^{230}Th/^{232}Th. Channel alluvium indicates a transition from interfluve surface to subsoil sources during flood (subsoil ~34% to ~91%, over about 8 km) and bank-full stages (subsoil ~9% to ~74%, over about 12 km), with distance downstream. These results indicate strong coupling between hillslope and channel processes, reflecting land use change from forested to agricultural, concentrated in lower Loco Bayou. This methodology shows that sediment sources can be differentiated based upon landscape placement where lithologic contrast is absent. The geochemistry, long half-lives, and fractionation of ^{238}U and ^{232}Th decay series radionuclides during pedogenic and fluvial processes in humid climates suggest that these methods are applicable in a wide variety of fluvial systems. *INDEX TERMS:* 1040 Geochemistry: Isotopic composition/chemistry; 1803 Hydrology: Anthropogenic effects; 1815 Hydrology: Erosion and sedimentation; 1824 Hydrology: Geomorphology (1625); *KEYWORDS:* natural radionuclides, fingerprinting, alluvium, source apportioning

Citation: Yeager, K. M., P. H. Santschi, J. D. Phillips, and B. E. Herbert, Sources of alluvium in a coastal plain stream based on radionuclide signatures from the ^{238}U and ^{232}Th decay series, *Water Resour. Res.*, *38*(11), 1242, doi:10.1029/2001WR000956, 2002.

1. Introduction

[2] Discerning the origin of fluvial sediment and source fluctuations over time is a critical question in hydrology, geology, geomorphology, and water resource management. Knowledge of fluvial sediment sources is important in many fields of environmental science, as sediment affects the fate and transport of pollutants [*Macklin et al.*, 1997; *Marcus et al.*, 2001], water quality [*Langedal*, 1997; *Swank et al.*, 2001], ecological health and diversity [*Rice et al.*, 2001; *Zajac and Whitlatch*, 2001], and reservoir design and sustainability [*Valero-Garces et al.*, 1999], to name just a few. In the U.S., for example, many specific water quality issues such as section 305 (Clean Water Act), nonpoint source pollution assessments and the monitoring of total maximum daily loads for sediment and sorbed pollutants may hinge directly on determining the source of sediment delivered to streams. Sources of sediment to river systems are not simple to measure or model at any scale. The case study presented here focuses on the development of methods for the delineation and quantification of sources of alluvial sediments in transient storage within an east Texas fluvial system. Spatial and temporal variations, both natural (climate and tectonics) and anthropogenic (agriculture and urbanization), influence the source flux, transport rate and residence time of alluvial sediments, which complicates field-based or mathematical attempts to address this question [*Roberts and Church*, 1986; *Kelsey et al.*, 1987; *Hoey*, 1992].

1.1. Previous Research

[3] Sources of alluvium to rivers have been assessed using a variety of tools including soil and sediment mineralogy [*Phillips*, 1992; *Woodward et al.*, 1992], combinations of lithogenic and atmospheric radionuclides [*Olley et al.*, 1993, 1997], heavy metals [*Passmore and Macklin*, 1994; *Lecce and Pavlowsky*, 2001], petrology [*Schneiderman*, 1995], and mineral magnetics [*Caitcheon*, 1998], and combinations of fallout radionuclides and geochemistry (C and N) [*Nagle and Ritchie*, 1999]. While this list is more illustrative rather than exhaustive, the common theme is that sediment source areas within a watershed have different physicochemical, mineralogical and other properties that may allow for an estimate of the relative contribution of these sources to stream sediments.

[4] Fallout radionuclides (^{137}Cs, ^{210}Pb, ^{7}Be) have been used to investigate soil erosion [*Quine and Walling*, 1991; *Branca and Voltaggio*, 1993; *Zhang et al.*, 1998], fluvial sediment yields and sediment budgets [*Allison et al.*, 1998; *Walling*, 1999], and resuspension and residence times [*Wallbrink et al.*, 1998; *Bonniwell et al.*, 1999]. Radionuclides in the ^{238}U and ^{232}Th decay series have also been used to address a range of problems in geology and fluvial geo-

[1]Department of Geology and Geophysics, Texas A&M University, College Station, Texas, USA.
[2]Now at Laboratory for Oceanographic and Environmental Research, Department of Oceanography, Texas A&M University, Galveston, Texas, USA.
[3]Laboratory for Oceanographic and Environmental Research, Department of Oceanography, Texas A&M University, Galveston, Texas, USA.
[4]Department of Geography, University of Kentucky, Lexington, Kentucky, USA.

0043-1397/02/2001WR000956$09.00

morphology, including provenance determination of coastal sediments [*Roberts and Plater*, 1999], fluvial overbank sedimentation rates [*Murray et al.*, 1990], and resolving fluvial sediment sources [*Olley and Murray*, 1994] and source fluxes [*Olley et al.*, 1993]. These radionuclides have been used either solely [*Olley*, 1994; *Olley et al.*, 1997] or together with fallout radionuclides [*Olley et al.*, 1993; *He and Owens*, 1995] to address fluvial source and transport problems. Additional examples can be found in the compilation on this subject by *Ivanovich and Harmon* [1992].

1.2. Secular Disequilibrium

[5] Use of radionuclides as tags to fingerprint sediment sources to fluvial systems is based on the application of secular disequilibrium, where the daughter concentration at any time t is

$$ {}^{t}N_d = N_p + [{}^{0}N_d - N_p]e^{-\lambda_d t}, \quad (1) $$

where ${}^{t}N_d$ and ${}^{0}N_d$ are daughter concentrations at time t and t = 0, respectively, N_p is the initial parent concentration, λ_d is the daughter decay constant, and e is the Naperian constant (2.718) [*Olley et al.*, 1997].

1.3. Thorium and Radium: Chemistry and Fractionation

[6] A principal assumption in tracer studies is that the marker(s) are conservative over a wide range of conditions, in this case, moving with sediment, while retaining the original source signature. Thorium is essentially insoluble ($<1 \times 10^{-4}$ ppb) [*Kaufman*, 1969], in surface water and does not undergo changes in oxidation state under normal *E*h-pH conditions [*Ivanovich and Harmon*, 1982]. It has a +4 charge, tends to strongly sorb onto suspended particulate matter, and thus it is almost exclusively transported on particulate matter in rivers [*Ivanovich and Harmon*, 1992]. Radium exists in one oxidation state in nature, Ra^{+2}. Its mobility is limited by coprecipitation in barite, calcite [*Tanner*, 1964], and hydrous oxides of Fe and Mn, adsorption (clays, quartz, and Fe (III) oxyhydroxides [*Riese*, 1982; *Ames et al.*, 1983]), and ion exchange. Radium in freshwater is strongly adsorbed to particulates.

[7] The relatively short-lived radionuclides such as ^{7}Be (53.5 days), ^{210}Pb (22 years), and ^{137}Cs (30 years), which are often used to assess geomorphic processes, may decay before reorganization and transport by pedogenic processes. Longer-lived radionuclides in the ^{238}U and ^{232}Th decay series can be profoundly fractionated and re-organized within surface environments over geologic timescales, especially where chemical, physical and biological processes are intense. Significant fractionation of radium isotopes from other U-series nuclides during weathering has been documented [*Rosholt*, 1982; *Muhs et al.*, 1990]. *Michel* [1984] showed recent additions of radium to surface soils based on radium excesses over ^{230}Th, without addressing the mechanism(s) responsible. Vegetation has a significant affinity for radium [*Popova et al.*, 1964; *Taskaev et al.*, 1977; *Linsalata*, 1994] and has been shown to be directly responsible for enrichment of radium in surface soils [*Greeman et al.*, 1999]. In contrast, thorium depletion in surface soils has been observed in a variety of settings and locations, including soils in California [*Hansen and Huntington*, 1969], soils in the Mississippi River drainage basin [*Rosholt et al.*, 1966], acidic soils observed by *Gueniot* [1983], and soils throughout the eastern United States [*Greeman et al.*, 1999]. *Greeman et al.* [1999] determined from soil extractions that depletion of thorium in surface horizons results in part from depletion of radionuclide-rich Fe-oxides via some combination of colloidal particle transport and solubilization of this phase. An additional possibility is that thorium is leached from the surface as dissolved organic complexes, as suggested by *Langmuir and Herman* [1980].

1.4. Experimental Approach

[8] This research is focused on delineation of two primary alluvial source compartments, surfaces of upland interfluves, and subsoils. Specifically, the surface component coincides with the upper ~20 cm of the soil profile, where organic content and vascular plant activity is greatest. Subsoil then is that portion of the soil profile which is found from ~20 cm depth to bedrock. Bedrock, where exposed, can also serve as a source of sediment to channel alluvium and is therefore also considered a part of the "subsoil" component. When related to alluvium in transient storage, these compartments allow the dominant erosion processes, sheet wash versus gully development at the watershed scale to be distinguished. ^{230}Th/^{232}Th values in soils and parent material have been shown to be equivalent [*Olley and Murray*, 1994], suggesting that these isotopes can be used to fingerprint fluvial sediment sources [*Olley et al.*, 1997]. It is expected that this ratio may also be useful in distinguishing contributions from surfaces of upland interfluves versus subsoil compartments. ^{226}Ra/^{232}Th has also been used as a source marker for soils and sediment [*Murray et al.*, 1990, 1991; *Olley et al.*, 1997]. ^{226}Ra/^{230}Th is also utilized here as it should mirror ^{226}Ra/^{232}Th results as the ratios of these elements are chemically equivalent, differing only in the half-life of the thorium nuclide and decay series origins for each set of ratios. Ra/Th ratios are anticipated to delineate surface and subsoil contributions, if surface radium enrichment coincides with thorium depletion.

[9] Given that these radionuclide signatures evolve in soils in response to external factors and in situ biogeochemical and pedogenic processes, and yet remain conservative over the relatively short timescales of erosion and fluvial transport, the radionuclide signatures of alluvial sediments reflect their original source compartment. Thus the primary objective of this case study is to test the use of isotope ratios of radium and thorium to fingerprint alluvium by source compartment as opposed to source lithology or discrete spatial location in a developed and hydrologically managed basin.

[10] The specific objectives of this study are to (1) use ^{238}U and ^{232}Th series radionuclides to fingerprint sediment source compartments within the lower Loco Bayou basin, (2) examine the relative importance of sheet wash and gully development on sediment erosion as a function of space and hydrologic flow, and (3) examine geomorphic and anthropogenic causes for systematic change in sediment sources of channel alluvium as a function of distance.

2. Materials and Methods

2.1. Study Basin

[11] The field site for this case study is the lower section of the Loco Bayou watershed, below Lake Nacogdoches in Nacogdoches County, Texas (Figure 1). The entire basin

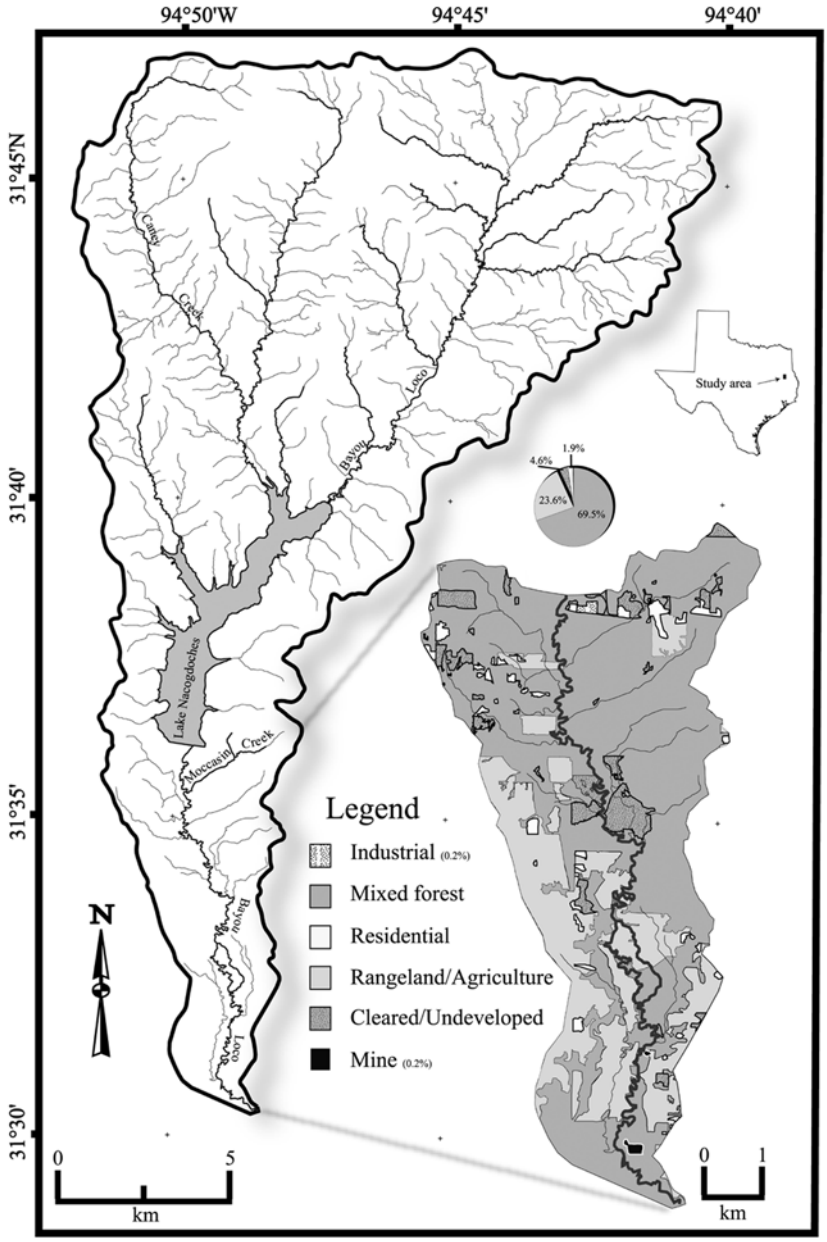

Figure 1. Loco Bayou watershed. The land use map is created from ground reconnaissance and 1 m resolution Digital Orthophoto Quarter-Quad images from 1996 and 1997.

has an area of 265 km^2, 9 km^2 of which is occupied by Lake Nacogdoches, with the lower section covering 37 km^2. Lake Nacogdoches provides the bulk of the drinking water for the city of Nacogdoches. When last surveyed in 1994, the lake had a storage capacity of 48,731,859 m^3, representing a 6.6% reduction in capacity since completion in 1976 (see the List of Lake Surveys Completed by The Texas Water Development Board Volumetric Survey Program at http://www.twdb.state.tx.us/assistance/lakesurveys/compsurveys.htm).

[12] Loco Bayou is in the Pineywoods region of the east Texas coastal plain. The climate is subtropical, with mean annual precipitation of 1200–1500 mm [*National Oceanic and Atmospheric Administration*, 2001]. While variable over the latter half of the 1990s because of consecutive droughts in the state, the distribution of precipitation is commonly bimodal in this region. The primary wet season here corresponds to January through April, often with a secondary peak in precipitation in early to late fall, with the summer months being the driest. The lower basin is predominantly forested (Figure 1); the main land use is agriculture, with minor portions of the basin utilized for residential areas, gravel mining, and forest clear-cuts, which vary spatially year to year. Total relief here is ~60 m; slopes prevail bordering the dam and valley walls in the north where forests dominate land cover. The southern half of the basin widens into a gently undulated floodplain, much of which has been cleared and utilized for agriculture.

[13] The bedrock geology of the lower basin is dominated by the Eocene Weches Formation, a glauconitic marine sand

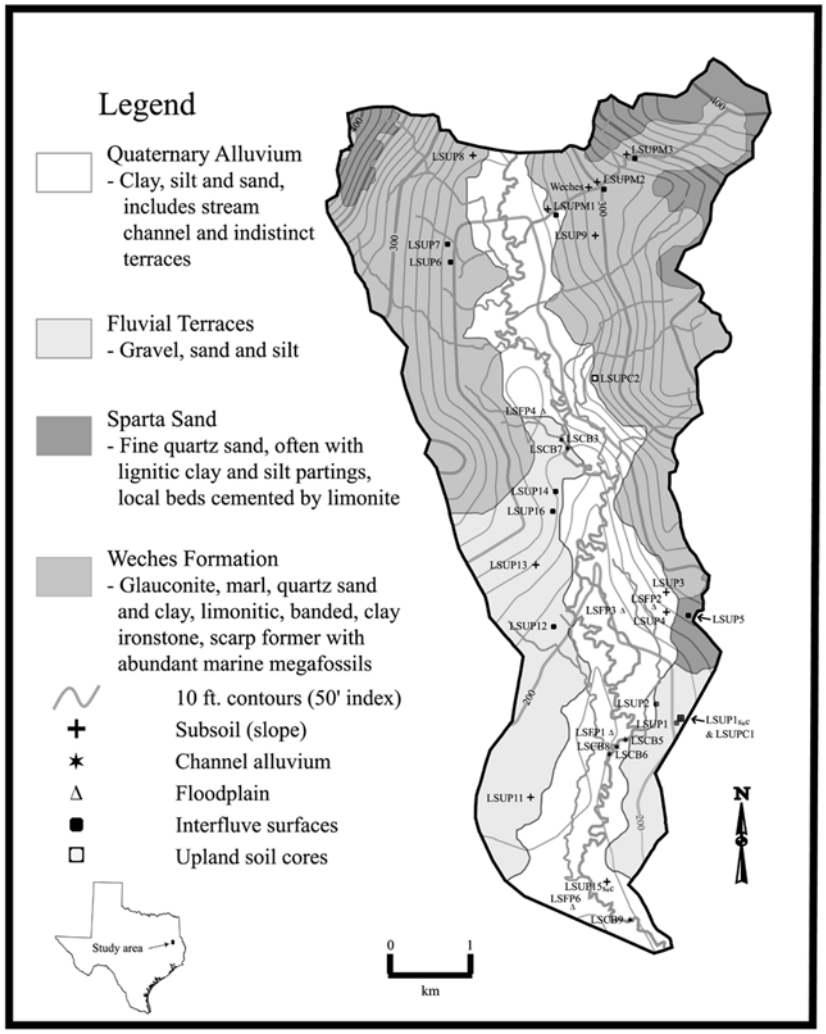

Figure 2. Lower Loco Bayou watershed geology and sample locations. The bedrock geology is digitized from the 1:250,000 scale Palestine sheet [*Shelby et al.*, 1968].

(Figure 2). This unit is exposed over ~0.5 km down reach of a culvert on Moccasin Creek (LSUPM2), a primary tributary of Loco Bayou that enters ~1 km south of the dam (Figure 2). Isolated patches of the up section, Eocene Sparta Sand, a limonitic coastal unit, can be found mainly in the headlands near the dam, but no outcrops were discovered. The channel itself is underlain by Quaternary alluvium, and the lowermost portion of the basin, near the confluence with the Angelina River, is bordered by Quaternary fluvial terrace deposits. The main channel can be characterized as degradational just south of the dam, where basal scour and tilted hardwoods indicate erosion and downcutting. Similar observations are made on the lower half of Moccasin Creek (Figure 2), south of the culvert. The Weches Formation is exposed here and incised; as one continues downgrade, bedrock is quickly buried, but evidence of downcutting persists, including steep channel walls over 3 m high at base flow, tilted hardwoods, and large rotational slumps. Moving south from confluence with Moccasin Creek, the channel meanders through cohesive floodplain loams with some evidence of lateral scour and spatially constrained channel degradation most usually associated with cattle crossings and bridges. The iron-rich rocks are expressed directly at Loco Bayou in the soils, which are categorized into three associations: the upland ridge, red land belt loams of the Nacogdoches-Trawick, sandier, hill slope soils of the Cuthbert-Tenaha, and terrace loams of the Attoyac-Bernaldo-Besner associations [*Dolezel*, 1980].

2.2. Particle Size Variability

[14] Differences in particle surface area have been shown to influence radionuclide adsorption [*Megumi et al.*, 1982], which is particularly important in fluvial systems, where transport results in sorting of materials by particle size and density [*Paola et al.*, 1992]. While an individual radionuclides activity concentration is a function of substrate surface area, daughter/parent ratios generally remain constant within analytical uncertainty [*Murray et al.*, 1990, 1991; *Olley et al.*, 1997]. This approach has been used when considering fallout radionuclides including ^{210}Pb, ^{137}Cs and ^{7}Be [*Bonniwell et al.*, 1999], and lithogenic radionuclides including radium and thorium [*Olley et al.*, 1993, 1997] in fluvial systems. We have attempted to minimize the effects of particle size variations by both analyzing a specific range

of particle sizes (<0.5 mm) and employing daughter/parent ratios.

2.3. Sampling

[15] Samples of channel alluvium, floodplain sediment and source area soils were collected from the near surface (0–2 cm). Source area samples were focused at actively eroding sites throughout the basin, concentrating on surfaces of upland interfluves and exposed subsoils on slopes (Figure 2). All samples were combined in the field, consisting of 8–10 subsamples collected over an approximately 10 m^2 area. Five samples of ''fresh'' bedrock were collected from the Weches Formation, where it outcrops in the channel of Moccasin Creek; these were combined and analyzed. Two soil cores were also collected. Alluvium is assumed to be derived from (1) soil erosion, (2) redistribution of sediments in storage, or, most likely, (3) a combination of processes 1 and 2, as the dam effectively limits the quantity of sediment available from the upper watershed [*Phillips*, 2001]. All source compartment and floodplain samples were collected from winter of 1999 through spring of 2001; sampling of alluvium was concentrated during flood (January–February 2001) and bank-full (April 2001) stages. Three water samples were collected at alluvial sampling sites during flood stage to assess radium in solution coinciding with annual maximum discharge and sediment transport capacity. Water samples were sequentially filtered in the field through 50, 20, 5, and 0.2 μm filters to remove suspended sediments and finally passed through two MnO_2 impregnated 0.5 μm filters to efficiently scavenge Ra in solution, as described by *Baskaran et al.* [1993]. MnO_2 filters were subsequently ashed and gamma counted.

2.4. Sample Processing and Radiochemistry

[16] Bulk samples were dried at 70°–80°C for 24 hours, then gently disaggregated with mortar and pestle and passed through 2 mm and 0.5 mm sieves. High-resolution gamma spectrometry was employed to resolve ^{228}Ra ($t_{1/2}$ = 5.75 years, via ^{228}Ac Eγ = 911 keV) and ^{226}Ra ($t_{1/2}$ = 1602 years, via ^{214}Pb Eγ = 352 keV), using Canberra HPGe well detectors and a multichannel analyzer, model 747. Samples were contained in plastic test tubes (inner diameter 1.3 cm and height 9.4 cm) and sealed with epoxy for 20 days in order for equilibrium between ^{226}Ra and its volatile daughter ^{222}Rn ($t_{1/2}$ = 3.8 days), an inert gas, to be reached. Owing to the range of sediment samples, standards were prepared and run on each detector in several geometries to determine representative efficiencies for each nuclide. Counting and efficiency errors based on standards were less than ±2%.

[17] Alpha spectrometry was employed to resolve ^{232}Th ($t_{1/2}$ = 1.39 × 10^{10} years), ^{230}Th ($t_{1/2}$ = 7.52 × 10^4 years), and ^{228}Th ($t_{1/2}$ = 1.91 years), using a Canberra alpha spectrometer, model 7404, mated to a Canberra multichannel analyzer, model 8224. Thorium samples were spiked with ^{229}Th tracer and completely digested (HF, HCL, and HNO_3) over heat. The solution was passed through two sets of anion exchange columns to selectively isolate thorium isotopes, as described by *Buesseler et al.* [1992]. The elution was acidified with H_2SO_4 and plated onto stainless steel planchets via sulfate electrodeposition prior to counting, according to methods described by *Hallstadius* [1984] and *Buesseler et al.* [1992]. Chemical recoveries for thorium isotopes averaged >70%.

[18] Relative source contributions were determined using a simple mixing model [*Olley et al.*, 1993];

$$AX + BY = C, \tag{2}$$

where A and B are the Ra/Th values for subsoil and interfluvial surface sources, respectively, C is the Ra/Th ratio of the output mix, and X and Y are the relative contributions of each, where X + Y = 1. This model does not consider nonlinearity in the ratios of the two independently varying activities [*Faure*, 1986; *Olley et al.*, 1993; *Kendall and McDonnell*, 1998]. The deviation from linearity is small for the measured range of ^{226}Ra, ^{230}Th, and ^{232}Th values and resultant ratios.

3. Results and Discussion

3.1. Sediment Sources

[19] Data for all samples are shown in Table 1, summary statistics and applied ratios are shown in Table 2, and end-member mixing results for alluvial samples are shown in Table 3. Core data (Figure 3) support Ra/Th fractionation in the soils of lower Loco Bayou, suggesting radium depletion coinciding with thorium enrichment with depth. Mean ^{226}Ra/^{232}Th, and ^{226}Ra/^{230}Th$_2$ signatures for interfluve surfaces versus subsoil compartments are statistically distinguishable, passing equal variance *t* tests, where $\alpha = 0.05$ ($p_1 = 0.003$ and $p_2 = 0.001$) (Figures 4a and 4b). While the difference between ^{230}Th/^{232}Th signatures for these compartments is not statistically significant, Figure 4c does graphically reflect Th enrichment at depth and depletion at the surface. Some signature overlap of these compartments is observed and was expected because of their contiguous relationship in the field.

[20] All three river water samples yielded no appreciable dissolved radium concentration during high discharge. A maximum value for ^{226}Ra of 0.001 Bq/L was determined, which falls at the lower range of observed concentrations in U.S. rivers [*Kraemer and Genereux*, 1998]. Also, examining particulate ^{228}Th/^{228}Ra data shows that although relatively enriched with ^{228}Th, the ratios are consistent within the mean error in alluvial samples (Figure 5). This ratio would change down-reach if recent adsorption of ^{228}Ra ($t_{1/2}$ = 5.75 years) had occurred, as ^{228}Th ($t_{1/2}$ = 1.91 years) would have insufficient time to grow into equilibrium with the recently adsorbed parent [*Olley et al.*, 1997]. These data support radium immobility in freshwater and a closed system following removal from the soil profile.

[21] These data unanimously show that subsoil materials become the dominant source of alluvium with increasing distance down reach from the dam (Table 3). Both ^{226}Ra/^{232}Th and ^{226}Ra/^{230}Th (Figures 6a and 6b) are in reasonable agreement, with ^{230}Th/^{232}Th data supporting the same trend (Figure 6c), while exhibiting linearity reflective of equilibrium. Differences in alluvial signatures between flood and bank-full stages are also observed. While no clear trend is evident for floodplain samples, values for their ratios are constrained by source end-members (Table 2).

3.2. Human Agency and Source Flux: Cause and Effect?

[22] Coupling of channel and hillslope processes can be strong, where material is transferred from hillslope to

Table 1. Activity Data for All Samples, With Propogated Errors as Discussed by *Choppin et al.* [1995][a]

Type	Sample	^{230}Th	^{226}Ra	^{232}Th	^{228}Ra	^{228}Th
Interfluvial	LSUP1	31.50 ± 3.01	36.90 ± 2.08	31.78 ± 3.01	25.83 ± 3.00	32.79 ± 3.09
	LSUP2	27.37 ± 2.36	31.64 ± 1.89	27.00 ± 2.31	20.22 ± 2.22	31.57 ± 2.65
	LSUP5	30.24 ± 2.24	26.56 ± 2.00	28.64 ± 2.12	15.86 ± 1.91	28.91 ± 2.14
	LSUP6	35.16 ± 2.68	27.10 ± 2.03	48.66 ± 3.64	21.40 ± 2.56	47.10 ± 3.54
	LSUP7	28.45 ± 2.15	23.48 ± 1.24	37.55 ± 2.78	34.92 ± 3.49	35.91 ± 2.67
	LSUP12	39.59 ± 3.14	36.90 ± 2.52	41.50 ± 3.26	30.52 ± 2.79	42.53 ± 3.34
	LSUP14	33.25 ± 2.52	41.12 ± 2.77	48.18 ± 3.57	29.86 ± 2.97	45.71 ± 3.39
	LSUP16	25.86 ± 2.41	45.13 ± 2.72	35.12 ± 3.06	39.91 ± 3.57	36.59 ± 3.18
	LSUPM1	41.00 ± 3.27	28.17 ± 1.55	77.15 ± 5.76	41.09 ± 3.38	82.33 ± 2.91
	LSUPM2	24.91 ± 1.97	23.66 ± 1.28	37.56 ± 2.84	24.96 ± 2.25	38.94 ± 2.94
	LSUPM3	20.84 ± 1.70	20.63 ± 0.90	22.89 ± 1.84	18.97 ± 1.75	22.85 ± 1.85
Subsoil	Weches Formation[b]	52.81 ± 4.16	19.62 ± 1.58	57.45 ± 4.50	84.79 ± 8.09	55.77 ± 4.34
Bedrock	LSUP1[c]	51.20 ± 3.63	43.33 ± 2.37	56.49 ± 3.98	48.93 ± 3.74	53.12 ± 3.76
Slope	LSUP1[d]	49.66 ± 3.61	38.23 ± 3.29	54.44 ± 3.94	55.06 ± 4.92	49.64 ± 3.61
Colluvium	LSUP3[d]	27.83 ± 2.48	20.81 ± 1.37	29.68 ± 2.62	18.23 ± 2.26	32.67 ± 1.53
	LSUP4[d]	38.40 ± 3.16	24.39 ± 0.97	42.91 ± 3.49	15.33 ± 1.29	47.30 ± 3.81
	LSUP8[d]	77.86 ± 5.71	47.13 ± 2.93	88.09 ± 6.43	52.87 ± 3.31	87.03 ± 6.36
	LSUP9[d]	53.91 ± 3.66	43.35 ± 2.56	95.94 ± 6.44	78.01 ± 4.07	95.77 ± 6.43
	LSUP11[d]	51.79 ± 4.29	46.89 ± 4.45	59.83 ± 4.86	62.12 ± 5.45	57.85 ± 4.72
	LSUP13[d]	53.76 ± 4.26	46.36 ± 2.93	63.92 ± 5.01	43.46 ± 3.89	64.14 ± 5.03
	LSUP15[d]	73.47 ± 6.15	31.66 ± 1.85	93.32 ± 7.56	29.06 ± 1.76	80.87 ± 3.47
	$LSUP15_c$	74.86 ± 6.64	44.08 ± 2.25	87.91 ± 5.87	55.62 ± 4.26	98.44 ± 7.65
	LSUPM1[d]	28.08 ± 2.18	22.67 ± 1.13	60.63 ± 4.41	44.92 ± 3.98	60.90 ± 5.59
	LSUPM2[d]	38.40 ± 2.8	22.97 ± 0.96	52.98 ± 3.79	33.17 ± 3.18	56.04 ± 3.77
	LSUPM3[d]	35.75 ± 2.55	22.76 ± 1.03	50.06 ± 3.52	34.89 ± 3.07	49.71 ± 4.92
Floodplain	LSFP1	35.41 ± 2.08	45.24 ± 2.19	35.13 ± 1.64	51.95 ± 2.42	43.37 ± 3.70
	LSFP2	37.15 ± 3.08	24.42 ± 2.28	42.66 ± 3.48	23.30 ± 2.91	42.40 ± 3.46
	LSFP3	29.10 ± 2.12	41.85 ± 2.70	37.69 ± 2.71	36.49 ± 3.24	39.59 ± 2.85
	LSFP4	65.10 ± 5.30	38.82 ± 1.43	61.47 ± 1.43	29.08 ± 2.53	59.00 ± 4.84
	LSFP6	77.82 ± 6.94	52.39 ± 3.24	90.36 ± 7.93	59.09 ± 5.31	99.08 ± 8.63
Alluvium	LSCB3	44.14 ± 3.67	40.17 ± 1.66	53.45 ± 4.32	40.93 ± 1.49	52.60 ± 4.26
	LSCB5	52.56 ± 4.24	39.48 ± 0.79	61.42 ± 4.87	34.65 ± 1.63	60.59 ± 4.81
	LSCB6	66.44 ± 3.19	42.57 ± 1.87	70.48 ± 6.94	39.90 ± 1.98	69.06 ± 6.86
	LSCB7	21.24 ± 1.88	20.57 ± 1.24	24.72 ± 2.13	21.71 ± 2.87	26.66 ± 2.29
	LSCB8	42.66 ± 2.96	36.16 ± 1.56	48.59 ± 4.10	34.81 ± 3.71	57.61 ± 4.29
	LSCB9	69.05 ± 3.64	47.65 ± 2.66	67.08 ± 4.94	41.74 ± 5.04	65.63 ± 4.85

[a] Activity data for all samples are given in Bq/kg.
[b] Sample is from bedrock.
[c] Sample is from colluvium.
[d] Sample is from slope.

channel rapidly and continuously, resulting in a perturbation sensitive channel. Conversely, a buffered system has significant floodplain or valley fill deposits, protecting hillslopes from basal erosion, while isolating the river from hillslope sediment supply. Upon initial inspection, lower Loco Bayou would appear buffered based on field observations. Exceptions are not spatially extensive and can be found immediately south of the dam and of a highway culvert that bisects Moccasin Creek at LSUPM2 (Figure 2). At these locations, channel degradation, basal scour, and tilted hardwoods all indicate erosion and downcutting, typical observations immediately downgrade from a dam or culvert. Moving south from the dam, Loco Bayou quickly spreads out into a meandering floodplain stream moving through loamy soils bordered by gentle terrain. *Phillips* [2001] and *Phillips and Marion* [2001] make similar observations, characterizing the floodplain of the lower basin as aggradational, with no apparent lack in sediment supply, estimating sedimentation by soil stratigraphic and dendrogeomorphic methods to be 44 mm/yr at the same location where the northernmost alluvial samples were collected for this research.

[23] Radionuclide data, however, suggest that hillslope and channel processes are strongly coupled. Radionuclide signatures indicate that alluvium is increasingly derived from subsoil with distance down reach for both flood and bank-full stages. The bulk of the northern half of the basin above the first set of alluvial samples is densely forested, and save for the areas immediately around the dam effluent and Moccasin Creek culvert, subsoil sediment sources are

Table 2. Radionuclide Activity Ranges and Mean Isotope Ratios in Loco Bayou Soil and Sediment Samples[a]

Compartment	n	^{232}Th	^{230}Th	^{228}Ra	^{226}Ra	$^{230}Th/^{232}Th$	$^{228}Ra/^{232}Th$	$^{226}Ra/^{232}Th$	$^{226}Ra/^{230}Th$	$^{228}Th/^{228}Ra$
Interfluvial surface	11	22.9–77.2	20.8–41.0	15.9–41.1	20.6–45.1	0.82 ± 0.09	0.73 ± 0.09	0.85 ± 0.09	1.03 ± 0.11	1.50 ± 0.19
Subsoil	14	29.7–95.9	27.8–77.9	15.3–84.8	19.6–47.1	0.81 ± 0.09	0.75 ± 0.09	0.55 ± 0.05	0.69 ± 0.07	1.56 ± 0.17
Alluvium	6	24.7–70.5	21.2–69.1	21.7–41.7	20.6–47.6	0.90 ± 0.10	0.69 ± 0.08	0.71 ± 0.07	0.80 ± 0.07	1.54 ± 0.18
Floodplain	5	35.1–90.3	29.1–77.8	23.3–59.0	24.4–52.4	0.92 ± 0.10	0.83 ± 0.09	0.84 ± 0.08	0.93 ± 0.09	1.50 ± 0.19

[a] Radionuclide activity ranges are given in Bq/kg.

Table 3. Ra/Th Mean and Discrete Values for Sources and Alluvium, Respectively

Sample	A ^{226}Ra/^{232}Th	B ^{226}Ra/^{230}Th	^{228}Th/^{228}Ra	Interfluvial A–B, %	Slopes A–B, %	Down-Reach Distance, km
Interfluvial surface (μ_i)	0.85 ± 0.09	1.03 ± 0.11	1.50 ± 0.19	...	...	...
Subsoil (μ_s)	0.55 ± 0.05	0.69 ± 0.07	1.56 ± 0.17	...	...	...
LSCB3[a]	0.75 ± 0.07	0.91 ± 0.09	1.29 ± 0.11	67–65	33–35	7.2
LSCB5[a]	0.64 ± 0.05	0.75 ± 0.06	1.75 ± 0.16	31–18	69–82	14.7
LSCB6[a]	0.60 ± 0.07	0.64 ± 0.04	1.73 ± 0.19	18–0	82–100	15.1
LSCB7[b]	0.83 ± 0.09	0.97 ± 0.10	1.23 ± 0.19	94–82	6–12	7.2
LSCB8[b]	0.75 ± 0.07	0.85 ± 0.07	1.66 ± 0.22	65–47	35–53	15.1
LSCB9[b]	0.71 ± 0.07	0.69 ± 0.05	1.57 ± 0.22	53–0	47–100	19.2

[a] This is January–February 2001 sampling.
[b] This is April 2001 sampling.

probably equal to or more likely of secondary importance relative to interfluvial surface supplies. This suggestion is supported by observations of consistent maximum values for interfluvial contribution at the northernmost sampling point during flood (~66%) and bank-full (~88%) stages. This implies an increase, moving north in lower Loco Bayou, in the importance of sheet and shallow rill erosion from uplands and a corresponding decrease in the importance of channel and gully erosion in the supply of channel alluvium. Land use significantly changes from dominantly forested to agricultural moving south from the northernmost alluvial sampling station. The majority of the lower basin is cleared land utilized for cattle grazing and agriculture (wheat, poultry, and dairy). While it would be an overgeneralization to characterize pastures and agriculturally developed floodplains as more prone to gully development and channel erosion than headwater forests, localized but significant subsoil contributions to alluvium are observed in this 37 km^2 basin. This is in spite of a generally aggrading floodplain due to the influence of stream flow management, the dam's influence on base level and channel processes, and impacts of landscape changes on soil erosion such as deforestation, road and bridge construction, and cattle ranching. Radionuclide data (Figures 6a, 6b, and 6c) are in congruence with this scenario, depicting alluvium as increasingly subsurface derived with distance downstream. The subsoil component comprises nearly all alluvium present (~91%) during flood by ~15 km and most (~74%) during bank-full stage by ~19 km downstream from the dam.

[24] Additional evidence of strong coupling is provided by the separation of alluvial samples between flood and bank-full stage events (Figures 6a, 6b, and 6c). During floods (LSCB 3, 5, and 6), subsoil contributions start out higher than at lower stages for the northernmost station and more rapidly progress toward complete dominance, which may reflect susceptibility of a developed and managed system to considerable subsurface erosion during high runoff events. Upland sediments may be rapidly flushed during high runoff events, whereas tributary and channel erosion and sediment remobilization in the main channel should increase as flows increase. Thus the subsoil source is more dominant at any given point during high flow, and its relative importance increases more rapidly downstream. During bank-full flows (LSCB 7, 8, and 9), subsoil contributions more gradually become dominant over a greater distance, ~74% of the total by about 19 km, very near to the basin outlet. This contrast may result from recovery of the system, where influx of subsoil materials has declined and alluvial sources are returning to a balance that better reflects the distribution of sources in the basin and their relationship to the channel under decreasing energy conditions.

[25] The gradient in sediment source compartment contributions to lower Loco Bayou channel alluvium observed by this technique over stream length has important management aspects. In the north, where land cover is dominated by forests, the contribution of interfluve surface sediments is more important, regardless of hydrologic stage. Although not entirely unexpected, this condition appears to mask the impact of localized channel degradation and scour associated with the dam effluent and Moccasin Creek tributary portions of the system, where subsoil contributions to

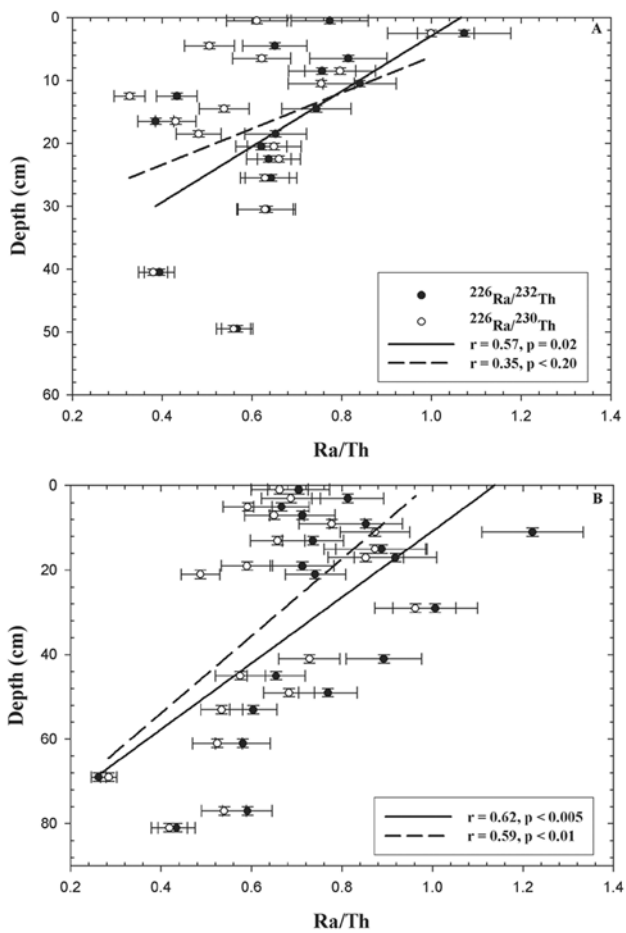

Figure 3. Loco Bayou soil cores ((a) LSUPC1 and (b) LSUPC2), suggesting isotope fractionation with depth.

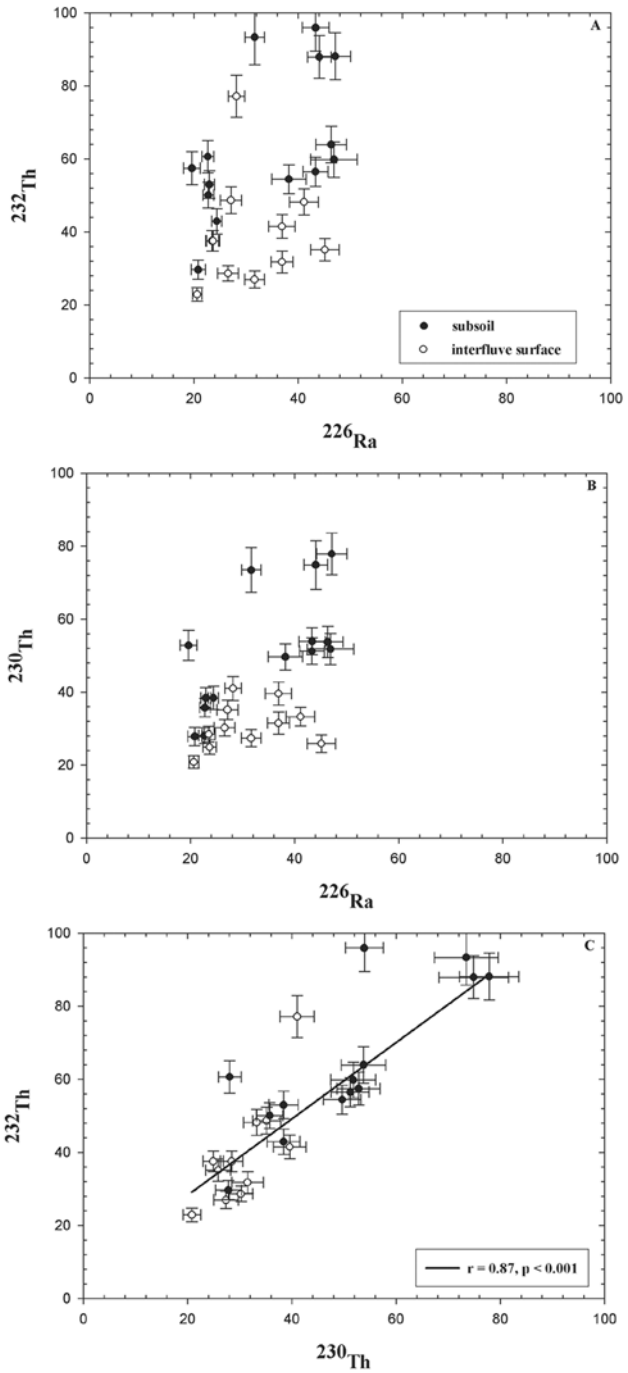

Figure 4. Source signatures for interfluvial surface and subsoil source compartments (Bq/kg): (a) ^{226}Ra/^{232}Th, (b) ^{226}Ra/^{230}Th, and (c) ^{230}Th/^{232}Th.

channel alluvium were expected to be relatively high. This is interpreted to reflect the dominance of sheet wash and shallow gullies as the primary sediment erosion and transport mechanism providing sediment to the stream channel here. This condition is most likely exacerbated by the clearing of land for development and logging practices that, while not areally extensive, are spatially skewed to the northern half of this basin. The increasing importance and eventual dominance of subsoil contributions to channel alluvium in lower Loco Bayou moving downstream is significant, implying that eroding channels, gullies, and highly concentrated erosion rather than general upland sheet-and-rill erosion is critical. This interpretation is strengthened by observations of land use that directly result in localized channel and riparian zone degradation, cattle trails and crossings, which are concentrated in the southern portion of the basin. Such a relationship has been observed by others [*Magilligan and McDowell*, 1997; *Lyons et al.*, 2000; *Flenniken et al.*, 2001], particularly in small streams like Loco Bayou [*Williamson et al.*, 1992], and relates well to the scenario offered by the radiochemical technique.

[26] Observations at lower Loco Bayou may provide insight into landscape sensitivity and feedback in response to development. Land use change in the Upper Mississippi Valley triggered hydrologic responses that were transmitted nearly simultaneously to all watershed scales and flood-driven hydraulic adjustments in channel and floodplain morphologies contributed to feedback effects, causing long-term lag responses [*Knox*, 2001]. There, agricultural land use had escalated landscape sensitivity to such a degree that modern process rates provide a very distorted representation of process rates that occurred in the geologic past prior to human disturbance.

[27] Research on effects of climate change on fluvial systems is sparse, compared to studies relating base level change to fluvial morphology and sediment transport capacity, and most of these studies focus on timescales greater than 10^3 years [*Blum and Tornqvist*, 2000]. Moreover, unique responses by fluvial systems to climate change, particularly over relatively short timescales ($\leq$100 years) are not well defined. *Knox* [1983] has shown that changes in global atmospheric circulation do influence both flood magnitudes and vegetation cover and that these two variables then interact to mutually effect fluvial morphology and sediment dynamics. While Texas has experienced several lasting and severe droughts during the 1990s, the short duration of climatic variability here, coupled with the ''overprinting'' on the system in the form of land utilization and hydrologic management, in particular, do not allow for definitive interpretations of climatic influence based on the radiochemical technique presented here. Techniques such as these, when combined with mineralogical or geochemical methods, may provide a valuable tool in the examination of

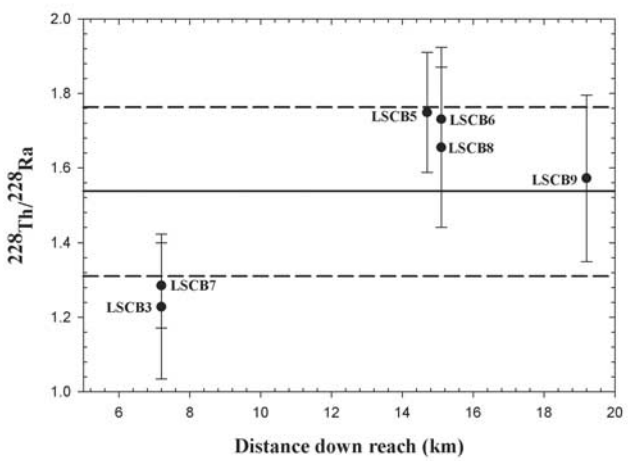

Figure 5. Alluvial signatures within mean error for ^{228}Th/^{228}Ra for all alluvial samples.

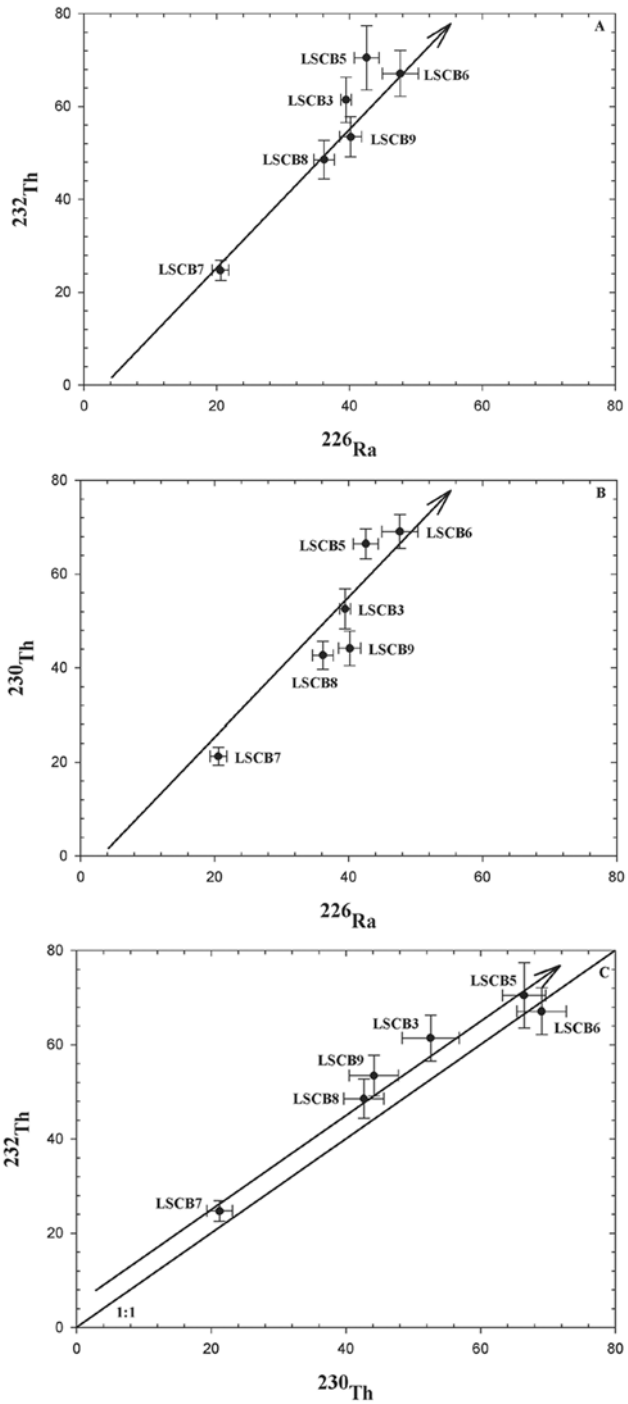

Figure 6. Loco Bayou alluvial signatures for January–February (LSCB 3, 5, and 6) and April (LSCB 7, 8, and 9) of 2001 (Bq/kg): (a) ^{226}Ra/^{232}Th, (b) ^{226}Ra/^{230}Th, and (c) ^{230}Th/^{232}Th. Arrows denote increasing downstream distance.

the effects of climate change in the short term (human scale) on fluvial systems. Their geochemical conservancy and long half-lives may be particularly useful to model changes in sediment source fluxes to alluvial deposits in river systems under a wide variety of settings.

3.3. Absence of ^{228}Ra Excess

[28] The prospect of resolving residence times of alluvium was also investigated using ^{228}Ra/^{232}Th. *Olley* [1994] observed ^{228}Ra concentrations in soils in excess of its parent ^{232}Th by as much as 30% and used this observation to estimate residence times of alluvial channel sediment [*Olley et al.*, 1997]. At lower Loco Bayou, ^{228}Ra was ubiquitously deficient relative to ^{232}Th in all samples collected (Table 2). Several contrasts between Loco Bayou and the field sites for *Olley et al.* [1997] exist, including bedrock geology, climate, and topography. These factors no doubt influence the general mobility of ^{228}Ra, the initial concentrations of both ^{228}Ra and ^{232}Th, as a function of parent rock lithology, and a host of biological and geochemical processes, which may be the cause for the observations of *Olley* [1994] and *Olley et al.* [1997].

4. Summary and Conclusions

[29] Throughout the lower Loco Bayou basin, samples of the Weches Formation, surfaces of upland interfluves and subsoil materials on slopes were collected from actively eroding sites. Two soil cores were collected and floodplain and channel alluvial sediments were sampled. Alluvial channel samples were collected during both flood and bank-full stages and stream water was filtered during flood stage to examine radium in solution. The isotope ratios ^{230}Th/^{232}Th, ^{226}Ra/^{232}Th, and ^{226}Ra/^{230}Th were employed to (1) determine if fractionation in the soil profile created discrete signatures for different spatial sediment source compartments, (2) allow for modeling of channel alluvium sediment sources and their change over distance or with hydrologic setting, and (3) relate results to coupling of hillslope and channel processes and land use in lower Loco Bayou.

[30] On the basis of the U/Th series radionuclide analyses of soils and sediments from lower Loco Bayou, Texas, we conclude the following.

1. The ^{226}Ra/^{232}Th and ^{226}Ra/^{230}Th data for interfluvial surfaces and subsoils produced discrete signatures, allowing for a simple mixing model to be applied to resolve relative contributions of each compartment to alluvial sediments. The ^{230}Th/^{232}Th data graphically support this distinction.
2. While exhibiting no clear spatial or temporal trends, floodplain sample ratios are constrained by soil compartment end-members.
3. Subsoil derived alluvial sediment became dominant with increasing distance downstream during both flood and bank-full stages. Separation of alluvial sediments between flood and bank-full stages indicate a more rapid and total dominance of subsoil sources over downstream length during flood and more gradual, less complete dominance during bank-full stage. This is interpreted as indicating strong coupling between hillslope and channel process in lower Loco Bayou, directly reflecting the impacts of human agency.
4. No excess of ^{228}Ra over its parent ^{232}Th was observed in soils and sediments, preventing use of ^{228}Ra/^{232}Th to estimate residence times of alluvium at lower Loco Bayou.
5. Agricultural development, while influencing alluvial sources and transport dynamics at lower Loco Bayou, may also be providing for a strongly coupled fluvial system, wherein landscape sensitivity to extrinsic forcing is enhanced. These relations are fundamental to our understanding of human influences on fluvial systems at any scale and warrant further investigation.

6. An important contribution to watershed-scale sediment transport modeling described herein is the ability to recognize and quantify sediment sources to the river not only by source rock lithology and its characteristic isotope signatures, where present, but also the ability to do the same for sediment based on its location on the landscape, whether lithologic contrast in isotopic signatures is or is not the case.

7. The ubiquity, chemical conservancy, long half-lives, ease of modeling, and wide climatic and geographic range over which fractionation of these primordial radionuclides in soils is expected represents an important tool in understanding fluvial processes. Additional research focusing on fractionation processes as related to both natural and anthropogenic factors and testing the applicability of these methods in larger, more geologically diverse watersheds is needed.

[31] **Acknowledgments.** Funding provided by the Texas Water Development Board, the Texas Water Resources Institute, the Geological Society of America, the Gulf Coast Association of Geological Sciences, and Texas A&M University is gratefully acknowledged. Cooperation of numerous landowners in allowing access to field sites is also appreciated. Thanks are also extended to Chris Courtney for field and laboratory assistance and to two anonymous reviewers who contributed to the improvement of this manuscript.

References

Allison, M. A., S. A. Kuehl, T. C. Martin, and A. Hassan, Importance of flood-plain sedimentation for river sediment budgets and terrigenous input to the oceans: Insights from the Brahmaputra-Jamuna River, *Geology*, *26*(2), 175–178, 1998.

Ames, L. L., J. E. McGarrah, and B. A. Walker, Sorption of trace constituents from aqueous solutions onto secondary minerals, II, Radium, *Clays, Clay Miner.*, *31*, 335–342, 1983.

Baskaran, M., D. J. Murphy, P. H. Santschi, J. C. Orr, and D. R. Schink, A method for rapid in situ extraction and laboratory determination of Th, Pb, and Ra isotopes from large volumes of seawater, *Deep Sea Res., Part I*, *40*, 849–865, 1993.

Blum, M. D., and T. E. Tornqvist, Fluvial responses to climate and sea-level change: A review and look forward, *Sedimentology*, *47*, suppl. 1, 2–48, 2000.

Bonniwell, E. C., G. Matisoff, and P. J. Whiting, Determining the times and distances of particle transit in a mountain stream using fallout radionuclides, *Geomorphology*, *27*, 75–92, 1999.

Branca, M., and M. Voltaggio, Erosion rate in badlands of central Italy—Estimation by radiocesium isotope ratio from Chernobyl nuclear accident, *Appl. Geochem.*, *8*(5), 437–445, 1993.

Buesseler, K. O., J. K. Cochran, M. P. Bacon, H. D. Livingston, S. A. Casso, D. Hirschberg, M. C. Hartman, and A. P. Fleer, Determination of thorium isotopes in seawater by non-destructive and radiochemical procedures, *Deep Sea Res.*, *39*, 1103–1114, 1992.

Caitcheon, G. G., The significance of various sediment magnetic mineral fractions for tracing sediment sources in Killimicat Creek, *Catena*, *32*, 131–142, 1998.

Choppin, G. R., J.-O. Liljenzin, and J. Rydberg. *Radiochemistry and Nuclear Chemistry*, 2nd ed., 707 pp., Butterworth-Heinemann, Woburn, Mass., 1995.

Dolezel, R., Soil survey of Nacogdoches County, Texas, report, 146 pp., Soil Conserv. Serv., Washington, D. C., 1980.

Faure, G., *Principles of Isotope Geology*, 2nd ed., 589 pp., John Wiley, New York, 1986.

Flenniken, M., R. R. McEldowney, W. C. Leininger, G. W. Frasier, and M. J. Trlica, Hydrologic responses of a montane riparian ecosystem following cattle use, *J. Range Manage.*, *54*(5), 567–574, 2001.

Greeman, D. J., A. W. Rose, J. W. Washington, R. R. Dobos, and E. J. Ciolkosz, Geochemistry of radium in soils of the eastern United States, *Appl. Geochem.*, *14*, 365–385, 1999.

Gueniot, B., Distribution et modes de fixation de l'uranium dans les grands types de pedogeneses climatiques et stationnelles sur roches cristallines, Ph.D. thesis, Univ. de Nantes, Nantes, France, 1983.

Hallstadius, L., A method for the electrodeposition of actinides, *Nucl. Instrum. Methods Phys. Res., Sect. A*, *223*, 266–267, 1984.

Hansen, R. O., and G. O. Huntington, Thorium movements in morainal soils of the High Sierra, California, *Soil Sci.*, *108*, 257–265, 1969.

He, Q., and P. Owens, Determination of suspended sediment provenance using caesium 137, unsupported lead 210, and radium 226: A numerical mixing model approach, in *Sediment and Water Quality in River Catchments*, edited by I. Foster, A. Gurnell, and B. Webb, pp. 207–227, John Wiley, New York, 1995.

Hoey, T., Temporal variations in bedload transport rates and sediment storage in gravel-bed rivers, *Prog. Phys. Geogr.*, *16*(3), 319–338, 1992.

Ivanovich, M., and R. S. Harmon (Eds.), *Uranium Series Disequilibrium: Applications to Environmental Problems*, 571 pp., Clarendon, Oxford, England, 1982.

Ivanovich, M., and R. S. Harmon (Eds.), *Uranium-Series Disequilibrium*: *Applications to Earth, Marine, and Environmental Sciences*, 910 pp., Clarendon, Oxford, England, 1992.

Kaufman, A., Thorium 232 concentration of surface ocean water, *Geochim. Cosmochim. Acta*, *33*, 717–724, 1969.

Kelsey, H. M., R. Lamberson, and M. A. Madej, Stochastic model for the long-term transport of stored sediment in a river channel, *Water Resour. Res.*, *23*, 1738–1750, 1987.

Kendall, C., and J. J. McDonnell (Eds.), *Isotope Tracers in Catchment Hydrology*, 839 pp., Elsevier Sci., New York, 1998.

Knox, J. C., Responses of river systems to Holocene climates, in *Late-Quaternary Environments of the United States*, vol. 2, *The Holocene*, edited by H. E. Wright Jr., pp. 26–41, Univ. of Minn. Press, Minneapolis, 1983.

Knox, J. C., Agricultural influence on landscape sensitivity in the upper Mississippi River Valley, *Catena*, *42*, 193–224, 2001.

Kraemer, T. F., and D. P. Genereux, Applications of uranium and thorium series radionuclides in catchment hydrology studies, in *Isotope Tracers in Catchment Hydrology*, edited by C. Kendall and J. J. McDonnell, pp. 679–722, Elsevier Sci., New York, 1998.

Langedal, M., The influence of a large anthropogenic sediment source on the fluvial geomorphology of the Knabeana-Kvina Rivers, Norway, *Geomorphology*, *19*, 117–132, 1997.

Langmuir, D., and J. S. Herman, Solubility of thorium in low temperature aqueous solutions, *Geochim. Cosmochim. Acta*, *44*, 1753–1766, 1980.

Lecce, S. A., and R. T. Pavlowsky, Use of mining-contaminated sediment tracers to investigate the timing and rates of historical flood plain sedimentation, *Geomorphology*, *38*, 85–108, 2001.

Linsalata, P., Uranium and thorium decay series radionuclides in human and animal foodchains—A review, *J. Environ. Qual.*, *23*, 633–642, 1994.

Lyons, J., B. M. Weigel, L. K. Paine, and D. J. Undersander, Influence of intensive rotational grazing on bank erosion, fish habitat quality, and fish communities in southwestern Wisconsin trout streams, *J. Soil Water Conserv.*, *55*(3), 271–276, 2000.

Macklin, M. G., K. A. Hudson-Edwards, and E. J. Dawson, The significance of pollution from historic metal mining in the Pennine orefields on river sediment contaminant fluxes to the North Sea, *Sci. Total Environ.*, *194/195*, 391–397, 1997.

Magilligan, F. J., and P. F. McDowell, Stream channel adjustments following elimination of cattle grazing, *J. Am. Water Resour. Assoc.*, *33*, 867–878, 1997.

Marcus, W. A., G. A. Meyer, and D. R. Nimmo, Geomorphic control of persistent mine impacts in a Yellowstone Park stream and implications for the recovery of fluvial systems, *Geology*, *29*(4), 355–358, 2001.

Megumi, K., T. Oka, K. Yaskawa, and M. Sakanoue, Contents of natural radioactive nuclides in soil in relation to their surface area, *J. Geophys. Res.*, *87*, 10,857–10,860, 1982.

Michel, J., Redistribution of uranium and thorium series isotopes during isovolumetric weathering of granite, *Geochim. Cosmochim. Acta*, *48*, 1249–1256, 1984.

Muhs, D. R., C. A. Bush, and J. N. Rosholt, Uranium series disequilibrium in Quaternary soils—Significance for ^{222}Rn hazard assessment, *U. S. Geol. Surv. Circ.*, *1033*, 39–44, 1990.

Murray, A. S., G. Caitcheon, J. Olley, and H. Crockford, Methods for determining the sources of sediments reaching reservoirs: Targeting soil conservation, *ANCOLD Bull.*, *85*, 61–70, 1990.

Murray, A. S., J. M. Olley, and P. J. Wallbrink, Radionuclides for analysis of sediments in water supply catchments, *Rep. 91/8*, 35 pp., Commonw. Sci. and Ind. Res. Organ., Canberra, ACT, Australia, 1991.

Nagle, G. N., and J. C. Ritchie, The use of tracers to study sediment sources in three streams in northeastern Oregon, *Phys. Geogr.*, *20*(4), 348–366, 1999.

National Oceanic and Atmospheric Administration, Regional Precipitation Monitoring Program, http://lwf.ncdc.noaa.gov/oa/ncdc.html, Natl. Clim. Data Cent., Asheville, N. C., 2001.

Olley, J. M., The use of ^{238}U and ^{232}Th decay series radionuclides in sediment tracing, 187 pp., Ph.D. thesis, Univ. of N. S. W., Kensington, Australia, 1994.

Olley, J. M., and A. S. Murray, Origins of the variability in the $^{230}Th/^{232}Th$ ratio in sediments, in *Variability in Stream Erosion and Sediment Transport*, edited by L. L. Olive, R. J. Loughran, and J. A. Kesby, *IAHS Publ.*, *224*, 65–70, 1994.

Olley, J. M., A. S. Murray, D. H. Mackenzie, and K. Edwards, Identifying sediment sources in a gullied catchment using natural and anthropogenic radioactivity, *Water Resour. Res.*, *29*, 1037–1043, 1993.

Olley, J. M., R. G. Roberts, and A. S. Murray, A novel method for determining residence times of river and lake sediments based on disequilibrium in the thorium decay series, *Water Resour. Res.*, *33*, 1319–1326, 1997.

Paola, C. G., R. Parker, R. Seal, S. K. Sinha, J. B. Southard, and P. R. Wilcock, Downstream fining by selective deposition in a laboratory flume, *Science*, *258*, 1757–1760, 1992.

Passmore, D. G., and M. G. Macklin, Provenance of fine-grained alluvium and late Holocene land-use change in the Tyne Basin, northern England, *Geomorphology*, *9*, 127–142, 1994.

Phillips, J. D., The source of alluvium in large rivers of the lower coastal-plain of North Carolina, *Catena*, *19*, 59–75, 1992.

Phillips, J. D., Sedimentation in bottomland hardwoods downstream of an east Texas dam, *Environ. Geol.*, *40*(7), 860–868, 2001.

Phillips, J. D., and D. A. Marion, Residence times of alluvium in an east Texas stream as indicated by sediment color, *Catena*, *45*, 49–71, 2001.

Popova, O. N., R. P. Kodaneva, and P. P. Vavilov, Distribution in plants of radium absorbed from the soil, *Sov. Plant Physiol.*, *11*, 371–375, 1964.

Quine, T. A., and D. E. Walling, Rates of soil-erosion on arable fields in Britain—Quantitative data from cesium-137 measurements, *Soil Use Manage.*, *7*(4), 169–176, 1991.

Rice, S. P., M. T. Greenwood, and C. B. Joyce, Tributaries, sediment sources, and the longitudinal organization of macroinvertebrate fauna along river systems, *Can. J. Fish. Aquat. Sci.*, *58*(4), 824–840, 2001.

Riese, A. C., Adsorption of radium and thorium onto quartz and kaolinite: A comparison of solution/surface equilibria models, Ph.D. thesis, 292 pp., Colo. Sch. of Mines, Golden, Colo., 1982.

Roberts, H. M., and A. J. Plater, U- and Th-series disequilibria in coastal infill sediments from Praia da Rocha (Algarve region, Portugal): A contribution to the study of late Quaternary weathering and erosion, *Geomorphology*, *26*, 223–238, 1999.

Roberts, R. G., and M. Church, The sediment budget in severely disturbed watersheds, Queen Charlotte Ranges, British Columbia, *Can. J. For. Res.*, *16*, 1092–1106, 1986.

Rosholt, J. N., Mobilization and weathering, in *Uranium Series Disequilibrium: Applications to Environmental Problems*, edited by M. Ivanovich and R. S. Harmon, pp. 167–180, Clarendon, Oxford, England, 1982.

Rosholt, J. N., B. R. Doe, and M. Tatsumoto, Evolution of the isotopic composition of uranium and thorium in soil profiles, *Geol. Soc. Am. Bull.*, *77*, 987–1004, 1966.

Schneiderman, J. S., Detrital opaque oxides as provenance indicators in River Nile sediments, *J. Sediment. Res., Sect. A*, *65*(4), 668–674, 1995.

Shelby, C. A., M. K. Pieper, A. C. Wright, D. H. Eargle, and V. E. Barnes, Palestine sheet, map, Bur. of Econ. Ecol., Univ. of Tex., Austin, 1968.

Swank, W. T., J. M. Vose, and K. J. Elliot, Long-term hydrologic and water quality responses following commercial clearcutting of mixed hardwoods on a southern Appalachian catchment, *For. Ecol. Manage.*, *143*, 163–178, 2001.

Tanner, A. B., Physical and chemical controls on distribution of radium-226 and radon-222 in ground water near Great Salt Lake, Utah, in *Natural Radiation Environment*, edited by J. A. S. Adams and W. M. Lowder, pp. 253–276, Univ. of Chicago Press, Chicago, Ill., 1964.

Taskaev, A. I., V. Y. Ovchenkov, R. M. Aleksakhin, and I. I. Shutomova, Uptake of ^{226}Ra by plants and change of its state in the soil plant tops-litterfall system, *Sov. Soil Sci.*, *9*, 79–85, 1977.

Valero-Garces, B. L., A. Nava, J. Machin, and D. Walling, Sediment sources and siltation in mountain reservoirs: A case study from the Central Spanish Pyrenees, *Geomorphology*, *28*, 23–41, 1999.

Wallbrink, P. J., A. S. Murray, J. M. Olley, and L. J. Olive, Determining sources and transit times of suspended sediment in the Murrumbidgee River, New South Wales, Australia, using fallout ^{137}Cs and ^{210}Pb, *Water Resour. Res.*, *34*(4), 879–887, 1998.

Walling, D. E., Linking land use, erosion and sediment yields in river basins, *Hydrobiologia*, *410*, 223–240, 1999.

Williamson, R. B., R. K. Smith, and J. M. Quinn, Effects of riparian grazing and channelization on streams in Southland, New Zealand, 1, Channel form and stability, *N. Z. J. Mar. Freshwater Res.*, *26*(2), 241–258, 1992.

Woodward, J. C., J. Lewin, and M. G. Macklin, Alluvial sediment sources in a glaciated catchment—The Voidomatis Basin, northwest Greece, *Earth Surf. Processes Landforms*, *17*(3), 205–216, 1992.

Zajac, R. N., and R. B. Whitlatch, Response of macrobenthic communities to restoration efforts in a New England estuary, *Estuaries*, *24*(2), 151–166, 2001.

Zhang, X., T. A. Quine, and D. E. Walling, Soil erosion rates on sloping cultivated land on the Loess Plateau near Ansai, Shaanxi Province, China: An investigation using ^{137}Cs and rill measurements, *Hydrol. Processes*, *12*(1), 171–189, 1998.

B. E. Herbert, Department of Geology and Geophysics, Texas A&M University, 257 M. T. Halbouty Building, College Station, TX 77843-3115, USA. (herbert@geo.tamu.edu)

J. D. Phillips, Department of Geography, University of Kentucky, 1453 Patterson Office Tower, Lexington, KY 40506-0027, USA. (jdp@pop.uky.edu)

P. H. Santschi and K. M. Yeager, Laboratory for Oceanographic and Environmental Research, Department of Oceanography, Texas A&M University, Ft. Crockett Campus, 5007 Ave. U, Galveston, TX 77551, USA. (santschi@tamug.edu; yeagerk@tamug.tamu.edu)

Towards an Integrated Water Policy Planning Model for the Texas High Plains

Basic Information

Title:	Towards an Integrated Water Policy Planning Model for the Texas High Plains
Project Number:	2001TX3301B
Start Date:	3/1/2001
End Date:	2/28/2002
Funding Source:	104B
Congressional District:	19
Research Category:	Not Applicable
Focus Category:	Management and Planning, Groundwater, Agriculture
Descriptors:	sustainable ground water use, dynamic efficiency, water policy analysis
Principal Investigators:	Biswaranjan Das

Publication

State:	Texas
Project Number:	TX3301
Title:	Towards an Integrated Water Policy Planning Model for the Texas High Plains
Project Type:	Research Project
Focus Category:	Management and Planning, Groundwater, Agriculture
Keywords:	sustainable ground water use, dynamic efficiency, water policy analysis
Start Date:	03/01/2001
End Date:	02/28/2002
Congressional District:	19
PI:	Biswaranjan Das Student, Texas Tech University email:biswaranjan.das@ttu.edu phone:(806) 742-2808

Abstract

The thrust of this project will be to develop a spatially and temporally disaggregated model for the water resources of the Texas High Plains. This water policy model will provide planners with a proactive planning tool that can be used to evaluate water policy and management decisions. The planning model will capable of addressing regional environmental, economic, and hydrologic concerns. This model will also be able to simulate the effects of such policies on smaller watersheds within the region. A generalized algebraic modeling system (GAMS) will be used to develop a spatially dynamic economic model, while data from the Texas Water Development Board will be incorporated into a water use model. These modeling tools will be linked to a groundwater model of the Ogallala Aquifer now being developed at Texas Tech University. The project should assist planners and water managers in evaluating the costs and benefits as well as the water resources implications of various management measures proposed for this region.

1. **Title:** Towards an Integrated Water Policy Planning Model for the Texas High Plains

2. **Focus Categories (to be completed by Institution personnel):**

3. **Keywords:** sustainable ground water use, water policy analysis, dynamic efficiency

4. **Duration:** 2 years beginning March 1, 2001

5. **Federal Funds Requested:** $5,000

6. **Non-Federal (matching) Funds Pledged:** Graduate Stipend for Biswaranjan Das ($12,000)

7. **Principal Investigator (graduate student):** Biswaranjan Das

   Co-Principal Investigator (faculty advisor): Dr. David B. Willis

8. **Congressional District: District 19**

9. **Statement of Critical Regional Water Problems:**

The Texas High Plains (THP) is facing many challenges in the allocation and management of its scarce water resources. Since World War II the THP economy has been strongly tied to irrigated agriculture. Recent drought experiences in combination with decreasing groundwater levels has made the THP critically aware that the region=s long-run economic viability is critically dependent upon optimally managing and conserving the region=s scarce water resources. Advances in irrigation technology in combination with once economically abundant Ogallala aquifer supplies, and low energy prices spurred large scale irrigation development throughout the 1950s and 1960s. The rapid development of irrigated agriculture resulted in annual groundwater extraction rates which often exceeded the recharge rate by a factor of ten. This mining of the aquifer quickly reduced aquifer thickness to the point where some areas of the aquifer lost 50 percent of its saturated thickness by the early 1980s relative to pre-irrigation development (Sweeten). The falling static water level sufficiently reduced well yields and increased pump lifts with the result that pumping cost increased by as much as 600% (in constant dollars) between 1952 and 1981 (Sweeten). Such dramatic increases in pumping cost made irrigation of marginally profitable lands unprofitable beginning in the late 1960's and irrigated acreage began to decline from a peak of nearly 8 million acres. Today, 5.25 million acres of crop land is irrigated in the THP which provides a $5.5 billion dollar impact on the THP economy (Arabiyat). Despite the reduction in irrigated acreage and the widespread adoption of more efficient irrigation technologies the static water table still continues to decline, albeit at a slower rate. The declining water table has increased the cost of water to both agricultural and non-agricultural interests. Moreover, it is likely that residential and non-agricultural industrial growth will increasingly compete for the limited groundwater supplies of the THP, as we move into the future, even though these users currently account for less than 5% of the regions water use.

10. **Nature, Scope, and Objectives of the Research:**

Given the increasing scarcity of the THP groundwater supplies and the impact groundwater has on the economic vitality of the region, we propose to use the Texas Water Resource Institute grant to augment our initial research effort to develop a spatially and temporally disaggregated water policy model for the THP. A comprehensive water policy model will provide planners with a pro-active planning tool and means to evaluate policies designed to address long-run bio-economic sustainability issues in the THP. A viable water policy planning model must be must be capable of addressing important region-wide economic, environmental, and hydrologic concerns, yet have sufficient spatial and temporal disaggregation to allow a comprehensive subregional analysis of the economic and biophysical impacts of each proposed policy. It is important for policy makers to have a credible tool which will allow them to accurately simulate the long-run economic and hydrologic consequences of a proposed water policy. For example, policy makers may wish to examine the benefits and costs of a policy which reduces agricultural diversions from the Ogallala aquifer, and/or determine when current agricultural use rates will begin to constrain non-agricultural water demands? Spatial subregional detail is essential to a viable planning model because it provides policy makers with a tool for targeting specific water uses and/or geographic regions which can most cost effectively achieve a policy dictated reduction in groundwater use?

Development of a credible regional water planning model will require constructing, linking, and calibrating a behaviorally based economic model to a hydrology model for the THP. The generalized algebraic modeling systems (GAMS) will be used to develop a spatially dynamic economic model (the behavioral response model). The economic model will employ a modular programing approach to allow the model to grow in complexity and sophistication over time. County specific data sets have been collected and assembled into representative farms by Terrrel (1998) for many of the THP counties. These representative farm data sets will initially be used to characterize the agricultural base of the THP. An agricultural water use survey currently being developed by the Department of Agricultural Economics at Texas Tech University will be mailed to a representative sample of the irrigated agricultural producers in the THP this spring. The collected survey data on water use, irrigation technology, and crop yields by soil types will be used to compliment Terrel=s data set and refine the economic response model. Additional data on use levels, and pump lifts has been collected from the Texas Water Development Board web site and will be used to both cross check the survey data and refine the economic model parameters.

A groundwater model for the southern Ogallala aquifer is currently being developed using the MODFLOW software program by Dr. Ken Rainwater (Dept. of Civil Engineering, Texas Tech University). The finite difference procedure used by the groundwater model to monitor groundwater elevation required a grid to be constructed on the land over the aquifer. All area within a specific grid cell is treated as a homogeneous unit. Current grid cell size is a quarter township (nine square miles). The aquifer grid provides the means to link the economic model to the subsurface groundwater model for purposes of monitoring changes in groundwater elevation resulting from recharge and groundwater pumping.

Once the economic and hydrology models are linked and calibrated the integrated policy model will be used to simulate the economic and hydrologic consequence of the status quo policy (current baseline policy) into the future under current property right structures (the right of capture) and individual economic incentives. Temporal and spatial accounts will be maintained with respect to

agricultural economic activity, groundwater use, and water table elevations. Given the common property nature of groundwater, individual economic incentives will be used to determine water use over time. Thus, under the baseline scenario, the aquifer will simply respond to the stresses placed upon it by individual economic agents acting in their economic self interest. However, as the aquifer is impacted by cumulative economically driven demands, prior water use decisions will likely determine what is economically viable (optimal) as we move into the future.

11. **Results Expected from this Project:**

Development of a comprehensive water policy planning model will provide planners with a pro-active planning tool. It will allow policy makers to identify subareas of the THP where significant differences exist (initially defined as counties) with respect to groundwater lift, water supplies, soil types, and agricultural response to scarce water supplies. Given these hypothesized differences a behaviorally driven integrated modeling framework will provide policy makers with a tool to target specific THP regions where policy incentives can most cost-effectively be used to enhance the overall long-run economic and hydrologic sustainability of the THP. The modeling framework will be capable of providing policy makers with an estimate of how rapidly the southern Ogallala aquifer is approaching economic depletion under current institutional structures.

The policy model, will also be used in post calibration policy runs to examine a variety of conservation policies. For example, given that agriculture currently uses in excess of 95% of the groundwater within the THP, region-wide water use constraints could be imposed upon agriculture to determine the agricultural cost relative to the baseline of implementing a policy which restricts agricultural diversions (and hence the compensation due agriculture for reducing their diversions). Existing data on alternative crop and livestock management strategies and expected advances in crop biotechnology could be included in the model as alternative production activities and evaluated to determine if these potential technologies can reduce the transitional cost of moving to a more sustainable water use policy. The impact of energy deregulation on groundwater pumping cost and the use of irrigated water could also be examined. Another future research extension would be to use the evolving model to examine the potential social gains that could be achieved by allow agriculture to market their water to residential or industrial users within the THP over time.

Assessing Water Quality Impacts of Nutrient Imports into an Urban Gradient

Basic Information

Title:	Assessing Water Quality Impacts of Nutrient Imports into an Urban Gradient
Project Number:	2001TX1561G
Start Date:	9/1/2001
End Date:	8/31/2003
Funding Source:	104G
Congressional District:	8th
Research Category:	Not Applicable
Focus Category:	Water Quality, None, None
Descriptors:	nonpoint source pollution, water quality
Principal Investigators:	Clyde L. Munster, Donald M Vietor

Publication

1. Hanzlik, J.E., C.L. Munster, D.M. Vietor, R.H. White. 2002. Locationof Turfgrass Production Sites using GIS in the North Bosque River Watershed. Proceedings, Total Maximum Daily Load (TMDL) Environmental Regulations Conference, ed. Ali Saley, 472-476, Fort Worth Texas, Martch 11013, 2002.
2. Vieter, D.M., R.H. White, C.L. Munster, and T.L. Provin. 2002. Reduced Nonpoint Source Pollution Through Manure Use and Export in Turfgrass Sod. In Proceedings Total Maximum Daily Load (TMDL) Environmental Regulations Conference, ed. Ali Saleh, 396-402. Fort Worth, TX, March 11-13, 2002
3. Hanzlik, J.E., C.L. Munster, D.M. Vietor, R.H. White. 2002. Locationof Turfgrass Production Sites using GIS in the North Bosque River Watershed. Proceedings, Total Maximum Daily Load (TMDL) Environmental Regulations Conference, ed. Ali Saley, 472-476, Fort Worth Texas, Martch 11-13, 2002.
4. Hanzlik, J.E., C.L. Munster, D.M. Vietor, R.H. White. 2002. Locationof Turfgrass Production Sites using GIS in the North Bosque River Watershed. Proceedings, Total Maximum Daily Load (TMDL) Environmental Regulations Conference, ed. Ali Saley, 472-476, Fort Worth Texas, March 11-13, 2002.

Assessment of River-Floodplain Aquifer Interactions

ANDREW S. ALDEN, Project Engineer
K. W. Brown Environmental Services, College Station, TX 77845

CLYDE L. MUNSTER, Assistant Professor
Agricultural Engineering Department, Texas A&M University, College Station, TX 77843-2117

Key Terms: ***Surface-Water/Ground-Water Interaction, Floodplain, Brazos River, Flow Sensor, Hydrogeology***

ABSTRACT

The interaction between the Brazos River and the adjacent floodplain aquifer was studied for 200 days in 1995 at a ground-water research site near College Station, Texas. Two In Situ Permeable Flow Sensors (ISPFS) and a grid of well nests were used to correlate river stage to the magnitude and direction of ground-water flow at depths of 13.7 m and 18.3 m in the unconfined alluvial aquifer. Linear relationships between ground-water flow and river stage were determined at each depth. The floodplain aquifer responded differently to changes in river stage at the 13.7 m and 18.3 m depths. The horizontal velocity, parallel and perpendicular to the river, decreased with increasing river stage and increased with decreasing river stage, at both depths. However, the rates of change varied between the two depths. This caused the magnitude and direction of ground-water flow to be different at the two depths. The upward vertical velocity increased with increasing river stage at the 13.7 m depth and decreased with increasing river stage at the 18.3 m depth. At the 13.7 m depth, vertical ground-water flow gradually changed from upward to downward flow with long term river stage decline. Downward ground-water flow was not observed at the 18.3 m depth. Assessment of river-aquifer interactions indicates that a direct and measurable relationship exists between river stage and ground-water flow components at the site. The magnitude and direction of ground-water flow in the alluvial floodplain aquifer may be predicted if river stage is known.

INTRODUCTION

Stream-Aquifer Interaction

Assessment of the interaction between ground water and surface water has become increasingly important as concern by regulatory agencies for the quality and quantity of water supplies has increased (Texas Water Commission, 1989). The quantification of the hydrologic connection between a stream and the adjacent aquifer is also important to agricultural, industrial, and municipal interests as competition for diminishing water supplies escalates (Postal, 1989).

The hydrologic relationship between streams and aquifers is often complex, especially in transient systems where stream stage fluctuates or ground water is pumped from the aquifer. From pump tests conducted along the Miami River near Venice, Ohio, Walton and others (1967) concluded that streambed infiltration could be estimated and that streambed losses were constant and at a maximum rate after the aquifer water table was below the streambed. Sophocleous and others (1987), used pump tests along the Arkansas River in Kansas to assess surface-ground-water interactions. They observed drawdown in wells on the opposite side of the river and the aquifer responded as a leaky confined aquifer. Actual stream losses were less than analytical solutions predicted. Dunlap and others (1985) used well level and river stage data in a modeling study of ground-water/surface-water interactions in the Arkansas River in Keary and Finney Counties, Kansas. This section of the Arkansas River has received little or no ground-water discharge since 1923. River recharge to the aquifer was controlled by streambed permeability and the hydraulic gradient between the river and the aquifer water table.

Johnson and others (1989) used test holes and monitoring wells to assess surface-water/ground-water interactions along Cottonwood Creek in Shasta and Tehama Counties, California. Ground water flowed principally within the most permeable aquifer material and recharge from the stream occurred if a downward gradient existed. Ground-water gradients were upward and no recharge from the stream was indicated when the stream channel crossed silt and clay formations. A study on the Nashua River in north-central Massachusetts by de Lima (1991) used infiltration tests to establish that the vertical hydraulic conductivities of the streambed ranged from 0.6 to 1.5 m/day. Sophocleous (1991) determined that ground-water level rises in the Great Bend Prairie aquifer of Kansas was caused by flooding in adjacent rivers. Wolf and Helgesen (1993) calculated an average aquifer

discharge of 0.8 m^3/s along a 222 km segment of the Kansas River between Wamego and Topeka, Kansas using 40 yr of data. Greeman (1995) summarized 2,328 water level measurement by the U. S. Geological Survey from 1985–1992 in the Calumet aquifer and surface-water levels in Northern Lake County, Indiana. Water tables sloped toward the streams in the study area and ground-water gradients increased with decreasing river stage.

The establishment of connections between surface and ground water has also led to increased concern for water quality (Texas Water Commission, 1989). Field studies by Ragan (1968) and Sklash and Farvoldon (1979) have shown rapid movement of contaminated ground water to nearby streams following rainfall events. In addition, contaminated surface water has the potential to degrade ground-water supplies. A study by Schulmeyer (1995) revealed that the water quality properties and constituents of the alluvial aquifer that served as a water supply for Cedar Rapids, Iowa, changed to follow the water quality trends of the Cedar River due to drawdown. Wang and Squillane (1994) detected herbicide transport from the Cedar River to floodplain wells up to 50 m from the river during high stream flow.

Field studies (Munster et al., 1996) and computer model simulations (Chakka and Munster, 1996) at the Brazos River ground-water research site have shown that river stage determines water levels in the floodplain aquifer. Infiltration from rainfall events has been shown to have little or no effect on ground-water levels. Rainfall events influence water levels primarily by increasing river stage through surface runoff. At the Brazos River research site, the floodplain aquifer typically discharges to the river. However, during high river stages, the aquifer is recharged by the river.

Research Objectives

The research objectives were to: a) assess ground-water/surfacewater interactions at two depths in the Brazos River floodplain aquifer and b) develop predictive relationships that would correlate ground-water flow to river stage at these two depths.

FIELD METHODS

The interaction between the Brazos River and the floodplain aquifer was evaluated at a ground-water research site located approximately 12 km west of College Station, Texas (Munster et al., 1996). The 8.5 hectare research site is located on a typical section of the lower Brazos River floodplain and is 183 m from the river (Figure 1). The unconfined, heterogeneous, alluvial aquifer is overlain by a Ships clay layer that is, on average, 7.3 m thick as shown in Figure 2. The site is underlain by an impermeable Yegua shale formation at a depth of 20.1 m (Cronin and Wilson, 1967). The aquifer gradually changes from a fine sand at a depth of 7.3 m to a coarse sand and gravel mixture at a depth of 20.1 m. Water levels in the aquifer typically fluctuate between 9 m and 10 m (elevations = 58.5 m and 57.5 m) below the surface. Slug and pump tests at the research site have yielded saturated hydraulic conductivity (K_{sat}) values that ranged from 3.2 to 150 m/day (Wrobleski, 1996). A comprehensive characterization of the Brazos River research site is included in Munster and others (1996).

Instrumentation at the site includes 36 partially screened piezometric wells, four 'water table' wells, two In Situ Permeable Flow Sensors (ISPFS), and an 0.2 m diameter pumping well. The piezometric monitoring wells are arranged in a three-by-three grid of well nests that is oriented parallel and perpendicular to the river (Figure 1). Each well nest contains four monitoring wells with 150 mm long, polyvinyl chloride (PVC), wire-wound well screens with 0.15 mm openings (Figure 2). Wells in each nest are numbered one through four. Well one is the shallowest and well four is the deepest. The well nest screens were located, on average, at depths of 7.3, 11.0, 14.5, and 18.4 m below the surface (Figure 2). The four 'water table' wells have 0.25 mm slotted openings and are screened throughout the thickness of the aquifer. Three 'water table' wells lie within the main well field grid and a fourth 'water table' well was installed at the river to monitor river stage (Figure 1). All monitoring well casings are 51 mm diameter, flush threaded, PVC. Water levels in all of the wells were continuously monitored and recorded in a system of four, independent data collection systems (Munster et al., 1996).

The In Situ Permeable Flow Sensor

Three ISPFSs have been installed at the research site. The first ISPFS installed (ISPFS one) proved to be defective and was abandoned. Two additional ISPFSs (two and three) were later installed and functioned properly during field testing conducted in 1995 (Alden and Munster, 1997). ISPFS two was installed near the B-WT water table well at a depth of 13.7 m (elevation = 53.8 m; Figure 3). ISPFS three was installed near the B-2 well nest at a depth of 18.3 m (elevation = 49.2 m; Figure 3). The placement of the ISPFSs was influenced by factors such as instrumentation access and proximity to the piezometers which were used for gradient analysis comparison.

The ISPFS measures ground-water flow using a thermal perturbation technique (Ballard, 1996) and is permanently installed in saturated, porous, unconsolidated media at the point where ground-water flow is to be determined. This is typically accomplished through use of the hollowstem auger drilling process. Natural backfill must collapse around the probe as the augers are removed to insure intimate contact between the aquifer formation and probe. This is typically accomplished through reverse rotation of the auger as it is pulled from

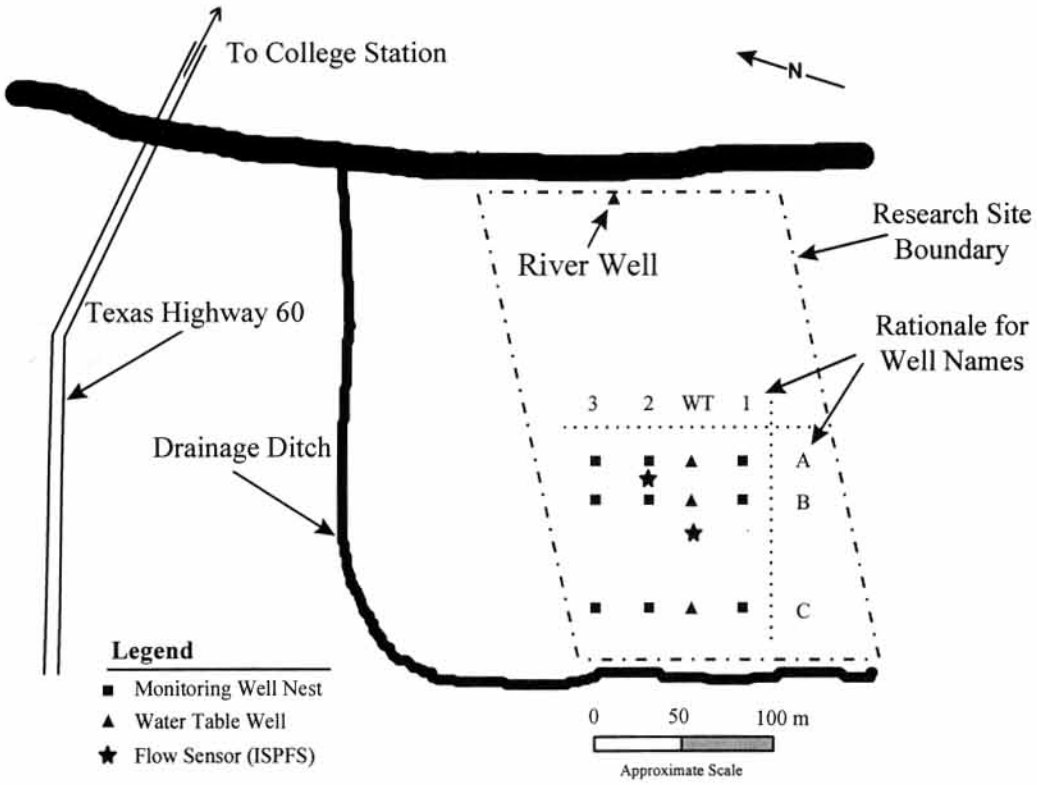

Figure 1. Plan view of the Brazos River Research Site.

the bottom of the borehole. A 25 mm diameter PVC conduit is connected to the device and extends to the surface to protect power and data wiring. ISPFS orientation is accomplished through alignment of the data wiring conduit with a known azimuth.

A resistance heater within the 0.76 m long, 50 mm diameter cylindrical sensor heats approximately one cubic meter of the surrounding aquifer. An array of 30 thermistors located below the surface of the sensor skin measures small variations in temperature that occur as a result of ground-water flow around the device. Post-manufacturing calibration of the sensor in an isothermal bath adjusts relative thermistor accuracy to approximately ±0.01°C. Computer analysis of temperature variations among the 30 thermistors using FLOW© allows determination of a Darcy flow rate and direction in three dimensions. FLOW© is a proprietary software program developed at Sandia National Laboratories for use with ISPFSs. Measurement of ground-water flow rates from 3×10^{-3} to 3×10^{-1} m/day at a resolution of 3×10^{-4} m/day are possible. Accuracy of direction measurement is estimated at ±10°. Instrument accuracy is highly dependent upon the thermal properties of the aquifer and the magnitude of velocities being measured (Ballard, 1994).

Above-ground instrumentation for the ISPFS includes a power supply and data acquisition equipment. Power requirements for the probe depend upon aquifer characteristics and typically range from 60 to 120 watts. The data acquisition equipment used in this test was manufactured by Campbell Scientific Inc., and includes a CR-10 datalogger, an AM416 4x16 relay multiplexer, a data storage module, and a MD9 serial interface module. Comparable data acquisition equipment from other manufacturers can be used.

After installation, the heater within the probe is activated to stabilize the temperature of the surrounding aquifer. Temperature data from 0.5 and 3.5 hours after initial heater start-up is used to produce a calibration file that adjusts the raw temperature data for the thermal properties of the media surrounding the probe. This calibration file is used for all subsequent measurement with this probe installation. Once thermistor temperatures stabilize, measurement of ground-water flow can begin. The time and frequency of discrete ground-water measurements is determined by datalogger programming parameters and options in the FLOW© software.

Data Collection

Data at the research site was collected from day 80 (March 21) to day 210 (July 29) of 1995. Water well levels, ISPFS data, and river stage were monitored. Water levels in the site wells were manually recorded on irregular intervals. ISPFS data was collected on six hour intervals and stored in two, independent and synchronized dataloggers. Power interruptions resulted in the loss of

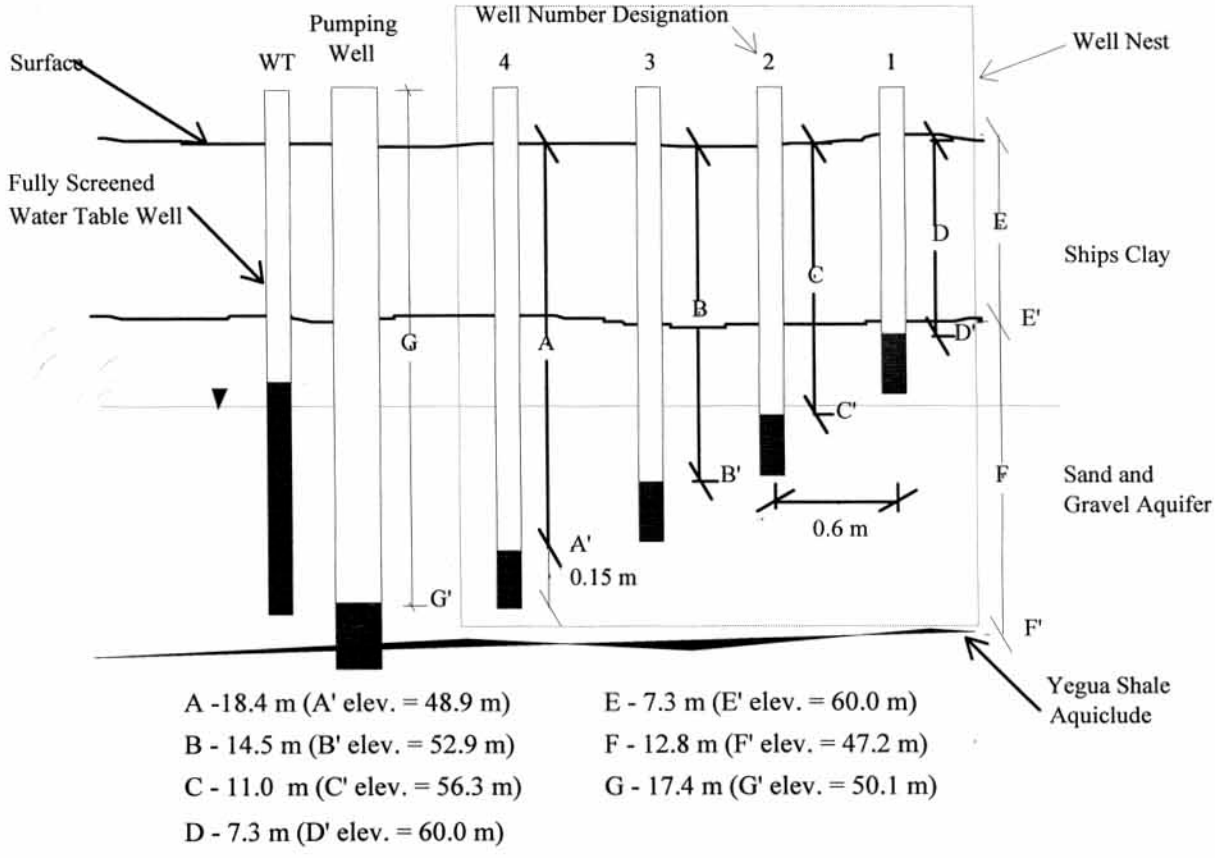

Figure 2. Elevation view of a typical well nest and water table well and the pumping well. The soil stratigraphy and average well screen depths and elevations with respect to mean sea level are also shown (not to scale).

data during the days 132–148 and 150–156 at ISPFS three. A combination of power interruptions and support equipment failure resulted in the loss of data from days 149–210 at ISPFS two.

River stage was approximated by piezometric data taken from a water table well located on the river bank. River well levels were collected every hour by a datalogger. Equipment failures resulted in loss of data on days 102–105, 111–115, 129–130, 131–135, 144–157, 166–168, and 171–174.

A pumping test was performed at the site from day 92 to 105 of 1995. A pumping rate of approximately 0.68 m^3/min was maintained in the 0.2 m pumping well during that period.

METHODS OF ANALYSIS

Piezometric Data

Water level data from the monitoring wells was used to determine horizontal and vertical gradients at two levels within the aquifer. These gradients were used to calculate the direction and magnitude of ground-water flow at each ISPFS location using Darcy's equation.

Piezometers used in the analysis were chosen based on close horizontal and vertical proximity to the applicable ISPFS. Averaging of piezometric data from multiple wells was performed where required to approximate water levels in the proximity of each ISPFS.

Piezometric Data at ISPFS Two

Piezometric wells in well nests A1, A2, B1, and B3 were used to calculate ground-water gradient components at ISPFS two as shown in Figure 4. The number three well in each well nest was chosen for the analysis due to proximity (in depth) to ISPFS two which is located at a depth of 13.7 m. Water table wells A-WT and B-WT were not used in the analysis since they are fully screened. Piezometers A1-3 and A2-3 were used to find the gradient parallel to the river. Water levels in the B1-3 and B2-3 wells were averaged to approximate a piezometric head at BW-T. Water levels from A1-3 and A2-3 were averaged to approximate a piezometric level at AW-T. The B1-3/B2-3 average and A1-3/A2-3 aver-age were used to calculate a gradient perpendicular to the river at ISPFS two as shown in Equation 1.

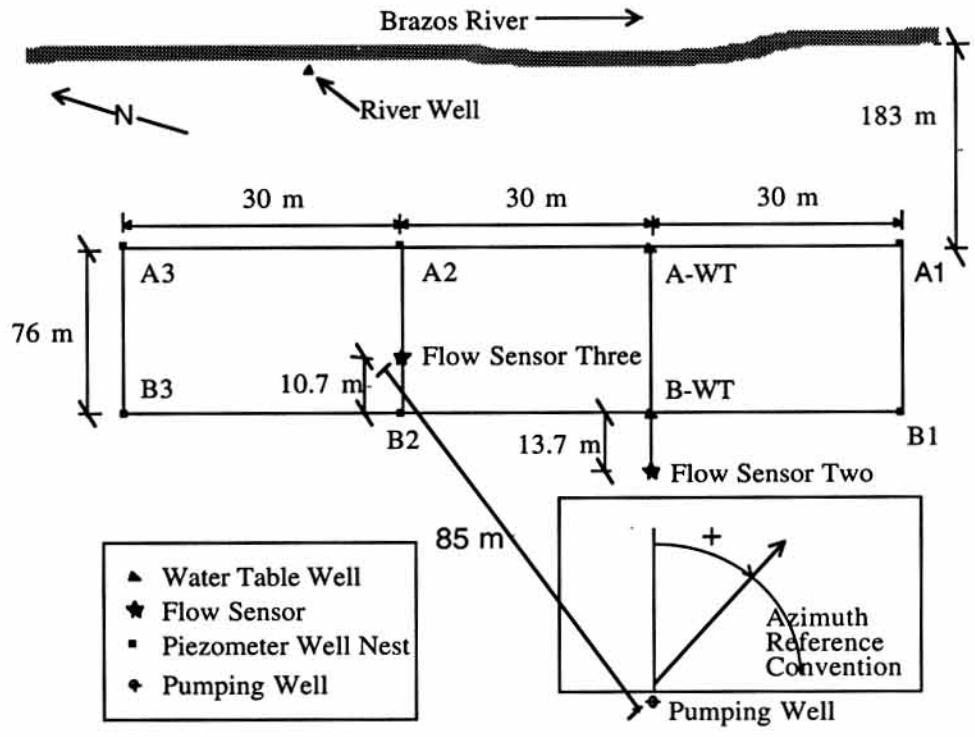

Figure 3. Plan view of the Brazos River Research Site with the location of piezometer well nests, water table wells and Flow Sensors (not to scale). The azimuth reference for ground-water flow direction is also shown.

$$G_{perp} = \left(\frac{[B1\text{-}3] + [B2\text{-}3]}{2} - \frac{[A1\text{-}3] + [A2\text{-}3]}{2} \right) \div l \qquad \text{Eq. 1}$$

Where:

G_{perp} = Hydraulic gradient at ISPFS two perpendicular to the river (m/m);

B1-3, B2-3, A1-3, A2-3 = Water levels in each well (m);

l = distance between the A and B rows of wells (76 m).

A summary of calculated ground-water gradients, horizontal velocities, and flow directions with respect to the river stage is shown in Table 1.

Piezometric Data at ISPFS Three

Piezometric wells in nests A2, A3, B2, and B3 were used to find ground-water gradient components at ISPFS three as shown in Figure 5. The number four well in each well nest was chosen for the analysis due to proximity (in depth) to ISPFS three. Wells B2-4 and A2-4 were used to determine a gradient perpendicular to the river. Wells A3-4 and A2-4 were used to find a gradient parallel to the river. An equipment malfunction resulted in the exclusion of well B3-4 from the analysis. A summary of calculated ground-water gradients, horizontal velocities, and flow directions for ISPFS two and three are shown with respect to the river stage in Tables 2 and 3, respectively.

Saturated Hydraulic Conductivity

Piezometric assessment of ground-water flow is based on the Darcy equation and is dependent upon a saturated hydraulic conductivity (K_{sat}) value for velocity determination. A K_{sat} value is not required for determining ground-water flow from ISPFS data.

Average saturated hydraulic conductivities values for each ISPFS location were calculated from piezometric and ISPFS data. Horizontal ground-water gradients calculated from piezometric data and horizontal velocities measured by the ISPFSs were used in the Darcy equation to calculate K_{sat} values (Tables 1 and 2) at discrete points in time.

The mean K_{sat} value at ISPFS two, at a depth of 13.7 m, was 28.9 m/day with a standard deviation of 1.01 m/day. The mean K_{sat} value at ISPFS three, at a depth of 18.3 m, was 16.5 m/day with a standard deviation of 2.13 m/day. These derived saturated hydraulic conductivities compare favorably to other hydraulic conductivities measured at the site using pump and slug tests (Table 3). The lower than expected values of K_{sat} at deeper aquifer depths in the gravel portion of the aquifer suggests that heterogeneities such as clay lenses may exist.

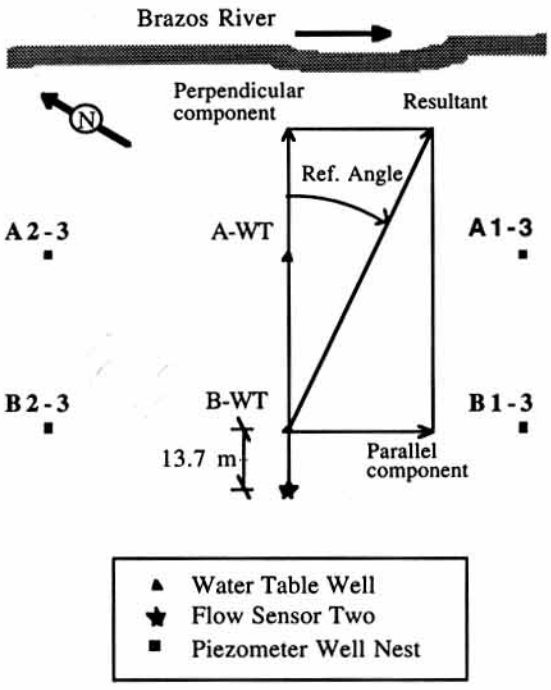

Figure 4. Plan view of wells used in gradient analysis at Flow Sensor two with the ground-water flow direction reference convention shown (not to scale).

ISPFS Data

Reduction of the raw temperature data from the ISPFSs was accomplished using the software program FLOW©. Calibration files developed during laboratory isothermal calibration and initial field operation are applied in FLOW© to convert raw temperature data to ground-water flow data.

RESULTS

Surface-water/ground-water interactions were assessed by evaluating the changes in ground-water flow induced by river stage fluctuations. Changes in the velocity and direction of ground-water flow were determined at depths of 13.7 m and 18.3 m in the aquifer. Changes in horizontal ground-water velocities, perpendicular and parallel to the river, and vertical ground-water velocities were calculated using piezometric and ISPFS data. An evaluation of the surface-water/ground-water interactions resulted in the observance of linear relationships between changes in river stage and changes in the ground-water flow components.

River-Aquifer Interaction

The ground-water flow components and river stage for days 8 to 208, 1995 at ISPFS locations two and three are shown in Figures 6 and 7, respectively. The flow components include horizontal ground-water velocity from piezometric and ISPFS data, vertical ground-water velocity from ISPFS data, and horizontal flow direction (azimuth) from piezometric and ISPFS data. Ground-water velocity and direction vary in response to gradient changes induced by river stage fluctuations. Large changes in ground-water velocity components and azimuth from day 92 to day 105 are due to pump tests conducted at the research site pumping well.

Horizontal ground-water velocities measured by piezometric and ISPFS methods compared very well as shown in Figures 6 and 7. At both depths (13.7 m and 18.3 m), the horizontal ground-water gradients and velocities were inversely related to river stage. Wolf and Helgesen (1993) reported that the ground-water flow to the Kansas River was slowed or even reversed due to increased water levels in the river. Similar trends were reported by Schulmeyer (1995) for the Cedar River in Iowa.

At the Brazos River research site, after the maximum river stage of 57.7 m on day 135, the horizontal velocity decreased to a minimum of 0.043 m/day at the 13.7 m depth and 0.019 m/day at the 18.3 m depth. After a low

Table 1. *Summary of hydraulic gradients from the monitoring wells and horizontal ground-water velocities from the Flow Sensor used to calculate K_{sat} at Flow Sensor two. Negative velocities indicate flow away from the river or upstream. The corresponding river stage is also shown.*

Day of Year 1995	River stage (m)	Hydraulic Gradient (m/m) Perpendicular	Parallel	Resultant	FS 2 Horiz. Vel. (m/day)	Calc. K_{sat} (m/day)
92	54.6	0.0023	0.0005	0.0024	0.067	28.32
105	56.0	–0.0007	0.0007	0.0010		
123	54.6	0.0022	0.0005	0.0023	0.068	29.60
137	57.3	–0.0005	0.0015	0.0015	0.043	27.76
142	55.5	0.0016	0.0005	0.0017	0.050	29.85
157	55.3	0.0020	0.0007	0.0021		
166	56.5	0.0010	0.0010	0.0014		
174	55.0	0.0026	0.0005	0.0026		
193	54.0	0.0036	0.0004	0.0037		
206	53.8	0.0038	0.0004	0.0038		
					AVERAGE =	28.9

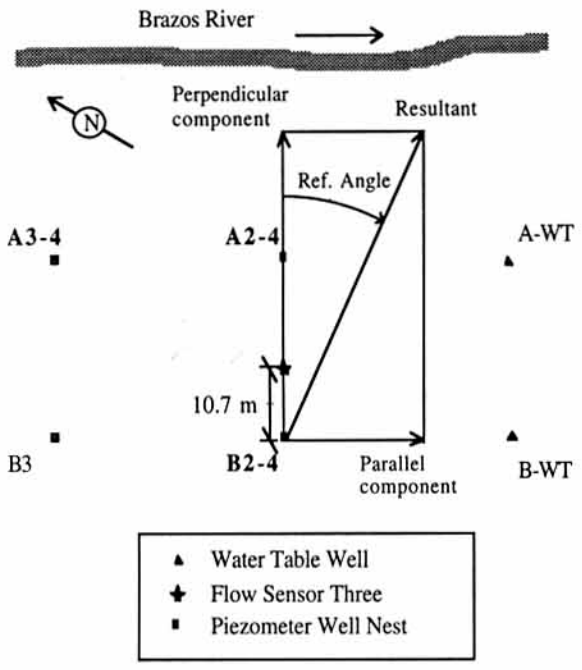

Figure 5. Plan view of piezometer wells used in gradient analysis at Flow Sensor three with the ground-water flow direction reference convention shown (not to scale).

river stage (54.3 m) on day 127, the horizontal velocity increased to 0.074 m/day at the 13.7 m depth and 0.044 m/day at the 18.3 m depth.

At the 13.7 m depth (ISPFS 2), vertical velocities varied from +0.018 m/day (upward) at maximum river stage on day 135 to –0.015 m/day (downward) at low river stage on day 127. At the 18.3 m depth (ISPFS 3), vertical velocities varied from +0.005 m/day (upward) on day 135 and 0.00 m/day on day 127.

Piezometer and ISPFS measured azimuths sometimes varied, especially at high or low river stages. While there was good agreement between ISPFS and piezometric measurement of azimuths at the ISPFS three location; measured azimuth values at the ISPFS two location vary by as much as 30°. At high river stage, ground-water flow was generally oriented in the downstream direction, while at low river stage ground-water flow was generally oriented perpendicular to the river. This type of flow orientation was also observed by Hibbs (1996) on the Colorado River near Bastrop, Texas.

At the 13.7 m depth, the azimuth of horizontal ground-water flow varied from 75° (90° is parallel to the river) at the highest river stage on day 135 to 15° (0° is perpendicular to the river) at low river stage on day 127. At the 18.3 m depth, the azimuth varied from 135° on day 135 to –15° (flow oriented upstream) on day 127. Ground-water flow in the upstream direction was also observed in the piezometric data and may be caused by heterogeneities inherent in fluvial deposits.

Ground-water flow was affected at both ISPFS locations during the pumping test (days 92 to 105). As shown in Figure 3, ISPFSs two and three were located 55 m and 85 m from the pumping well, respectively. The well screen of the pumping well was located from 17.0 m to 21.6 m below the surface. Therefore ISPFS two was above the well screen at 13.7 m and ISPFS three was at the same level as the well screen at 18.3 m.

The direction of ground-water flow changed immediately at ISPFS three. The azimuth changed from –14.4° to 116° very rapidly (approximately 1 day), indicating a direct hydraulic connection between the aquifer at ISPFS three and the pumping well. The final azimuth at ISPFS three was 143° at the end of the pump test. At ISPFS two, the direction of ground-water flow changed gradually from 28.4° to 100.0° during the 13-day pump test.

At ISPFS three the horizontal ground-water velocity increased from 0.034 m/day to 0.063 m/day and the upward vertical velocity changed from 0.017 m/day to 0.014 m/day during the pumping test. The horizontal ground-water velocity at ISPFS two responded in the opposite direction as the velocity decreased from 0.06 m/day to

Table 2. *Summary of hydraulic gradients and Flow Sensor horizontal ground-water velocities used to calculate K_{sat} at Flow Sensor three. Negative velocities indicate flow away from the river or upstream. The corresponding river stage is also shown.*

Day of Year 1995	River Stage (m)	Hydraulic Gradient (m/m) Perpendicular	Parallel	Resultant	FS 3 Horiz. Vel. (m/day)	Calc. K_{sat} (m/day)
88	54.7	0.0014	–0.0009	0.0017		
92	54.6	0.0020	–0.0001	0.0020	0.031	15.47
105	56.0	–0.0022	0.0011	0.0024		
123	54.6	0.0020	–0.0002	0.0021	0.037	18.04
137	57.3	–0.0006	0.0010	0.0012		
142	55.5	0.0016	–0.0002	0.0016		
157	55.3	0.0019	0.0001	0.0019	0.026	13.56
166	56.5	0.0008	0.0008	0.0011	0.022	19.36
174	55.0	0.0023	–0.0004	0.0024	0.043	18.42
193	54.0	0.0032	–0.0006	0.0033	0.052	15.66
206	53.8	0.0034	–0.0006	0.0035	0.05	14.91
						AVERAGE = 16.5

Table 3. *Summary of K_{sat} values in the alluvial aquifer at the Brazos River site.*

Location	Source	Average Depth (m)	Average K_{sat} (m/day)	Wells Used in Analysis
Flow Sensor Two	Flow Sensor	13.7	28.9	N.A.
	Pump Test[1]	14.9	60.6	B1-3, B2-3
	Slug Test[2,4]	14.9	19.0	B1-3, B2-3
	Slug Test[3,4]	14.9	32.3	B1-3, B2-3
Flow Sensor Three	Flow Sensor	18.3	16.5	N.A.
	Pump Test[1]	18.8	58.2	A2-4, B2-4
	Slug Test[2,4]	18.8	3.2	A2-4, B2-4
	Slug Test[3,4]	18.8	3.6	A2-4, B2-4

[1] (Wrobleski, 1996)
[2] Bouwer and Rice analysis (Bouwer, 1989)
[3] Hvorslev analysis (Hvorslev, 1951)
[4] (Alden and Munster, 1997)

0.032 m/day during the pumping test. The vertical velocity at ISPFS two initially increased in the upward direction from 0.00 m/day to 0.09 m/day, then steadily decreased to a downward flow of –0.01 m/day by the end of the pump test.

The relationships between river stage and the ground-water flow components at each ISPFS location were evaluated (Figures 8 and 9). Parallel and perpendicular horizontal ground-water velocities were derived from piezometric data, and vertical ground-water velocities were from ISPFS data. Ground-water flow data from the pump test period (day 92 to 105) was not used in the analysis. Linear regression equations were developed to permit horizontal ground-water velocities, parallel and perpendicular to the river, and vertical ground-water velocities, to be estimated from river stage. The direction of ground-water flow could then be calculated from the predicted horizontal and vertical ground-water velocities.

Similar responses to river stage changes were apparent in the perpendicular and parallel horizontal ground-water velocities at the 13.7 m and 18.3 m depths. For increasing river stage, the perpendicular velocity decreased and the parallel velocity increased. However, the horizontal velocity changes induced by river stage fluctuations at the 13.7 m depth were much greater than those at the 18.3 m depth. At the 13.7 m depth, the perpendicular velocity varied from 0.11 m/day to –0.02 m/day; whereas, at the 18.3 m depth, the perpendicular velocity varied from 0.06 m/day to –0.01 m/day.

Distinctly different responses to river stage were observed in the vertical ground-water velocities at each ISPFS location. At the 13.7 m depth, increasing river stage increased the vertical upward velocity. At the 18.3 m depth, increasing river stage decreased the vertical upward velocity. These different responses may be attributed to aquifer heterogeneities, such as clay lenses or high permeability zones, that resulted from fluvial deposition.

A reversal of vertical ground-water flow from upward to downward occurs when the river stage drops below 53.6 m at the 13.7 m depth and when the river stage rises above 57.4 m at the 18.3 m depth. River stages between 53 m to 58 m were recorded during the investigation and are typical near the Brazos River research site.

SUMMARY

The floodplain aquifer responded differently at the two depths to changes in river stage due to aquifer heterogeneity. The horizontal velocity (parallel and perpendicular), at both depths, decreased with increasing river stage and increased with decreasing river stage. However, the rates of change varied between the two depths, and consequently, the direction of ground-water flow was very seldom, if ever, in the same direction at the two depths.

In addition, the vertical velocity responded in opposite directions due to river stage fluctuations. At the 13.7 m depth, the vertical velocity increased upward with increasing river stage while at the 18.3 m depth, the upward vertical velocity decreased with increasing river stage. At the 13.7 m depth, vertical ground-water flow was directly related to river stage fluctuations. As the river stage began to rise, vertical ground-water flow gradually changed from downward flow to upward flow. As the river stage began to decline, the vertical ground-water flow gradually changed from upward to downward flow. Reversal of vertical ground-water flow occurred at a river stage of approximately 53.6 m.

At the 18.3 m depth, the vertical ground-water velocity fluctuated very little in response to changes to river stage. The flow was always in an upward direction except at very low river stages where the vertical velocity approached zero.

Calibration of piezometric data with ISPFS data produced saturated hydraulic conductivities of 28.9

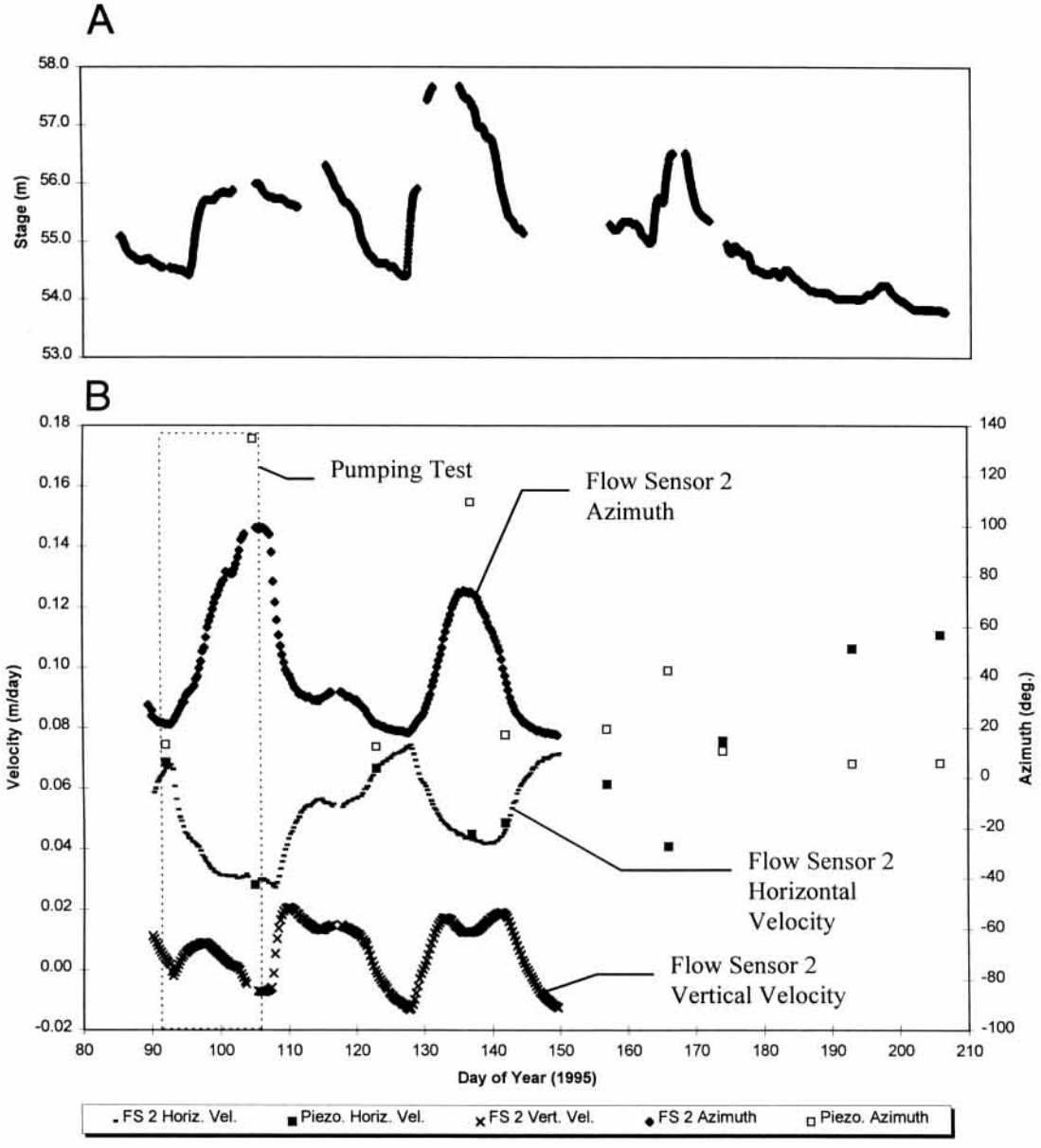

Figure 6. A) River stage from day 80 to 210, 1995. B) Ground-water flow components from piezometric and Flow Sensor data at the Flow Sensor two location from day 80 to 210, 1995. A K_{sat} value of 28.8 m/day was used in piezometric calculations. Negative vertical velocities indicate downward flow.

m/day and 16.5 m/day at depths of 13.7 m and 18.3 m, respectively.

CONCLUSIONS

Ground-water flow in aquifers are often idealized with flow in the same horizontal and vertical direction throughout the depth of the aquifer. However, in floodplain aquifers that are primarily influenced by fluctuations in the adjacent stream, the magnitude and direction of ground-water flow can vary significantly with depth.

ISPFS and piezometric data were used to assess the interaction between the Brazos river and the floodplain aquifer at two depths, 13.7 m and 18.3 m. Changes in the magnitude and direction of ground-water flow induced by river stage fluctuations and a pumping test were studied for 200 days in 1995. In general, the ISPFS values and piezometric values were in close agreement.

Linear relationships between river stage and the magnitude and direction of horizontal and vertical ground-water flow in the floodplain aquifer were developed. In addition, saturated hydraulic conductivity (K_{sat}) values at two depths in the aquifer were derived using piezometric and ISPFS data. These K_{sat} compared favorably to K_{sat} values determined from pump and slug tests performed at the research site.

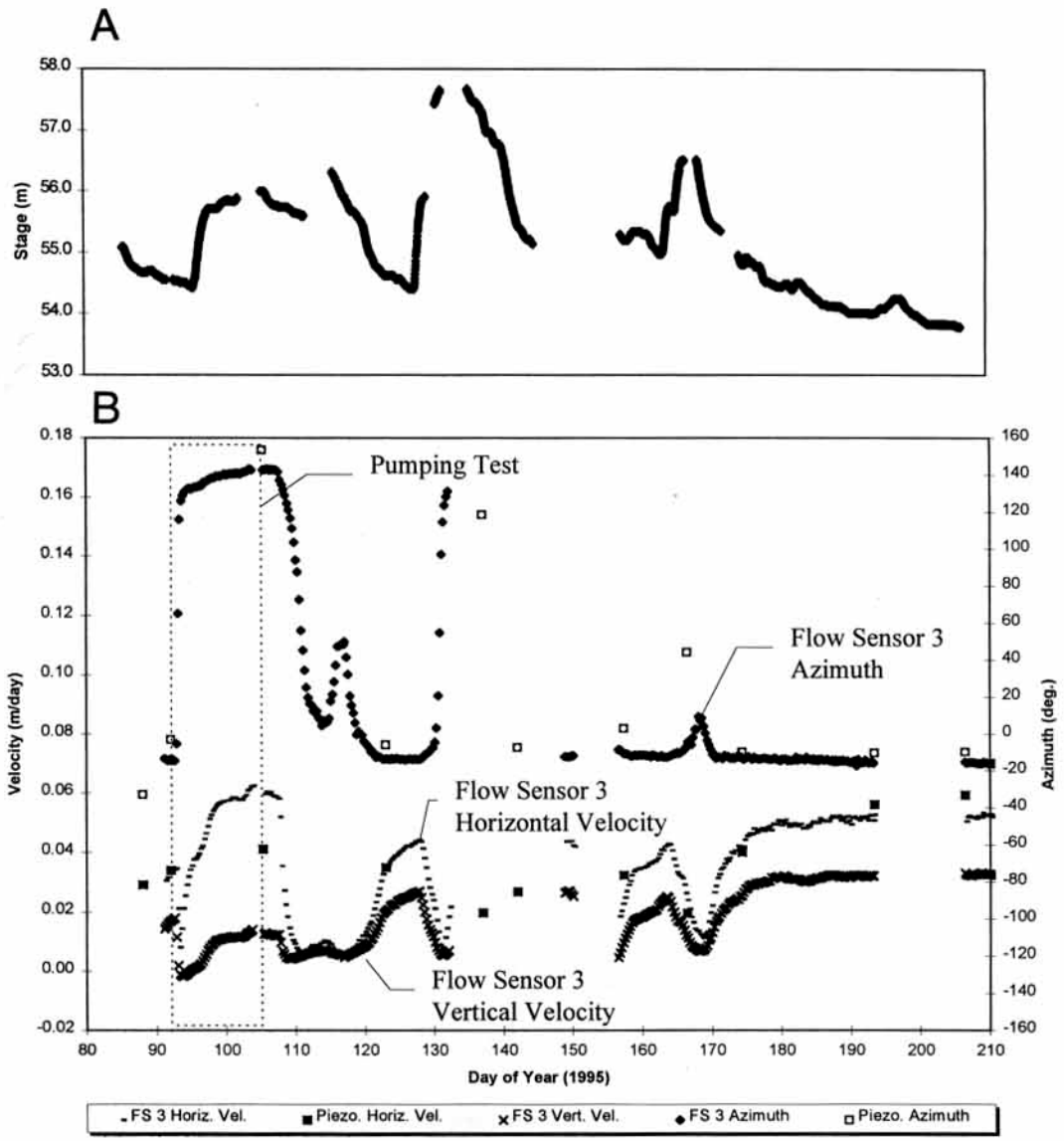

Figure 7. A) River stage from day 80 to 210, 1995. B) Ground-water flow components from piezometric and Flow Sensor data at the Flow Sensor three location from day 80 to 210, 1995. A K_{sat} value of 16.5 m/day was used in piezometric calculations. Negative vertical velocities indicate downward flow.

Evaluation of river-aquifer interaction suggests that a direct and measurable connection exists between river stage and ground-water flow components. Derivation of linear regressions for each ground-water flow component at depths of 13.7 m and 18.3 m, suggests that horizontal and vertical ground-water velocity and direction of horizontal ground-water flow may be predicted if river stage is known.

ACKNOWLEDGMENTS

The authors thank Sanford Ballard of Sandia National Laboratories and Jim Gibson of SIE, Inc. for their assistance.

REFERENCES

ALDEN, A. S. AND MUNSTER, C. L., 1997, Field test of the in situ permeable groundwater flow sensor: *Ground Water Monitoring and Remediation,* Vol. XVII, No. 3, pp. 81–88.

BALLARD, S., 1994, *In Situ Permeable Flow Sensors at the Savannah River Integrated Demonstration: Phase II Results:* SAND94-1958, Sandia National Laboratories, Albuquerque, NM.

BALLARD, S., 1996, The In Situ Permeable Flow Sensor: a ground-water flow velocity meter: *Ground Water,* Vol. 34, No. 2, pp. 231–240.

BOUWER, H., 1989, The Bouwer and Rice slug test—an update: *Ground Water*, Vol. 27, No. 3, May–June, pp. 304–309.

CHAKKA, K. B. AND MUNSTER, C. L., 1996, Simulation of groundwater–surface water interactions on the lower reach of the Brazos River, in *Proceedings, UCOWR '96, Integrated Management*

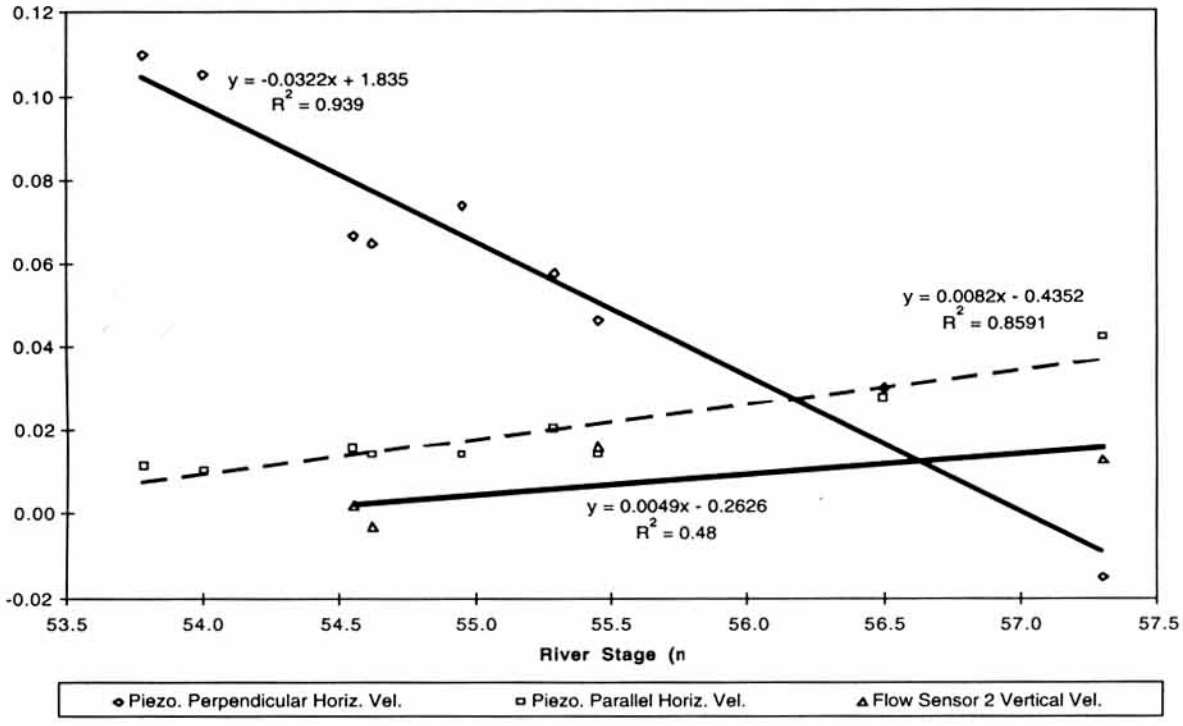

Figure 8. Ground-water flow components from piezometric and Flow Sensor data at the Flow Sensor two location at various river stages. A K_{sat} value of 29.8 m/day was used in piezometric velocity calculations. Negative vertical velocities indicate downward flow. Linear regression lines, formulas, and R^2 values for each ground-water flow component data set are shown. Statistics are based on a 95 percentile confidence interval.

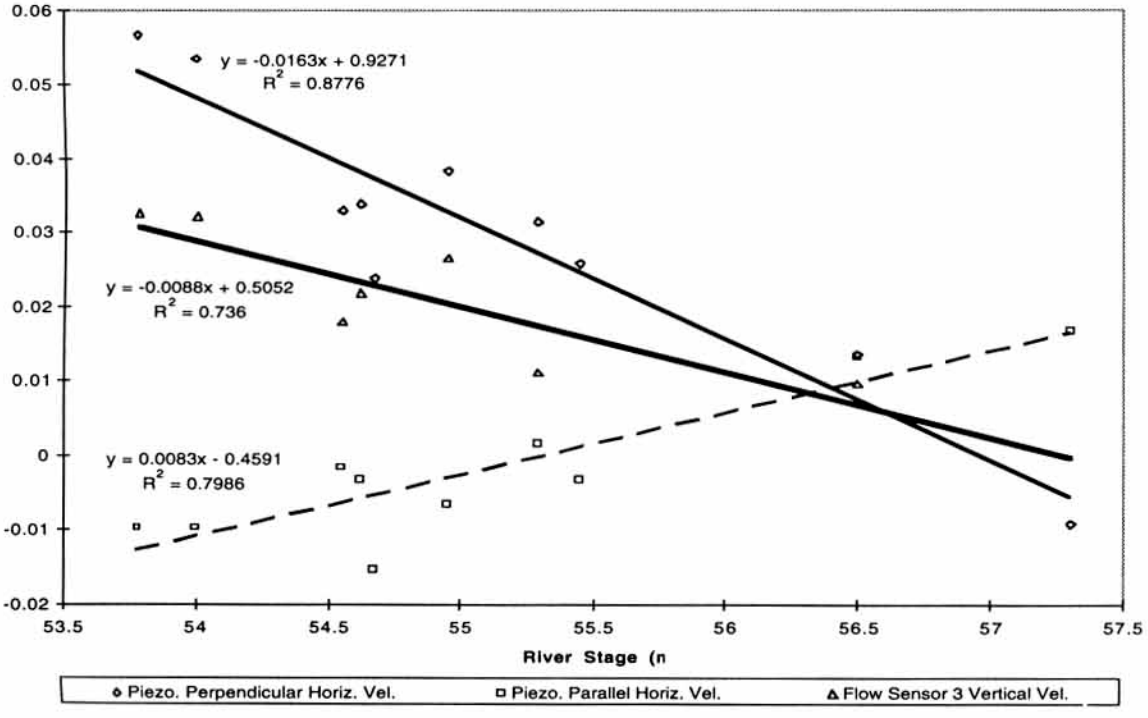

Figure 9. Ground-water flow components from piezometric and Flow Sensor data at the Flow Sensor three location at various river stages. A K_{sat} value of 16.5 m/day was used in piezometric velocity calculations. Negative vertical velocities indicate downward flow. Linear regression lines, formulas, and R^2 values for each ground-water flow component data set are shown. Statistics are based on a 95 percentile confidence interval.

of Surface and Ground Water, July 30–August 2, pp. 213–228.

CRONIN, J. G. AND WILSON, C. A., 1967, *Ground Water in the Flood-Plain Alluvium of the Brazos River, Whitney Dam to Vicinity of Richmond, Texas,* U.S. Geological Survey, Texas Water Development Board, Report 41: Texas Water Development Board, Austin, TX, 206 p.

DE LIMA, V., 1991, *Stream-Aquifer Relations and Yield of Stratified-Drift Aquifers in the Nashua River Basin, Massachusetts*, U. S. Geological Survey Water Resources Investigations Report 88-4147: U. S. Geological Survey, Denver, CO, 47 p.

DUNLAP, L. E.; LINDGREN R. J.; AND SAUER C. G., 1985, *Geohydrology and Model Analysis of Stream-Aquifer System Along the Arkansas River in Kearny and Finney Counties, Southwestern Kansas*, U. S. Geological Survey Water Supply Paper 2253: U. S. Geological Survey, Denver, CO, 52 p.

GREEMAN, T. K., 1995, *Water Levels in the Calumet Aquifer and Their Relation to Surface-Water Levels in Northern Lake County, Indiana, 1985–92*, U.S. Geological Survey Water-Resources Investigations Report 944110: U. S. Geological Survey, Denver, CO, 61 p.

HIBBS, B. J., 1996, Issues of streamflow depletion by high capacity water wells in alluvial aquifers adjacent to Texas rivers, in *Proceedings, UCOWR '96, Integrated Management of Surface and Ground Water*, July 30–August 2, pp. 200–212.

HVORSLEV, M., 1951, *Time Lag and Soil Permeability in Ground-Water Observations:* Waterways Experiment Station, U. S. Army Corps of Engineers, Vicksburg, MS.

JOHNSON, M. J.; HOUSTON, E. R.; AND NEIL, J. M., 1989, *Test Holes for Monitoring Surface-Water/Ground-Water Relations in the Cottonwood Creek Area, Shasta and Tehama Counties, California, 1984–85*, U. S. Geological Survey Water-Resources Investigations Report 88-4090: U. S. Geological Survey, Denver, CO, 28 p.

MUNSTER, C. L.; MATHEWSON, C. C.; AND WROBLESKI, C. L., 1996, The Texas A&M University Brazos River hydrologic field site: *Environmental and Engineering Geoscience*, Vol. II, No. 4, Winter, College Station, TX, pp. 517–530.

POSTAL, S., 1989, Water for agriculture: facing the limits: *World Watch Paper,* No. 93, p. 53.

RAGAN, R. M., 1968, An experimental investigation of partial area contributions: *International Association of Hydrogeology Science Publication*, No. 76, pp. 241–249.

SCHULMEYER, P. M., 1995, *Effect of the Cedar River on the Quality of the Ground-Water Supply for Cedar Rapids, Iowa,* U. S. Geological Survey Water-Resources Investigations Report 94-4211: U. S. Geological Survey, Denver, CO, 68 p.

SKLASH, M. G. AND FARVOLDON, R. N., 1979, The role of groundwater in storm runoff. In Back, W. and Stephenson, D. A. (Editors), *Contemporary Hydrogeology:* Elsevier Scientific Publishers Company, New York, NY, pp. 45–65.

SOPHOCLEOUS, M. A., 1991, Stream–floodwave propagation through the Great Bend alluvial aquifer, Kansas: field measurements and numerical simulations: *Journal of Hydrology,* Vol. 124, pp. 207–228.

SOPHOCLEOUS, M. A.; TOWNSEND, M. A.; VOGLER, L. D.; MCCLAIN, T. J.; MARKS, E. T.; AND COBLE, G. R., 1987, Experimental studies in stream-aquifer interaction along the Arkansas River in Central Kansas, field testing and analysis: *Journal of Hydrology,* Vol. 98, pp. 249–273.

TEXAS WATER COMMISSION, 1989, *Ground-Water Quality of Texas, an Overview of Natural and Man-Affected Conditions,* Report 89-01: Texas Water Commission, Austin, TX, 197 p.

WALTON, W. C.; HILLS, D. L.; AND GRUNDEEN, G. M., 1967, *Recharge From Induced Streambed Infiltration Under Varying Groundwater-Level and Stream Stage Conditions,* Minnesota Water Resources Research Center, Bulletin 6: Minnesota Water Resources Research Center, St. Paul, MN.

WANG, W. AND SQUILLANE, P., 1994, Herbicide interchange between a stream and the adjacent alluvial aquifer: *Environmental Science Technology,* Vol. 28, pp. 2336–2344.

WOLF, R. J. AND HELGESEN, J. O., 1993, *Ground- and Surface-Water Interaction Between the Kansas River and Associated Alluvial Aquifer, Northeastern Kansas,* U. S. Geological Survey Water-Resources Investigations Report 92-4137: U. S. Geological Survey, Denver, CO, 49 p.

WROBLESKI, C. L., 1996, *An Aquifer Characterization at the Texas A&M University Brazos River Hydrologic Field Site, Burleson County, Texas:* Masters Thesis, Department of Geology, Texas A&M University, College Station, TX, 127 p.

ATRAZINE AND NITRATE TRANSPORT TO THE BRAZOS RIVER FLOODPLAIN AQUIFER

K. B. Chakka, C. L. Munster

ABSTRACT. *The potential for contamination of groundwater and surface water from agricultural chemicals used on river floodplains is a serious concern in many parts of the United States. An agricultural research site located near College Station, Texas, was instrumented to determine the fate of agricultural chemicals typically applied to the Brazos River floodplain. Nine well nests were installed in a 3×3 grid pattern, parallel and perpendicular to the river. Each well nest has four monitoring wells screened at various depths throughout the aquifer. Ammonium-nitrate fertilizer and the herbicide atrazine were applied to this research site at the time a corn crop was planted in 1994 and 1995. Groundwater and river samples were periodically collected and tested for nitrate-N, ammonium-N, and atrazine. Increases in nitrate-N in the groundwater were not observed due to high background concentrations of nitrate-N. Ammonium-N was not detected in the groundwater above background concentrations (<1 mg/L) due to nitrification of ammonium-N to nitrate-N in the clay soil. Atrazine was detected in the groundwater 24 days after the second application indicating preferential flow through the Ships clay surface layer that was 6 m thick. A pump test that was conducted at the research site just after the second atrazine application facilitated the movement of atrazine to a depth of 18 m.*

Keywords. *Atrazine, Nitrate-N, Groundwater, Clay soil, Brazos River flood plain.*

On river floodplains, nonpoint source transport of agricultural chemicals in runoff or groundwater can have a significant impact on river water quality. Many river floodplains in East Texas have been identified as locations that are highly susceptible to nonpoint source groundwater contamination. The Texas Water Commission (TWC) has used the DRASTIC system to assess the groundwater pollution potential of the various hydrogeologic settings in the state of Texas. The word DRASTIC is an acronym for the input parameters required by the EPA model (U.S. Environmental Protection Agency, 1987); depth to water, net recharge, aquifer media, soil media, topography, vadose zone impact and hydraulic conductivity. The DRASTIC model, which is a systematic approach to groundwater pollution potential mapping, consistently ranks the river floodplains of East Texas in the highest risk category (Texas Water Commission, 1989). Fertile floodplains are used extensively for agricultural production. However, floodplain aquifers are often in direct hydraulic connection with the adjacent streams, making this geographical area particularly vulnerable to nonpoint source contamination from agriculture.

A maximum contaminant level (MCL) for drinking water has been established for nitrate-N (10 mg/L) and atrazine (3 µg/L) (United States Environmental Protection Agency (USEPA), 1990a). The presence of nitrate-N in groundwater in excess of 10 ppm has proven to be hazardous to human health, especially for infants (USEPA, 1985). Atrazine is soluble in water (33 mg/L), has low adsorption to organic matter (K_{oc} = 100 mL/g) and a relatively long half-life (60 days) in soil (Thooko et al., 1994). These chemical properties facilitate atrazine transport through the soil profile and into the groundwater. However, several factors influence the concentration of agricultural chemicals in groundwater. These include land use, depth of groundwater below land surface, hydrogeologic conditions of the site and soil hydrologic group (Mueller et al., 1995).

Concern for water quality in the rural United States has increased in the past decade. Nonpoint source pollution and watershed protection have been identified as areas of special attention (Knopman and Smith, 1993). To address these concerns, Congress appropriated funds in 1986 for the United States Geological Survey (USGS) to begin a pilot program in seven project areas to develop and refine the National Water-Quality Assessment (NAWQA) Program (Mueller et al., 1995).

National reviews of existing water quality data have proven valuable in describing the occurrence and distribution of nitrate-N in the groundwater of the United States. Hallberg (1989) has reported that nitrate contamination of groundwater occurs in parts of the northeastern, midwestern, and West Coast states. Spalding and Exner (1993) have reported that groundwater beneath agricultural areas in large parts of the southeastern and north-central states was not contaminated with nitrate-N. The USEPA (1990b) reported that only 1.2% of 566 samples collected from public supply wells in 1988 exceeded the nitrate MCL.

In the U.S., the detection of pesticides in drinking water supplies is extremely low (Southwick et al., 1992). However, sound water quality management requires research to

Article was submitted for publication in June 1996; reviewed and approved for publication by the Soil & Water Div. of ASAE in February 1997. Presented as ASAE Paper No. 95-2434.

The authors are **Kesava B. Chakka**, Research Associate, and **Clyde L. Munster**, Assistant Professor, Department of Agricultural Engineering, Texas A&M University, College Station, Tex. **Corresponding author:** Clyde L. Munster, Texas A&M University, Agric. Engineering Dept., 201 Scoates Hall, College Station, TX 77843-2117; tel.: (409) 847-8793; fax: (409) 845-3932; e-mail: <munster@agen.tamu.edu>.

minimize future possible contamination. Evidence exists that herbicides can move into shallow aquifers underlying highly permeable, irrigated, sandy soils (Anderson, 1987). However, with few exceptions, the concentration of atrazine in the groundwater is well below the 3 µg/L MCL (Mueller et al., 1995). A field study conducted by Delin et al. (1995) reported that 58% of the 361 samples collected from a 160-acre farm detected atrazine. Most detections were at trace concentrations, between the detection limit of 0.01 µg/L and the reporting limit of 0.04 µg/L. Blanchard et al. (1995) reported that atrazine concentrations in the groundwater in the Goodwater Creek watershed in north-central Missouri frequently exceeded the 3 µg/L drinking water standard. Fractures which occur throughout the Goodwater Creek study area occupy less than 1% of the soil volume but make the overlying 3-m thick clay layer as permeable as sand.

Increasing our knowledge of the fate of agricultural chemicals applied to the environment will improve our ability to predict the occurrence of these chemicals in shallow aquifers. A field-scale study has been initiated to improve the understanding of processes associated with agricultural chemical transport on river floodplains. A research site has been instrumented along the Brazos River at the Texas A&M University Research Farm near College Station, Texas (Wrobleski, 1996). A primary research objective was to monitor the fate of atrazine and nitrate-N applied to the Brazos River floodplain. This article summarizes the groundwater quality data collected at the research site from February 1994 through August 1995. The objective of this research study was to monitor the changes in groundwater quality, throughout the depth of a floodplain aquifer, in response to surface applied atrazine and ammonium-nitrate fertilizer, for two growing seasons.

Site Description

A research site on the Brazos River was instrumented at the Texas A&M University research farm, approximately 11 km southwest of Bryan-College Station, in Burleson County, Texas (Munster et al., 1996a). The site is located between a drainage ditch that is approximately 5 m deep and the Brazos River which is approximately 193 m from the boundary of the research site (fig. 1). The drainage ditch drains a large portion of the 600 ha farm and is the outlet for surface runoff from the research site. The drainage ditch, which was always dry until surface runoff events occurred, was not sampled or monitored for runoff volume.

The surface layer at the research site is a Ships clay unit (very fine, mixed, thermic chronic Hapluderts) that uniformly varies in depth from 9.1 m near the river to 6.1 m near the ditch with an average thickness of 7.6 m. A floodplain aquifer located below the clay layer changes gradually from a fine sand at a depth of 6 m to a coarse sand and gravel mixture at a depth of 20 m. The aquifer is underlain by an impermeable Yegua shale formation at a depth of 20 m as shown in figure 2.

Field and laboratory studies measured low saturated hydraulic conductivities (1 mm/day at 150 mm depth) for the Ships clay. However, the clay has a high shrink-swell capacity that produces large cracks or macropores during dry periods (Lin, 1995). Ships clay soils are generally low in organic carbon, less than 1% (Lin, 1995), which indicates a low capacity to organically adsorb agricultural chemicals. Soluble agricultural chemicals can potentially be transported through the soil profile via infiltration through these macropores.

The average annual precipitation at this site is approximately 1000 mm. Rainfall is not uniformly distributed throughout the year. The wettest months are

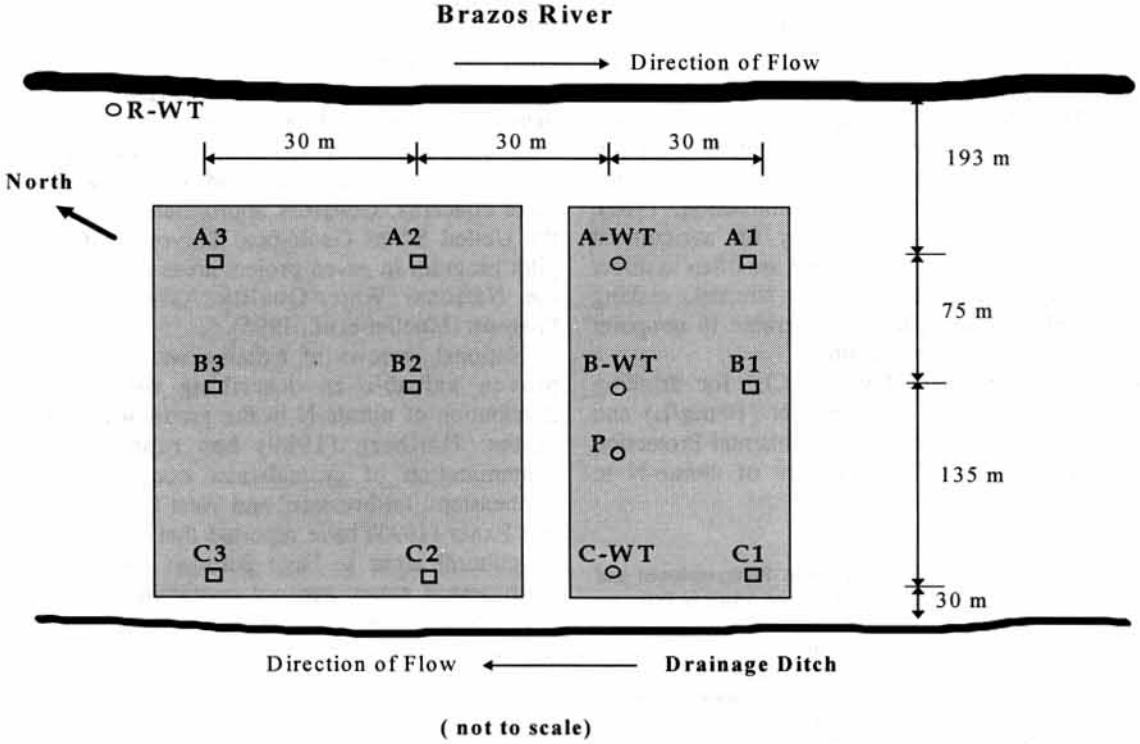

Figure 1–Well Field Layout at the Texas A&M University Research Farm near College Station, Texas, including nine well nests (A1, A2, A3, B1, B2, B3, C1, C2, C3), four water table wells (A-WT, B-WT, C-WT and R-WT), and a 200-mm diameter pumping well (P).

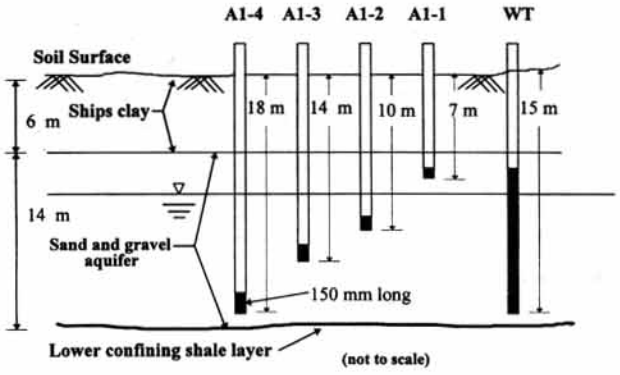

Figure 2–A typical cross-section view of a well nest with four monitoring wells (A1-1, A1-2, A1-3, and A1-4) and a water table well with the soil layers also shown.

April, May, and September and the driest months include March, July, and August. During the summer, rainfall often occurs as short-duration, high-intensity convective thunderstorms. These thunderstorms often occur at times when large macropores or cracks are visible in the surface soil. The total rainfall from day 115 through day 365 in 1994 was 883 mm. The total rainfall measured at the site through day 215 in 1995 was 456 mm.

The research site uniformly slopes (0.5%) toward the drainage ditch. An average of 6.5% of the rainfall left the research site as surface runoff during the groundwater study (Munster et al., 1995).

Groundwater Instrumentation

The 2.4-ha research site was instrumented for groundwater monitoring. Nine well nests were installed in a 3×3 grid that is parallel and perpendicular to the river (fig. 1). Each well nest has four monitoring wells typically labeled as shown in figure 2. These monitoring wells were constructed of 51-mm diameter flush threaded, polyvinyl chloride (PVC) well casing with 150 mm long screens. The well screens, which are wire wound PVC with 0.15 mm openings, are evenly spaced throughout the depth of the sand and gravel aquifer (fig. 2). The 150-mm long screens allowed sampling at discreet points in the saturated aquifer. In addition to the nested wells, four water table monitoring wells, which are fully screened, were located as shown in figure 1. The fully screened wells, which are labeled "water table" wells, have slotted screens with 0.25-mm wide openings. The R-WT water table well was located as close as possible to the river to monitor river stage (fig. 1).

A 203-mm diameter pumping well with a submersible pump rated at 750 L/min was also installed at the research site to evaluate the aquifer characteristics during pump tests. Two pump tests were conducted at the research site during the study period. The pump tests were part of another research study. The first pump test was conducted between day 35 and day 43, 1995, and the second test was conducted between day 92 and day 105, 1995. The average flow rate of the pump tests was approximately 750 L/min.

Water levels were monitored continuously by well head devices installed on each monitoring well. The wellhead device was mounted on top of the monitoring well casings (Munster et al., 1996b). Groundwater flow at the research site was toward the river with an average gradient of 0.0046 m/m (Munster et al., 1996a). However, when the pump tests were conducted, a reversal of groundwater flow toward the pumping wells was observed at the research site in the A and B row wells.

Chemical Application

The site was a pasture with scrub trees prior to 1994. Corn was planted at the research site using ridge till cultivation on day 111 in 1994 and on day 81 in 1995. Granular ammonium nitrate fertilizer was broadcast, and liquid atrazine was sprayed over the entire field at the time of planting. The granular fertilizer (34% nitrogen) and the atrazine application rates are summarized in table 1.

Sampling

All monitoring wells (except the dry 7-m wells) and the river were sampled during each sampling round. A total of 421 groundwater samples and 13 river samples were obtained from 13 sampling rounds (table 2). Background samples were collected prior to the application of the chemicals on day 55 in 1994 and on day 70 in 1995.

Three of the four wells in each well nest were sampled during each sampling event. The shallowest monitoring well in each well nest (fig. 2), located just below the clay layer, was never below the water table and therefore was never sampled. The aquifer was unconfined during the entire study period.

The groundwater sampling protocol followed standard EPA procedures (Exner and Spalding, 1985). Prior to obtaining a sample, each monitoring well was purged three well volumes in order to obtain a representative groundwater sample. Once the wells were purged, groundwater samples were collected and transferred to polyethylene sample bottles and chilled in the field. The sample bottles were transported to the laboratory and refrigerated until chemical analysis was performed.

Table 1. Schedule of chemical applications

Chemical	Day	Application Rate
Fertilizer	111 (1994)	482 kgN/ha
Atrazine	111 (1994)	2.18 kg/ha*
Fertilizer	81 (1995)	200 kgN/ha
Atrazine	81 (1995)	2.80 kg/ha*

* Active ingredient.

Table 2. Schedule of groundwater sampling conducted at the research site

Sampling Round	Day (Year)	No. of Samples	Days after Application
1	55 (1994)	30	Background
2	127 (1994)	33	16
3	144 (1994)	33	33
4	158 (1994)	33	47
5	187 (1994)	33	76
6	231 (1994)	34	120
7	267 (1994)	33	156
8	323 (1994)	34	212
9*	70 (1995)	33	324
10	105 (1995)	32	24
11	137 (1995)	32	56
12	175 (1995)	33	94
13	217 (1995)	33	136

* Background sampling round for second chemical application.

Typically, samples were analyzed within one week after collection. Purging and sampling were accomplished with polyethylene bailers and disposable nylon rope. Each well had a dedicated bailer with new rope each sampling round. The purged water was placed in 19 L buckets and disposed of outside the research plot. After each sampling round the rope was discarded and the bailers were decontaminated for reuse. River samples were grab samples from the bank.

Field measurements of groundwater chemistry were also obtained for each well sample. Field measurements included pH, eH, and conductivity. The groundwater pH ranged from 7.4 in the deep wells to 6.5 in the shallow wells. The eH measurements of groundwater samples ranged from −0.001 mV to 0.030 mV. The shallow monitoring wells had higher Eh values than the medium and deep wells. The Eh values in all the monitoring wells decreased over the study period. The electrical conductivity of groundwater samples ranged from 1000 to 2400 μS. Samples from the shallow wells had higher conductivities than samples from the medium and deep wells. Conductivities also increased in all monitoring wells over the study period.

For quality assurance of laboratory analytical procedures, at least one field blank and three duplicate samples were collected during each sampling round. A total of 36 duplicate samples were analyzed during study. The duplicate sample analyses were generally in good agreement. Nitrate and atrazine concentrations in the field blanks were always below the detection limits.

Analysis of Samples

The groundwater and river samples were analyzed for nitrate-N, ammonium-N, and atrazine concentrations. The nitrate-N and ammonium-N concentrations were analyzed using colorimetric methods (USEPA, 1979; Flore and O'Brien, 1962) by the Soil, Water and Forage Testing Laboratory at Texas A&M University. Groundwater and river samples from sample rounds 1 to 6 were tested for atrazine concentrations using gas chromatography at the Blackland Research Laboratory in Temple, Texas. All groundwater and river water samples from sample rounds 6 to 13 were tested for atrazine concentrations using enzyme immunoassay analysis (EIA) (Cook and Linden, 1995) at the Agricultural Engineering Department at Texas A&M University. Gas chromatography/mass spectrometry (GCMS) was used to verify 39 samples of the EIA analysis.

Results and Discussion

Nitrate-N

The average and standard deviations of concentrations of nitrate-N in the nine shallow wells, eight medium wells (well C2-3 not available), and nine deep wells are shown in table 3. The average screen depth below the surface for the shallow wells was 10 m, 14 m for the medium wells, and 18 m for the deep wells. During the 13 sampling rounds, the nitrate-N concentrations in the shallow wells ranged from 0.59 to 8.51 mg/L with an average of 5.52 mg/L. In the medium wells, the nitrate-N concentration ranged from 0.39 to 1.90 mg/L with an average of 0.97 mg/L. In the deep wells, the nitrate-N concentration ranged from 0.00 to 1.82 mg/L with an average of 0.25 mg/L.

Table 3. Average nitrate-N concentrations with standard deviations detected in groundwater samples from the shallow, medium, and deep wells and the Brazos River from February 1994 to August 1995

Days after Application (Sampling Round)	Shallow Wells 9.8 m to 12.5 m		Medium Wells 14.0 m to 16.1 m		Deep Wells 17.1 m to 19.2 m		River Water
	Avg.* (mg/L)	Std. Dev.† (mg/L)	Avg. (mg/L)	Std. Dev. (mg/L)	Avg. (mg/L)	Std. Dev. (mg/L)	(mg/L)
Background (1)	7.31	5.14	0.92	0.88	0.08	0.11	0.81
16 (2)	7.33	4.59	1.30	1.78	0.09	0.11	1.16
33 (3)	7.80	5.52	1.78	1.69	0.12	0.07	0.70
7 (4)	8.51	5.81	1.18	1.54	0.15	0.06	0.20
76 (5)	6.36	5.47	0.78	1.27	0.14	0.16	0.05
120 (6)	6.03	6.06	1.10	1.55	0.13	0.18	0.05
156 (7)	5.90	3.99	0.98	1.40	0.13	0.19	0.10
212 (8)	3.56	5.44	0.54	0.68	1.82	3.86	0.70
324 (9)	5.80	4.38	0.49	0.88	0.08	0.11	0.20
24‡ (10)	6.88	4.90	0.39	0.61	0.00	0.00	0.50
56‡ (11)	3.11	2.28	0.43	0.48	0.05	0.00	0.50
94‡ (12)	2.52	2.82	1.90	4.08	0.10	0.00	0.1
136‡ (13)	0.59	1.01	0.80	1.29	0.32	0.67	0.1

* Average.
† Standard deviation.
‡ Days after second chemical application.

The average for the shallow wells (5.52 mg/L) is approximately six times higher than average of the medium wells (0.97 mg/L). The average of the deep wells (0.25 mg/L) is approximately 3.5 times lower than the medium wells and 21 times lower than the shallow wells. The nitrate-N levels in the river ranged from 0.05 to 1.16 mg/L with an average concentration of 0.40 mg/L during the 13 sampling rounds.

A high degree of spatial variability was noticed from all the sampling rounds. Samples from the C-row monitoring wells showed higher concentrations of nitrate-N than the other wells, resulting in high standard deviations. During sampling rounds 6, 8, 12, and 13 the standard deviation was higher than the mean of concentrations in the shallow wells (table 2).

The nitrate-N and atrazine concentrations for the shallow wells in the A, B, and C row well nests are shown in figures 3-5. Nitrate-N and atrazine concentrations in the water table wells and the Brazos River are shown in figure 6. The average nitrate-N concentrations decreased in the shallow wells with increasing distance from the ditch (figs. 3-5). The spatial variability of nitrate-N concentrations in the medium and deep wells was less than that in the shallow wells based on the higher standard deviations for the shallow wells as shown in table 3.

In the shallow wells, the average nitrate-N concentration in the C-row (closest to the ditch) for sampling round 1 was approximately 16 mg/L, while the A and B row averages were approximately 2.5 mg/L (figs. 3-5). This may indicate direct interaction between the irrigation drainage ditch and the shallow wells in the C-row. After sampling round 1, the NO_3-N concentrations in the shallow wells in the C-row steadily declined to the same concentration levels as the A and B-row shallow wells. The shallow wells do not give any solid evidence of increased nitrate concentrations due to the ammonium nitrate fertilizer that was applied on day 111, 1994 and day 81 in 1995.

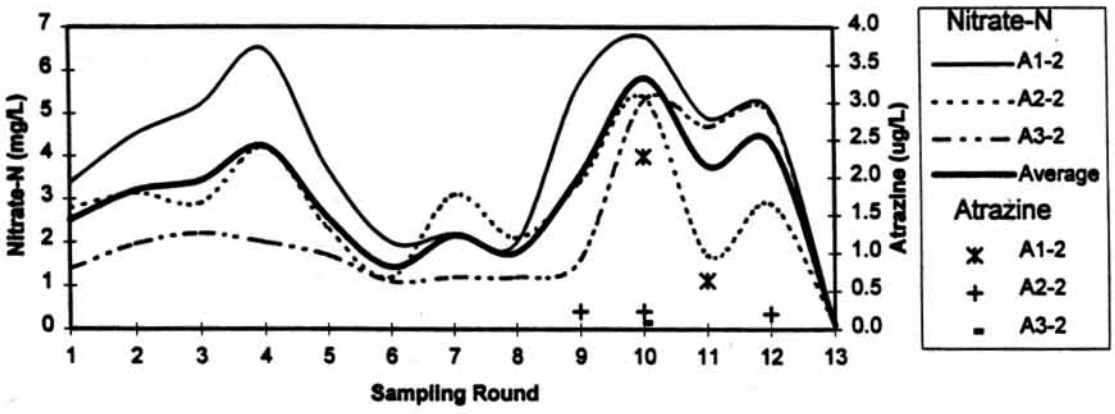

Figure 3–Nitrate-N and atrazine concentrations in the shallow wells (10.3 m to 12.5 m) of A-row well nests.

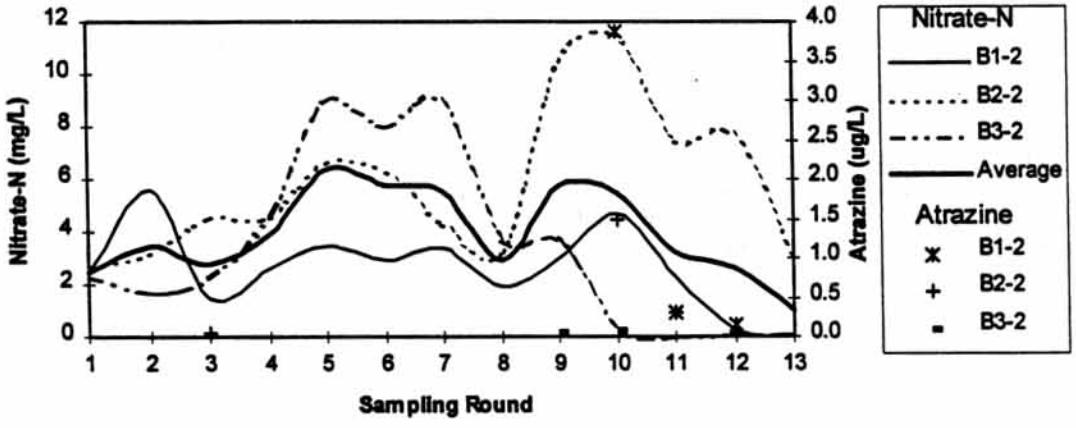

Figure 4–Nitrate-N and atrazine concentrations in the shallow wells (10.0 m to 12.6 m) of B-row well nests.

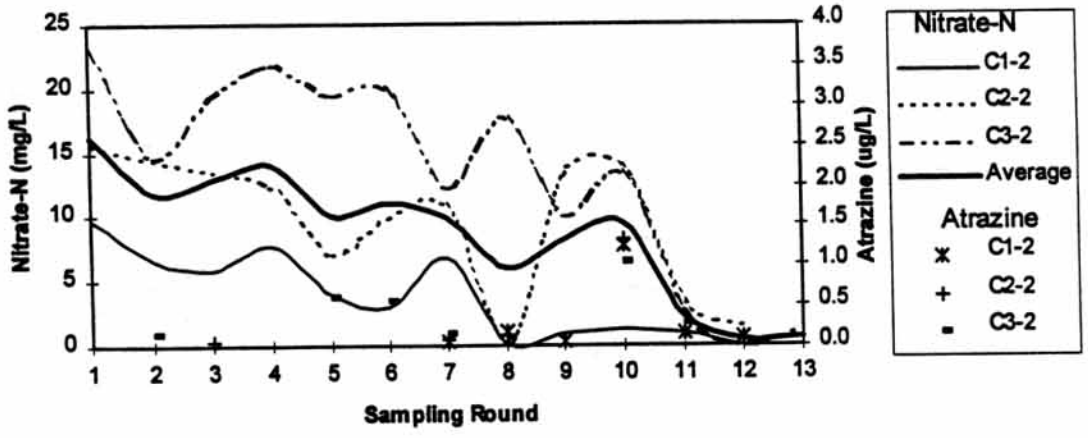

Figure 5–Nitrate-N and atrazine concentrations in the shallow wells (9.75 m) of C-row well nests.

The average nitrate-N concentrations in the shallow, medium and deep wells of the A, B, and C rows are listed in table 4. Although there are high nitrate-N concentrations in the C-row shallow wells, the C-row medium wells have very low concentrations. The average concentration in the C-row shallow wells was approximately 8.88 mg/L while the average of the C-row medium wells was 0.10 mg/L, which is 90 times smaller than the shallow wells. The C-row medium wells do not appear to be hydraulically connected with the C-row shallow wells. In addition, the A and B-row medium wells have an overall average concentration of 1.22 mg/L, which is 12 times larger than the C-row medium wells. All deep wells at the study site generally had low concentrations of nitrate-N (<0.05 mg/L). However, high concentrations of nitrate-N (3.8 mg/L and 11.6 mg/L) were detected twice in the deep wells.

Ammonium-N

The nitrification of ammonium-N to nitrate-N generally occurs quite quickly in moist clay soils (Tisdale et al.,

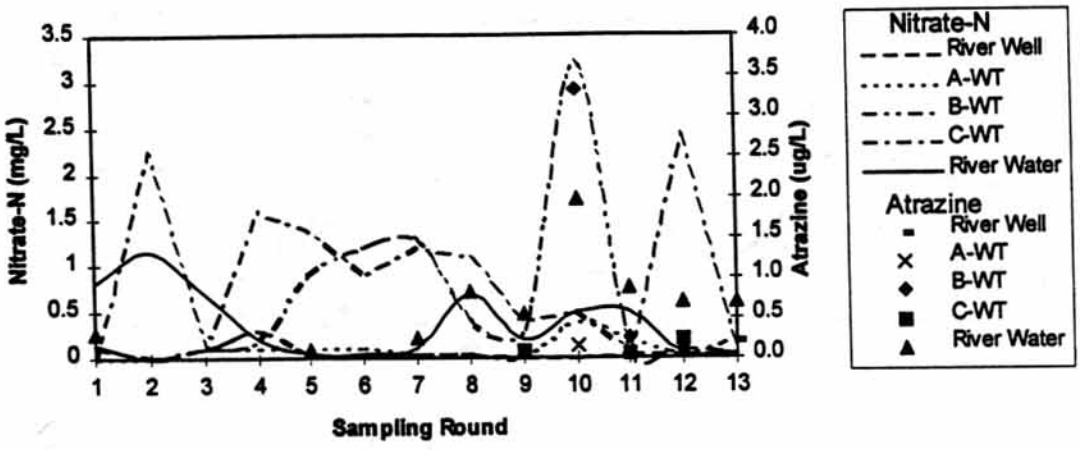

Figure 6–Nitrate-N and atrazine concentrations in the river well, water table wells, and in the Brazos River.

1985). This occurred at the research site as the ammonium-N concentrations in all wells at the study site were very low, ranging from 0.2 mg/L to 1.0 mg/L. The C-row shallow wells, which had the highest concentrations of nitrate-N, did not have high concentrations of ammonium-N. The concentrations of ammonium-N did not change appreciably in any of the wells throughout the study period. All groundwater samples had concentrations of ammonium-N below 1.0 mg/L. The ammonium-N analysis indicates no trends or changes in the concentrations during the study period. This analysis was discontinued after sampling round seven but was restarted after the application of fertilizer for the second crop period.

Atrazine

The atrazine concentrations detected in the groundwater during the 13 sampling rounds are summarized in table 5. Atrazine was detected consistently in the shallow wells of the C-row near the ditch. Atrazine concentrations are plotted with nitrate-N on figures 3-6. Detection of atrazine was not affected by the first pump test, which was conducted between sampling rounds 8 and 9 just prior to the second chemical application. However, atrazine movement was affected by the pump test conducted on days 92 to 104, 1995, which occurred between sampling rounds 9 and 10. An increase of the vertical hydraulic gradients, due to the pump test and several rainfall events, facilitated the transport of atrazine through the aquifer and resulted in detection of atrazine in five of the nine deep wells. The atrazine data presented in table 5 indicated the movement of the surface applied chemicals to the shallow wells within 24 days during a period of pump testing when increased vertical hydraulic gradients were established.

While the concentration of nitrate-N does not indicate any particular trend, the atrazine concentrations detected in sample round 10 provided evidence of macropore flow through the 6-m thick clay layer to the groundwater. The second application of atrazine occurred on day 81, 1995. Sampling round 10 took place on day 105, 24 days after application. After the atrazine was applied, a pump test using the 0.20-m diameter well was conducted from day 92 to day 107. During the pump test, the vertical groundwater gradients increased approximately 8 times from 0.0022 m/m pre-pumping to 0.0178 m/m post-pumping. In addition, two large rainfall events occurred on days 94 and 95, 13 days after application, totaling 68.6 mm of rainfall. From surface runoff studies at this site (Munster et al., 1995), a maximum of 18% of the rainfall typically runs off. Therefore, at least 55 mm of rainfall infiltrated by day 96. This infiltration transported the atrazine from the surface through the 6 m thick clay layer to the sand aquifer by macropore flow. Once in the sand aquifer, the large vertical gradients generated by the pump test accelerated the transport of atrazine through the sand and gravel aquifer. Atrazine was detected in all nine shallow wells, seven of eight medium wells, and five of nine deep wells during sampling round 10.

Table 4. Average nitrate-N concentrations in the shallow, medium, and deep wells in A, B, and C-Rows for all 13 sampling rounds

Average Nitrate-N Concentrations	Shallow Wells (mg/L)	Medium Wells (mg/L)	Deep Wells (mg/L)
A-Row	2.99	1.22	0.13
B-Row	3.95	1.25	0.18
C-Row	8.88	0.10	0.51

Table 5. Atrazine concentrations detected in the groundwater and the Brazos River from February 1994 to August 1995

Days After Application (Sampling Rd.)	No. of Samples with Atrazine Detects			Max. Conc.* (µg/L)	River Water (µg/L)
	Shallow	Medium	Deep		
Background (1)	0	0	0	0.0	0.30
16(2)	1	0	1	0.15	0.00
33 (3)	1	0	0	0.05	0.00
47 (4)	0	0	0	0.00	0.00
76 (5)	1	0	0	0.60	0.10
120 (6)	1	0	0	0.56	0.00
156 (7)	3	0	0	0.16	0.26
212 (8)	3	0	0	0.17	0.83
324 (9)	3	0	1	1.23	0.56
24† (10)	9	7	5	3.87	1.98
56† (11)	5	2	1	0.64	0.87
94† (12)	5	0	3	0.22	0.70
136† (13)	0	0	2	0.26	0.71

* Maximum concentration.
† Days after second chemical application.

SUMMARY

A field-scale research site has been instrumented to study the potential for nonpoint source contamination from agricultural chemicals on the Brazos River floodplain. A total of 421 groundwater and 13 river water samples were obtained in 13 sampling rounds from February 1994 to August 1995. These samples were analyzed for nitrate-N, ammonium-N and atrazine. Fertilizer and atrazine were applied in April 1994 and March 1995. Over the study period, the average nitrate-N concentrations were 5.52 mg/L in the shallow wells, 0.97 mg/L in the medium wells, and 0.25 mg/L in the deep wells. From the nitrate and ammonium water quality data, there was no direct evidence of transport of surface applied nitrate-N to the groundwater. This was due to the relatively high nitrate concentrations already present in the groundwater.

Although the aquifer is overlain by a surface clay soil 6 m thick, there is evidence of atrazine transport to the groundwater after the second application in March 1995. Sample round 10, which was conducted 24 days after application, detected atrazine concentrations in 21 of 26 monitoring wells. The maximum atrazine concentration for sample round 10 was 3.87 µg/L. This is 11 times higher than the average maximum concentration of 0.36 µg/L for all other sample rounds. A pump test conducted just prior to sample round 10 facilitated the movement of atrazine through the sand aquifer. However, atrazine had to first travel through the 6 m clay layer to reach the sand aquifer. The rapid chemical transport to the sand aquifer indicates macropore flow in the clay soil and supports the research findings by Blanchard et al. (1995), in a claypan soil watershed. Atrazine was a better indicator of macropore flow than nitrate due to the zero background concentrations of atrazine in the groundwater.

Two crop periods were monitored during the years 1994 and 1995. There is a large difference between the crop periods in terms of number of detections of atrazine in groundwater. Only four of 132 samples collected during the crop period in 1994 detected atrazine. During 1995, 37 of 133 samples detected atrazine. The atrazine application rate during 1995 was 28% higher than the application rate during 1994. Approximately 27.5% of the total samples collected during the year 1995 resulted in atrazine detects, compared to 3% in 1994. Possible explanations for an increase in 1995 include a series of rainfall events that occurred within 15 days after chemical application; a pump test that was conducted between days 92 and 104; and 28% higher atrazine application rate. Atrazine was detected in the shallow wells in the C-row during sampling rounds 2, 5, 10, 11, and 12. This indicates that there may be movement of atrazine from the irrigation ditch to the C-row shallow wells. However, further evaluation is needed since the drainage water in the irrigation ditch was not sampled during the study period.

REFERENCES

Anderson, J. H. 1987. Agriculture and natural resources: The broadening horizon. In *Rural Groundwater Contamination*, eds. F. M. D'ltri and L. G. Wolfson. Chelsea, Mich.: Lewis Publ. Inc.

Blanchard, P. E., W. W. Donald and E. E. Alberts. 1995. Herbicide concentrations in groundwater in a claypan soil watershed. In *Proc. Clean Water - Clean Environ. — 21st Century,* Vol. 1-Pesticides. St. Joseph, Mich.: ASAE.

Cook, S. M. F. and D. R. Linden. 1995. Immunoassay suitability for measuring atrazine in a silt loam soil. In *Proc. Clean Water - Clean Environ. — 21st Century,* Vol. 1-Pesticides. St. Joseph, Mich.: ASAE.

Delin, G. N, M. K. Landon, J. A. Lamb, R. H. Dowdy and J. L. Anderson. 1995. Transport of agricultural chemicals to groundwater. In *Proc. Clean Water - Clean Environ.— 21st Century,* Vol. 1-Pesticides. St. Joseph, Mich.: ASAE.

Exner, M. E. and R. F. Spalding. 1985. Groundwater contamination and well construction in Southeast Nebraska. *Ground Water* 23(1):26-34.

Hallberg, G. R. 1989. Nitrate in groundwater in the United States. In *Nitrogen Management and Ground-water Protection.* ed. R. F. Follet, 35-74. New York, N.Y.: Elsevier Science Publ. Co.

Knopman, D. S. and R. A. Smith. 1993. Twenty years of the Clean Water Act. *Environ.* 35(1):17-41.

Lin, H. 1995. Hydraulic properties and macropore flow of water in relation to soil morphology, Ph.D. thesis. College Station, Tex.: Texas A&M University.

Mueller, D. K., P. A. Hamilton, D. R. Helsel, K. J. Hitt and B. C. Ruddy. 1995. Nutrients in groundwater and surface water of the United States — An analysis of data through 1992. USGS Water Resour. Inv. Rep. 95-4031. Denver, Colo.

Munster, C. L., C. C. Mathewson and C. L. Wrobleski. 1996a. The Texas A&M University Brazos River hydrologic field site. *Environ. Eng. Geosci.* (In Press).

Munster, C. L., J. E. Parsons and R. W. Skaggs. 1996b. Using the personal computer for water table management. *Appl. Eng. Agric.* (In Press).

Munster, C. L., B. M. Schneider and J. R. Vogel. 1995. Chemical and sediment transport in surface runoff (Part 1: Field study). ASAE Paper No. 95-2697. St. Joseph, Mich: ASAE.

O'Brien, J. E. and J. Flore. 1962. Automation in sanitary chemistry — Parts 1 and 2. Determination of nitrates and nitrites. *Wastes Eng.* 33(March):128 and 33(May):238.

Southwick, L. M., G. H. Willis and H. M. Selim. 1992. Leaching of atrazine from sugarcane in southern Louisiana. *J. Agric. Food Chem.* 40(7):1264-1268.

Spalding, R. F. and M. E. Exner. 1993. Occurrence of nitrate in groundwater. *J. Environ. Quality* 22(3):392-402.

Texas Water Commission. 1989. Plate 2 — Groundwater pollution potential, agricultural sources. In *Groundwater Quality of Texas*. Report 89-01. Austin, Tex.

Thooko, L. W., R. P. Rudra, W. T. Dickinson, N. K. Patni and G. J. Wall. 1994. Modeling pesticide transport in subsurface drained soils. *Transactions of the ASAE* 37(4):1175-1181.

Tisdale, S. L., W. L. Nelson, J. D. Beaton and J. L. Halvin. 1985. *Soil Fertility and Fertilizers*. New York, N.Y.: Macmillan.

U.S. Environmental Protection Agency. 1990a. Maximum contaminant levels (subpart B of 141, Nat. primary drinking water reg.). In *U.S. Code of Federal Regulations*, Title 40, Parts 100-149:559-563. Washington, D.C.: U.S. GPO.

————. 1990b. National survey of pesticides in drinking water wells, Phase I report. USEPA Report 570/9/9-90-015. Washington, D.C.: Office of Water, Office of Pesticides and Toxic Substances.

————. 1987. DRASTIC: A standardized system for evaluating ground water pollution potential using hydrogeologic settings. USEPA Report 600/2-87/035. Ada, Okla.: Robert S. Kerr Environmental Research Lab.

————. 1985. Nitrate/Nitrite health advisory (draft). Washington, D.C.: Office of Drinking Water.

————. 1979. *Methods for Chemical Analysis of Water and Wastes*. Washington, D.C.

Wrobleski, C. L. 1996. An aquifer characterization at the Texas A&M University Brazos River hydrologic field site, Burleson Co., Texas, M.S. thesis. College Station, Tex.: Texas A&M University.

The Texas A&M University Brazos River Hydrogeologic Field Site

By Clyde Munster, Christopher Matthewson, Christine Wrobleski

Published in Volume II, Number 4
Journal of Environmental & Engineering Geoscience
Winter 1996

The Texas A&M University Brazos River Hydrogeologic Field Site

CLYDE MUNSTER, Assistant Professor
Agricultural Engineering Department, Texas A&M University, College Station, TX 77843-2117

CHRISTOPHER MATHEWSON, Professor
Department of Geology and Geophysics, Texas A&M University, College Station, TX 77843-3115

CHRISTINE WROBLESKI
Radian International, Austin, TX 78720-1088

Key Terms: ***Test Site, Ground Water, Hydrogeology, Floodplain, Brazos River, Monitoring Wells, Surface-Ground-Water Interactions***

ABSTRACT

A ground-water test site on the Brazos River floodplain has been instrumented and characterized for research, education and the assessment of ground-water technology. This 8.5 ha (21 ac) site, known as the Brazos River Site, is located near College Station, Texas, on the Texas A&M University Research Farm and is intended to function as a test facility for the development of new and innovative technologies. The site is overlain by a surface clay layer that extends to an average depth of 7.6 m (24.9 ft). Below the clay is an alluvial, heterogeneous unconfined aquifer that is approximately 13.4 m (44.0 ft) thick. The aquifer, which is in direct hydraulic connection with the Brazos River, is comprised of a fluvial deposited upward fining sequence of gravel, sand, silt and clay. At an average depth of 21 m (69 ft), the site is underlain by an impermeable shale formation. The Brazos River Site has nine well nests, arranged in a 3 x 3 grid, oriented parallel and perpendicular to the river. Each well nest consists of four monitoring wells that are screened at different intervals throughout the aquifer that are instrumented to monitor water levels. The site has a large diameter pumping well and an injection well for forced gradient tracer studies. Other site instrumentation includes weather stations, surface runoff collection systems to quantify and sample runoff, and experimental 3-D ground-water velocity meters.

INTRODUCTION

The U. S. government has recently recognized the need for ground-water testing facilities for technology development. In 1990, the U. S. congress authorized the Strategic Environmental Research and Development Project (SERDP) under the auspices of the Department of Energy (DOE), Department of Defense (DOD) and the Environmental Protection Agency (EPA). One of the goals of SERDP is a project to develop six Restoration Technology Demonstration Sites across the United States. These sites will provide the ability to demonstrate technologies developed either in the Federal or private sector (1994 Annual Report and Five Year [1994–1998] Strategic Investment Plan [SERDP, 1994]).

To accommodate the growing need for ground-water testing facilities, the Texas A&M University Brazos River Hydrogeologic Field Site, known as the Brazos River Site, has been established on the Brazos River floodplain in Burleson County near College Station, Texas. The Brazos River Site has three missions: research, education and assessment of new and innovative ground-water technology. This site is available to all segments of the ground-water industry for field research, technology development, equipment and procedure testing, and education. The Brazos River Site is intended to function in the same capacity as standardized test sites for other engineering disciplines. An existing model would be the National Geotechnical Experimentation Sites that were established by the Federal Highway Administration to "develop practical, cost-effective technology for bridge foundations, retaining walls and embankments" (DiMillino and Prince, 1993).

The Brazos River Site was initially establish in 1993 with funding from the Texas Water Research Institute and Texas A&M University to investigate the fate of agricultural chemicals applied to river floodplains. The site was instrumented for ground-water and surface runoff research and agricultural chemicals were monitored in the soil, ground water and surface runoff during the growing seasons of 1994 and 1995 (Munster et al., 1995; Chakka and Munster 1996a).

Since 1993, numerous research investigations have been conducted at the Brazos River Site. Site research

projects have included, bacteriophage tracer tests under pumped gradient conditions (Vogel et al., 1996), ground-water surface-water interactions (Chakka and Munster, 1996b), surface electromagnetic investigations to identify subsurface permeability (Everett et al., 1996) and macropore transport studies.

As a result of these research projects, extensive ground-water instrumentation has been installed, the hydrogeology has been characterized and the ground-water surface-water interactions have been assessed at the site. In addition, the U. S. Geological Survey (USGS) computer model, Variably Saturated Two-Dimensional Transport (VS2DT) was successfully used to simulate ground-water flow and chemical transport at the Brazos River Site (Chakka and Munster, 1996b).

SITE DESCRIPTION

The Brazos River Site is a 8.5 ha (21 ac) field research site located on the Brazos River floodplain at the Texas A&M University Research Farm. Covering approximately 15 percent of the state, the Brazos River basin is the largest in Texas, traversing 1,931 km (1,200 mi) from the high plains of west Texas to the Gulf of Mexico while dropping 1,402 m (4,600 ft; Epps, 1973). The Brazos River Site is approximately 201 km (125 mi) from the river mouth at Freeport, Texas (Figure 1).

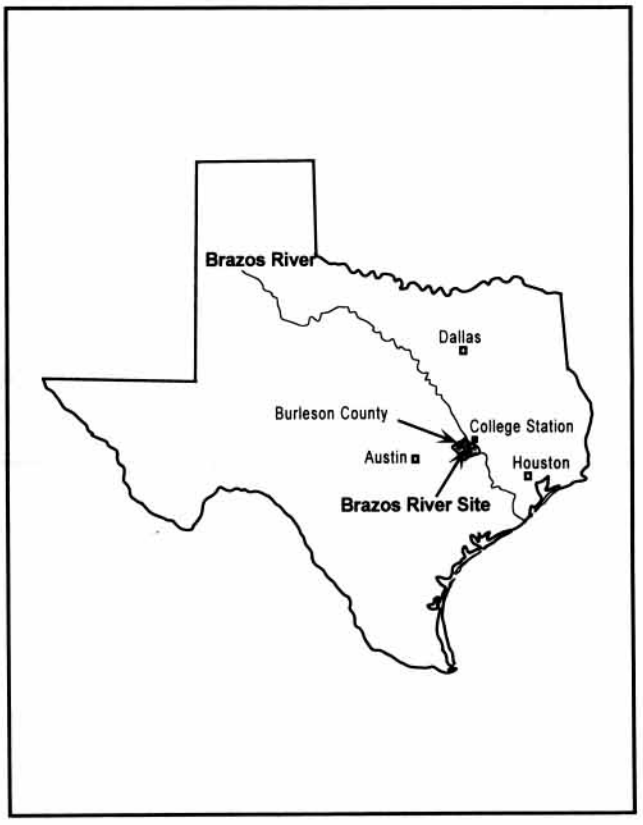

Figure 1. Location of the Brazos River Site in Burleson County, Texas.

The Brazos River Site is located on the western side of the Brazos River 0.8 km (0.5 mi) downstream from the Highway 60 bridge (Figure 2). At this point on the Brazos River, the floodplain extends approximately 8 km (5 mi) to the west with no floodplain to the east where the river abuts terrace deposits.

In the vicinity of the research site, the Brazos River has an average slope of 0.20 m/km (1.071 ft/mi) and a sinuosity of 1.8 (Gillespie, 1992). Flow rates measured at the Highway 21 bridge, approximately 19.3 km (12 mi) upstream, and river stages measured at the research site for 1994 and 1995 are shown in Table 1. The average flow rate varied from a low of 30.0 m^3/s (1,059 ft^3/s) in July to a high of 218.6 m^3/s (7,720 ft^3/s) in May. During this time period the river stage varied from 55.79 m (183.0 ft) in August to 58.67 m (192.5 ft) in May.

The average meteorological conditions near the Brazos River Site are shown in Table 2. The average yearly rainfall rate is 992.6 mm (39.1 in) with May and September being the wettest months and July the driest month. The average yearly total potential evapotranspiration (PET) rate, calculated using the Penman PET method, is 1,758.6 mm (69.2 in.; Dugas and Ainsworth, 1983).

The research site is located on the West Gulf Coastal Plains section of the Coastal Plains Province. The geology of the Coastal Plains Province consists of sedimentary bedrock ranging in age from the Cretaceous to recent, dipping gently southeastward toward the Gulf of Mexico and striking roughly parallel to the coastline. The bedrock underlying the Brazos River in the study area is of early Tertiary age. The Yegua Formation underlies the alluvial deposits at the Brazos River Site. The Yegua Formation is approximately 335 m (1,100 ft) thick, consisting of mudstones and clayey sandstones, with some interbeds of lignite and bentonitic mudstones (Yancy and Davidoff, 1991). It is the mudstones of the bentonitic Easterwood Member of the Yegua which form an impermeable boundary beneath the alluvium at the research site.

Currently, the land use at the research site is a mixture of cultivated agricultural land and pasture. A corn crop was grown in the surface runoff plots A and B in the spring and summer of 1994 and 1995 (Figure 3). These areas were left fallow after the corn was harvested. The remainder of the site is pasture. The research site is bounded by an orchard to the north and by woods and agricultural land to the south and by agricultural land to the west as shown in Figure 2. There are no irrigation wells or water supply wells in the vicinity that affect ground-water flow at the site.

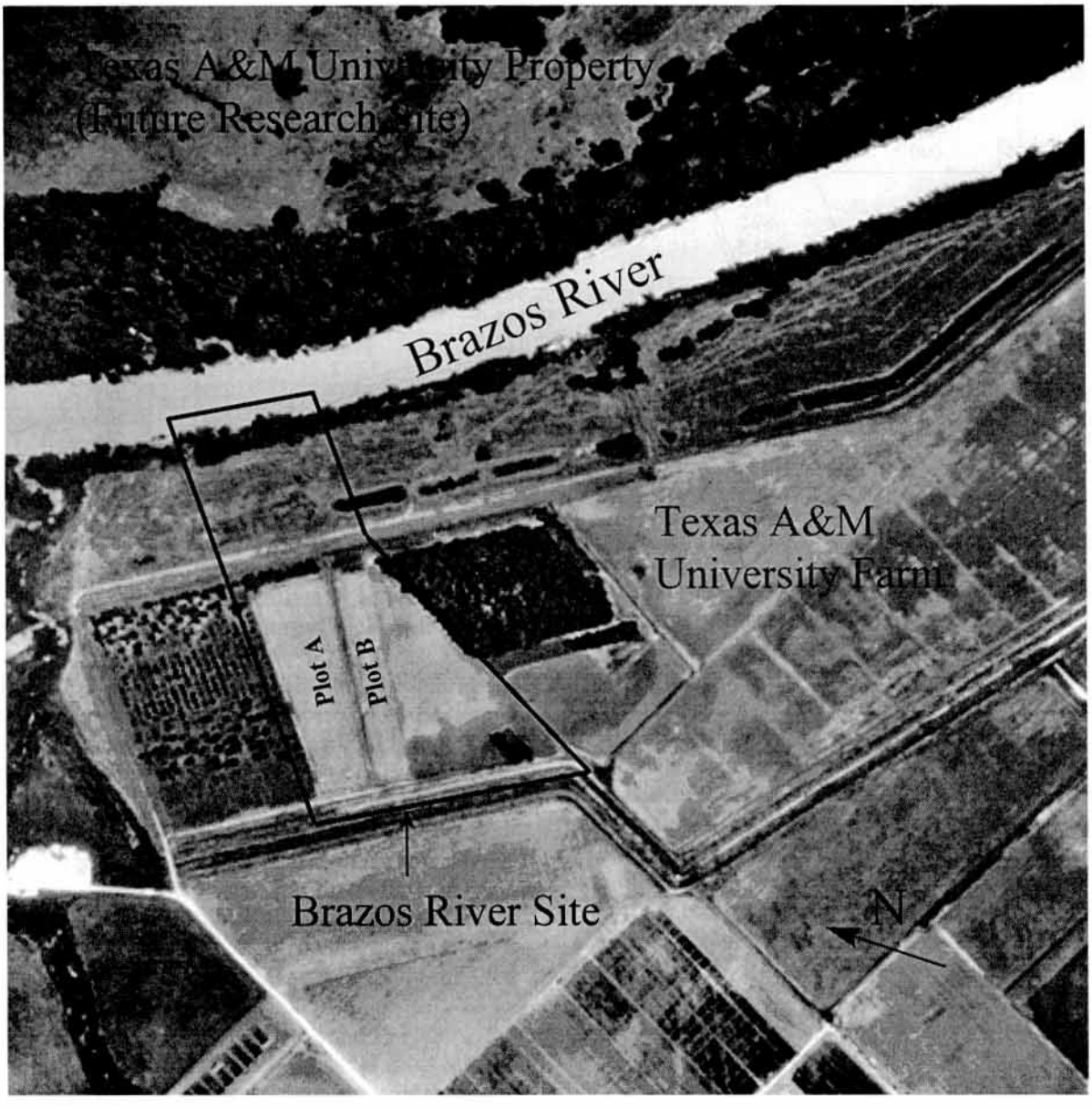

Figure 2. Aerial photograph of the Brazos River Site.

Site Hydrogeology

The lower reach of the Brazos River valley alluvium, in the vicinity of College Station, Texas, is a series of terraces and floodplain deposits. The floodplain deposits are the primary ground-water sources in the valley for irrigation and water supply. Recharge to the alluvium is primarily from precipitation on the floodplain and losses are through evaporation, transpiration and well withdrawals. The floodplain aquifer is typically unconfined, however, confined conditions are found below restrictive clay layers interbeded within the sand and gravel aquifer.

The floodplain alluvium discharges to the lower reach of the Brazos River during normal or low river stages. However, during high river stage, surface water discharges to the floodplain alluvium (near river) and is accompanied by a rise of the water table in the alluvium.

The hydraulic conductivities of the floodplain alluvium range from 0.1 mm/d (0.004 in./d) in the clay deposits to 100 m/d (328 ft/d) in coarse gravel layers. An average transmissivity for the floodplain of the lower reach of the Brazos River was reported by Cronin and Wilson (1967) to be 522 $m^3/d/m$ (42,000 gpd/ft).

Table 1. *The average monthly river stage of the Brazos River with respect to mean sea level measured at the Brazos River Site and Brazos River flow rates from the USGS meteorological station at the Highway 21 bridge approximately 19.3 km (12 mi.) upstream from the research site.*

	1994		1995		Average	
Month	stage (m)	flow (m^3/s)	stage (m)	flow (m^3/s)	stage (m)	flow (m^3/s)
January	–	37.6	57.482	171.5	57.482	70.1
February	–	89.2	57.056	54.6	57.056	48.8
March	–	63.5	57.147	249.1	57.147	104.8
April	56.141	28.0	58.580	341.5	57.361	123.4
May	58.397	247.4	58.945	401.4	58.671	218.6
June	57.543	134.4	58.275	272.5	57.909	136.9
July	56.324	30.1	57.117	59.1	56.721	30.0
August	56.111	22.4	55.471	323.2	55.791	115.4
September	56.995	23.8	–	59.1	56.995	27.9
October	56.568	76.2	–	36.8	56.568	38.4
November	56.538	71.1	–	30.9	56.538	34.7
December	58.366	216.4	–	26.4	58.366	83.0

Hydrostratigraphy

The Brazos River Site is located between the Brazos River and a deep drainage ditch as shown in Figure 3. The cross section A–A' on Figure 3 is shown in Figure 4. The research site is overlain by a clay layer that varies depth from 9.1 m (29.9 ft) near the river to 6.1 m (20.0 ft) near the ditch. The surface is flat with an average uniform slope of 0.5 percent away from the river. However, the site is bisected by an old flood control levee that runs parallel to the river (Figure 4).

The site is underlain at approximately 21 m (68.9 ft) by an impermeable Yegua shale formation (Cronin and Wilson, 1967). A heterogeneous, unconsolidated sand and gravel aquifer with clay lenses is located between the clay and shale layers (Figure 4). The aquifer is unconfined and grades from a fine sand at the top to course sand and gravel at the bottom.

Table 2. *Average monthly air temperature, rainfall and potential evapotranspiration (PET) at the Brazos River Site.*

Month	Average Air Temperature* (°C)	Average Rainfall* (mm)	Average PET** (mm)
January	9.2	67.3	71.3
February	11.3	66.5	92.8
March	15.7	65.5	136.4
April	20.1	85.9	153.0
May	23.7	121.9	186.0
June	27.1	93.5	210.0
July	28.7	58.2	232.5
August	28.9	61.5	213.9
September	25.9	123.7	165.0
October	20.8	96.8	133.3
November	15.4	80.0	90.0
December	10.8	71.9	74.4
Average	19.8	82.7	146.6
Total	–	992.6	1,758.6

*Data from Easterwood Airport (State Climatologist Office, Department of Meteorology, Texas A&M University).
**PET values from Dugas and Ainsworth (1983).

The clay is classified as a Ships clay (very fine, mixed, thermic Chromic Hapluderts) and exhibits extensive shrink-swell properties. The average texture of the Ships clay to a depth of 1.22 m (4.0 ft) is: 1.1 percent sand, 29.9 percent silt and 69.0 percent clay (Lin, 1995). The clay has a very low saturated hydraulic conductivity. However, the clay also has high shrink-swell properties that creates cracks or macropores in unsaturated conditions (Lin, 1995).

The transition from clay to sand is very abrupt with a 0.3 m (1.0 ft) to 0.6 m (2.0 ft) sandy clay layer between the clay and the sand. The sand layer extends from the clay unit to a shale formation that underlays the entire site. The shale is a confining layer that is located at a depth of approximately 21 m (69 ft) below the surface (Figure 4).

The sand layer grades from fine sand at the top to coarse sand with cobbles at the bottom. The aquifer is primarily unconfined with the water table in the top of the sand layer at a depth of approximately 9.1 m (30 ft). There is the possibility that this aquifer can become a confined aquifer system if the water table rises higher than the top of the sand layer into the clay zone. The river stage varies widely but is generally located in the bottom of the sand layer.

Cores were obtained to the depth of the shale unit using a hollow-stem auger drill rig equipped with a split barrel sampler. The clay is a continuous stratigraphic unit that contains numerous cracks and fissures and is interbedded with thin silt layers. The sand and gravel aquifer has clay and silt layering.

Hydraulic Aquifer Properties

The clay unit has been tested for saturated conductivity to a depth of 0.46 m (1.5 ft) using both field and

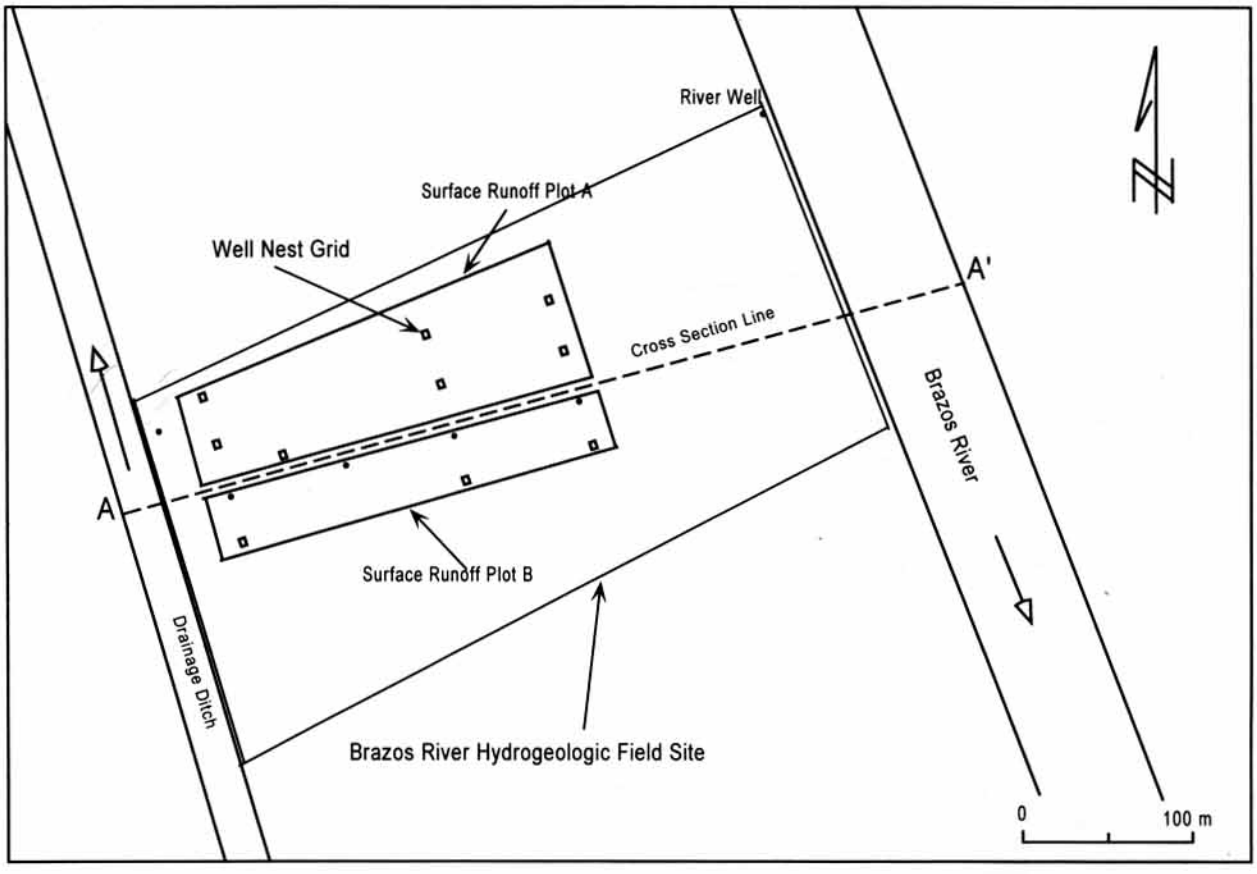

Figure 3. Plan view of the Brazos River Site which extends from the drainage ditch to the Brazos River, consisting of the well nest grid, surface runoff plots and the river well.

laboratory methods (Table 3). A constant head permeameter was used in the field for *in situ* testing (Amoozegar, 1989). The constant head test for saturated conductivity was also conducted in the laboratory using soil cores, 76 mm (3 in.) in diameter and 76 mm (3 in.) long.

Two pump tests have also been conducted using the site pumping well. A summary of the pump test results is shown in Table 4. The average saturated hydraulic conductivity for the entire sand and gravel aquifer is 83 m/d (272 ft/d; Wrobleski, 1996).

Ground-Water Quality

In general, the chemical character of the floodplain aquifer along the lower reach of the Brazos River is predominately calcium bicarbonate (Harlan, 1990). The ground water at the Brazos River Site is extremely hard ($CaCO_3$ = 538.3 mg/L) with a bicarbonate concentration of 640 mg/L (Table 5).

The ground water at the Brazos River Site is neutral (pH = 7.0) with a total dissolved solids concentration of 694 mg/L and high concentrations of iron (0.6 mg/L) and manganese (0.4 mg/L). A complete analysis of the water quality at the Brazos River Site is presented in Table 5.

Existing Test Facilities

Monitoring Well Network

In order to monitor ground-water flow and water quality at a field scale, a total of nine well nests were installed at the research site (Figure 5). The well nests were located in a 3 x 3 grid parallel to and perpendicular to the river. Each well nest has four monitoring wells with 152 mm (6 in.) long screens that are located at average depths of 7.2 m (23.6 ft), 11.0 m (36.1 ft), 14.8 m (48.6 ft), and 18.3 m (60.0 ft) as shown in Figure 6. The well screen of the deepest well in each well nest is located approximately 1.5 m (4.9 ft) above the impermeable shale layer. The well screen of the shallowest well in each well nest is located just below the clay layer. The well screens of the remaining two wells in each well nest are evenly spaced vertically between the deepest well and the shallowest well. The well nests permit water samples and pressure measurements to be taken at discrete points within the aquifer.

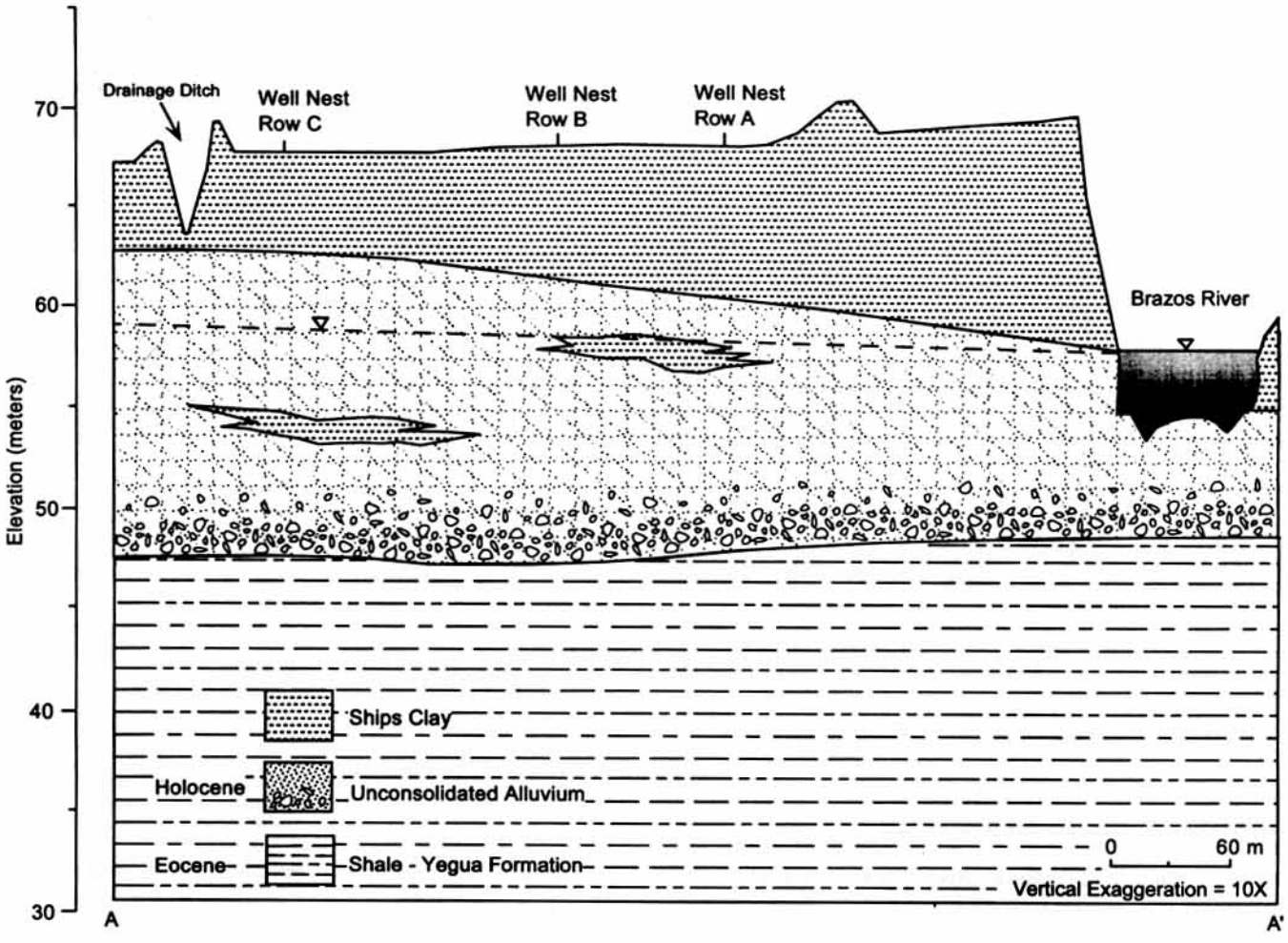

Figure 4. The Brazos River Site geologic cross-section A–A1 from Figure 3.

Four additional wells at the research site are fully screened throughout the sand and gravel aquifer. These "water table" wells provide a composite ground-water sample as well as an average aquifer water level. One fully screened well is located as close as possible (approximately 15 m [49 ft]) to the river. The water level in this well is used to approximate river stage. To reduce field error in water level measurements, the top of each well casing at the site has the same elevation (68.48 m [224.67 ft]). The top of the river well casing is 3.0 m (9.8 ft) below the top of the other wells because the ground elevation near the river is lower.

All wells are constructed of 0.05 m (2 in.) diameter, flush threaded polyvinyl chloride (PVC) well casing. The 0.15 m (6 in.) long well screens are wire wound PVC screens with 0.12 mm (0.005 in.) openings. The fully screened wells have 0.25 mm (0.010 in.) slotted screens.

The Brazos River Site also has an injection well (I-WT) with a well nest (V1) that is designed for tracer studies in response to pumped gradient conditions (Figure 5). The injection well and tracer well nest are located in a line with the pumping well and the C2 well nest.

Table 3. *Saturated hydraulic conductivity values for the surface clay soil at the Brazos River Site using field and laboratory test procedures.*

Depth (m)	Constant Head (Lab) (mmd^{-1})	Constant Head (Field) (mmd^{-1})	Average (mmd^{-1})
0.15	21.5	10.9	16.2
0.30	112.0	122.6	117.3
0.46	–	3.7	3.7

Table 4. *Saturated hydraulic conductivity values for the sand aquifer at the Brazos River Site from pump test analysis.*

Wells Tested	Average Depth (m)	Average Ksat (m/d)	Standard Deviation (m/d)	Coeff. of Variability (%)
7	10.4	83.1	8.5	10.2
6	14.3	81.3	9.7	11.9
7	18.5	83.8	15.3	18.3

Table 5. *Ground-water quality at the Brazos River Site.*

Chemical	9.7 m Depth Concentration (mg/L)	14.3 m Depth Concentration (mg/L)	18.3 m Depth Concentration (mg/L)	Average Concentration (mg/L)
Alkalinity ($CaCO_3$)	390.0	262.0	260.0	304.0
Aluminum (Al)	0.020	0.020	0.181	0.074
Antimony (Sb)	0.002	0.002	0.004	0 003
Arsenic (As)	0.002	0.002	0.002	0.002
Barium(Ba)	0.110	0.125	0.136	0.124
Beryllium (Be)	0.002	0.002	0.002	0.002
Bicarbonate ($2CO_3$)	587	654	680	640
Boron (B)	0.300	0.300	0.400	0.333
Bromide (Br)	0.27	0.72	0.64	0.50
Cadmium (Cd)	0.0005	0.005	0.001	0.0007
Calcium (Ca)	150	143	149	147
Carbonate (CO_3)	0	0	0	0
Chloride (Cl)	26	52	48	42
Chromium (Cr)	0.010	0.010	0.010	0.010
Cobalt (Co)	0.010	0.010	0.010	0.010
Copper (Cu)	0.004	0.004	0.004	0.004
Dissolved Solids	628	718	737	694
Fluoride (F)	0.3	0.3	0.1	0.2
Hardness ($CaCO_3$)	527	572	516	538
Iron (Fe)	0.013	0.976	0.908	0.632
Lead (Pb)	0.005	0.005	0.005	0.005
Lithium (Li)	0.026	0.030	0.038	0.031
Magnesium (Mg)	37	52	35	41
Manganese (Mn)	0.0046	0.530	0.579	0.371
Mercury (Hg)	0.00013	0.00013	0.00013	0.00013
Molybdenum (Mo)	0.050	0.050	0.050	0.050
Nickel (Ni)	0.010	0.010	0.010	0.010
Nitrate (NO_3)	5.9	1.1	0.2	2.4
Nitrate N (NO_3-N)	1.34	0.25	0.05	0.55
Nitrite N (NO_2-N)	0.01	0.01	0.01	0.01
Nitrogen (NH_3-N)	0.06	0.66	0.14	0.30
Nitrogen (TKN)	0.4	1.1	0.7	0.7
Phosphorus (P)	0.03	0.01	0.03	0.02
Potassium (K)	2.2	4.1	4.3	3.5
Selenium (Se)	0.004	0.004	0.004	0.004
Silica (Si)	17	15	13	15
Silver (Ag)	0.010	0.010	0.010	0.010
Sodium (Na)	42	61	94	66
Strontium (Sr)	1.2	1.6	0.5	1.1
Sulfate (SO_4)	58	67	59	61
Thallium (Tl)	0.002	0.002	0.002	0.002
Vanadium (V)	0.010	0.010	0.010	0.010
Zinc (Zn)	0.0224	0.0252	0.0202	0.0226
Conductivity (µmho)	980	1115	1170	1088
pH	6.90	7.00	7.10	7.00
Temperature (°C)	21	21	21	21

Data from the Texas Water Development Board, 1994.

Instrumentation

All monitoring wells in the well nest grid are equipped with well head devices that are used to continuously monitor water levels (Figure 7). The well head devices consists of a float, pulley, potentiometer and counter weight (Munster et al., 1996). The float rides on the water surface and turns the pulley that is connected to a potentiometer that varies voltage from 0 to 2 volts. The potentiometers have been calibrated in the lab to determine the linear relationship between a change in voltage and a change in float elevation. Under ideal field conditions, the float, pulley, potentiometer and counter weight system can monitor well water levels within ±25 mm (1 in.) of actual levels.

Three data loggers are used to collect well water level data at the research site. Each data logger collects water level data from a well nest row aligned parallel to the

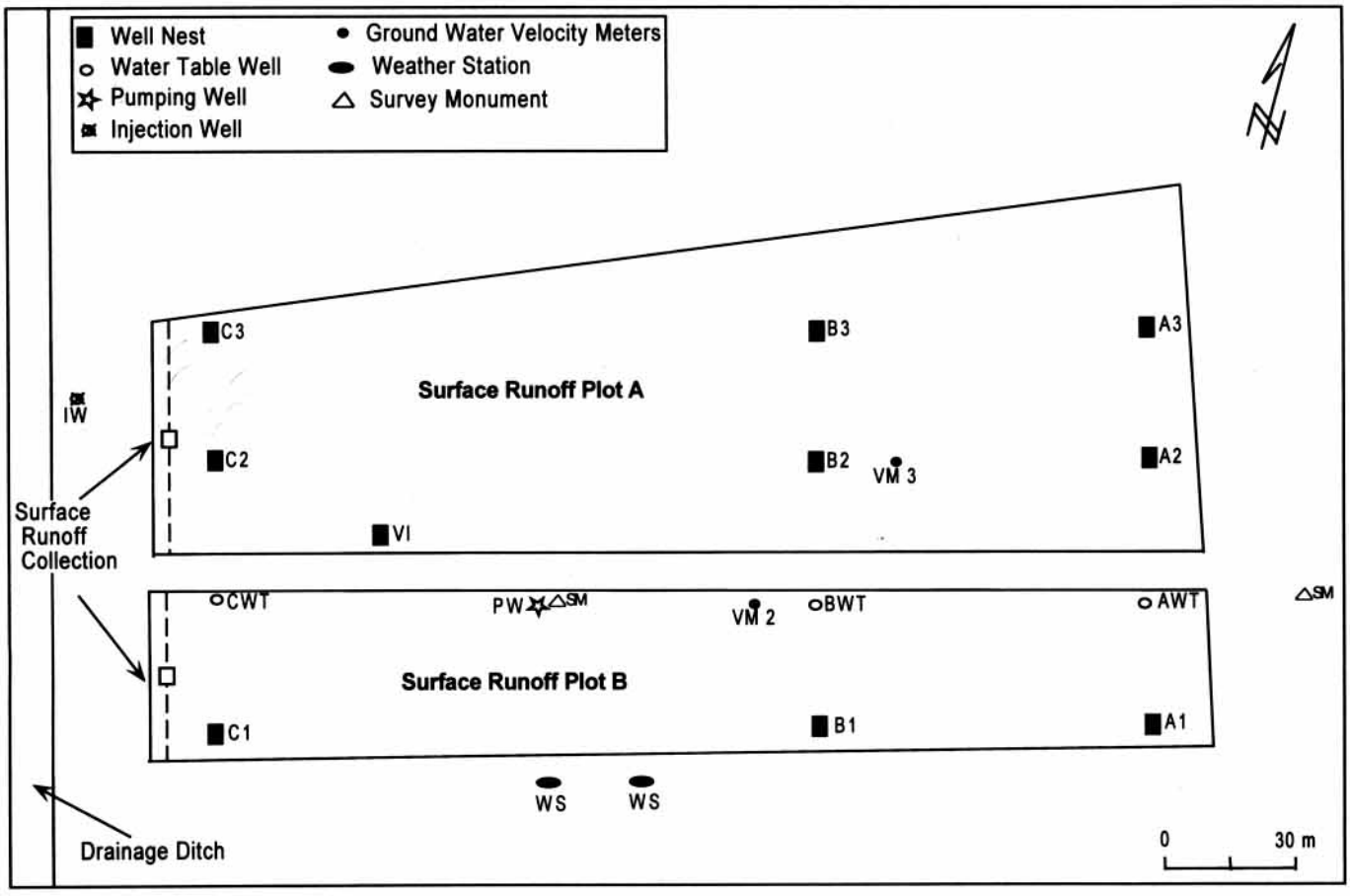

Figure 5. Detailed plan view of the Brazos River Site well field, including well nests, water table wells, a pumping well, an injection well, ground-water velocity meters, surface runoff plots and collection systems, weather stations, and two survey monuments.

river (12 wells) plus a water table well. An additional datalogger is dedicated to data collection at the river well. The data loggers provide an excitation voltage (2V) and records the date, time and the variable voltage on each potentiometer every six hours.

The data is downloaded in the field using a laptop computer and the ending water level depth is manually measured. The voltages are converted to water level elevations in the laboratory using the starting depth to the water, which is also manually measured at the start of the data collection period, and the calibration factor. The last calculated water level is compared to the ending field measured level to determine accuracy.

Pumping Well

A 0.20 m (8 in.) diameter well has been located in the middle of the monitoring well field to simulate a typical floodplain irrigation well as well as for aquifer pump tests. This well is constructed with flush threaded PVC well casing with 3.2 mm (0.125 in.) slotted screen that is 4.6 m (15 ft) long. The slotted screen is located in the coarse sand and gravel layer from 18.0 m (59 ft) to 21.6 m (71 ft) below the surface.

A 0.15 m (6 in.) submersible pump has been installed in the 0.20 m (8 in.) diameter well. This single stage centrifugal pump is powered by a 3 phase, 480 volt, 7.5 hp motor. Electrical power has been installed at the site to power the pump and other instrumentation. The well head on the 0.20 m (8 in.) diameter well has a pressure gauge, flowmeter and gate valve.

The outflow from the pumping well is transported away from the research site using 0.20 m (8 in.) irrigation pipe. In addition to the flowmeter at the wellhead, the flow rate is quantified using a 0.3 m (1 ft) H flume that is equipped with a datalogger to continuously record flume water levels. The H flume is installed at the end of the irrigation piping just prior to discharge into the drainage ditch.

Ground-Water Velocity Meters

The site has two, experimental, three-dimensional ground-water velocity meters. These velocity meters are non recoverable, *in situ* devices that determine the magnitude and direction of ground-water flow in three dimensions (Alden and Munster, 1995). The three-dimensional velocity meters are 0.76 m (2.5 ft) long and 0.05

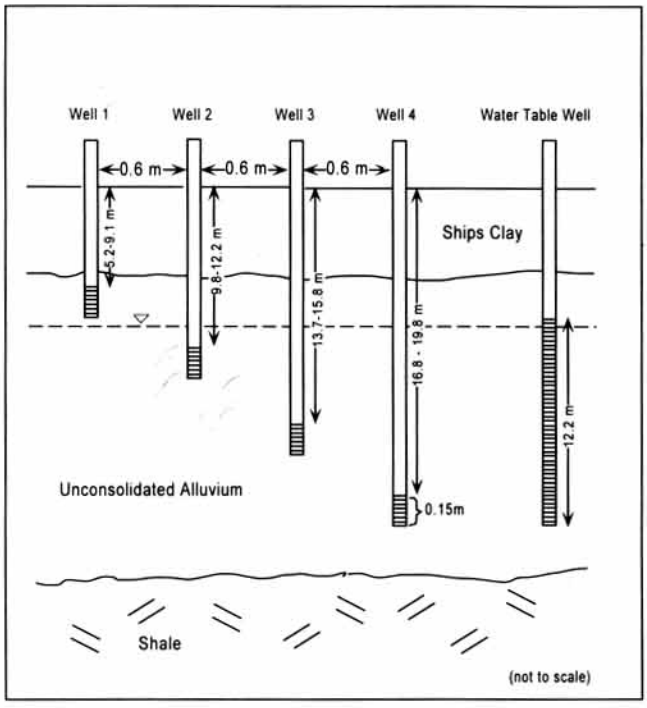

Figure 6. Well nest layout and water table well at the Brazos River Site. Each nest contains four wells; individuals wells are 0.6 m apart and vary in depth from 5.2 m to 19.8 m. The water table wells are fully screened and extend to a depth of approximately 20 m.

m (2 in.) in diameter. These devices contain electrical resistance heating units with 30 thermocouples located throughout the meter. The meter is attached to 25 mm (1 in.) PVC conduit through which the power supply and data cables are routed to the surface. The associated surface instrumentation includes; a data logger, multiplexer, storage module, power supply, solar panel, and battery. The electrical requirements vary from 60 to 120 watts depending upon aquifer characteristics.

The velocity meters have been installed within the grid of well nests (Figure 5). The meter located near the B2 well nest is 18.3 m (60.0 ft) deep and the meter near the B-WT well is 13.7 m (44.9 ft) deep.

Surface Runoff

The research site is subdivided into two experimental plots for surface runoff studies. Clay berms, approximately 0.3 m (1 ft) high, were installed to define a 0.8 ha (2.0 ac) plot (plot B) and 1.6 ha (4.0 ac) plot (plot A). Each experimental plot has a uniform slope of 0.1 percent toward the drainage ditch. All surface runoff from each plot is quantified and sampled for chemical and sediment analysis.

The surface runoff instrumentation consists of a collector pipe that runs the width of the field, inlet box, flume transition box (1.2 m [3.9 ft] long x 0.6 m [2.0 ft] wide) and 0.3 m (1 ft) H flume. The H flume, which can measure flow rates up to 0.06 m^3/sec (2.1 ft^3/sec) discharges into the deep drainage ditch with a free out fall. The H flume has a stilling well with a float-pulley-potentiometer system that is connected to a data logger. The data logger records potentiometer voltages every minute. The float pulley potentiometer system has been calibrated in the laboratory to determine the linear relationship between float travel and voltage change. Using the voltages recorded by the data logger, the depth of water in the H flume can be determined each minute during a surface runoff event. The flow rate is then determined using published depth-discharge data for this standard H flume.

Surface Runoff Sampling

Two automated samplers at each plot are used to obtain surface runoff samples from the flume transition box. These weather proof samplers are activated automatically by a moisture sensor and are highly programmable. Composite samples in glass or plastic bottles can be obtained throughout the surface runoff event. The samplers are powered by a 12-V marine battery that is recharged by a solar cell.

The surface runoff sample bottles are transported to the laboratory immediately after each runoff event. In the laboratory, each surface runoff sample is subdivided into appropriate containers for the various analyses and refrigerated until transfer to the analytical laboratory.

Meteorological Equipment

There is a permanent weather station located at the research site. The instrumentation at this weather station includes; wind speed and direction at 2 m (6.6 ft) and 6 m (19.7 ft) heights, air temperature, soil temperature, relative humidity, solar radiation, tipping bucket rain gage, pan evaporation and leaf wetness. This data is transmitted to the Meteorological Department at Texas A&M University using radio frequency transmission.

In addition, there are three portable weather stations located at the research site. A standard field weather station continuously records air temperature, relative humidity, soil temperature, wind speed and direction, solar radiation, and rainfall data.

Summary of Research Conducted at the Brazos River Site

Research projects at the Brazos River Site have investigated ground-water/surface-water interactions, agricultural chemical transport, water quality of the ground water, surface runoff and river water, site characterization, measurement of crop evapotranspiration rates, virus transport under pumped gradient conditions,

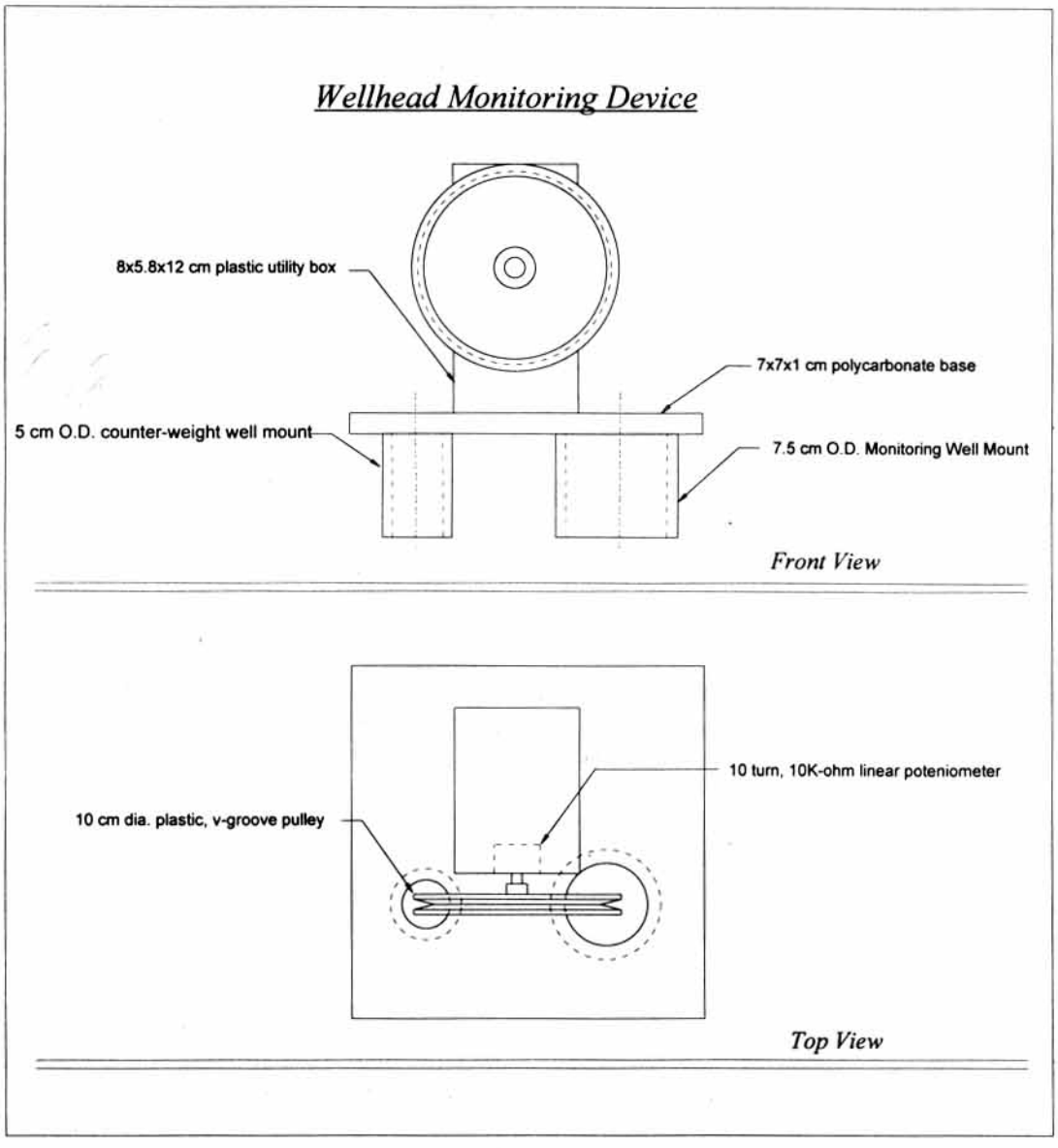

Figure 7. Front and top view of the well head device used to monitor water level elevations.

electromagnetic (EM) subsurface characterization, and simulation of contaminate and virus transport in variably saturated ground water.

Ground-Water Flow System

The well nests provide data to calculate horizontal and vertical ground-water pressure gradients. The vertical gradients are determined from water levels in the wells at each well nest. The horizontal gradients are determined by the differences in the water levels in wells screened at approximately the same level between well nests. Horizontal gradients are determined between well nest rows A, B and C, as well as the river well.

From April 1994 to April 1995 the river stage fluctuated between 58.4 m (191.6 ft), on day 144 (1994), to 55.9 m (183.4 ft), on day 267 (1994), as shown in Figure 8. Monthly horizontal gradients measured between the C-WT well and the A-WT well and between the C-WT well and the R-WT well are also shown in Figure 8. The in-field gradients between the C-WT to A-WT wells ranged from 0.0014 m/m to 0.0031 m/m with an average of 0.0024 m/m. The distance between the C-WT well and the A-WT well is 213 m (699 ft). The A-WT well is 163 m (535 ft) from the river. The gradients between the research site and the river (C-WT to R-WT) ranged from 0.0009 m/m to 0.0066 m/m with an average of 0.0046 m/m. The R-WT well is approximately 15 m (49 ft) from the river.

From April 1994 to April 1995, the horizontal ground-water flow was always toward the river. Water table contour maps from August 1994 at low river stage

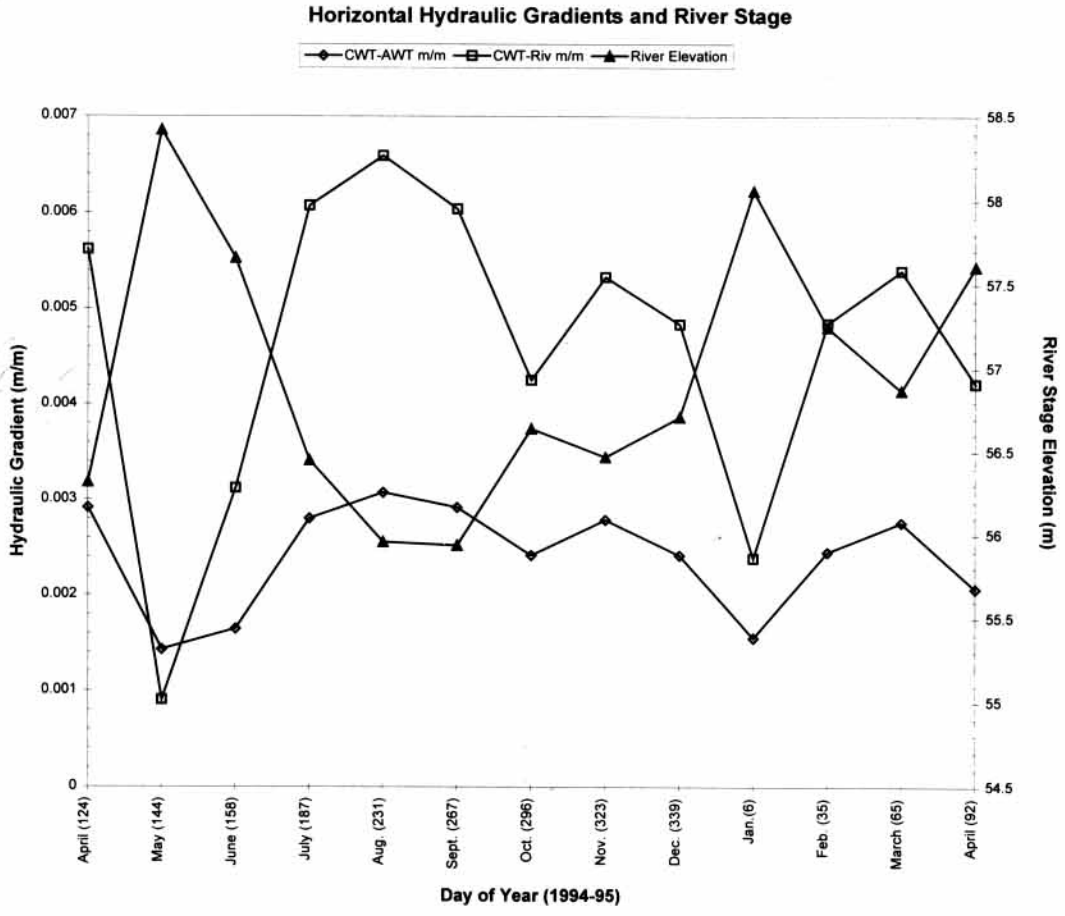

Figure 8. Horizontal hydraulic gradients and river stage at the Brazos River Site.

(56.1 m [183.98 ft]) and April 1994 at high river stage (58.6 m [192.25 ft]) show that as river stage rises, the water table at the research site increases and gradients toward the river decrease (Figure 9).

River stage has an inverse affect on the ground-water gradients. When river stage increased, ground-water gradients always decreased and when river stage decreased, ground-water gradients always increased. The minimum ground-water gradients occurred during maximum stage. The maximum ground-water gradients occurred during a period of near lowest river stage.

The agricultural chemical transport studies have verified the presence of macropore flow through the surface clay layer to the floodplain aquifer. Surface applied chemicals were detected 24 days after application in 21 out of 26 monitoring wells sampled at the research site (Chakka and Munster, 1996a). In addition, the macropores in the clay soil and the flat topography resulted in low runoff volumes at the site. The average runoff event was only 6.5 percent of the total rainfall with a maximum runoff of 18.8 percent in a two-year study (Munster et al., 1995).

The USGS model, VS2DT, has successfully simulated macropore transport through the clay surface layer, ground-water flow, aquifer river interactions and chemical transport at the Brazos River Site. The model simulations have been validated and calibrated using field data. From a two-year simulation, the average discharge from the aquifer to the Brazos River was 0.023 $m^3/s/km$ (1.30 $ft^3/sec/mi$) at normal or low river stage. During high river stage, the average river recharge to the floodplain aquifer was 0.022 $m^3/s/km$ (1.26 $ft^3/sec/mi$; Chakka and Munster, 1996a).

Model simulations of macropore infiltration and transport of surface applied atrazine (a herbicide) to the floodplain aquifer were completed. In a two-year study, an average of 11 percent of the total atrazine applied was transported to the sand and gravel aquifer (Chakka, 1996).

The Computalog Corporation of Fort Worth, Texas, has used the Brazos River Site to develop and field test an *in situ* permeable ground-water flow sensor. The flow sensor was evaluated under natural and pumped gradient conditions at the research site (Alden and Munster, 1996a, 1996b). Preliminary tests indicate that the flow sensor is a useful tool in determining the direction and magnitude of ground water in three dimensions.

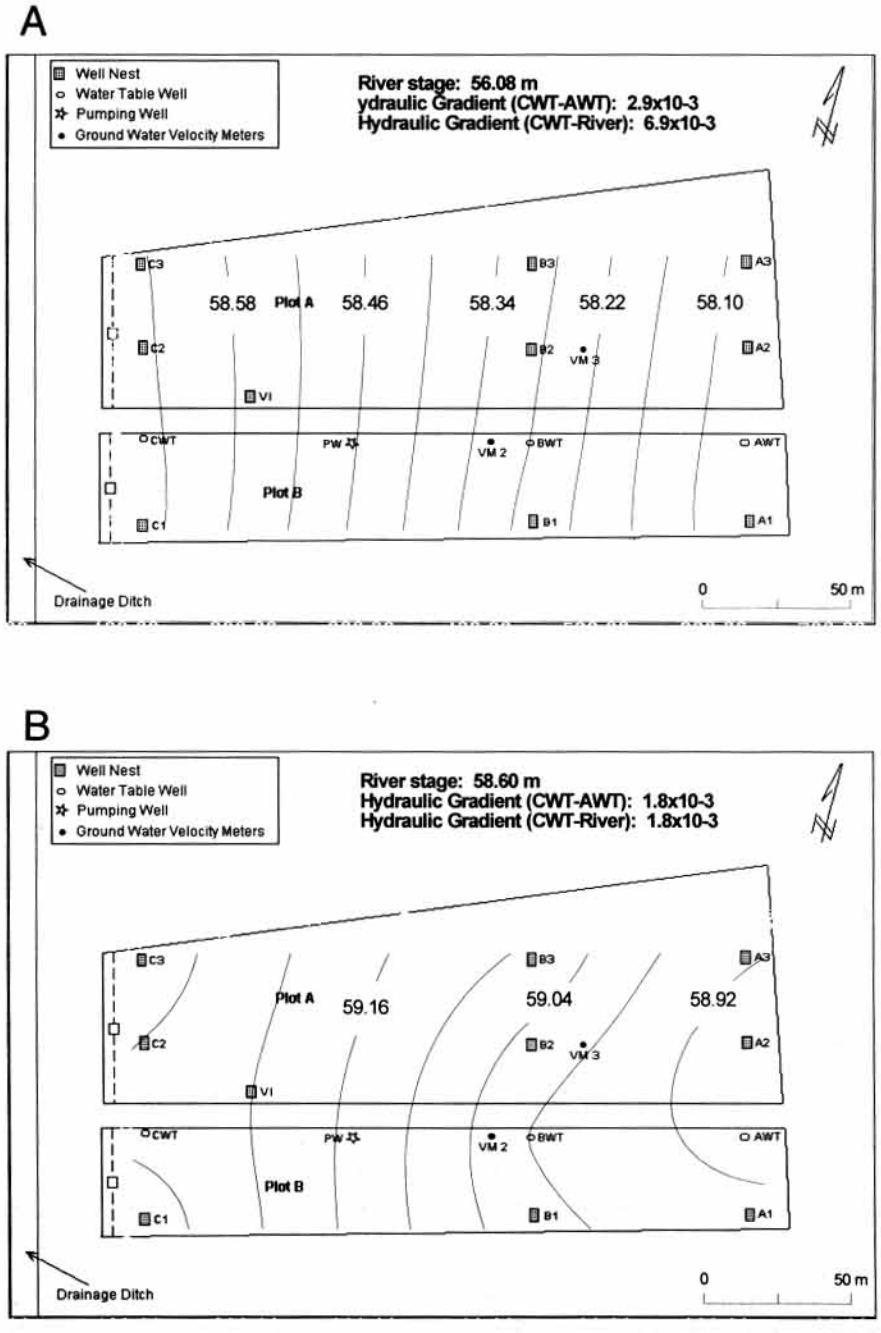

Figure 9. Water table contour maps at the Brazos River site at (A) low, and (B) high river stage with calculated hydraulic gradients.

FUTURE PLANS

The Brazos River Site is available for any research project that is approved by the Texas A&M University System and that is consistent with the educational, research and technology development mission of the Brazos River Site. The possible uses of the research site for ground water, surface runoff, evapotranspiration and soil investigations are listed in Table 6.

The recruitment of industry cooperation has been limited during the initial development of the Brazos River Site. Now that the site has been instrumented and an initial assessment of the hydrogeologic site characteristics completed, a concerted effort will be initiated to solicit industry utilization of the Brazos River Site.

The Brazos River Site database includes information on site characterization, water quality, meteorology, ground-water flow, river levels, surface runoff, land use, and soil properties and will continue to be expanded and enhanced. A graphical information system (GIS) database to incorporate all of the information

Table 6. *Possible uses of the Brazos River Site for field research, technology development and education.*

Field Research	Technology Development	Education
	Ground Water	
natural gradient conditions	flow sensors	saturated zone
pump gradient conditions	saturated zone	unsaturated zone
flow and chemical transport	unsaturated zone	flow measurement
saturated zone	electro-magnetic surface sensors	sampling techniques
unsaturated zone	soil layer determination	pump test evaluation
surface water interactions	aquifer properties	slug tests
tracer tests	drilling procedures	drilling procedures
land-use affects	sampling techniques	electro-magnetic sensors
model simulations	well water level sensors	tracer tests
	model development	model simulation
	Surface Runoff	
quantity	instrumentation	volume measurement
quality	quantify volumes	sampling techniques
sediment	sampling	sediment
chemical transport	sampling techniques	chemicals
macropore infiltration	chemical transport	land use affects
irrigation affects	sediment	irrigation affects
land-use affects		model simulations
model simulations		
	Evapotranspiration	
quantity	instrumentation	meteorological
land-use affects	meteorological	measurements
model simulation	measurement techniques	instrumentation
		modeling
	Soil Investigations	
infiltration	moisture sensors	sampling techniques
macropore flow	macropore flow	moisture measurement
moisture content	quantification	infiltration measurement
quality	sampling	irrigation procedures
chemical transport	irrigation application	
phytoremediation		
irrigation		
land-use effects		

from the research site is a priority for future site development.

Currently there are plans to expand the Brazos River Site to Texas A&M University property on the other side of the Brazos River adjacent to the existing site. This 121 ha (300 ac) site, which also borders the Brazos River, is situated on terrace deposits and has little or no floodplain. The hydrogeology of this new site will be completely different from the existing site. This will offer Brazos River Site users a wider variety of options for research, testing and evaluation.

ACKNOWLEDGMENTS

This research was supported in part by grants from the Texas Water Resource Institute and the Texas A&M University Research Enhancement Program. We thank Mr. Lloyd Morris, P.E., L.D., in the Department of Geology and Geophysics at Texas A&M University and Mr. Al Nelson at the Texas A&M University Research Farm for their assistance in the installation of the field instrumentation and the site characterization.

REFERENCES

ALDEN, A. S. AND MUNSTER, C. L., 1996a, Assessment of River-floodplain aquifer interactions: *Ground Water,* in review.

ALDEN, A. S. AND MUNSTER, C. L., 1996b, Field test of the *in situ* permeable groundwater flow sensor: *Ground Water Monitoring & Remediation,* in review.

ALDEN, A. S. AND MUNSTER, C. L., 1995, Field test of a 3-D groundwater flow sensor. In Charbeneau, Randall J., *Ground-water Management,* Proceedings of the International Symposium sponsored by the Water Resources Engineering Division, ASCE, in conjunction with the ASCE's First International Conference on Water Resources Engineering in San Antonio, Texas, August 14–16: American Society of Civil Engineers, New York, NY, pp. 181–186.

AMOOZEGAR, A., 1989, A compact constant-head permeameter for measuring saturated hydraulic conductivity of the vadose zone: *Soil Science Society of America Journal,* Vol. 53, pp. 1356–1361.

CHAKKA, K. B., 1996, *Evaluation and Simulation of Non-Point Source Agricultural Chemical Transport in Variably Saturated Soil Medium:* Ph.D. Dissertation, Texas A&M, University, College Station, TX, 191 p.

CHAKKA, K. B. AND MUNSTER, C. L., 1996a, The fate of agricultural chemicals applied to the Brazos River floodplain: groundwater quality: *Transactions of ASAE,* in review.

CHAKKA, K. B. AND MUNSTER, C. L., 1996b, Simulation of groundwater-surface water interactions on the lower reach of the Brazos River, in *Proceedings of the Universities Council on Water Resources Annual Meeting on Integrated Management of Surface and Ground Water,* July 30–August 2, San Antonio, Texas, pp. 213–228.

CRONIN, J. G. AND WILSON, C. A., 1967, *Ground Water in the Floodplain Alluvium of the Brazos River, Whitney Dam to Vicinity of Richmond, Texas:* U.S. Geological Survey, Texas Water Development Board, Report 41, Austin, TX, 206 p.

DIMILLINO, A. F. AND PRINCE, G. C., 1993, National geotechnical experimentation sites: *Public Roads*, Vol. 57, No. 2, Autumn, pp. 17–22.

DUGAS, W. A. AND AINSWORTH, C. G., 1983, *Agroclimatic Atlas of Texas, Part 6: Potential Evapotranspiration:* The Texas Agricultural Experiment Station, The Texas A&M University System, College Station, TX.

EPPS, L. W., 1973, *A Geologic History of the Brazos River,* Baylor Geological Studies Bulletin No. 24: Department of Geology, Baylor University, Waco, TX, p. 44.

EVERETT, M. E.; BURDEN, C.N.; SANANIKONE, K.; AND HERBERT, B. E., 1996, Progress in interpretation of transient electromagnetic data in terms of subsurface permeability, in *Symposium on the Application of Geophysics to Engineering and Environmental Problems,* Keystone, Colorado, April 28–May 1.

GILLSEPIE, B. M., 1992, *The Nature of Channel Planform Change: Brazos River, Texas:* Unpublished Ph.D. Dissertation, Department of Geography, Texas A&M University, College Station, TX, p. 307.

HARLAN, S. K., 1990, *Hydrogeologic Assessment of the Brazos River Alluvial Aquifer, Waco to Marlin, Texas:* Unpublished Master's Thesis, Department of Geology, Baylor University, Waco, TX, p. 98.

LIN, H., 1995, *Hydraulic Properties and Macropore Flow of Water in Relation to Soil Morphology:* Unpublished Ph.D. Dissertation, Texas A&M University, College Station, TX, 228 p.

MUNSTER, C. L.; SCHNEIDER, B. M.; AND VOGEL, J. R., 1995, *Chemical and Sediment Transport in Surface Runoff: A Field Study,* ASAE Paper No. 952697: ASAE, St. Joseph, MI.

MUNSTER, C. L.; PARSONS, J. E.; AND SKAGGS, R. W., 1996, Using the personal computer for water table management: *Applied Engineering in Agriculture:* ASAE, St. Joseph, MI, in review.

SERDP, 1994, *Annual Report and Five-Year (1994–1998) Strategic Investment Plan*: Department of Defense, Department of Energy and the U.S. Environmental Protection Agency, Strategic Environmental Research and Development Program (SERDP), A Partnership to Improve the Environment, September: SERDP Program Office, Arlington, VA, 302 p.

VOGEL, J. R.; DOWD, S. E.; MUNSTER, C. L.; PILLAI, S.; AND CORAPCIOGLU, M. Y., 1996, Large-scale virus transport through a sandy aquifer under a forced gradient, in *Proceeding of the ASCE Texas Section Conference*, Beaumont, Texas, April 12.

WROBLESKI, C. L. 1996, *An Aquifer Characterization at the Texas A&M University Brazos River Hydrologic Field Site, Burleson County, Texas:* M.S. Thesis, Department of Geology & Geophysics, Texas A&M University, College Station, TX, p. 127.

YANCY, T. E. AND DAVIDOFF, A. J., 1991, *Paleogene Sequence Stratigraphy in the Brazos River Valley, Texas,* Field Trip Guidebook of the Gulf Coast Association of Geological Society, p. 112.

MODELING MACROPORE TRANSPORT OF AGRICULTURAL CHEMICALS ON A RIVER FLOODPLAIN: ATRAZINE TRANSPORT SIMULATION

K. B. Chakka, C. L. Munster

ABSTRACT. *The United States Geological Survey (USGS) model Variably Saturated Two Dimensional Transport (VS2DT) was used to simulate macropore transport of atrazine through a highly structured clay soil to a sand and gravel floodplain aquifer at a field research site in Burleson County, Texas. A simulation of preferential flow through the surface clay was successfully coupled with a simulation of groundwater flow in a floodplain aquifer. Simulated groundwater flow and atrazine transport compared favorably with field measured values. The water levels in the floodplain aquifer were primarily influenced by fluctuations in river stage. Simulated groundwater and surface water flows into and out of the aquifer were calculated. Groundwater discharge from the aquifer to the river averaged 0.023 $m^3/s/km$ during low river stages. Surface water recharge to the aquifer averaged 0.022 $m^3/s/km$ during high river stages. Simulated atrazine transport through the clay soil domain resulted in atrazine losses (percent of total applied) of 7% in 1994 and 15 % in 1995. A pumping test at the research site and more rainfall in 1995 than in 1994 resulted in simulated atrazine transport to the bottom of the sand and gravel aquifer (19 m). Atrazine was not transported to the river in groundwater flow during model simulations. Simulated atrazine concentrations were validated using measured concentrations throughout the study period.* **Keywords.** *Modeling, Macropore flow, Atrazine transport, Groundwater, Surface water recharge, Floodplain aquifer.*

Groundwater flow and chemical transport in a floodplain aquifer are influenced by the stage of the adjacent stream. The region of surface water-groundwater interactions in stream beds is known as the "hyporheic zone" (White et al., 1992). Groundwater and surface water interaction studies of the hyporheic zone have traditionally concentrated on a hydrologic balance analysis. Quantification of discharge or recharge rates was primarily based on large scale average hydraulic gradients, gross estimates of saturated hydraulic conductivities and stream flow measurements. Using these methods, approximate estimates of the groundwater discharge into the lower reach of the Brazos River along one bank are between 0.006 to 0.01 $m^3/s/km$ (Cronin and Wilson, 1967).

The potential for agricultural chemicals to contaminate groundwater is a growing concern in the United States since chemicals associated with agriculture have been found in private and public drinking water. In addition, the degradation of surface water bodies has been attributed, in part, to polluted groundwater that discharges into bays, lakes, and streams (Kellogg et al., 1992).

Jakeman et al. (1990) derived a model for simulating groundwater transport of a conservative solute along the River Murray, in Australia, that was in direct connection with the aquifer. The model simulations indicated that stream salinity increased substantially due to aquifer discharge to the stream. The groundwater and surface water interactions were also successfully monitored in the Rio Grande de Manati, in Puerto Rico, using an innovative application of ^{222}Rn as a geochemical tracer (Ellins et al., 1990). Using estimates of groundwater influx and stream flow loss obtained through the measurement of ^{222}Rn, independent estimates of groundwater discharge from Puerto Rico's North Coast Limestone Aquifer to the Rio Grande de Manati, recharge from the stream to the aquifer, and storage changes in the aquifer were obtained.

Modeling the field scale movement of chemicals in unsaturated soil is of interest to both the public and private sectors and has become an area of active research in numerous environmentally related disciplines (Bronswijk et al., 1995). However, the experimental data needed to validate existing solute transport models and to facilitate the development of more refined simulations is very limited. Several new theoretical transport models have been developed. However, these remain largely untested, due to the lack of large-scale solute transport experiments under natural field conditions.

Several existing agricultural chemical transport models have been modified for macropore flow transport. Ahuja et al. (1993) assessed the Agricultural Research Service Root Zone Water Quality Model (RZWQM) for simulating macropore flow and chemical transport in a silty clay loam. Up to 8% of the surface applied atrazine was transported through macropore flow. The GLEAMS (Groundwater Loading Effects of Agricultural Management Systems) model (Leonard et al., 1987) has been modified to simulate water and chemical transport in cracking clay soils (Morari and Knisel, 1997). The modified GLEAMS model successfully simulated pesticide transport from the root zone in field validation studies. Chung et al. (1992) developed the ADAPT (Agricultural Drainage and

Article was submitted for publication in February 1997; reviewed and approved for publication by the Soil & Water Div. of ASAE in August 1997.

The authors are **Kesava B. Chakka**, Technical Consultant, Deloitte & Touche Consulting Group, DRT Systems, Houston, Tex.; and **Clyde L. Munster, *ASAE Member Engineer***, Assistant Professor, Department of Agricultural Engineering, Texas A&M University, College Station, Tex. **Corresponding author:** Dr. Clyde L. Munster, Department of Agricultural Engineering, MS 2117, Texas A&M University, College Station, TX 77843-2117; tel.: (409) 847-8793; fax: (409) 845-3932; e-mail: <munster@agen.tamu.edu>.

Pesticide Transport) model by combining algorithms from GLEAMS and DRAINMOD (Skaggs, 1978). ADAPT is a water table management model that incorporates macropore flow in the transport of water through the soil. The model successfully simulated subsurface drainage and surface runoff for long term field data.

The United States Geological Survey (USGS) groundwater model Variably Saturated Two Dimensional Transport (VS2DT) (Lappala et al., 1987; Healy, 1990) simulates groundwater flow and chemical transport in two dimensions and was applied to a research site on the Brazos River floodplain. This site is characterized by a macroporous surface clay unit that overlies a sand and gravel aquifer that is in direct hydraulic connection with the Brazos River. A new methodology for VS2DT was developed to simulate preferential flow and aquifer-river interactions (Chakka and Munster, 1997). The flow domains for the clay unit and aquifer were de-coupled requiring two separate model simulations. Conceptualized macropores were used to simulate preferential flow in the clay unit. Then, output from the clay flow domain simulation was used as model input into the aquifer flow domain simulation.

The hydrogeology of the research site and the two-dimensional flow domain used to simulate field conditions were presented by Chakka and Munster (1997). In addition, details for: the finite difference grids used to discretize the clay soil and aquifer flow domains, the boundary conditions that were applied, the soil properties used as model inputs, the atrazine properties required for chemical transport simulation, and the methodology used to introduce surface runoff into the macropores were presented by Chakka and Munster (1997).

The objective of this article is to present the VS2DT simulation results of macropore infiltration, groundwater flow and atrazine transport at the Brazos River research site for the crop growing periods of 1994 and 1995. Macropore infiltration rates through the clay soil are quantified and the influence of river stage on aquifer recharge and discharge is detailed. Model simulation results were validated using field measured data. The objectives of the atrazine transport simulations were to: (1) quantify the transport of surface applied atrazine through the macropores in the clay soil flow domain; and (2) simulate the movement of atrazine in the sand and gravel floodplain aquifer that is in direct connection with the Brazos River.

Model Simulations

The variably saturated soil medium was simulated for two crop periods. The first simulation period was from day 111 to 221 in 1994. The second simulation period was from day 81 to 193 in 1995. These simulation periods correspond to the growing seasons for the corn crop planted at the research site. The soil properties used in the model simulations were the same for both the 1994 and 1995 simulations. However, rainfall and evapotranspiration changed depending on field measured values.

The clay soil flow domain was decoupled from the sand and gravel aquifer requiring two simulations. First, infiltration and transport through the clay soil was modeled using meteorological data from the research site. Next, transport through the sand and gravel aquifer was simulated using inputs from the clay soil simulation as well as groundwater and river stage data from the research site.

The initial conditions for the simulation in the clay soil flow domain are defined in terms of water content. Soil samples collected on the first day of the simulation were analyzed for moisture content and used as initial water content for the clay soil modeling. The initial conditions for the simulation in the aquifer flow domain are defined in terms of measured water table elevation. The simulation periods started on the day atrazine was applied to the research site. Atrazine concentrations were input to the surface nodes in the model based on the application rate (Chakka and Munster, 1997).

The decay constant was based on the half life of atrazine. The half life value in various soils ranged from 15 to 77 days. However, sand and gravel aquifers with aerobic conditions generally have lower half life values (Acock and Herner, 1995). Therefore, a half life of 63 days was used for the clay soil (decay constant = 0.011) and a half life of 33 days was used for the aquifer simulation (decay constant = 0.021).

Adsorption was assumed to be equilibrium controlled. The Freundlich adsorption constant (K_d) used for atrazine in the clay soil was 2.4 mg/L (Acock and Herner, 1995). In the aquifer simulations, the sorption was effectively turned off by setting K_d to zero (Chakka and Munster, 1997).

Simulation Results — Water Flow

Clay Soil with Macropores

The simulated moisture content in the clay soil flow domain was computed by averaging the moisture content at each node, in each soil layer, including the macropore nodes. This was compared to field measured values. The volumetric water content of the clay soil was determined whenever soil samples were collected for chemical analyses. The volumetric water contents were an average of two composited samples from eight random locations at the research site to a depth of 1.05 m, in 0.15 m increments. For comparison, the average absolute deviation (AAD) of the measured and simulated water contents was calculated for each sampling day for all the soil layers. The AAD was calculated as:

$$AAD = \frac{\sum_{i=1}^{n} |M_i - S_i|}{n} \quad (1)$$

where

M = field measured value
S = model simulated value
n = number of field measured values

The AAD values for the simulated and measured soil-water contents for 1994 and 1995 are presented in table 1.

The simulated water contents closely approximated the measured values for most of the simulation period as shown in table 1. The simulated and field measured water contents of the soil layers below the 0.375 m depth exhibited small variation. However, the simulated water contents of the soil layers were consistently less than the field measured values. The measured moisture content in the clay soil to a depth of 0.375 m varied from 0.210 to 0.326 depending upon meteorological conditions.

Table 1. The absolute average deviation (AAD) between measured and simulated volumetric water content in the clay soil flow domain with percent deviation from the average measured values in 1994 and 1995

Depth (mm)	Day (yr) θ*	165 (1994) θ	186 (1994) θ	194 (1994) θ	115 (1995) θ	160 (1995) θ	191 (1995) θ
75	Sim.†	0.281	0.277	0.277	0.283	0.278	0.278
	Mea.‡	0.215	0.277	0.205	0.28	0.272	0.272
225	Sim.	0.215	0.212	0.212	0.218	0.214	0.214
	Mea.	0.180	0.247	0.241	0.212	0.233	0.233
375	Sim.	0.215	0.210	0.249	0.218	0.211	0.211
	Mea.	0.233	0.233	0.282	0.244	0.248	0.248
525	Sim.	0.219	0.209	0.256	0.24	0.208	0.208
	Mea.	0.301	0.214	0.288	0.277	0.309	0.309
75	Sim.	0.222	0.210	0.209	0.262	0.209	0.209
	Mea.	0.275	0.243	0.246	0.308	0.211	0.211
825	Sim.	0.275	0.224	0.218	0.271	0.220	0.220
	Mea.	0.325	0.251	0.267	0.267	0.282	0.282
975	Sim.	-	-	-	0.279	0.261	0.261
	Mea.	-	-	-	0.323	0.348	0.348
Avg.	Sim.	0.237	0.224	0.237	0.253	0.229	0.224
	Mea.	0.254	0.244	0.255	0.273	0.272	0.249
AAD		0.050	0.021	0.042	0.024	0.045	0.037
Dev. (%)§		19.7	8.4	16.5	8.7	16.5	14.8

* Volumetric water content.
† Simulated.
‡ Measured.
§ (AAD/Average Measured) × 100.

In the model simulations, the clay soil layer was unable to meet the evaporative demand during the simulation periods with the exception of a few days following rainfall events. Bare soil evaporation and plant transpiration was used by the model to meet the potential evapotranspiration (PET) demands. PET was calculated by the Penman combination equation as modified by Businger, Penman, Long, Monteith, and van Bavel (Jensen et al., 1990). During the study period in 1994, the cumulative calculated PET was approximately 780 mm as shown in figure 1A. The total simulated ET losses were 196 mm with bare soil accounting for 39.5 mm and 156.5 mm from transpiration. During the study period in 1995, the cumulative calculated PET was approximately 810 mm over a period of 111 days as shown in figure 1B. The total simulated evaporative losses were 220 mm with bare soil evaporation at 107 mm and transpiration at 113 mm. The limiting soil water conditions, due in part by the macropore infiltration in the clay flow domain, were observed throughout the simulation period in both years.

The volume of recharge through the preferential flow paths to the sand and gravel aquifer was calculated on a daily basis by the clay soil simulation. The macropore nodes (fig. 4, Chakka and Munster, 1997), with high saturated hydraulic conductivity and low porosity, quickly transported the surface infiltration to the bottom of the clay layer. Generally, flow out of the clay soil flow domain, even on days with rainfall events that did not produce simulated surface runoff, occurred with a lag of 1 to 2 days after a rainfall event as shown in figure 2. Successive rainfall events accelerated flow out of the domain. The non-macropore nodes in the clay soil flow domain did not contribute infiltration to the sand and gravel aquifer. However, the moisture content in the adjacent nodes along the macropore paths increased during the simulation due to matrix flow between the soil pores. An increase in moisture content was observed for a distance of 200 to 300 mm (2 to 3 nodes) around the macropore flow paths.

The recharge from the clay soil simulation was used as input to the sand and gravel aquifer on a daily basis. In 1994, 234 mm of rainfall was measured at the research site during the simulation period. The simulated flow out of the clay domain was 56 mm and the simulated surface runoff losses were 12.4 mm. In 1995, 355 mm of rainfall was measured at the research site during the simulation period. The simulated flow out of the clay soil flow domain was 81 mm and the simulated surface runoff losses were 19.7 mm. In 1995, eight rainfall events that occurred between days 81 and 94 contributed to higher percentage of macropore flow than in 1994.

Sand and Gravel Aquifer

Groundwater flow in the sand and gravel aquifer was modeled after completion of the clay soil flow domain simulation. Simulated groundwater flow out of the bottom of the clay domain was used as a daily input into the aquifer model (fig. 3). The nodes on the top boundary, BE, (fig. 3, Chakka and Munster, 1997) of the aquifer flow domain were spaced 3 m apart which corresponded to the 3 m width of the clay soil domain. The nodes on BE were specified as flux boundaries or no flow boundaries depending upon outflow results from the clay simulation. The daily measured water levels in the monitoring wells R-WT and C-WT (fig. 3) were used as the right and left boundary conditions, respectively. The bottom of the aquifer flow domain, CD, (fig. 3, Chakka and Munster, 1997) was always a no flow boundary.

Simulated water levels in the B-WT and A-WT wells were compared to daily measured water levels in 1994 and 1995 as shown in figures 4 and 5. Measured and simulated water levels in A-WT differed by more than 0.1 m at the start of the simulation from days 112 to 129 in 1994 (fig. 4A). However, during the remaining simulation period, the simulated water levels closely matched the field measured values (fig. 4). The effects of river stage on water levels in the floodplain aquifer was effectively simulated by the VS2DT model in 1994.

The river stage fluctuated more in the 1995 simulation than in the 1994 simulation. As shown in figure 3A, the river stage rose quickly to a single peak on day 135 and then gradually declined. However, in 1995 (fig. 3B), the river stage peaked twice on days 115 and 134 with a sharp drop in river stage between peaks. In addition, a pump test at the research site was also conducted between days 92 and 104 in 1995. The measured water levels in the A-WT and B-WT wells dropped in response to the pump test as shown in figure 5.

As in the 1994 simulation (fig. 4), the field measured values in 1995 were also higher than the simulated values (fig. 5) at the start of the simulation period. The difference between measured and simulated values at the A-WT well, which is closer to the river, is generally greater than at the B-WT well. Simulated water levels dropped in response to the pump test at the B-WT well but lagged the field

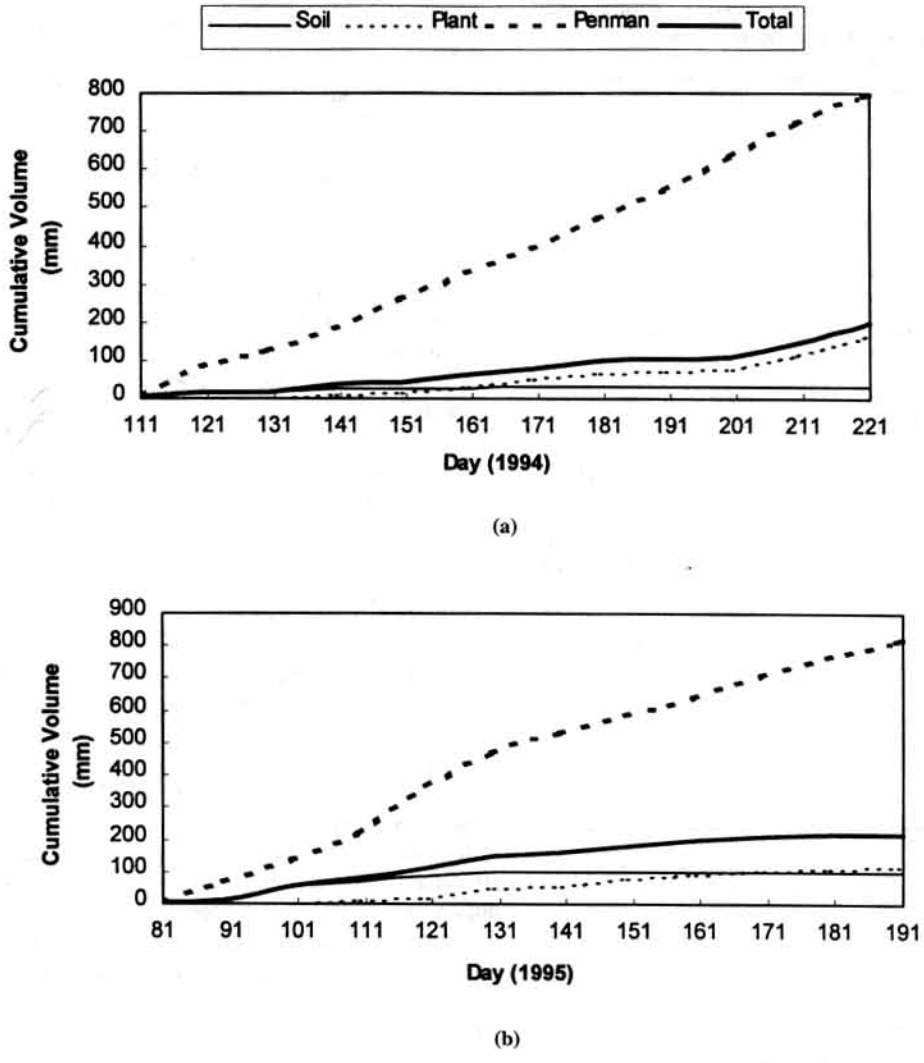

Figure 1–Simulated soil evaporation and plant transpiration losses with PET as calculated by a modified Penman method (Jensen et al., 1990) for the (a) 1994 growing season, and (b) 1995 growing season.

measured response by one day (fig. 5). The sharp drop due to pumping measured in the field at the A-WT well was not simulated by the model. However, simulated water levels at the A-WT well leveled out during the pumping test. After the pumping test, measured and simulated values closely matched until a sharp rise in the river stage occurred between days 121 and 131. Again the field measured well water levels increased faster than the simulated water levels (fig. 5).

The simulated cumulative volume of groundwater and surface water entering and leaving the aquifer domain for 1994 and 1995 shown in figure 6. Between day 128 and

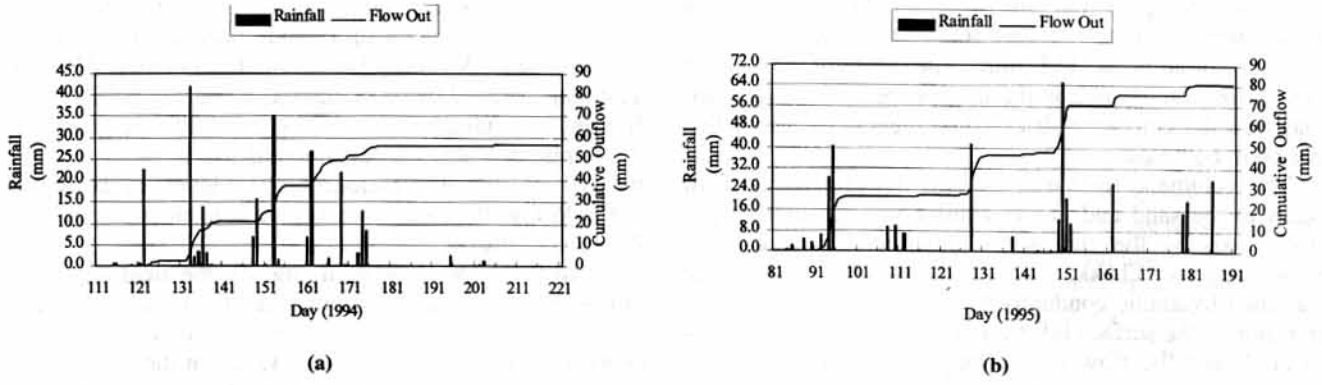

Figure 2–Cumulative simulated outflow from the bottom of the clay soil flow domain with rainfall record for the (a) 1994 growing season, and (b) 1995 growing season.

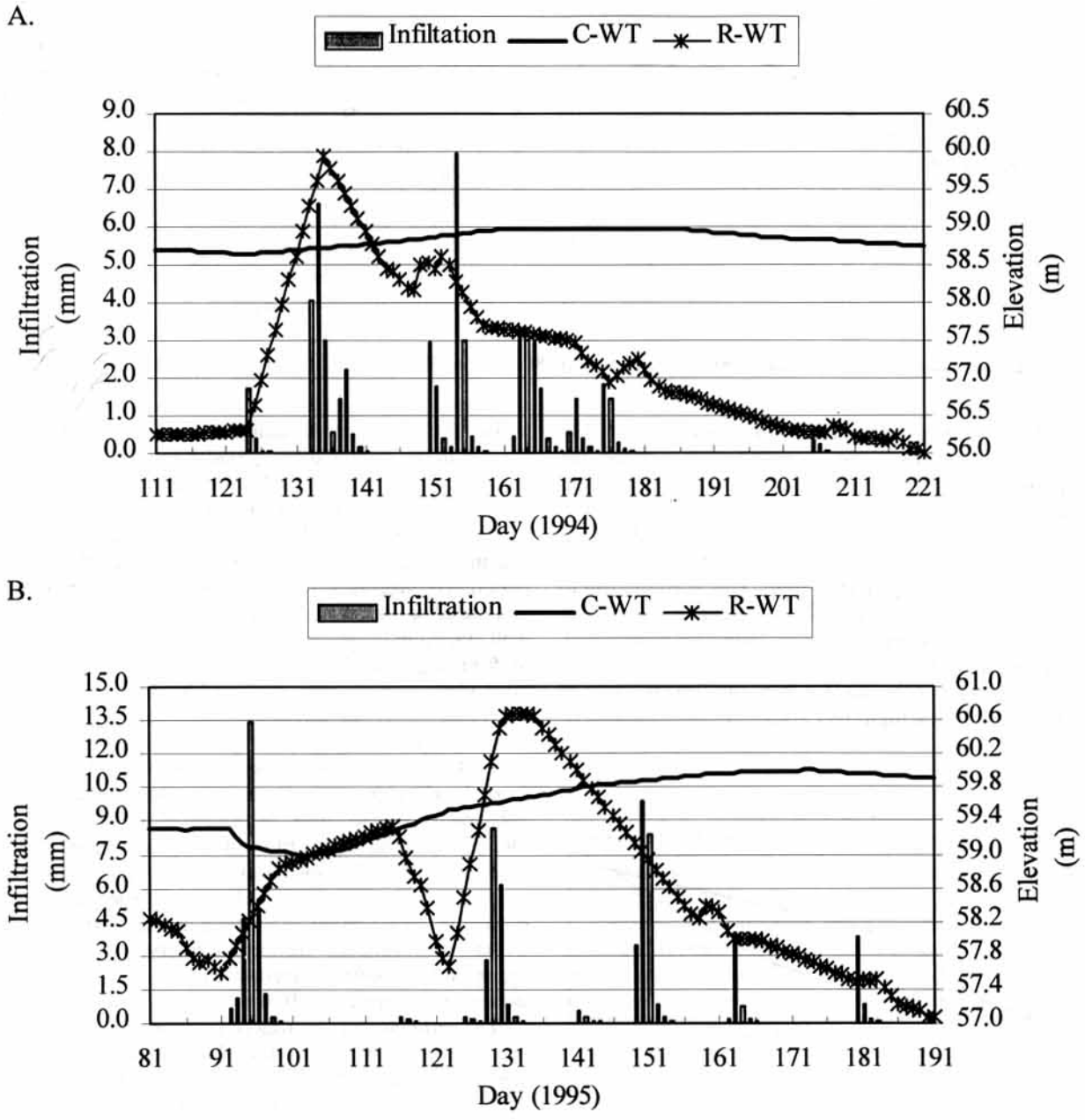

Figure 3–Boundary conditions used in the aquifer simulations that include measured water levels in the C-WT and R-WT wells and simulated outflow from the clay soil domain for (a) 1994, and (b) 1995.

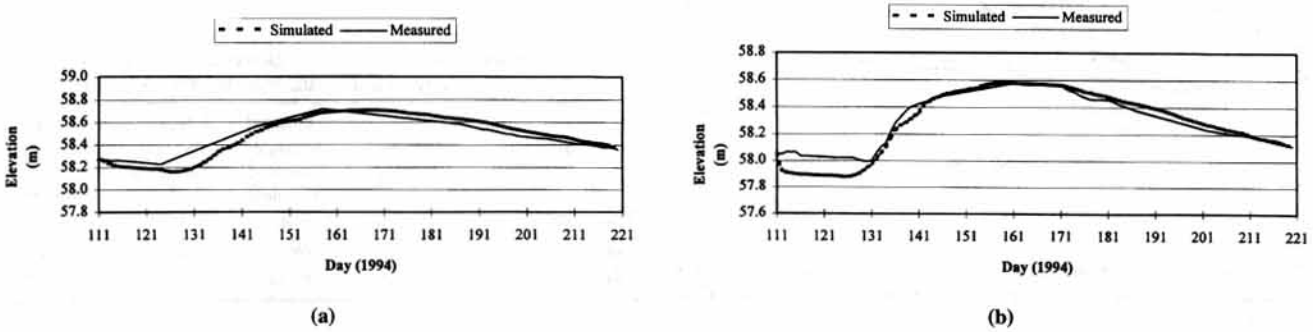

Figure 4–Measured and simulated water table levels for days 111 to 221 in 1994 in the (a) B-WT well, and the (b) A-WT well.

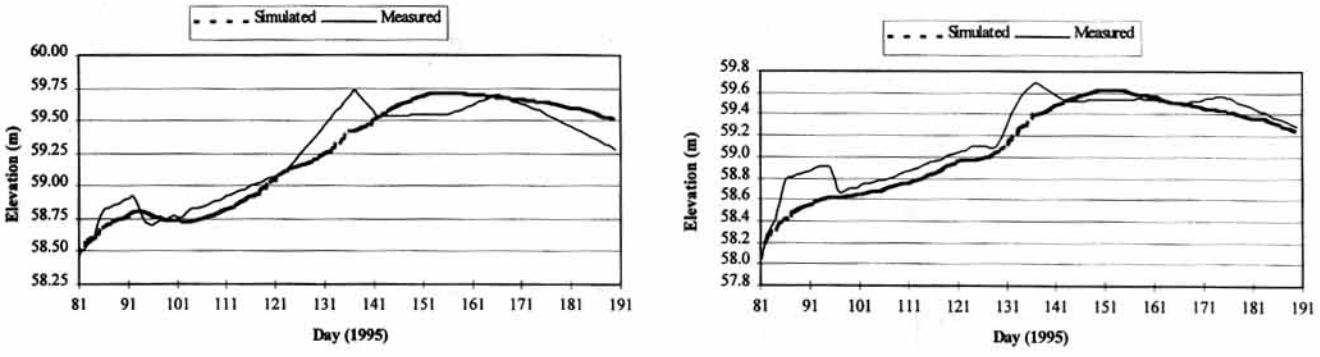

Figure 5–Measured and simulated water table levels for days 81 to 191 in 1995 at the (a) B-WT well and the (b) A-WT well.

155 in 1994, the river was high with a peak on day 135 (fig. 3A). During this period, groundwater entered the domain from both the left and right boundaries and the water levels in the C-WT well steadily rose as indicated in figure 3A. The total groundwater discharge from the flood plain aquifer to the Brazos river was 237.9 m^3/m during the 110 day simulation period in 1994. This is equivalent to a simulated flow rate of 0.025 $m^3/s/m$. The cumulative surface water flow entering the right boundary during high river stage was 37.9 m^3/m. This is equivalent to a simulated recharge of the aquifer from the Brazos River of 0.026 $m^3/s/km$ during high river stages in 1994.

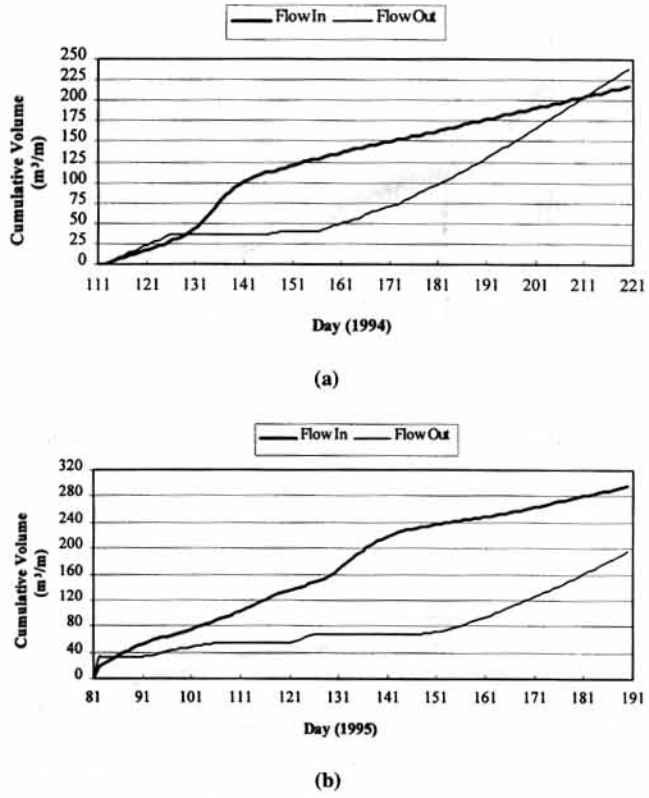

Figure 6–Simulated cumulative groundwater flow and river water into and out of the sand and gravel aquifer for (A) days 111 to 221 in 1994, and (B) days 81 to 191 in 1995.

In 1995, simulated cumulative flow into the aquifer from both the right and left boundaries was 298 m^3/m. The cumulative outflow to the Brazos River was 196.5 m^3/m. The excess groundwater that resulted from the difference between the inflow and outflow was stored in the aquifer causing water levels to rise during the 1995 simulation period. The well A-WT started with an elevation of 58.0 m and ended at a level of 59.2 m (fig. 5A) while at B-WT the well started with an elevation of 58.5 m ended at a level of 59.5 m (fig. 5B). The simulated water levels at the water table wells continuously increased between days 81 to 154 due to elevated river stages.

The total simulated discharge entering the Brazos River in 1994 and 1995 is summarized in table 2. The discharge from the alluvium to the Brazos river was reported to range between 0.006 to 0.01 $m^3/s/km$ (Cronin and Wilson, 1967). This value was estimated using an average hydraulic gradient of 0.0017, transmissibility of 200 $m^3/m/day$ and a saturated thickness of 6.1 m. For comparison of simulated discharge with Cronin and Wilson reported values, the average simulated transmissibility of aquifer was approximately 440 $m^3/m/day$ and the average simulated saturated thickness was 10.6 m.

The influence of macropore flow on water levels in the saturated zone was investigated by an aquifer simulation without flow from the unsaturated zone at the top boundary (BE). A maximum difference of 0.001 m in water table levels resulted when simulations with and without surface infiltration were compared. Therefore, water table levels were primarily influenced by the dynamic boundary conditions induced by river stage fluctuations. Surface infiltration had little effect on water table levels in the floodplain aquifer.

Table 2. Summary of simulated discharge and recharge at the Brazos River research site with reported average values

Year	Simulated Aquifer Discharge ($m^3/s/km$)	Reported Average Discharge* ($m^3/s/km$)	Simulated Average Saturated Thickness (m)	Reported Average Saturated Thickness (m)	River Recharge to Aquifer ($m^3/s/km$)
1994	0.025	0.006 - 0.01	10.09	6.1	0.026
1995	0.021	0.006 - 0.01	11.14	6.1	0.018

* Cronin and Wilson (1967).

Simulation Results — Atrazine Transport

Simulation results were compared to field measured values at the groundwater research site on the Brazos River. Soil samples were obtained to a depth of 1.05 m (Chakka, 1996). From day 55, 1994 to day 217, 1995, 13 sampling events were conducted to monitor the transport of atrazine in the soil and groundwater. A total of 185 soil samples and 426 groundwater samples were analyzed for atrazine (Chakka and Munster, 1997a). The detection limit of the soil analysis was 0.0075 mg/kg. Groundwater samples analyzed for atrazine concentrations had a detection limit of 0.05 µg/L.

Clay Soil with Macropores

The herbicide atrazine was directly sprayed on the clay soil when the corn crop was planted at an application rate of 2.18 kg/ha in 1994 and 2.8 kg/ha in 1995 (active ingredient). To simulate the atrazine application, the soil water in the surface nodes was assigned atrazine concentrations of 17.4 mg/L in 1994 and 22.4 mg/L in 1995. These initial concentrations assumed that the atrazine was applied uniformly over the soil surface and were based on the initial soil water content on the day of application.

The concentration of chemical losses in the runoff was also based on observations at the research site. The mass of chemicals lost in surface runoff was adjusted daily by a second order polynomial that was used to compute the surface runoff concentration as a function of the time after chemical application (Chakka and Munster, 1997).

No chemical losses were simulated in the water leaving the domain due to evaporation. However, the model did simulate chemical losses by plant root uptake associated with transpiration. The atrazine concentration in the macropore infiltration leaving the bottom of the clay soil domain was equal to the atrazine concentration at the exit node.

Simulated atrazine transport for days 111 and 221 in 1994 and 81 to 193 in 1995 were compared to measured field data as shown in table 3. Simulated concentrations were determined from the total mass of atrazine in each soil layer and weight of soil in that layer. Soil samples were collected in 150 mm layers to a depth of 1.05 m. The average sample depth was reported in table 3.

In 1994, 13 days after the first application, atrazine was detected in the field to an average depth of 375 mm. During the first two sampling events, samples were only collected to a depth of 450 mm. By 54 days after the first application, the simulated and measured concentrations in soil were very similar, except at the soil surface. It is interesting to note that atrazine was detected in the field to an average depth of 825 mm. However, all of the samples collected at the 525 mm depth were non-detect. This supports the hypothesis of chemical movement through preferential flow. Atrazine may have followed inclined macropore flow paths. When vertical soil samples were collected, there was a possibility of not intercepting the inclined macropore flow paths.

At 84 days after the first application, atrazine concentrations in soil approached the analytical detection limit (0.0075 mg/kg). Modeling was discontinued 110 days after application in 1994 as the maximum simulated atrazine concentration in soil was 0.001 mg/kg except at the surface nodes where the concentration was 0.015 mg/kg. The high concentrations at the surface nodes was due to the accumulation of atrazine at the surface nodes, due to evaporation.

Table 3. Measured and simulated atrazine concentrations in the clay soil flow domain in 1994 and 1995

DAA*		13 (1994)	27 (1994)	54 (1994)	84 (1994)	34 (1995)	79 (1995)	112 (1995)
Depth (mm)		(mg/kg)	(mg/kg)	(mg/kg)	(mg/kg)	(mg/kg)	(mg/kg)	(mg/kg)
75	Sim.†	0.781	0.411	0.150	0.060	0.152	0.102	0.020
	Mea.‡	0.535	0.469	0.054	0.041	0.017	0.013	0.019
225	Sim.	0.092	0.061	0.013	0.007	0.074	0.015	0.010
	Mea.	0.165	0.150	0.014	0.011	0.009	0.011	0.009
375	Sim.	0.061	0.061	0.018	0.011	0.044	0.013	0.008
	Mea.	0.042	0.046	0.011	0.008	0.008	0.012	0.014
525	Sim.	ns**	ns	0.020	0.012	0.036	0.011	0.006
	Mea.	ns	ns	0.000	0.008	0.000	0.011	0.010
675	Sim.	ns	ns	0.019	0.011	0.024	0.010	0.005
	Mea.	ns	ns	0.018	0.008	0.008	0.000	0.018
825	Sim.	ns	ns	0.021	0.011	0.018	0.009	0.005
	Mea.	ns	ns	0.015	0.000	0.010	0.008	0.016
975	Sim.	ns	ns	ns	0.014	0.018	0.012	0.007
	Mea.	ns	ns	ns	0.008	0.010	0.011	0.009
AAD§		0.113	0.054	0.022	0.007	0.043	0.015	0.005
% Dev.‖		36.188	30.394	54.232	39.778	83.128	61.628	61.148

* Days after application.
† Simulated.
‡ Measured.
§ Average Absolute Deviation.
‖ (AAD/Average Measured) × 100.
** ns = No sample.

The first soil sampling event in 1995 occurred 34 days after the second chemical application. Measured atrazine concentrations were low or non-detect (525 mm depth) while simulated concentrations were higher in all soil layers. By 79 days after application, both simulated and measured atrazine concentrations approached the analytical detection limit (0.0075 mg/kg). However, simulated concentrations at the surface layer were still higher than measured values. The atrazine concentrations in all the soil layers below the 375 mm depth exhibited little variation during the entire modeling period. The nodes that exhibited considerable variation in the concentrations below 375 mm depth were the nodes adjacent to the macropore paths. The gradual reduction in atrazine concentrations in soil samples from the first crop year were not repeated in the second crop year. The measured atrazine concentrations were in the same range as the simulated concentrations, including the surface layer, 110 days after the second chemical application.

Mass Balance for Atrazine

The total mass of atrazine applied to the 3 m wide section considered in the surface clay layer simulation was 6540 µg in 1994 and 8400 µg in 1995. The mass balance summary for atrazine in the surface layer simulations for 1994 and 1995 is shown in figure 7. In 1994, 110 days after application, simulated results indicated that approximately 69% of the atrazine decayed (63 day half life), 10% of the

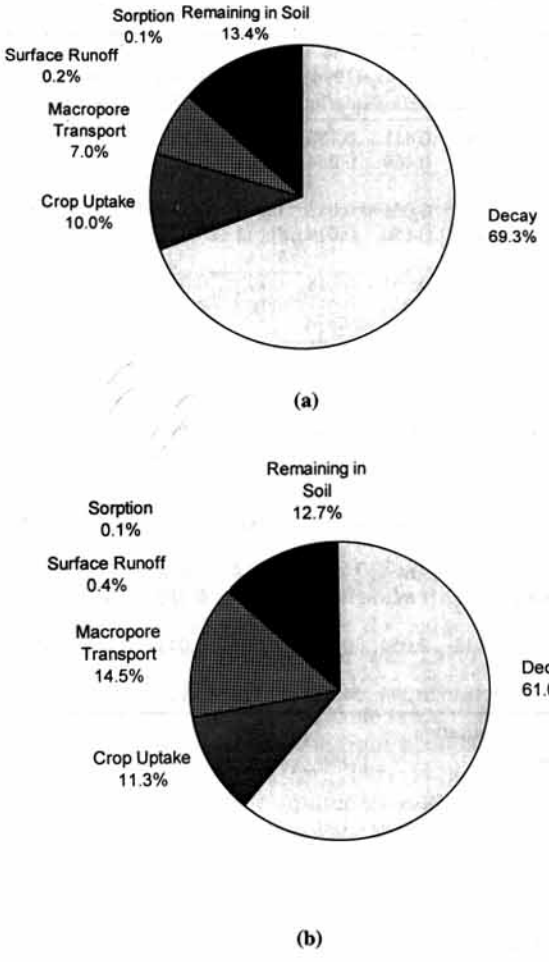

Figure 7–Atrazine mass balance summary for simulated transport in the clay soil domain in percent of the total applied after (a) 110 days in 1994, and (b) 112 days in 1995.

atrazine was taken up by the crop, approximately 7% was transported through the surface clay layer to the top of the sand and gravel aquifer, 0.1% remained sorbed onto the soil and 0.2% was lost in the surface runoff during the simulation period (fig. 7a). Approximately 13% of the atrazine remained in solution in the soil profile after 110 days of simulation.

In 1995, after 112 days of simulation, approximately 61% of the atrazine decayed, 11.3% of the atrazine was taken up by the crop, approximately 14.8% was transported through the surface clay layer to the top of the sand and gravel aquifer, 0.1% remained sorbed onto the soil and 0.4% was lost in the surface runoff during the simulation period (fig. 7a). In 1995, approximately 12.7% of the atrazine remained in solution in the soil profile after 112 days of simulation.

The model did not simulate atrazine losses due to volatilization. The K_d value of 2.4 mL/g used in atrazine simulations resulted in a net adsorption of 0.1% of the total applied atrazine. The average loss of atrazine due to surface runoff was 0.3%. This closely matched measured atrazine losses (0.15%) at the site (Munster et al., 1995).

Atrazine Flux Out of the Clay Soil Flow Domain

The atrazine flux in the simulated macropore flow out of the clay surface layer domain in 1994 and 1995 is summarized in figure 8. Atrazine transport out of the surface domain was always associated with water flux resulting from the rainfall events. In the 1994 simulations, the total mass of atrazine that entered the saturated zone was 478 µg. This was approximately 7% of the total 1994 atrazine application. The maximum atrazine loading in 1994 occurred during the first big rainfall event on day 121, 11 days after application. The total rainfall during the 1994 simulation was 233 mm.

For the 1995 simulation, the total mass of atrazine that entered the saturated zone was 1240 µg. This was approximately 14.5 % of the total atrazine applied in 1995. As shown in figure 8b, 75% of the total atrazine transported to the aquifer in 1995 occurred between days 90 and 94 (10-14 days after application). This was in response to the multiple rainfall events that occurred during this time period. The total rainfall for the 1995 simulation was 354 mm.

Sand and Gravel Aquifer Simulations

Simulated atrazine losses from the bottom of the clay soil domain were input to the top BE boundary of the sand and gravel aquifer, between the A-row and C-row wells, on a daily basis (fig.1, Chakka and Munster, 1997). A solute flux boundary condition was used in the model simulations to transfer atrazine from the clay soil domain to the aquifer domain.

A zero solute flux boundary condition was specified at the BC boundary where groundwater enters the aquifer domain (fig. 2, Chakka and Munster, 1997). At the DE boundary, the water leaving the domain had an atrazine

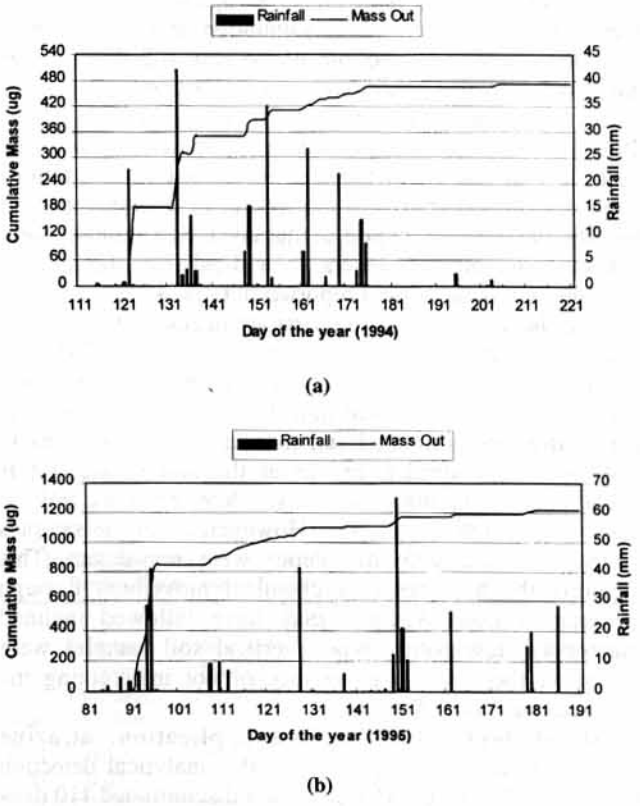

Figure 8–Simulated cumulative atrazine flux out of the surface clay layer with rainfall records for (a) 1994, and (b) 1995.

concentration equal to the concentration of the groundwater at the exit nodes. The river water entering the domain at the DE boundary was considered to be solute free. The bottom CD boundary of the flow domain was a no flow boundary. Groundwater leaving the aquifer domain on the right side DE boundary had the same atrazine concentrations as the DE boundary nodes. However, during the 110 and 112 day simulations in 1994 and 1995, atrazine did not reach the river boundary.

The simulated atrazine concentrations in the saturated domain for 1994 and 1995 were compared to the average measured concentrations in the groundwater at the same depth as shown in table 4. The simulated concentrations were obtained by averaging concentrations in the grid nodes at the same depth as the monitoring wells. Atrazine concentrations detected at the nine monitoring well nests were used for comparison with simulated concentrations. The number of samples with atrazine detects and the maximum concentrations are shown in table 4.

Transport simulations in the aquifer domain indicated that very low levels of atrazine (concentration = 0.001 µg/L) had reached the water table by 11 days after application in 1994, following the first rainfall event. However, simulated atrazine concentrations in the saturated zone were almost always below the analytical detection limit of 0.05 µg/L throughout the 1994 simulation period. The highest simulated concentration in the saturated zone was 0.09 µg/L, at the top of the water table. In model simulations, approximately 3.5% of the total applied atrazine was transported to the aquifer between 8 and 15 days after application. However, the atrazine quickly dissipated due to decay and dilution after reaching the aquifer. Simulated atrazine concentrations were considered to be insignificant for values less than 0.001 µg/L.

During the simulation period for 1994, the aquifer was sampled four times. Atrazine concentrations found in the groundwater samples from the monitoring wells in 1994 were random without any trends. The first sampling event in 1994 occurred 16 days after the first atrazine application. Two out of 26 groundwater samples analyzed contained atrazine. However, the transport simulations indicated no atrazine in the saturated zone during this period.

Table 4. Field measured and simulated atrazine concentrations in the groundwater from the nine shallow, eight medium, and nine deep monitoring wells

Days After Application (Year)	Shallow Wells 9.7 – 12.2 m			Medium Wells 13.7 – 15.9 m			Deep Wells 16.8 – 19.8 m		
	No. of Detects*	Max. Meas. Conc.† (µg/L)	Avg. Sim. Conc.‡ (µg/L)	No. of Detects	Max. Meas. Conc. (µg/L)	Avg. Sim. Conc. (µg/L)	No. of Detects	Max. Meas. Conc. (µg/L)	Avg. Sim. Conc. (µg/L)
16 (1994)	1	0.150	0.000	0	0.000	0.000	1	0.110	0.000
33 (1994)	1	0.050	0.000	0	0.000	0.000	0	0.000	0.000
47 (1994)	0	0.000	0.002	0	0.000	0.000	0	0.000	0.000
76 (1994)	1	0.600	0.068	0	0.000	0.005	0	0.000	0.000
24 (1995)	9	3.870	0.081	7	0.570	0.002	5	0.230	0.000
56 (1995)	5	0.640	0.117	2	0.070	0.051	1	0.050	0.012
94 (1995)	5	0.020	0.061	0	0.000	0.030	3	0.070	0.048

* Number of groundwater samples from the shallow, medium, and deep wells with atrazine detections.

† Maximum atrazine concentration measured in the groundwater from the shallow, medium, and deep wells.

‡ Average simulated atrazine concentrations in the groundwater for the shallow, medium, and deep well depths.

During the second sampling round 33 days after application, one shallow well sample out of 26 samples analyzed contained atrazine. Again, the transport simulation did not result in atrazine concentrations above the analytical detection limit in the saturated zone 33 days after the application.

Model simulations resulted in atrazine transport to the shallow well depth, 47 days after application, with an average concentration of 0.002 µg/L (table 4). However, all field samples were below the analytical detection limit of 0.05 µg/L. During the next sampling round, 76 days after application, atrazine was transported to the shallow well depth at an average concentration of 0.068 µg/L and to the medium well depth at an average concentration of 0.005 µg/L in model simulations. One shallow well sample, collected 76 days after application, contained atrazine.

The detects in well samples from 1995 were less random than in 1994. During the 1995 simulation time period, the monitoring wells were sampled 24, 56, and 94 days after the second atrazine application. In the first sampling round, 21 out of 26 groundwater samples contained atrazine (Chakka and Munster, 1997a). The rapid transport of atrazine to the sand and gravel aquifer was due to several rainfall events that occurred between 5 to 13 days after application and a pumping test at the site pump well that continuously pumped 972 m^3/d from day 11 to day 23 after application.

The 1995 transport simulations in the aquifer domain indicated that atrazine had reached the water table 18 days after the second application. Simulated atrazine transport to the aquifer, by day 24 after application, was approximately 4.5 times higher than the atrazine transported in 1994. At 24 days after application, the average simulated atrazine concentrations were 0.081 µg/L at the shallow well depth, 0.002 µg/L at the medium well depth and 0.000 µg/L at the deep well depth. This compares with maximum field measured values of 3.870 µg/L, 0.570 µg/L, and 0.230 µg/L in the shallow, medium and deep wells, respectively. Five out of the 9 deep wells sampled in the field contained atrazine. The pumping test contributed to rapid movement of atrazine to the deeper zones in the aquifer in the field. The vertical gradients that developed during the pump test and quickly transported atrazine deep into the aquifer were not effectively simulated by the model.

Atrazine was detected in 5 shallow wells, 2 medium wells, and 1 deep well in the field 56 days after application (table 4). Transport simulations also resulted in atrazine transport to shallow (average concentration = 0.117 µg/L), medium (average concentration = 0.051 µg/L) and deep well depths (average concentration = 0.012 µg/L).

Between 56 and 94 days after application, the average simulated concentrations in the shallow and medium wells decreased as did the field measured concentrations (table 4). However, there was an increase in the average simulated concentrations in the deep wells. On day 94 after application, simulated atrazine concentrations closely matched measured field concentrations at all well depths. The monitoring wells were not sampled between days 94 and 112 after application in 1995. Model simulations were discontinued 112 days after application after simulated atrazine concentrations were less than 0.001 µg/L throughout the aquifer.

During both simulation periods, atrazine did not reach the river boundary. Atrazine was transported horizontally beyond the A-row wells a distance of 27 m during the 1994 simulation and 43 m during the 1995 simulation.

Summary and Conclusions

Groundwater flow and atrazine transport through conceptualized macropores was simulated during the crop periods of 1994 and 1995 using the model VS2DT. The macropores were represented by porous media with high hydraulic conductivity and low porosity. Surface runoff was introduced into the macropore channels and the flow out of the clay soil was simulated on a daily basis. The groundwater and atrazine flux output from the clay domain were used as input for the sand and gravel aquifer simulations.

The interactions between the floodplain aquifer and the Brazos river were then simulated using the VS2DT model. Groundwater levels and river stage were monitored at the study site during the crop periods in 1994 and 1995. The daily measurements obtained from the field were used as model inputs for groundwater flow simulations. Measured and simulated water levels matched very closely throughout the study period. The simulated discharge into and out of the aquifer was determined on a daily basis. The simulated groundwater discharge rate entering the Brazos River, during normal or low river stage, was 0.025 $m^3/s/km$ in 1994 and 0.021 $m^3/s/km$ in 1995. During periods of high river stage, the simulated recharge rates from the river to the aquifer were 0.025 $m^3/s/km$ in 1994 and 0.018 $m^3/s/km$ in 1995.

Simulated atrazine concentrations in the clay soil domain compared favorably to measured soil concentrations to a depth of 1 m. A mass balance of the clay soil simulations quantified atrazine decay, sorption, crop uptake, surface runoff, soil residue, and macropore transport out of the clay domain for each year. Atrazine losses in macropore flow were 7% (of total applied) in 1994 and 15% in 1995. Increased atrazine losses in 1995 were due to a series of rainfall events immediately after the 1995 application and a 28% increase in the 1995 atrazine application rate.

Simulated atrazine concentrations in the aquifer generally reflected the field measured atrazine concentrations in 1994 and 1995. Atrazine was transported to a depth of 19 m in the 1995 simulations due to increased loading from the clay soil domain and groundwater withdrawals from a pumping well at the research site. Atrazine was also detected in the wells at the research site at the 19 m depth in 1995.

In summary, the use of the USGS model VS2DT was validated for groundwater flow and agricultural chemical transport in a complex flow domain that included macropore flow and groundwater-surface water interactions. The use of two transport simulations, one for the clay soil domain and one for the sand and gravel aquifer, permitted a detailed macropore characterization to be coupled with a field scale aquifer system. The model simulations of groundwater flow and atrazine transport compared favorably to field measured values.

References

Acock, B. and A. Herner. 1995. Agricultural research services pesticides properties database. In *Clean Water-Clean Environment-21st Century*, Conf. Proc., Vol. 1: Pesticides. St. Joseph, Mich.: ASAE.

Ahuja, L. R. , D. G. DeCoursey, B. B. Barnes and K. W. Rojas. 1993. Characterization of macropore transport studied with the ARS root zone water quality model. *Transactions of the ASAE* 36(2):369-380.

Bronswijk, J. J. B., W. Hamminga and K. Oostindie. 1995. Field scale solute transport in a clay soil. *Water Resour. Res.* 31(3): 517-526.

Chakka, K. B. 1996. Evaluation and simulation of non-point source agricultural chemical transport in variably saturated soil medium. Ph.D. thesis. College Station, Tex: Department of Agricultural Engineering, Texas A&M University.

Chakka, K. B. and C. L. Munster. 1997a. Atrazine and nitrate transport to Brazos River floodplain. *Transactions of the ASAE* 40(3):615-621.

Chakka, K. B. and C. L. Munster. 1997. Modeling macropore transport of agricultural chemicals on a river floodplain: Model formulation. *Transactions of the ASAE* 40(5):1355-1362.

Chung, S. O., A. D. Ward and C. W. Schalk. 1992. Evaluation of the hydrologic component of the ADAPT water table management model. *Transactions of the ASAE* 35(2):571-579.

Cronin J. G. and C. A. Wilson. 1967. Groundwater in the floodplain alluvium of the Brazos River, Whitney Dam to Vicinity of Richmond, Texas. Rep. No. 41. Austin, Tex.: Texas Water Development Board.

Ellins, K. K., A. Roman-Mas and R. Lee. 1990. Using ^{222}Rn to examine groundwater/subsurface discharge interaction in the Rio Grande de Manati. *J. Hydrol.* 115(1):319-341.

Healy, R. H. 1990. Simulation of solute transport in variably saturated porous media with supplemental information on modifications to the U.S. Geological Survey's computer program VS2D. Rep. 90-4025. Denver, Colo.: Water-Resources Investigations.

Jakeman, A. J., D. R. Dietrich and G. A. Thomas. 1990. Solute transport in a stream aquifer system: Application of model identification to the River Murray. *Water Resour. Res.* 25(10): 2177-2185.

Jensen, M. E., R. D. Burman and R. G. Allen. 1990. *Evapotranspiration and Irrigation Water Requirements*. New York, N.Y.: ASCE.

Kellogg, R. L., M. S. Maizel and D. W. Goss. 1992. Agricultural chemical use and groundwater quality: Where are the potential problem areas? Washington, D.C.: United States Dept. of Agriculture, NRCS.

Lappala, R. W., R. W. Healy and E. P. Weeks. 1987. Documentation of computer program VS2D to solve the equations of fluid flow in variably saturated porous media. Rep. 83-4099. Denver, Colo.: Water-Resources Investigations.

Leonard, R. A., W. G. Knisel and D. A. Still. 1987. GLEAMS: Groundwater loading effects of agricultural management systems. *Transactions of the ASAE* 30(2):1403-1418.

Morari, F. and W. G. Knisel. 1997. Modifications of the GLEAMS model for cracking clay soil. *Transactions of the ASAE* 40(5):1337-1348.

Munster, C. L., B. M. Schneider and J. R. Vogel. 1995. Chemical and sediment transport in surface runoff: A field study. ASAE Paper No. 95-2697. St. Joseph, Mich.: ASAE.

Skaggs, R. W. 1978. A water table management model for shallow water table soils. Technical Report No. 134. Raleigh, N.C.: Water Resources Research Inst., University of North Carolina, NC State University.

U.S. Environmental Protection Agency. 1992. The national survey of pesticides in drinking water wells: Phase II report, Another look. EPA 570/09-91-020. Washington, D.C.: USEPA.

White, D. S., S. P. Hendricks and S. L. Fortner. 1992. *Groundwater and Surface Water Interactions and the Distributions of Aquatic Macrophytes*, Proc. 1st Int. Conf. Groundwater Ecology. Bethesda, Md.: Am. Water Resources Association.

MODELING MACROPORE TRANSPORT OF AGRICULTURAL CHEMICALS ON A RIVER FLOODPLAIN: MODEL FORMULATION

K. B. Chakka, C. L. Munster

ABSTRACT. *Modeling methods were developed to simulate groundwater flow and atrazine transport at a research site on the Brazos River floodplain. Conceptualized macropores were utilized to simulate preferential flow through a highly structured clay soil. The United States Geological Survey (USGS) model, Variably Saturated Two Dimensional Transport (VS2DT), was used to simulate macropore transport of agricultural chemicals through the soil to a sand and gravel aquifer. The clay soil flow domain was decoupled from the sand and gravel aquifer. Transport simulation in the aquifer used inputs from the simulation of transport through the clay soil. The model simulated variably saturated flow in the macropores, clay soil matrix and floodplain aquifer using the Richards equation and chemical transport using the advection-dispersion equation. The flow domains for the clay soil and aquifer were detailed. Model inputs for groundwater flow and atrazine transport and the associated boundary conditions are presented.* **Keywords.** *Modeling, Macropore flow, Clay soil, Groundwater, Agricultural chemicals, Chemical transport, Floodplain aquifer.*

The U.S. Environmental Protection Agency (USEPA) reports that at least 46 pesticides have been detected in groundwater in 26 states as a result of normal agricultural practices (USEPA, 1988). A number of large water quality surveys have been conducted to assess the extent of agricultural chemical contamination. In a nationwide survey, the USEPA analyzed 65,865 samples from community water wells and rural household wells between 1971 and 1991 for 126 pesticides and pesticide metabolites (USEPA, 1992). The data indicated that one or more pesticides in excess of health standards were detected in 14.4% of the samples analyzed (USEPA, 1992).

The transport of agricultural chemicals to the groundwater may occur rapidly in soils with macropores. Detection of agricultural chemicals in drainage discharge has been reported following the first post-application rainfall (Kladivoko et al., 1991). Similar trends were observed by Gish et al. (1991) and Smith et al. (1990), where high concentrations of pesticides were measured in shallow groundwater.

In preferential flow, infiltration is transported laterally and vertically through the soil in large macropores (Beven, 1989). Preferential flow may also be characterized by non-uniform unstable wetting fronts (Hill and Parlange, 1972) and funnel flow (Kung, 1990a,b). Funnel flow is characterized by many random macropore channels near the surface, which consolidate to fewer, well defined preferential paths with increasing depth.

Article was submitted for publication in February 1997; reviewed and approved for publication by the Soil & Water Div. of ASAE in August 1997.

The authors are **Kesava B. Chakka**, Technical Consultant, Deloitte & Touche Consulting Group, DRT Systems, Houston, Tex.; and **Clyde L. Munster, *ASAE Member Engineer***, Assistant Professor, Department of Agricultural Engineering, Texas A&M University, College Station, Tex. **Corresponding author:** Dr. Clyde L. Munster, Department of Agricultural Engineering, MS 2117, Texas A&M University, College Station, TX 77843-2117; tel.: (409) 847-8793; fax: (409) 845-3932; e-mail: <munster@agen.tamu.edu>.

In clay soils, preferential flow paths are created by surface cracks that extend below the surface and channelize flow through the porous media (Lawes et al., 1982). High infiltration rates have been reported for small macropores (Beven, 1989). Macropore flow velocities reported by Beven (1989) range from 0.25 to 2.08 mm/s inferring high hydraulic conductivities.

Unfortunately, very few models exist that can predict the preferential transport of pesticides. Steenhuis et al. (1994), Chen and Wagnet (1992), and Ray et al. (1996) made attempts to model chemical transport through preferential flow. Steenhuis et al. (1994) derived expressions for distance traveled, arrival time, and concentration of preferential transport in a conceptual model where a layer near the surface becomes saturated and distributes water and solute to the preferential flow paths. Ray et al. (1996) developed a simulation model capable of describing the preferential movement of water and pesticides in macroporous soils based on a conceptual dual-porosity approach.

Simulation models without macropore transport are widely used for predicting water and solute transport through unsaturated soil (Healy, 1990; van Genuchten, 1980; Gee et al., 1991). However, significant discrepancies between model results and field measurements are often observed due to macropore transport. Traditional models using average soil properties, underpredict chemical transport in macroporous soils (Jury and Fluhler, 1992; Steenhuis et al., 1990).

The objective of this research article is to present the methods used to simulate macropore transport of atrazine through a clay soil to the underlying sand and gravel floodplain aquifer using the United States Geological Survey (USGS) model, Variably Saturated Two Dimensional Transport (VS2DT) (Lappala et al., 1987; Healy, 1990). VS2DT was then used to simulate flow through a variably saturated floodplain aquifer in direct hydraulic connection with the adjacent river.

  0001-2351 / 97 / 4005-1355

Multi-domain models were presented in the past by Gwo et al. (1995) and Hutson and Wagenet (1995). These studies indicated that a multi-domain approach described the field scale processes better than a single domain approach. Gerke and van Genuchten (1993) stated that the non-equilibrium conditions associated with preferential flow severely limit the ability of single continuum models to predict flow and transport phenomena in macroporous media.

This article will present the hydrogeology of the floodplain research site and the flow domains that were used in the model simulations. Modeling the clay soil flow domain with conceptualized macropores and the methodology used to infiltrate surface runoff will be detailed. The methods used to simulate the sand and gravel aquifer flow domain under natural gradient and pumped gradient conditions will also be presented. The model inputs required for groundwater flow and atrazine transport and the associated boundary conditions for both flow domains at the floodplain research site are given. A companion article will present results of the groundwater flow and atrazine transport simulations.

Research Site

A 8.5 ha groundwater research site on the Brazos River floodplain approximately 11 km southwest of College Station, Texas, was used for model simulations (Munster et al., 1996). The site was located between a deep (5 m) drainage ditch and the Brazos River (fig. 1). The surface layer at the research site was a Ships clay unit (very fine, mixed, thermic chronic Hapluderts) that was approximately 6 m thick. A floodplain aquifer located below the clay layer changed gradually from a fine sand at a depth of 6 m to a coarse sand and gravel mixture at a depth of

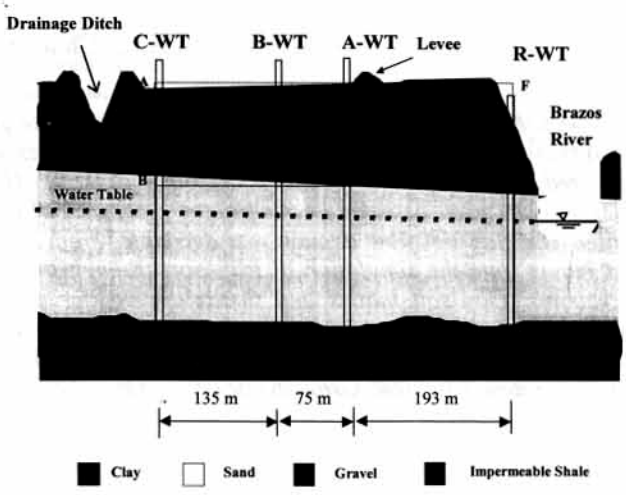

Figure 2–Cross-section of the Brazos River research site with the water table wells (A-WT, B-WT, C-WT, and R-WT) that are fully screened throughout the aquifer, the soil layers, and the flow domain (A, B, C, D, E, and F) simulated by the model (not to scale).

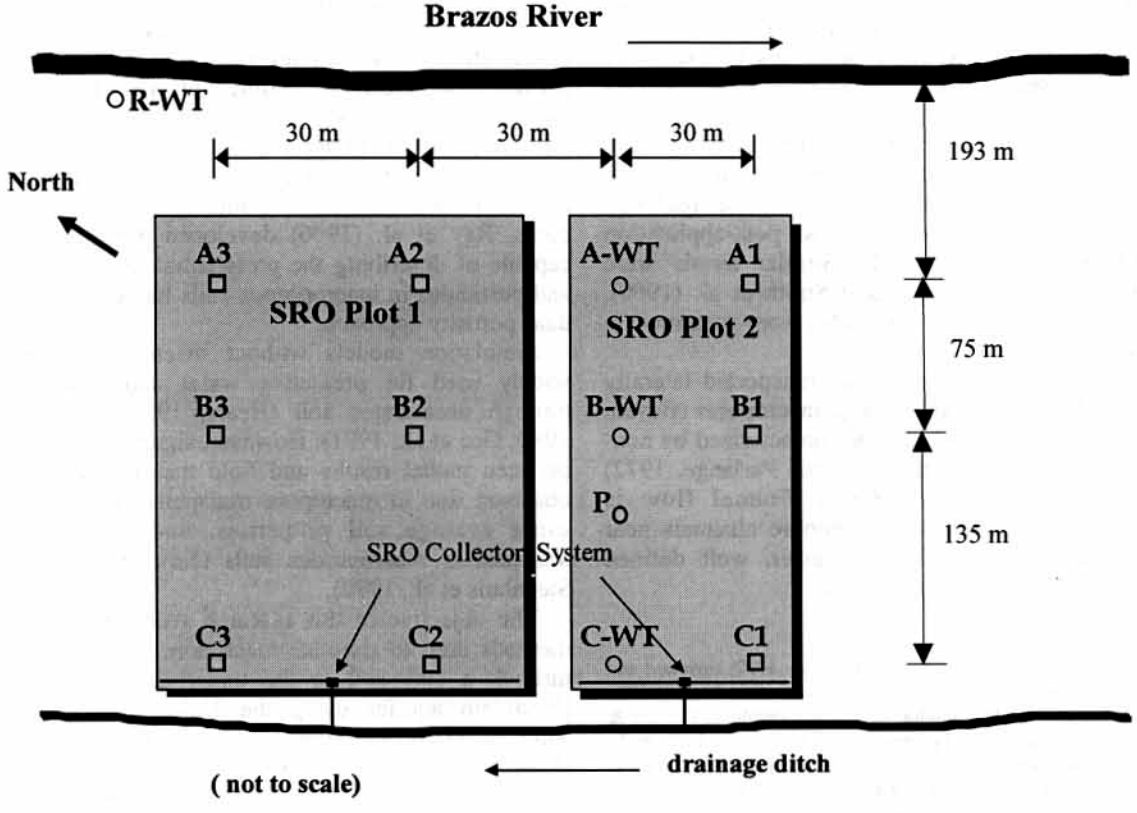

Figure 1–The Brazos River research site with two surface runoff (SRO) plots that include nine well nests (A1, A2, A3, B1, B2, B3, C1, C2, C3), four water table wells (A-WT, B-WT, C-WT, and R-WT), and a 200 mm diameter pumping well (P).

20 m. The aquifer was underlain by an impermeable Yegua shale formation at a depth of 20 m (fig. 2).

Field and laboratories studies measured low saturated hydraulic conductivities (1 mm/day at 150 mm depth) for the Ships clay at the research site. However, this mixture of kaolinite and montmorillonite clay has a high shrink-swell capacity that produces large cracks or macropores during dry periods (Lin, 1995). Ships clay soils are generally less than 1% organic carbon (Lin, 1995), which indicates a low capacity to organically adsorb agricultural chemicals (Hassett and Banwart, 1989). Therefore, soluble agricultural chemicals have the potential to be transported through the soil profile with infiltration through these macropores. Detectable levels of pesticides can result even though a small fraction of chemicals that are surface applied escape the root zone and reach groundwater through the macropores (Heuvelman et al., 1993; Chakka and Munster, 1997). Rainfall events that follow extended dry periods produce little or no surface runoff, with most of the surface runoff flowing into the cracks or macropores (Munster et al., 1995).

The research site was instrumented for groundwater and surface runoff monitoring. A total of nine well nests were installed in a 3 × 3 grid that was parallel and perpendicular to the river (fig. 1). Each well nest had four monitoring wells. There were also four "water table" wells that were fully screened throughout the aquifer. The R-WT water table well was located approximately 20 m from the river to monitor river stage.

A pump test was conducted in 1995 to determine aquifer properties by analyzing drawdown in the wells at the site. The research site was subdivided into two surface runoff plots with surface runoff collector systems in each plot (fig. 1). All surface runoff was quantified from each plot and sampled throughout each runoff event (Munster et al., 1995).

The site was not used for agricultural production prior to 1994. A corn crop was planted between the drainage ditch and levee (fig. 2) using ridge-till cultivation in 1994 and 1995. Liquid atrazine was applied at the time of planting at an average rate of 2.49 kg/ha of active ingredient. No atrazine was applied to the pasture between the levee and river. Surface applied atrazine was detected in the groundwater 24 days after application indicating preferential flow at the research site in 1995 (Chakka and Munster, 1997).

Computer Model

The United States Geological Survey (USGS) computer model Variably Saturated Two Dimensional Transport (VS2DT) was used to simulate groundwater flow and chemical movement at the research site. The model, written in ANSI FORTRAN, solves the Richards' equation for groundwater flow and the advection-dispersion equation for chemical transport in both saturated and unsaturated conditions (Lappala et al., 1987; Healy, 1990). The model uses two-dimensional finite difference methods. The spatial derivatives for the governing partial differential equations are approximated using central differences between adjacent nodes. The time derivatives are approximated using a fully implicit backward scheme. The matrix of finite difference equations are solved using the strongly implicit procedure (Lappala, 1987).

The VS2DT model has been extensively verified for groundwater flow and chemical transport using analytical solutions (Healy, 1990). VS2DT has also been validated for agricultural chemical transport using field measured values. VS2DT simulations of the transport of the pesticide aldicarb through the soil and groundwater at an agricultural research site closely matched field measured values (Munster et al., 1994).

For VS2DT model simulations, the recharge period was set to one day, with an initial time increment of 1.0E-06 day for the unsaturated zone and 1.0E-14 day for the sand and gravel aquifer. These initial time increments were increased by a factor of 2.1 when a stable solution was achieved and reduced by a factor of 0.1 when non-stable conditions existed. All simulation input variables were determined either experimentally or from the literature.

Simulation Domain

The flow domain at the research site was approximated by a two dimensional rectangular section in the X-Z plane as shown in figure 2. The porous media layers in the flow domain (A, B, C, D, E, and F) were approximated as shown in figure 3. The average depth for each layer was determined from soil sampling and well installation observations at the site.

Soil layers 1 and 2 were characterized by very low saturated hydraulic conductivity clays with preferential flow paths from cracking and soil structure (Lin, 1995). Aquifer layers 1 and 2 formed the water bearing aquifer which was unconfined during the study period. Below the water table, aquifer layer 1 exhibited "flowing sand" conditions during the well installation process. Aquifer layer 2 was highly permeable with coarse gravel and cobbles (Wrobleski, 1996).

Simulation Methods

Macropore channels were incorporated into the surface clay layers in the simulation model to match the field observations. To facilitate macropore modeling, the clay soil layers were decoupled from the sand and gravel aquifer. A flow domain in the clay soil 3 m in length (A′, B′, E′, and F′), was selected for detailed modeling as shown in figure 4.

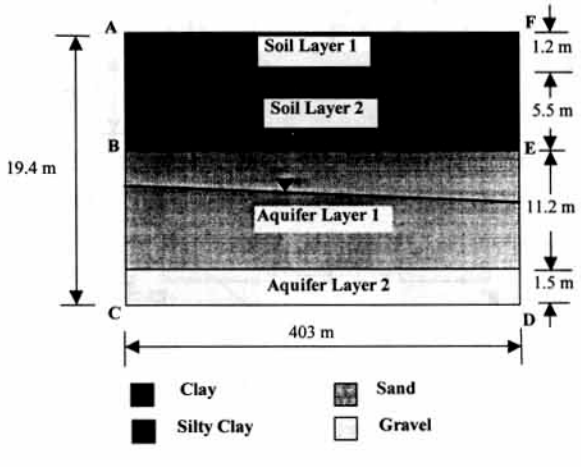

Figure 3–The porous media layers used to approximate the flow domain at the Brazos River research site with a typical water table location also shown.

De-coupling the two flow domains required two separate simulations to be performed. First, the clay domain model simulated macropore flow and incorporated the meteorological processes and chemical applications. The daily flux of solute from the bottom of the clay section was used as input for the sand and gravel aquifer simulations. Then the sand and gravel aquifer model simulated chemical transport and groundwater-surface water interactions from the clay domain model. However, chemical flux inputs were restricted to the chemical application zone between the drainage ditch and the levee.

This modeling approach assumed that a 3 m long clay section could adequately represent the infiltration process in a clay soil that was 6.7 m deep. Another assumption was that the sand and gravel aquifer did not contribute to the evaporation processes at the surface.

Modeling Clay Soil with Macropores

The flow domain for the surface soil layer (A′, B′, E′, F′) was 3 m long and 6.7 m deep with conceptualized macropores as shown in figure 4. The works by Lin (1995) and Heuvelman et al. (1993) in Ships clay soil reported a macropore system with many chaotic preferential flow paths near the surface that merged with depth to fewer, well-defined macropores. The macropore spacing at the surface coincided with the spacing of the furrows formed during ridge-till cultivation. The macropores in figure 4 represented areas of high hydraulic conductivity and low porosity within the soil.

A finite difference grid consisting of 32 nodes in the vertical direction (6.7 m) and 31 nodes in the horizontal direction (3.0 m) was used for numerical simulation of the clay soil flow domain. Horizontally, all the nodes were equally spaced at 0.097 m. Vertically, variable node spacing was used. Vertical node spacing was gradually increased from 0.05 m at the surface to 0.20 m in the clay layer. Node spacing was also gradually decreased to 0.05 m at the clay-silty clay interface. In the silty clay porous medium the spacing was gradually increased from 0.05 m to 0.20 m and was also gradually reduced to 0.05 m near the BE boundary.

The nodes representing the macropores were arranged in a horizontal and vertical stair-step configuration to create the 45° angle. This permitted horizontal and vertical flow between the nodes as required by the finite difference method.

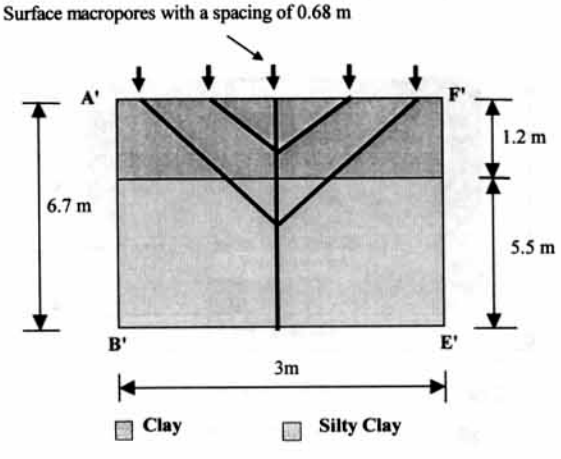

Figure 4–Conceptualized macropores in the clay soil flow domain in a 3 m long cross-section (A′, B′, E′, and F′) considered for detailed modeling of the clay soil from 403 m long clay soil flow domain (A, B, E, and F in fig. 1).

Boundary Conditions

The boundary conditions used to simulate groundwater flow changed daily based on field observations. The groundwater flow boundary conditions for the cross-section considered in the clay soil flow domain (fig. 4) are as follows:

A′F′ = constant head or specified flux boundary
A′B′ = no flow boundary
B′E′ = seepage face
E′F′ = no flow boundary

The boundary A′F′ is either a specified flux or a constant head boundary depending upon the meteorological conditions. The maximum specified flux out of the domain at the A′F′ boundary was the potential evapotranspiration (PET) rate determined daily from meteorological conditions. Typically, the maximum flux out of the domain at A′F′ was not achieved due to limiting soil-water availability. On days with rainfall, the specified flux was into the domain at a rate that distributed the rainfall over a 24 h period. If the rainfall rate exceeded the soil infiltration capacity, then ponding occurred and the A′F′ boundary became a constant head boundary. From field observations, when the depth of ponded water exceeded 50 mm, surface runoff occurred. The boundary B′E′ was defined as a seepage face where only flow out of the domain was permitted.

Chemical boundary conditions were specified for the clay soil flow domain at the A′F′ boundary. In the field, the herbicide atrazine was directly sprayed onto the clay soil. To simulate the atrazine application, the nodes at the A′F′ boundary were assigned atrazine concentrations based on field measured water content values on the day of application and the mass of atrazine active ingredient applied to the soil.

To simulate the atrazine application, the nodes at the A′F′ boundary were assigned the atrazine application concentration. At the bottom boundary (B′E′), the chemical flux out of the domain was equal to the rate of water flux times the concentration of the chemical at the exit node.

Potential Evapotranspiration

Daily PET values were used in the model to establish maximum rates for soil evaporation and plant transpiration. The potential evapotranspiration values were calculated using a Penman combination equation as modified by Businger, Penman, Long, Monteith, and van Bavel (Jensen et al., 1990). The data obtained from a weather station at the site was used to compute the PET values using the combination equation. Fallow conditions existed at the time the corn crop was planted. Therefore, 100% of the PET flux was assigned to soil evaporation. However, as the corn crop began to grow, the PET flux was incrementally shifted to plant transpiration. By day 70 after planting, 100% of the PET flux was assigned to plant transpiration. Plant transpiration was extracted from the soil profile according to a specified root growth function from Molz (1981). The soil-water leaving the domain in the form of evaporation was considered to be solute free by the model. The water extracted by the roots due to

transpiration had the same chemical concentration as the soil-water in the nodes near the roots. Root extraction represented plant uptake of the solute.

Surface Runoff Simulation

A critical component in modeling macropore infiltration was surface runoff and the associated chemical losses. The average surface runoff measured at the research site in 1994 and 1995 was 5 to 8% of the rainfall (Munster et al., 1995). Therefore, a maximum of 5% of the rainfall was allowed to runoff in the simulation based on surface runoff studies at the site.

To represent actual field conditions, the runoff and chemical losses were simulated in the following manner. The rainfall on any particular day was distributed evenly over the surface of the clay soil flow domain. At the end of the daily simulation, the potential surface runoff was calculated as follows:

$$SRO_{pot} = R - I - DS \quad (1)$$

where

SRO_{pot} = potential surface runoff without forced macropore infiltration (mm)
R = rainfall (mm)
I = infiltration on the day of rainfall without forced macropore infiltration (mm)
DS = depression storage (mm)

The depressional storage is a function of surface roughness. A depressional storage depth of 50 mm was used in the model simulations based on field observations.

If the SRO_{pot} was less than 5% of the rainfall, then there was no forced macropore infiltration and simulated surface runoff (SRO) equaled SRO_{pot}. However, if the SRO_{pot} was greater than 5% of the rainfall, then simulated surface runoff (SRO) equaled 5% of the rainfall and forced macropore infiltration was calculated as follows:

$$I_{macro} = SRO_{pot} - 0.05\,(R) \quad (2)$$

where I_{macro} = forced macropore infiltration (mm).

I_{macro} was reapplied using a specified flux boundary condition at the macropore nodes on the surface, as shown in figure 4, on the following day. This forced surface runoff into the macropore nodes as observed in the field. If rainfall occurred on consecutive days and forced macropore infiltration was required on the second day, the rainfall was distributed evenly over the entire domain and the flux into the macropore nodes was the sum of rainfall flux and I_{macro} from the previous day.

The concentration of chemical losses in the runoff was also based on observations at the research site in 1994 (Munster et al., 1995). The mass of atrazine lost in surface runoff was adjusted daily by a second order polynomial. This polynomial was used to compute atrazine concentrations in the surface runoff as a function of the time after chemical application. The second-order polynomial that was derived from a regression analysis of the measured concentrations of the surface runoff was:

$$Y = 0.0381\,X^2 - 4.5374\,X + 136.43 \quad (3)$$

where

Y = concentration of atrazine in surface runoff in µg/L
X = days after application

The regression analysis was based on the atrazine concentrations detected in the surface runoff events that were monitored during the growing season in the year 1994. The average measured concentrations in the surface runoff and the second order polynomial used to estimate the surface runoff concentration are shown in the figure 5.

Model Inputs for the Clay Soil with Macropores

VS2DT required seven soil properties to be input for each soil layer; anisotropic ratio for saturated hydraulic conductivity (vertical/horizontal), the saturated horizontal hydraulic conductivity (K_{sat}) in units of L/T, the specific storage (S_s) in units of 1/L, the porosity (ϕ), the bubbling pressure (h_b) in units of L, the residual volumetric water content (θ), and the pore size distribution index (λ). In the absence of experimental data, literature values were used for model simulations (Lappala 1987).

The surface clay soil profile was divided into three soil types. The macropores were assumed to be porous media channels with high saturated hydraulic conductivity and low porosity. The soil properties used for the simulation of the clay soil are presented in table 1. The saturated hydraulic conductivity values and the Brooks and Corey parameters (Brooks and Corey, 1964) for the clay soil and silty clay layers were determined from laboratory and field tests. The hydraulic conductivity of the macropore flow channels was calibrated by comparing model simulations to field observations of atrazine transport and groundwater levels. The macropore specific storage values and the Brooks and Corey parameters were from the literature for a coarse sand (Lappala, 1987).

Seven soil and chemical variables were required for chemical transport simulation in each soil layer. The chemical transport parameters included: longitudinal dispersivity (α_L), transverse dispersivity (α_T), molecular diffusion (D_m), decay constant, bulk density (ρ_b), Freundlich adsorption constant (K_d), and the Freundlich exponent (n). The soil and chemical properties used in the transport simulation are shown in table 2. The decay constant (0.011) used in the clay layer simulation was based on a clay soil half life of 63 days (Acock and Herner, 1995).

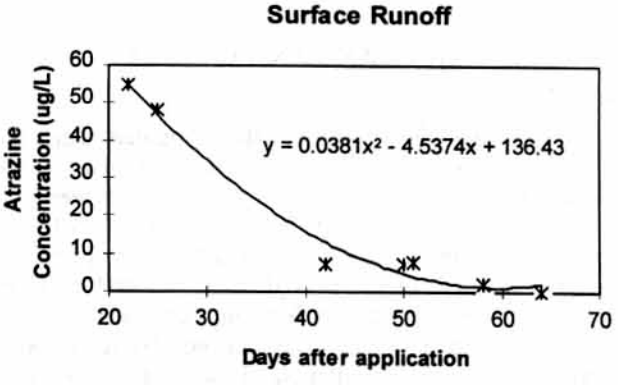

Figure 5–Surface runoff concentrations for atrazine in 1994 and a best-fit polynomial used to estimate atrazine losses in surface runoff. The concentrations below detection limit were not included.

Table 1. The soil properties used in the flow simulations for the clay soil and the aquifer flow domains

Soil Depth (m)	Medium	Ksat* (H/V Ratio)	Ksat† (m/d)	S_s‡	φ§	h_b‖ (m)	θ#	λ**
0-1.2	Clay	1	0.011	1.0E-06	0.45	–0.60	0.25	1.3
1.2 - 6.7	Silty clay	1	0.10	1.0E-06	0.40	–0.40	0.15	0.51
——	Macropore	1	100	1.0E-06	0.25	–0.18	0.08	2.5
6.7 – 17.9	Sand	1	40††	1.0E-06	0.30	–0.15	0.01	1.58
17.9 – 19.4	Gravel	1	140‡‡	1.0E-06	0.30	–0.10	0.01	2.3

* Assumed anisotropy ratio for saturated hydraulic conductivity.
† Saturated hydraulic conductivity obtained from laboratory analysis of soil samples, pump test, and from model calibrations.
‡ Assumed specific storage values.
§ Porosity values obtained from Brooks and Corey (1964).
‖ Bubbling pressure head obtained from laboratory studies for clay layer and literature values for other soil mediums (Brooks and Corey, 1964).
\# Residual water content obtained from laboratory studies for clay layer and literature values for other mediums (Brooks and Corey, 1964).
** Pore size distribution index obtained from laboratory studies for clay layer and literature values for other soil mediums (Brooks and Corey, 1964).
†† A reduced saturated hydraulic conductivity value of 4 m/d was used within 40 m of the river. This value was calibrated from model simulations.
‡‡ A reduced saturated hydraulic conductivity value of 14 m/d was used within 40 m of the river. This value was calibrated from model simulations.

Table 2. Soil and chemical properties used for atrazine transport simulations in the clay soil and aquifer flow domains

Soil Depth (m)	Medium	α_L* (m)	α_T* (m)	D_m† (m^2/d)	De-cay‡ Con-stant (d^{-1})	ρ_b§ (kg/ L)	K_d‖ (L/kg)	n#
0-1.2	Clay	0.1	0.1	1.0E-6	0.011	1.30	2.4	1.0
1.2-6.7	Silty Clay	0.1	0.1	1.0E-6	0.011	1.40	2.4	1.0
——	Macropore	0.2	0.2	1.0E-6	0.011	1.35	2.4	1.0
6.7-17.9	Sand	3.0	3.0	1.0E-6	0.021	1.50	0.0	-
17.9-19.4	Gravel	3.0	3.0	1.0E-6	0.021	1.60	0.0	-

* Longitudinal and transverse dispersivity values obtained from Gelhar et al. (1985).
† Assumed molecular diffusion values.
‡ Decay constant from Acock and Herner (1995).
§ Bulk density based on the laboratory tests for clay layer and particle size analysis and obtained from literature for other soil mediums (Rawls and Brakensiek, 1983).
‖ Freundlich adsorption constant from Acock and Herner (1995).
\# Assumed Freundlich exponent.

Modeling the Sand and Gravel Aquifer

The flow domain for the variably saturated, sand and gravel aquifer is shown in figure 3 (B, C, D, and E). The sand layer was approximately 11.5 m thick and overlies a 1.2 m gravel layer. The R-WT well and the C-WT well (fig. 2) formed the right and left boundaries, respectively. The overall length of the flow domain was 403 m. Even though clay lenses with low hydraulic conductivity were expected to be present in the aquifer, no clay lenses were identified during the installation of the monitoring wells. Therefore, average saturated hydraulic conductivity values were used in the sand and gravel layers.

The finite difference grid used to simulate the aquifer consisted of 142 nodes in the horizontal direction (403 m) and 57 nodes in the vertical direction (12.7 m) for a total of 8094 nodes. Variable spacing was used in both the horizontal and vertical directions. The horizontal nodes were spaced 3 m apart except near the boundaries BC and DE. The nodal spacing was gradually reduced to 0.5 m at these boundaries. The vertical node spacing gradually increased from 0.05 m near the BE boundary to 0.4 m in the sand aquifer. The spacing was then gradually reduced to 0.05 m at the sand-gravel interface. In the gravel layer, the vertical spacing was gradually increased from 0.05 m at the sand-gravel interface to 0.2 m and then gradually reduced to 0.05 m at the CD boundary.

Pump Test Simulation

A pumping test that was conducted at the site between days 92-104, in 1995, was simulated by the model. The pumping test was conducted in the pump well (fig. 1) at an average flow rate of 972 m^3/d. The analysis of the drawdown data in the site monitoring wells resulted in a range of hydraulic conductivities varying from 50 to 150 m/d (Wrobleski, 1996).

To simulate the pumping test, six nodes located along the well screen of the pump well were assigned flux boundary conditions for discharge out of the flow domain. The pumping rate of 972 m^3/d was converted to a specified flux boundary condition for the two-dimensional simulation as follows. The radius of the cone of depression during the pumping test was determined to be 200 m from field observations (Wrobleski, 1996). The pump discharge rate of 972 m^3/day was evenly distributed around the circumference of the cone of depression. This resulted in 0.774 m^3/m/day from one direction or 1.55 m^3/m/day from both sides of the well screen. This two dimensional pumping flux was equally distributed to the six nodes at pumping well screen for a specified boundary condition flux of 0.258 m^3/day at each node.

Boundary Conditions

The boundary conditions used to simulate groundwater flow in the sand and gravel aquifer changed daily based on field observations. The groundwater flow boundary conditions for the cross section shown in figure 3 are:

BE = specified flux boundary
BC = specified pressure head boundary
CD = no flow boundary
DE = specified pressure head boundary

The specified flux boundary condition at BE was based on the simulated water flux out of the clay soil domain. The 3 m nodal spacing along BE in the aquifer corresponded to the 3 m spacing of the macropore channel outlet from the clay soil domain. The specified pressure head boundary at DE was based on daily water levels in the R-WT well at the river. The no flow boundary condition at CD was due to the impermeable shale formation. The pressure head boundary at BC was based on daily water level in the C-WT well.

The only chemical boundary condition for the aquifer flow domain was a specified flux at the boundary BE. The simulated chemical flux out of the clay soil domain was input as a specified flux into the aquifer above runoff plots one and two (fig. 1) at the boundary BE. The water leaving the domain at the boundary DE was assumed to have the

same concentration as the boundary nodes. The water entering the domain through the BC and DE boundaries was assumed to be solute free.

Model Inputs for the Sand and Gravel Aquifer

The saturated hydraulic conductivity values for the aquifer domain were calibrated using model simulations. The hydraulic conductivities for the sand and gravel were adjusted over the range of pump test values (50-150 m/d) until model simulations closely matched field water table observations. The calibrated saturated hydraulic conductivities used in the model simulations were 40 m/d for the sand and 140 m/d for the gravel as shown in table 1.

The saturated hydraulic conductivities in the aquifer domain were reduced near the river to produce the high head losses that typically occur at groundwater-surface water interfaces (Ellins et al., 1990; Jakeman et al., 1990). The hydraulic conductivities were reduced to 4 m/d for the sand and 14 m/d for the gravel and were extended 40 m from the river based on the calibration of model simulations to observed water levels. This reduction of permeability is generally attributed to an accumulation of silts and clays in the sand and gravel aquifer from surface water infiltration.

The soil, aquifer, and chemical properties used in the chemical transport simulation are shown in table 2. Atrazine half life values in aquifers with aerobic conditions are typically lower then the half life values in anaerobic clay soils (Acock and Herner, 1995). Therefore, in chemical transport simulations, a half life of 33 days (decay constant = 0.021) was used in the sand and gravel aquifer and a half life of 63 days (decay constant = 0.011) was used in the clay soil (Hartley and Kidd, 1987).

Summary and Conclusions

Field observations of preferential flow in clay soils is documented in the literature. However, macropore flow is not effectively simulated using conventional modeling procedures. A conceptual simulation method was presented that considers groundwater infiltration and chemical movement through macropores. A clay soil and sand-gravel aquifer continuum was decoupled into two flow domains. The flow in the clay soil domain was dominated by the macropore flow. Conceptualized macropore channels were located in the soil medium based on field research by Lin (1995) and Heuvelman et al. (1993). These macropore channels were characterized as porous media with high hydraulic conductivity and low porosity.

The simulation method used to model macropore transport of water and chemicals through the soil to the aquifer considered both matrix flow and preferential flow. Flow through the clay domain, including the macropores, and flow in the aquifer domain was governed by the Richards equation. Chemical transport was governed by the advection-dispersion equation. A companion article documents groundwater flow and chemical transport simulation results.

References

Acock, B. and A. Herner. 1995. Agricultural research services pesticides properties database. In *Clean Water-Clean Environment-21st Century,* Conf. Proc., Vol. 1: Pesticides. St. Joseph, Mich.: ASAE.

Alden, A. S. and C. L. Munster. 1995. Field test of a 3-D groundwater flow sensor. In *Groundwater Management Proc. International Symp.,* 181-186, ed. R. J. Charbeneau, sponsored by the Water Resour. Engr. Div., ASCE, New York. New York, N.Y.: ASCE.

Beven, K. J. 1989. Interflow. In *Unsaturated Flow in Hydrologic Modeling*, 191-219, ed. H. J. Morel Seytoux. Dortretcht, The Netherlands: Kluwer Acad. Pub.

Brooks, R. H. and A. T. Corey. 1964. Hydraulic properties of porous media. *Hydrology Papers*. Fort Collins, Color.: Water Resources Center, Colorado State Univ.

Chakka, K. B. and C. L. Munster. 1997. Atrazine and nitrate transport to Brazos River floodplain. *Transactions of the ASAE* 40(3):615-621.

Chen, C. and R. J. Wagenet. 1992. Simulation of water and chemicals in macropore soils. Part 2. Application of linear filter theory, *J. Hydrol.* 130(1):127-149.

Ellins, K. K., A. Roman-Mas and R. Lee. 1990. Using ^{222}Rn to examine groundwater-subsurface discharge interaction in the Rio Grande de Manati. *J. Hydrol.* 115(1):319-341.

Gee, G. W., T. Kincaid, R. J. Lenhard and C. S. Simons. 1991. Recent studies of flow and transport in the vadose zone. *Rev. Geophysics* 29(Suppl. Pt. 1):227-239.

Gelhar, L. W., A. Mantoglou, C. Welty and K. R. Rehfeldt. 1985. A review of field scale physical solute transport processes in saturated and unsaturated porous media, Report: EPRI EA-4190. Palo Alto, Calif.: Electric Power Research Institute.

Gerke, H. H. and M. T. van Genuchten. 1993. A dual-porosity model for simulating the preferential movement of water and solutes in structured porous media. *Water Resour. Res.* 29(2):305-319.

Gish, T. J., A. R. Isensee, R. G. Nash and C. S. Helling. 1991. Impact of pesticides on shallow groundwater quality. *Transactions of the ASAE* 34(4):1745-1753.

Gwo, J. P., P. M. Jardine, G. V. Wilson and G. T. Yeh. 1995. A multiple pore region concept to modeling transfer in subsurface media. *J. Hydrol.* 164(1):217-237.

Hassett, J. J. and W. L. Banwart. 1989. The sorption of nonpolar organics by soils and sediments. In *Reactions and Movement of Organic Chemicals in Soils*, 31-44. SSSA No. 22. Madison, Wis.: Soil Sci. Soc. America and Am. Soc. Agronomy.

Healy, R. H. 1990. Simulation of solute transport in variably saturated porous media with supplemental information on modifications to the U.S. Geological Survey's computer program VS2D. Rep. 90-4025. Denver, Colo.: Water-Resources Investigations.

Heuvelman, W. J., K. J. McInnes, L. P. Wilding and C. T. Hallmark. 1993. Water and solute flow in a highly-structured soil. Technical Rep. 161. College Station, Tex.: Texas Water Resources Institute.

Hill, D. E. and J. Y. Parlange. 1972. Wetting front instability in layered soils. *SSSA J.* 36(5):697-702.

Hutson, J. L. and R. J. Wagenet. 1995. A multiregion model describing water flow and solute transport in heterogeneous soils. *SSSA J.* 59(3):743-751.

Jakeman, A. J., D. R. Dietrich and G. A. Thomas. 1989. Solute transport in a stream aquifer system: Application of model identification to the river Murray. *Water Resour. Res.* 25(10):2177-2185.

Jensen, M. E., R. D. Burman and R. G. Allen. 1990. *Evapotranspiration and Irrigation Water Requirements*. New York, N.Y.: ASCE.

Jury, W. A. and H. Fluhler. 1992. Transport of chemical through soil: Mechanisms, models and field applications. *Adv. Agron.* 47:141-201.

Kladivoko, E. J., E. E. VanScoyoc, E. J. Monke, K. M. Oates and W. Pask. 1991. Pesticide and nutrient movement into subsurface tile drains on a silt loam soil in Indiana. *J. Environ. Qual.* 20(1):264-270.

Kung, K. J. S. 1990a. Preferential flow in a sandy vadose soil: 1. Field observations. *Geoderma* 46(1):51-58.

Kung, K. J. S. 1990b. Preferential flow in a sandy vadose soil: 2. Mechanism and implications. *Geoderma* 46(1):59-71.

Lappala, R. W., R. W. Healy and E. P. Weeks. 1987. Documentation of computer program VS2D to solve the equations of fluid flow in variably saturated porous media. Rep. 83-4099. Denver, Colo.: Water-Resources Investigations.

Lawes, J. B., J. H. Gilbert and R. Warington. 1982. *On the Amount and Composition of the Rain and Drainage Water Collected at Rothamstead.* London, England: William Clowes & Sons Ltd.

Lin, H. 1995. *Hydraulic Properties and Macropore Flow of Water in Relation to Soil Morphology.* Unpubl. Ph.D. diss. College Station, Tex.: Texas A&M University.

Molz, F. J. 1981. Models of water transport in the soil-plant system — A review. *Water Resour. Res.* 17(5):1245-1260.

Munster, C. L., C. C. Mathewson and C. L. Wrobleski. 1996. The Texas A&M University Brazos River hydrologic field site, *Environ. and Eng. Geosci.* II(4) Winter:517-530.

Munster, C. L., B. M. Schneider and J. R. Vogel. 1995. Chemical and sediment transport in surface runoff (Part 1: field study). ASAE Paper No. 95-2697. St. Joseph, Mich.: ASAE.

Munster, C. L., R. W. Skaggs, J. E. Parsons, R. O. Evans, J. W. Gilliam, M. A. Breve. 1994. Simulating aldicarb transport in a drained field. *Transactions of the ASAE* 37(6):1817-1824.

Rawls W. J. and D. L. Brakensiek. 1983. A procedure to predict infiltration parameters. In Conf. Proc. *Advances in Infiltration,* 102-112. St. Joseph, Mich.: ASAE.

Ray, C., C. W. Boast, T. R Ellsworth and A. J. Valocchi. 1996. Simulation of the impact of agricultural management practices on chemical transport in macropore soils. *Transactions of the ASAE* 39(5):1697-1707.

Smith, M. C., D. L. Thomas, A. B. Bottcher and K. L. Campbell. 1990. Measurement of pesticide transport to shallow groundwater. *Transactions of the ASAE.* 33(5):1573-1582.

Steenhuis, T. S., J. Y. Parlange, C. J. Ritsema and L. W. Dekker. 1994. Overview of solute modeling in fingered and macropore pore for homogeneous and structured soils. ASAE Paper No. 94-2530. St. Joseph, Mich.: ASAE.

Steenhuis, T. S., J. Y. Parlange and M. S. Andreini. 1990. A numerical model for preferential solute movement in structured soils. *Geoderma* 46(1):193-208.

U.S. Environmental Protection Agency. 1992. The national survey of pesticides in drinking water wells: Phase II report, Another look. EPA 570/09-91-020. Washington, D.C.

————. 1988. Pesticides in groundwater data base: 1988 interim report. Washington, D.C.: Office of Pesticide Programs.

van Genuchten, M. T. 1980. A closed form equation for predicting the hydraulic conductivity of unsaturated soils. *SSSA J.* 44(5):892-898.

Wrobleski, C. L. 1996. An aquifer characterization at the Texas A&M Univ. Brazos River hydrologic field site, Burleson Co., Texas. Unpubl. M.S. thesis. College Station, Tex.: Department of Geology, Texas A&M University.

Field Test of the In Situ Permeable Ground Water Flow Sensor

by Andrew S. Alden and Clyde L. Munster

Abstract

Two in situ permeable flow sensors, recently developed at Sandia National Laboratories, were field tested at the Brazos River Hydrologic Field Site near College Station, Texas. The flow sensors use a thermal perturbation technique to quantify the magnitude and direction of ground water flow in three dimensions. Two aquifer pumping tests lasting eight and 13 days were used to field test the flow sensors. Components of ground water flow as determined from piezometer gradient measurements were compared with ground water flow components derived from the 3-D flow sensors. The changes in velocity magnitude and direction of ground water flow induced by the pump were evaluated using flow sensor data and piezometric analyses. Flow sensor performance closely matched piezometric analysis results. Ground water flow direction (azimuth), as measured by the flow sensors and derived in the piezometric analysis, predicted the position of the pumping well accurately. Ground water flow velocities measured by the flow sensors compared well to velocities derived in the piezometric analysis. A significant delay in flow sensor response to relatively rapid changes in ground water flow was observed. Preliminary tests indicate that the in situ permeable flow sensor provides accurate and timely information on the velocity magnitude and direction of ground water flow.

Pages 81-88

Introduction

Various in situ and well casing ground water flow sensors have been developed to monitor ground water flow. Portable in situ ground water flow meters were successfully used to evaluate shallow ground water flow around lakes during septic leachate surveys in Michigan and Minnesota (Kerfoot 1979; Kerfoot and Skinner 1981). Heat pulse probes for fully penetrating slotted wells designed for ground water flow measurement in two and three dimensions were developed by Kerfoot (1982). Ground water flow measurements using a two-dimensional heat pulse probe in monitoring wells at landfill sites were validated by subsequent investigations and long-term monitoring (Guthrie 1986). However, Melville et al. (1985) tested a two-dimensional heat pulse ground water flow meter under controlled laboratory conditions and found that small channelization between the slotted well casing and the probe could invalidate the flow meter response. Kerfoot (1988) provided recommendations for monitoring well construction and a new calibration procedure to increase the accuracy of heat pulse ground water flow meters.

The In Situ Permeable Flow Sensor

The flow sensor is 0.76 m long, 50 mm in diameter, and is permanently installed in saturated, porous, unconsolidated media at the point where ground water flow is to be determined. The flow sensor contains a resistance heater that

continuously heats the aquifer and an array of 30 thermistors located along the probe to measure temperature variations induced by ground water flow. Once the probe has been installed and calibrated, the velocity magnitude and direction of ground water flow, in three dimensions, is measured using a thermal perturbation technique. Analysis of raw temperature data using the proprietary software FLOW© allows near real-time measurement of a Darcy velocity vector. Ground water flow components are measured in a volume of approximately one cubic meter surrounding the probe. Measurement of ground water flow rates from 1×10^{-3} to 1 m/day are possible. Accuracy of direction measurement is estimated at $\pm 10°$ (Ballard 1996; Ballard et al. 1994; Ballard et al. 1996).

Previous Work

In 1994, a pump test was used to evaluate the effectiveness of the flow sensor at the Savannah River Site. Flow sensors were able to measure ground water flow velocities as low as 8.64×10^{-3} m/day with direction (azimuth) uncertainty values of $\pm 7°$ to $\pm 30°$. Values of measurement uncertainty were highly dependent upon pumping rate (Ballard 1994; Ballard et al. 1996).

In 1995, a flow sensor was used to assess the hydraulic characteristics at an underground oil storage facility in Weeks Island, Louisiana. The development of a sinkhole in the sandy sediments above a salt dome was an indication of possible intrusion of saltwater into the oil storage facility. A flow sensor was installed in a sand-filled fissure in the top of the dome at a depth of 76 m. Information gathered during a 17-day period indicated that probable contamination of the repository was occurring as water flowed downward through the crevice into the salt dome (Ballard and Gibson 1995).

In tests conducted at the Brazos River Site, long-term flow sensor and piezometric data were used to derive local saturated hydraulic conductivities. Comparison of the calculated hydraulic conductivities to those found in pump and slug tests at the site was used as a basis for evaluation of the velocity meter. Saturated hydraulic conductivities of 28.9 and 16.5 m/day were derived at depths of 13.7 and 18.3 m, respectively (Alden and Munster 1997).

Flow Sensor Tests

Test Overview

Flow sensor information and piezometric data from monitoring wells were collected during two aquifer pump tests at the Brazos River Research Site. The influence of pumping on ground water flow was determined using flow sensor output and piezometric data. The direction and magnitude of ground water flow obtained from the two independent flow sensors was compared to ground water flow components derived from a gradient analysis of piezometric data during the pump tests.

Test Site Description

The pump tests were performed at the Brazos River Hydrologic Field Site (Brazos River Site), which is located approximately 12 km west of College Station, Texas. The four-hectare site lies approximately 200 meters from the Brazos River, as shown in Figure 1. The alluvial aquifer at the site changes gradually from a fine sand at a depth of 8 meters to a coarse sand and gravel mixture at a depth of 21 meters. The aquifer is overlain by a surface layer of ships clay (very fine, mixed, thermic chromic hapluderts) that extends to a depth of 8 meters and is underlain by an impervious Yegua shale formation at 21 meters (Wrobleski 1996). Water levels in the aquifer typically fluctuate between 9 and 10 meters below the surface. Two pump tests were conducted using the site pumping well (Munster et al. 1996). The saturated hydraulic conductivity was determined at 20 site monitoring wells. In addition, slug tests were performed on 14 monitoring wells at the research site (Alden 1996). The pump and slug tests yielded a range of saturated hydraulic conductivity values from 3.4 to 83 m/day. Testing at the site suggests that saturated hydraulic conductivity values do not necessarily increase with depth. This may be attributed to the existence of clay lenses and other discontinuities often found in fluvial aquifers. Direct interaction between river stage and aquifer level has been observed (Alden and Munster 1997).

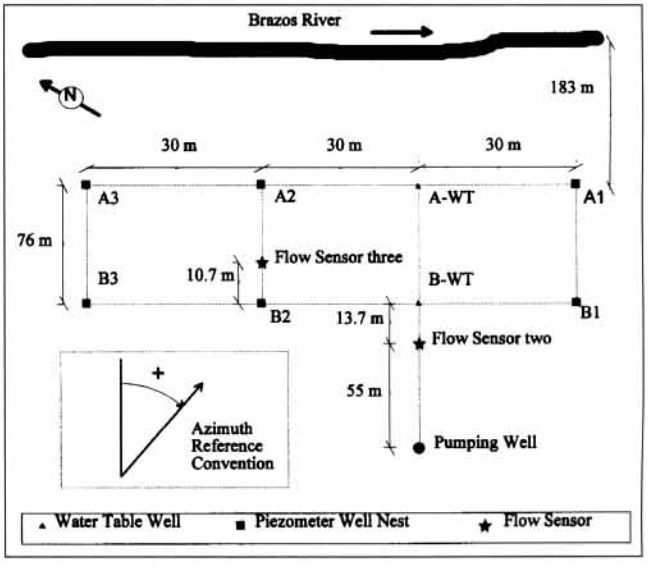

Figure 1. Plan view of the research site with the location of the piezometer well nests, water table wells, pumping well, and flow sensors (not to scale). A diagram of the ground water flow direction convention is also shown.

Instrumentation at the site includes 36 partially screened piezometric wells, four fully screened "water table" wells, two 3-D ground water flow sensors, and an 0.20-m-diameter pumping well, as shown in Figure 1 (Munster et al. 1996). The piezometric monitoring wells are arranged in a rectangular grid of well nests that is oriented parallel and perpendicular to the river (Figure 1). Each well nest contains four monitoring wells with short 150-mm-long polyvinyl chloride (PVC) wire-

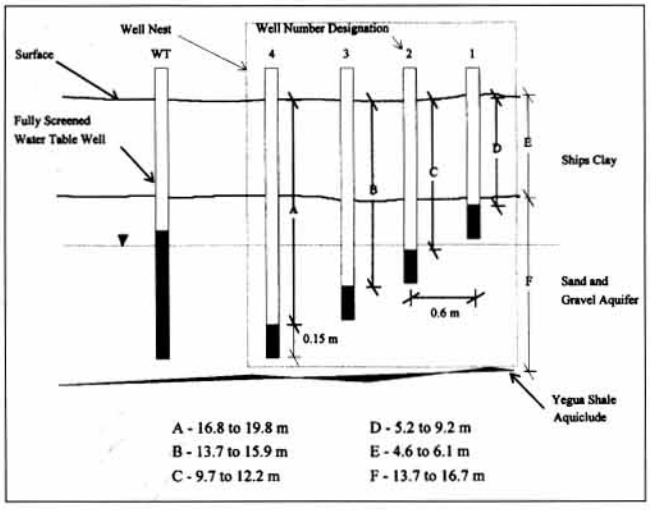

Figure 2. Elevation view of a typical well nest and water table well with soil stratigraphy and range of piezometer well screen depths shown (not to scale).

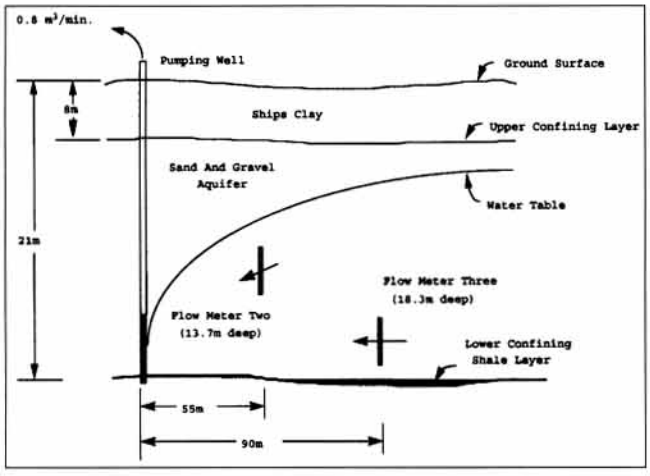

Figure 3. Elevation view of the pumping well and 3-D flow sensors at the Brazos River Site with soil stratigraphy also shown (not to scale).

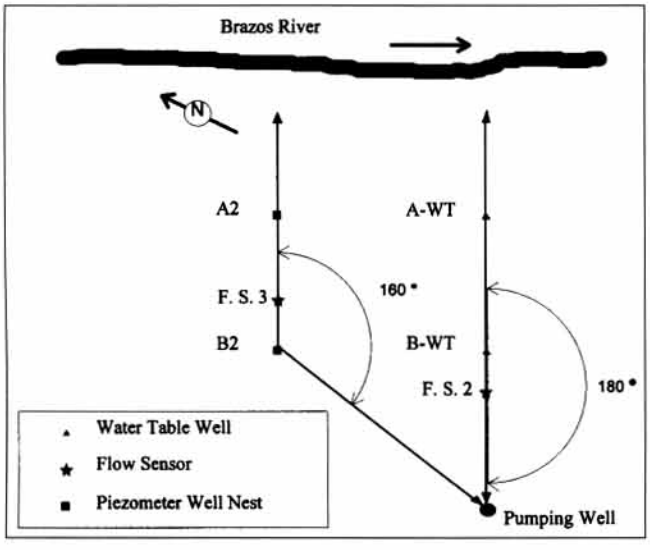

Figure 4. Diagram showing the geometric relationship between flow sensors two and three and the pumping well (not to scale). The true azimuth for the pumping well with respect to flow sensor three is 160° and to flow sensor two is 180° as shown.

wound (0.152-mm openings) well screens, which act as piezometers (Figure 2), that are numbered from one to four. The number one well is the shallowest and the number four well is the deepest. A typical well nest has screens located at 9, 12, 15, and 18 meters below the surface. The four "water table" wells are screened throughout the thickness of the aquifer with 0.254-mm slotted openings. Three water table wells lie within the main wellfield grid and one has been installed at the river to monitor river stage. All monitoring wells are 50.8-mm-diameter flush-threaded polyvinyl chloride (PVC). Water levels within all of the wells were continuously monitored and recorded in a system of four independent data collection systems (Munster et al. 1996).

Flow sensors were installed at the B-WT well and well nest B-2 at depths of 13.7 and 18.3 meters, respectively, as shown in Figures 1 and 3. Placement of the flow sensors was influenced by factors such as instrumentation access, distance from the pumping well, and proximity to the piezometers used in the gradient analysis. The geometric relationship between flow sensors two and three and the pumping well is shown in Figures 3 and 4.

Test Description

Two pump tests were used to evaluate flow sensor performance. The first pump test was conducted for eight days from Day 35 to Day 43, 1995. The second pump test was conducted for 13 days from Day 92 to Day 105, 1995. Flow sensor heaters and data acquisition equipment were activated three days prior to pumping to allow for temperature stabilization of the probe and surrounding aquifer. Water levels in the piezometer well system were measured manually prior to pumping to initialize the well data collection system. During the pump tests, a constant flow rate of approximately 0.8 m^3/min. was monitored by an in-line flow meter. All water from the pump test was transported off site to a nearby irrigation ditch using irrigation pipe. Immediately prior to the end of the pump test, all piezometric data was downloaded and well water levels were measured manually to reinitialize the well data collection system for aquifer recovery. Flow sensor and piezometric data collection intervals ranged from one minute at the start of the test to 360 minutes at the end of the test.

Methods of Analysis

Piezometric Data

Water level data from the monitoring wells was used to determine horizontal and vertical gradients at various levels within the aquifer. The piezometers analyzed were chosen based on horizontal and vertical proximity to the applicable velocity meter. The gradients between wells were used to calculate the direction and magnitude of ground water flow using Darcy's equation (Equation 1) and trigonometric analysis.

$$V = K_{sat} \times \frac{dH}{dL} \quad (1)$$

Where:

V = Darcy velocity (m/day)
K_{sat} = saturated hydraulic conductivity (m/day)
H = total head (m)
L = length (m)

In previous testing at the research site, saturated hydraulic conductivity values for each flow sensor installation location were determined through pump and slug tests. At flow sensor two, K_{sat} values ranged from 25.7 m/day (slug test) to 60.6 m/day (pump test). At flow sensor three, K_{sat} values ranged from 3.4 m/day (slug test) to 58.2 m/day (pump test) (Alden and Munster 1997). These K_{sat} values were used in the piezometric analysis to determine a range of ground water velocities for comparison to flow sensor results.

Piezometric Data at Flow Sensor Two

Piezometric wells in well nests A1, A2, B1, and B3 were used to calculate ground water gradient components at flow sensor two as shown in Figure 5. Piezometers A1-3 and A2-3 were used to find a gradient parallel to the river. The values for wells B1-3 and B2-3 were averaged to approximate water levels at flow sensor two. Values for A1-3 and A2-3 were also averaged and used in conjunction with the B1-3 / B2-3 average to derive a gradient perpendicular to the river (Equation 2):

$$G_{perp} = \left(\frac{B1\_3 + B\_32}{2} - \frac{A1\_3 + A2\_3}{2}\right) \div l \quad (2)$$

Where:

G_{perp} = Hydraulic gradient perpendicular to the river at flow sensor three (m/m)
B1-3, B2-3, A1-3, A2-3 = Water levels in respective wells(m)
l = distance between respective averaged points (m)

Piezometric Data at Flow Sensor Three

Piezometric wells in well nests A2, A3, B2, and B3 were used to find ground water gradient components at flow sensor three as shown in Figure 6. Wells B2-4 and A2-4 were used to determine a gradient perpendicular to the river. Wells A3-4 and A2-4 were used to find a gradient parallel to the river.

Flow Sensor Data

Raw temperature data from the flow sensor probe was used in FLOW to calculate the magnitude and direction of ground water flow for each velocity meter. Output from FLOW was transformed to yield the influence of pumping on the direction and magnitude of ground water flow. Options within FLOW allow for various data manipulations such as vector addition and

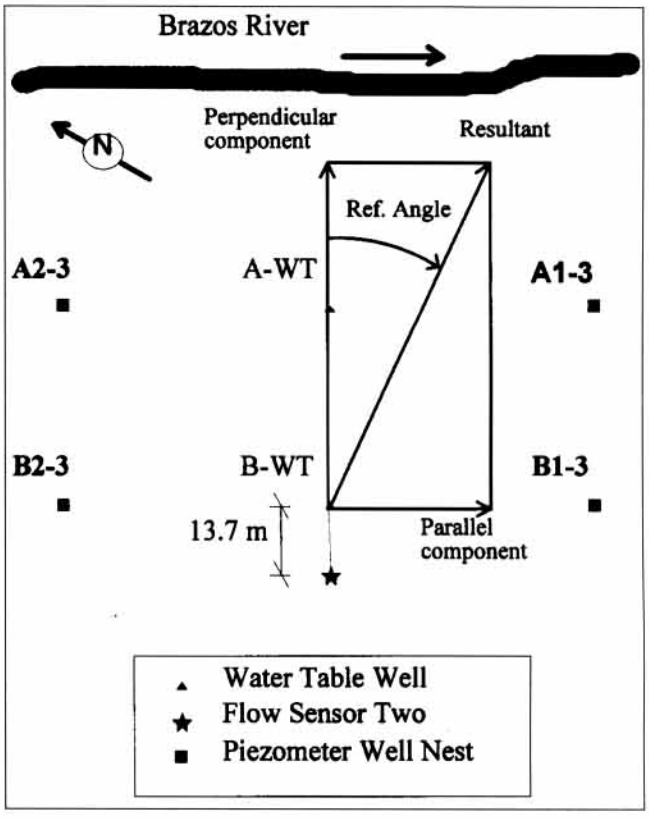

Figure 5. Plan view of the monitoring wells near flow sensor two (not to scale). Piezometric data from the bold-labeled wells was used to calculate ground water flow for comparison to flow sensor two output. The vector orientation convention is also shown.

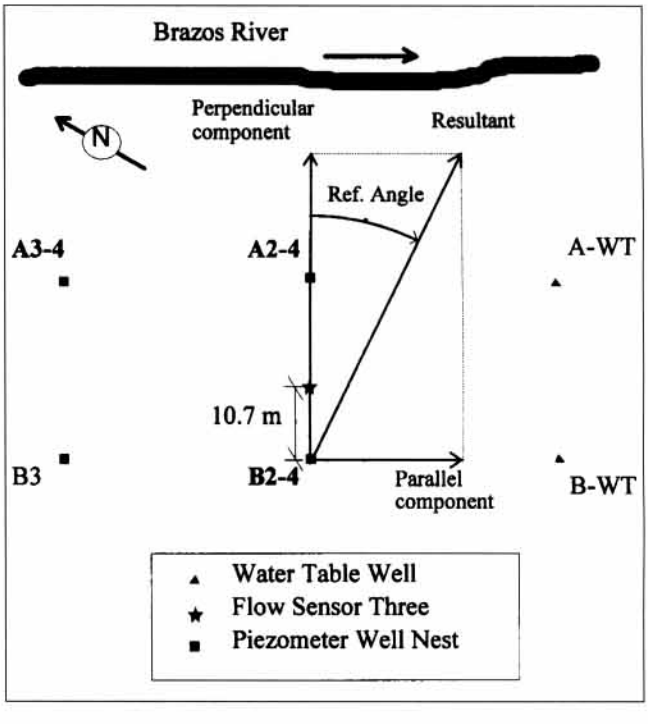

Figure 6. Plan view of the monitoring wells near flow sensor three (not to scale). Piezometric data from the bold-labeled wells was used to calculate ground water flow for comparison to flow sensor three output. The vector orientation convention is also shown.

data averaging (Ballard et al. 1994; Ballard 1996). Average ground water flow, as measured by the flow sensors immediately prior to pumping, was used as the background vector in the analysis of flow sensor data during the pump test.

Net Flow as a Basis of Comparison

A background ground water flow vector was derived at each flow sensor location using flow vectors found immediately prior to pumping. Manual well soundings were used as a basis for calculation of background ground water flows for use with the piezometric data. Respective background (prepumping) flow vectors were then subtracted from gross flow (during pumping) vectors to yield flow components due to pumping (net flow) as shown in Figure 7. The effects of river stage fluctuation are not considered in this analysis.

Net horizontal ground water velocities and azimuths are used as a basis of comparison between flow sensor and piezometric results. Net horizontal velocities from flow sensor results and piezometric analysis are compared to each other. Net azimuths from flow sensor results and piezometric analysis are compared to the known values of 180° for flow sensor two and 160° for flow sensor three as shown in Figure 4.

Results

The ground water flow components calculated from the flow sensor data and the gradient analysis of the piezometer wells are shown in Figures 8 through 11. Instability in the azimuth values at the beginning of each test are due to the extremely low initial net velocities. As pumping continues, the horizontal direction (azimuth) converges quickly to a final value. However, the measured velocities converge to final values much more slowly as the aquifer is drawn down. Net vertical velocity values as measured by the flow sensors are shown in Figures 8 through 11 for informational purposes and were not used in evaluation of the flow sensors.

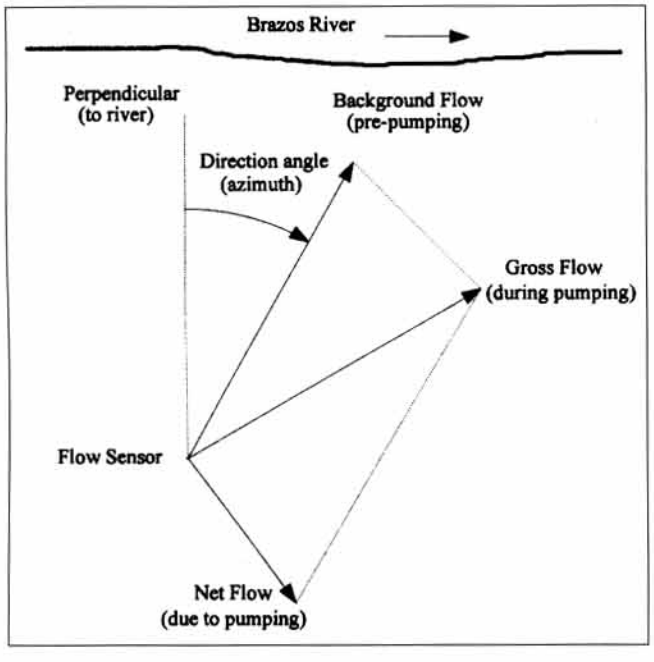

Figure 7. Plan view of the ground water flow vector subtraction convention used for derivation of net flow in the analysis of flow sensor and piezometric data. The direction (azimuth) convention is also shown.

Pump Test One

Pump test one started at 11:40 a.m. of Day 35, 1995, and ended at 3:15 p.m. of Day 43, 1995. A power failure during the period from Day 38 to Day 41 resulted in the loss of data from both flow sensors. All data shown for the flow sensors during this period has been linearly interpolated. Flow sensor response to changes in ground water velocity at the beginning of each pump test is slower than that observed in the piezometric data. This occurred in all pump tests and may be due to the nature of the thermal phenomena that the flow sensor is dependent upon for its operation. Delays in flow sensor response to rapid changes in ground water velocity may result as heat is "flushed" from the 1 m^3 volume around the velocity meter. The time of this delay is directly dependent upon the ground water velocity and may be considered as the "thermal time lag"; thermal time lag is defined here as the time required for ground water temperatures to stabilize in the vicinity of the flow sensor.

Flow Sensor Two

The ground water flow components for flow sensor two during the first pump test are shown in Figure 8. The azimuths of net horizontal flow as calculated by the flow sensor and piezometers converged quickly to 180° and 200°, respectively. The actual azimuth for the pumping well with respect to flow sensor two is 180° (Figure 4). The maximum net horizontal velocities using the saturated hydraulic conductivities from the slug tests (25.7 m/day) and the pump tests (60.6 m/day) were 0.04 and 0.1 m/day, respectively. The maximum net horizontal velocity measured by flow sensor two was 0.03 m/day. Vertical downward velocity increased from approximately zero to 0.01 m/day during initial pumping and then decreased to approximately 0.004 m/day in the latter portion of the test. The piezometric data displays a much faster reaction to aquifer pumping than does the flow sensor. The thermal lag time exhibited by the flow sensor is approximately two days.

Flow Sensor Three

The ground water flow components for flow sensor three during the first pump test are shown in Figure 9. The azimuths for net horizontal flow as calculated by the flow sensor and piezometers converge to 145° and 155°, respectively. The actual azimuth for the pumping well with respect to flow sensor three is 160° (Figure 4). The maximum net horizontal velocities using the saturated hydraulic conductivities from the slug tests (3.4 m/day) and the pump tests (58.2 m/day) were 0.020 and 0.220 m/day, respectively. Vertical downward velocity increased from approximately zero to 0.01 m/day at the

beginning of the pump test and remained at that level for the duration of pumping. The maximum net horizontal velocity measured by flow sensor two was 0.063 m/day. The flow sensor thermal lag is approximately two days.

Pump Test Two

Pump test two started at 4:30 p.m. of Day 92, 1995, and ended at 12:00 p.m. of Day 105, 1995. Again, a difference in velocity measurement response is evident at both flow sensors. Reversal of background ground water flow gradients was observed toward the latter part of the test period. A longer pumping period during pump test two and an increase in river stage resulted in reversal of ground water flow toward the river in the latter portions of the pump test.

Flow Sensor Two

The ground water flow components at flow sensor two during the second pump test are shown in Figure 10. The azimuths for net horizontal flow as calculated by the flow sensor and piezometers converged quickly to approximately 175°. The actual azimuth for the pumping well with respect to flow sensor two is 180° (Figure 4). The maximum net horizontal velocities using the saturated hydraulic conductivities from the slug tests (25.7 m/day) and the pump tests (60.6 m/day) were 0.08 and 0.19 m/day, respectively. The maximum net horizontal velocity measured by flow sensor two was 0.068 m/day. Vertical flow was upward during the first half of the pump test and downward during the second half of the test at maximum velocities of approximately 0.01 m/day. The flow sensor thermal lag time is approximately two days.

Flow Sensor Three

The ground water flow components for flow sensor three during the second pump test are shown in Figure 11. The azimuths for net horizontal flow as calculated by the flow sensor and piezometers converged quickly to approximately 152° and 158°, respectively. The actual azimuth for the pumping well with respect to flow sensor three is 160° (Figure 4). The maximum net horizontal velocities using the saturated hydraulic conductivi-

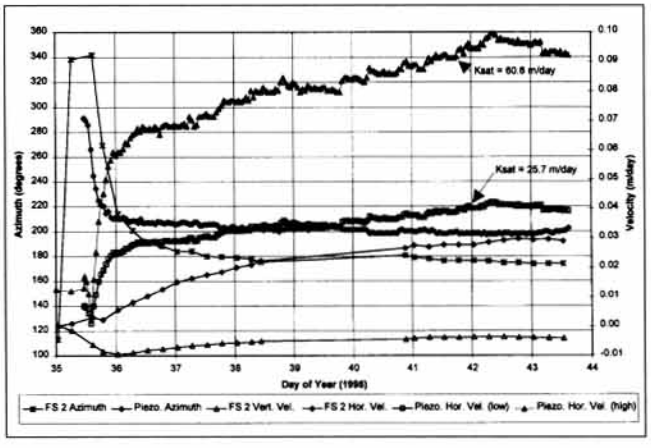

Figure 8. Net velocity magnitude and direction of ground water flow at flow sensor two during pump test one from piezometric and flow sensor data. The horizontal saturated hydraulic conductivity used in the piezometric analysis was 28.9 m/day. Negative vertical velocities indicate downward flow.

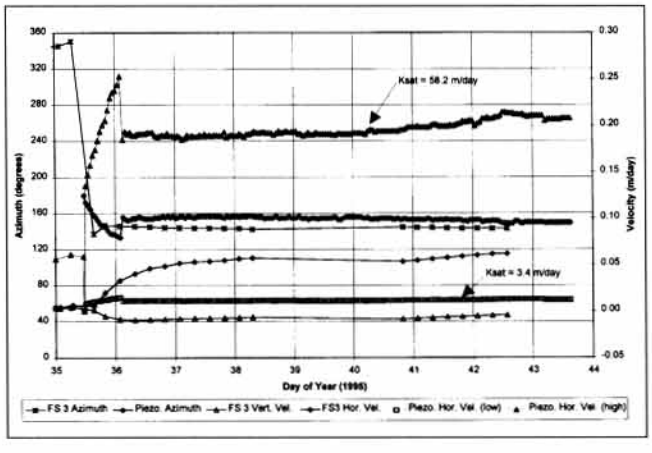

Figure 9. Net velocity magnitude and direction of ground water flow at flow sensor three during pump test one from piezometric and flow sensor data. The horizontal saturated hydraulic conductivity used in the piezometric analysis was 16.5 m/day. Negative vertical velocities indicate downward flow.

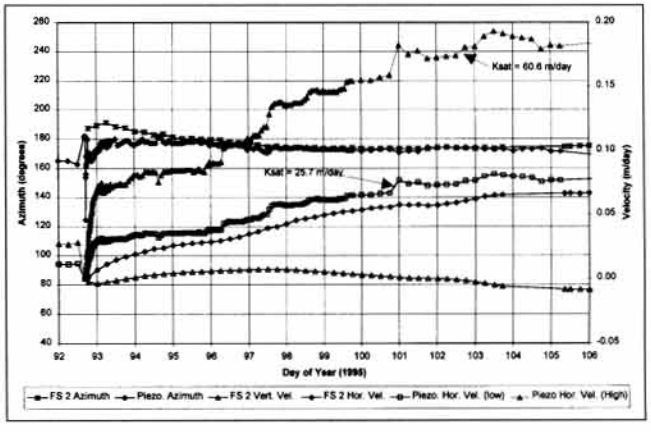

Figure 10. Net velocity magnitude and direction of ground water flow at flow sensor two during pump test two from piezometric and flow sensor data. The horizontal saturated hydraulic conductivity used in piezometric analysis was 28.9 m/day. Negative vertical velocities indicate downward flow.

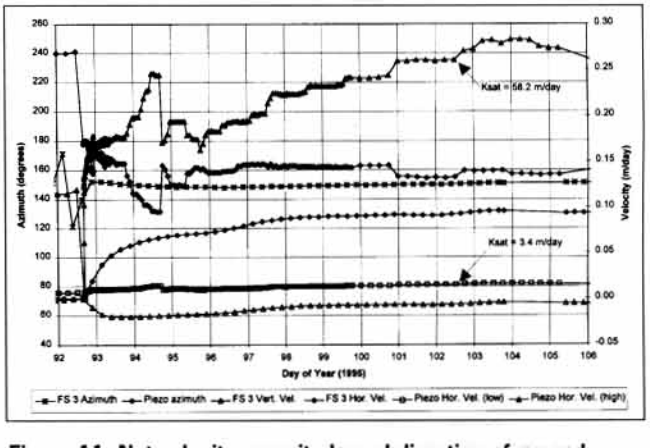

Figure 11. Net velocity magnitude and direction of ground water flow at flow sensor three during pump test two from piezometric and flow sensor data. The horizontal saturated hydraulic conductivity used in piezometric analysis was 16.5 m/day. Negative vertical velocities indicate downward flow.

Table 1
Summary of Net Horizontal Ground Water Flow Components from Piezometric and Flow Sensor Data for Pump Tests 1 and 2

		Pump Test 1			Pump Test 2		
		Azimuth (deg.)		Velocity	Azimuth (deg.)		Velocity
Location	Method	Measured	Actual	(m/day)	Measured	Actual	(m/day)
FS 2	Flow Sensor	180	180	0.030	175	180	0.068
FS 2	Piezometer (K = 25.7 m/d)	200	180	0.040	175	180	0.080
FS 2	Piezometer (K = 60.6 m/d)	200	180	0.100	175	180	0.190
FS-3	Flow Sensor	145	160	0.063	152	160	0.095
FS 3	Piezometer (K = 3.4 m/d)	150	160	0.020	158	160	0.020
FS 3	Piezometer (K = 58.2 m/d)	150	160	0.220	158	160	0.270

Table 2
Summary of Flow Sensor Uncertainty Values from Pump Tests 1 and 2

		Pump Test 1			Pump Test 2		
Flow Sensor	Measurement	Low	High	Average	Low	High	Average
2	Horizontal Velocity (m/day)	0.04	0.04	0.04	0.03	0.05	0.04
2	Azimuth (degree)	5.00	9.50	7.40	6.10	11.00	9.60
3	Horizontal Velocity (m/day)	0.00*	0.03	0.02	0.03	0.04	0.04
3	Azimuth (degree)	0.00*	17.20	4.86	5.41	34.07	7.80

* Values shown as zero due to truncation of nonzero digits.

ties from the slug tests (3.4 m/day) and the pump tests (58.2 m/day) were 0.020 and 0.270 m/day, respectively. The maximum net horizontal velocity measured by flow sensor two was 0.095 m/day. Vertical downward velocity increased from near zero to 0.02 m/day during initial pumping and then decreased to approximately 0.008 m/day in the latter portion of the test.

Summary of Results

A summary of measured net ground water flow values from pump tests one and two is shown in Table 1. The velocity magnitude and direction of ground water flow shown in Table 1 are taken from discrete points in time where maximum measured velocities are observed. Table 2 shows values of uncertainty associated with the flow sensor data. Options within FLOW allow for the output of uncertainty data for each velocity and azimuth measurement. Uncertainty data is based on a Monte Carlo technique using a 95 percent confidence interval. Levels of measurement uncertainty generally decrease as ground water velocity increases (Ballard et al. 1994; Ballard 1996). Minimum, maximum, and average values of the uncertainty data associated with the pump tests are shown in Table 2.

Conclusions

The in situ permeable flow sensor is easy to use and relatively inexpensive. The velocity magnitude and direction of ground water flow are measured directly at a single point (one cubic meter) within the aquifer. Knowledge of hydraulic conductivity and aquifer stratigraphy is not required and results are available immediately and continuously after installation, warm-up, and calibration are completed.

Flow vectors measured using piezometric and flow sensor data correlated well. The azimuths obtained from both methods predicted the approximate position of the pumping well at both flow sensor locations accurately. Ground water velocities measured by the flow sensors compared favorably to a range of velocities calculated in piezometric analyses using saturated hydraulic conductivity values from slug tests and pump tests. The flow sensor's dependence upon thermal phenomena in its operation may limit its application in situations where ground water velocities change rapidly. This is generally not the case in most ground water studies, but could occur where ground water flow is influenced by pumps or streams. Preliminary tests indicate the in situ permeable flow sensor to be a useful tool in determining the direction and magnitude of ground water flow in three dimensions.

References

Alden, A.S. 1996. *Field testing of an in situ permeable flow sensor*. Master's thesis, Dept. of Civil Engineering, Texas A&M University, College Station, Texas.

Alden, A.S., and C.L. Munster. 1997. Assessment of river-floodplain interactions. *Environmental and Engineering Geoscience* 3, no. 4: in press.

Ballard, S. 1996. The in situ permeable flow sensor: A ground water flow velocity meter. *Ground Water* 34, no. 2: 231-240.

Ballard, S., G.T. Barker, and R.L. Nichols. 1996. A test of the in situ permeable flow sensor at Savannah River, South Carolina. *Ground Water* 34, no. 2: 389-396.

Ballard, S., and J. Gibson. 1995. Groundwater flow velocity measurements in a sinkhole at the Weeks Island strategic petroleum reserve facility, Louisiana. In *Proceedings of the Symposium on the Applications Geophysics to Engineering and Environmental Problems*, 931-935, by Environmental and Engineering Geophysical Society. Englewood, Colorado: EEGS.

Ballard, S., G.T. Barker, and R.L. Nichols. 1994. The in situ permeable flow sensor: A device for measuring ground water flow velocity. Sand93-2765. Albuquerque, New Mexico: Sandia National Laboratories.

Ballard, S. 1994. In situ permeable flow sensors at the Savannah River integrated demonstration: Phase II results. SAND94-1958. Albuquerque, New Mexico: Sandia National Laboratories.

Guthrie, M. 1986. Use of a Geo Flowmeter for the determination of ground water flow direction. *Ground Water Monitoring Review* 6, no. 1: 81-86.

Kerfoot, W.B. 1988. Monitoring well construction and recommended procedures for direct groundwater flow measurements using a heat-pulsing flowmeter. In *Ground-water contamination: Field methods, ASTM STP 963*, ed. Nina I. McClelland, 146-161. Philadelphia, Pennsylvania: American Society for Testing and Materials.

Kerfoot, W.B. 1982. Comparison of 2-D and 3-D groundwater flowmeter probes in fully-penetrating monitoring wells. In *Proceedings of the Second National Symposium on Aquifer Restoration and Ground Water Monitoring*, 264-268, by National Water Well Association. Worthington, Ohio: NWWA.

Kerfoot, W.B., and S.M. Skinner. 1981. Septic leachate surveys for lakeside sewer needs evaluation. *Journal Water Pollution Control Federation* 53, no. 12: 1717-1725.

Kerfoot, W.B. 1979. Septic system leachate surveys for rural lake communities: A winter survey of Otter Tail Lake, Minnesota. In *Individual Onsite Wastewater Systems*, 435-470. Ann Arbor, Michigan: Ann Arbor Science.

Melville, J.G., F.J. Moltz, and O. Guven. 1985. Laboratory investigation and analysis of a ground-water flowmeter. *Ground Water* 23, no. 4: 486-495.

Munster, C.L., C.C. Mathewson, and C.L. Wrobleski. 1996. The Texas A&M University Brazos River hydrologic field site. *Environmental and Engineering Geoscience* 2, no. 4: 517-530.

Wrobleski, C.L., 1996. *An aquifer characterization at the Texas A&M University Brazos River Hydrologic Field Site, Burleson Co., Texas*. Master's thesis, Texas A&M University, College Station, Texas.

Biographical Sketches

Andrew S. Alden *is an environmental engineer with K.W. Brown Environmental Services (501 Graham Rd., College Station, TX 77845). He has worked on projects including aquifer characterization using conventional and experimental methods, assessment of ground water contamination from landfills and petroleum exploration and distribution operations, the suitability of wetland plants in a constructed wetland, and regulatory review under RCRA and TSCA. He received a B.S. in mechanical engineering technology and an M.S. in civil engineering (environmental option) from Texas A&M University. He is registered as an engineer in training in Texas, and is a member of the ASCE*

Clyde L. Munster*, P.E., is an assistant professor in the Agricultural Engineering Department at Texas A&M University, College Station, Texas. His primary research interests are field, laboratory, and computer modeling studies of contaminant transport through soil and ground water. Dr. Munster received a B.S.C.E. in 1980 and an M.S.C.E. in 1981 from Virginia Tech, and a Ph.D. in agricultural engineering in 1992 from North Carolina State University.*

Information Transfer Program

Information Transfer

PI: Ric Jensen

Publication of research results summaries in quarterly newsletter, New Waves; examination of one water resource issue in depth in quarterly newsletter, Texas Water Resources. Publication of fact sheets on on-site septic systems. Conducting workshops on source water protection, cross-connection protection; conducting conferences on dissemination of water resources information on the World Wide Web. Publication of technical reports on funded water resources research.

Summarizes information about water resources research projects at Texas universities through newsletters, reports, WWW sites, and listservs. This project provides news relating to university research in water resources. An e-mail list in compiles and distribute timely information about Texas water issues, as well as research opportunities. Through our publications program, we reach more than 20,000 readers.

Work continued to educate the public about the importance of university research in water resources matters. Outreach materials were developed for printed newsletters, technical reports, web site sites, and electronic mailng list. Products discussed such issues as the prospects for implementing brush control to boost water yields; the involvement of university researchers in the water planning process in Texas; the future of rice irrigation in Texas, and efforts of the USGS to study water quality through its NAWQA program. Technical reports for this project covered such issues as monitoring groundwater supplies in the Trinity Aquifer of Central Texas; identifying opportunities for water conservation in the Lower Rio Grande Valley; use of filtration to treat surface waters and reduce dependence on chemicals; insitutional strategies to manage waters in the Rio Grande during droughts; the economic impact of coastal tourism; and site-specific data on how to increase water supplies through brush control in eight regions of Texas. TWRI personnel, including the PI, gave many presentations at meetings, workshops and conferences. TWRI continues to emphasize research results in such issues as rural [onsite] wastewater systems [septic tanks and drainfields] and water conservation and reuse. We are now working with the Texas Rural Water Assn to help them with outreach and communications and training efforts, and recently worked with them to and Mississippi State University to sponsor a workshop on cross connections, which is an issue that affects many small water systems. Publications: Jensen, Ric, Editor, New Waves newsletter, 2001. [Four issues]. Jensen, Ric, Editor, Texas Water Resources newsletter, 2001. [Four issues]. Jensen, Ric, Editor. Texas On-Site Insights newsletter, 2001. [Four issues]. Jensen, Ric.

Information Transfer

Basic Information

Title:	Information Transfer
Project Number:	2001TX3321B
Start Date:	3/1/2001
End Date:	2/28/2002
Funding Source:	104B
Congressional District:	8
Research Category:	Not Applicable
Focus Category:	Law, Institutions, and Policy, Management and Planning, Waste Water
Descriptors:	technology transfer, information dissemination, world wide web, public education
Principal Investigators:	Ric Jensen, Jan Gerston

Publication

1. Bush, Peter, Kevin Dennehy, Bruce Moring, 2001. The USGS National Water Quality Assessment Program in Texas: A consistent, long-term approach to understanding water quality in three regions of the state, Texas Water Resources newsletter, v. 26, n.1, April 2002
2. Jensen, Ric. 2001 Creating Regional Water Plans under SB1: University researchers, Extension personnel, and graduate students contribute to analyze water supplies, economics, and policies, Texas Water Resources Newsetter, v. 26, n.2, August 2001.
3. Jensen, Ric. 2001. Can Brush Control Increase Water Yields? Field Studies, modeling by universities and agencies estimate site-specific costs and benefits, Texas Water Resources newsletter, v. 26, n.3, December 2001.
4. Jensen, Ric, 2002, TWRI Research Projects Fund Graduate Students, Faculty throughout Texas: Projects address wide range of issues, including water quality, water use, modeling, Texas Water Resources newsletter, v.26, n.4, May 2002.

Information Transfer
Texas Water Resources Institute

PI: Ric Jensen
co-PI: Jan Gerston
3/1/01 to 2/28/02
Texas Water Resources Institute
College Station, TX

Publication of research results summaries in quarterly newsletter, New Waves; examination of one water resource issue in depth in quarterly newsletter, Texas Water Resources. Publication of fact sheets on on-site septic systems. Conducting workshops on source water protection, cross-connection protection; conducting conferences on dissemination of water resources information on the World Wide Web. Publication of technical reports on funded water resources research.

Summarizes information about water resources research projects at Texas universities through newsletters, reports, WWW sites, and listservs. This project provides news relating to university research in water resources. An e-mail list in compiles and distribute timely information about Texas water issues, as well as research opportunities. Through our publications program, we reach more than 20,000 readers.

Work continued to educate the public about the importance of university research in water resources matters. Outreach materials were developed for printed newsletters, technical reports, web site sites, and electronic mailng list. Products discussed such issues as the prospects for implementing brush control to boost water yields; the involvement of university researchers in the water planning process in Texas; the future of rice irrigation in Texas, and efforts of the USGS to study water quality through its NAWQA program. Technical reports for this project covered such issues as monitoring groundwater supplies in the Trinity Aquifer of Central Texas; identifying opportunities for water conservation in the Lower Rio Grande Valley; use of filtration to treat surface waters and reduce dependence on chemicals; insitutional strategies to manage waters in the Rio Grande during droughts; the economic impact of coastal tourism; and site-specific data on how to increase water supplies through brush control in eight regions of Texas. TWRI personnel, including the PI, gave many presentations at meetings, workshops and conferences. TWRI continues to emphasize research results in such issues as rural [onsite] wastewater systems [septic tanks and drainfields] and water conservation and reuse. We are now working with the Texas Rural Water Assn to help them with outreach and communications and training efforts, and recently worked with them to and Mississippi State University to sponsor a workshop on cross connections, which is an issue that affects many small water systems. Publications: Jensen, Ric, Editor, New Waves newsletter, 2001. [Four issues]. Jensen, Ric, Editor, Texas Water Resources newsletter, 2001. [Four issues]. Jensen, Ric, Editor. Texas On-Site Insights newsletter, 2001. [Four issues]. Jensen, Ric.

Impact: This project provides timely information about news relating to university research in water resources. Currently, one of our most valuable services are electronic mailing list in which are compiled and distributed timely information about Texas water issues, as well as research opportunities. Through our publications program, we reach more than 20,000 readers. During 2001, we helped publicize, sponsor, administer a wide range of research projects. TWRI communicated information about opportunities for scientists to become involved in water research, and transmitted information about results from water resources projects to key clients and the general public.

Information Transfer

Basic Information

Title:	Information Transfer
Project Number:	2001TX9B
Start Date:	3/1/2001
End Date:	2/28/2002
Funding Source:	104B
Congressional District:	8
Research Category:	Not Applicable
Focus Category:	None, None, None
Descriptors:	information transfer, technology transfer
Principal Investigators:	Ric W. Jensen, Jan Robin Gerston

Publication

1. Gerston, Jan, Mark MacLeod, C. Allan Jones, 2002. Efficient Water Use for Texas: Policies, Tools, and Management Strategies, Texas Water Resources Institute, Texas A&M University, College Station, Texas, 32 pp.
2. Jensen, Ric, 2000, "Texas' Water Recreation Treasures: State Rivers, Streams, and Lakes Provide Outstanding Recreation Opportunities, but can these Waters be Protected?" Texas Water Resources newsletter, v 25, n.3
3. Jensen, Ric, 2000, "What is the Future of Rice Irrigation? Pending Water Shortages, Increased Water Demands, Poor Econonomies and Policies may Threaten the Texas Rice Industry and Perhaps the Environment, Texas Water Resources newsletter, v. 25, n.4.
4. Bush, Peter, Kevin Dennehy, Bruce Moring, 2001, "The USGS National Water-Quality Assessment Program in Texas: A Consistent, Long-term Approach to Understanding Water Quality in Three Regions of the State," Texas Water Resources newsletter, v. 26, n.1
5. Jensen, Ric, 2001, Creating Regional Water Plans under SB1: University Researchers, Extension Personnel, and Graduate Students Contribute to Analyze Water Supplies, Economics, and Policies, Texas Water Resources newsletter, v. 26, n.2

Student Support

Student Support					
Category	**Section 104 Base Grant**	**Section 104 RCGP Award**	**NIWR-USGS Internship**	**Supplemental Awards**	**Total**
Undergraduate	3	6	0	0	9
Masters	5	3	0		8
Ph.D.	7	0	0	0	7
Post-Doc.	0	0	0	0	0
Total	15	9	0	0	24

Notable Awards and Achievements

Publications from Prior Projects

None